

## Enzymatic hydrolysis of cellulose

a kinetic comparison of the two cellobiohydrolases Cel6A and Cel7A from *Hypocrea jecorina*

Badino, Silke Flindt

*Publication date:*  
2018

*Document Version*  
Publisher's PDF, also known as Version of record

*Citation for published version (APA):*  
Badino, S. F. (2018). *Enzymatic hydrolysis of cellulose: a kinetic comparison of the two cellobiohydrolases Cel6A and Cel7A from Hypocrea jecorina*. Roskilde Universitet.

### General rights

Copyright and moral rights for the publications made accessible in the public portal are retained by the authors and/or other copyright owners and it is a condition of accessing publications that users recognise and abide by the legal requirements associated with these rights.

- Users may download and print one copy of any publication from the public portal for the purpose of private study or research.
- You may not further distribute the material or use it for any profit-making activity or commercial gain.
- You may freely distribute the URL identifying the publication in the public portal.

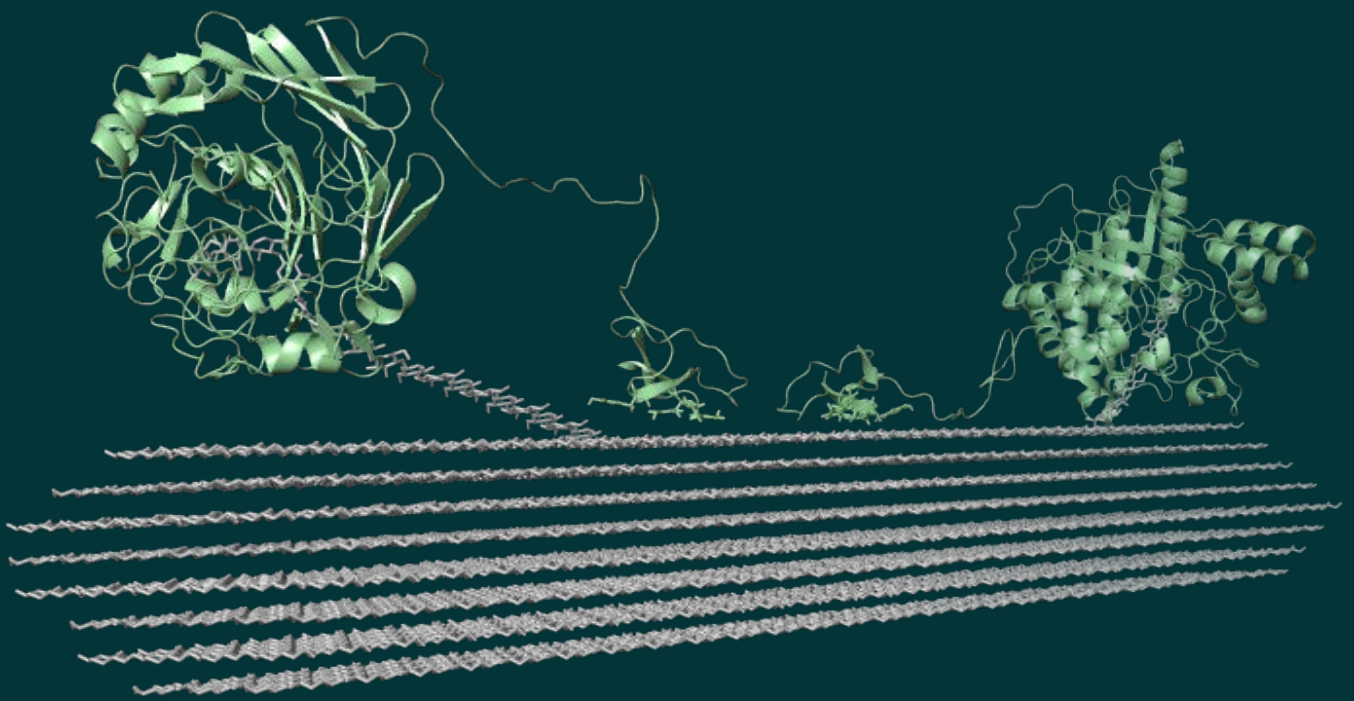
### Take down policy

If you believe that this document breaches copyright please contact [rucforsk@ruc.dk](mailto:rucforsk@ruc.dk) providing details, and we will remove access to the work immediately and investigate your claim.

# Enzymatic Hydrolysis of Cellulose

---

A Kinetic Characterization of the  
Cellobiohydrolases Cel6A and Cel7A



**Silke Flindt Badino**

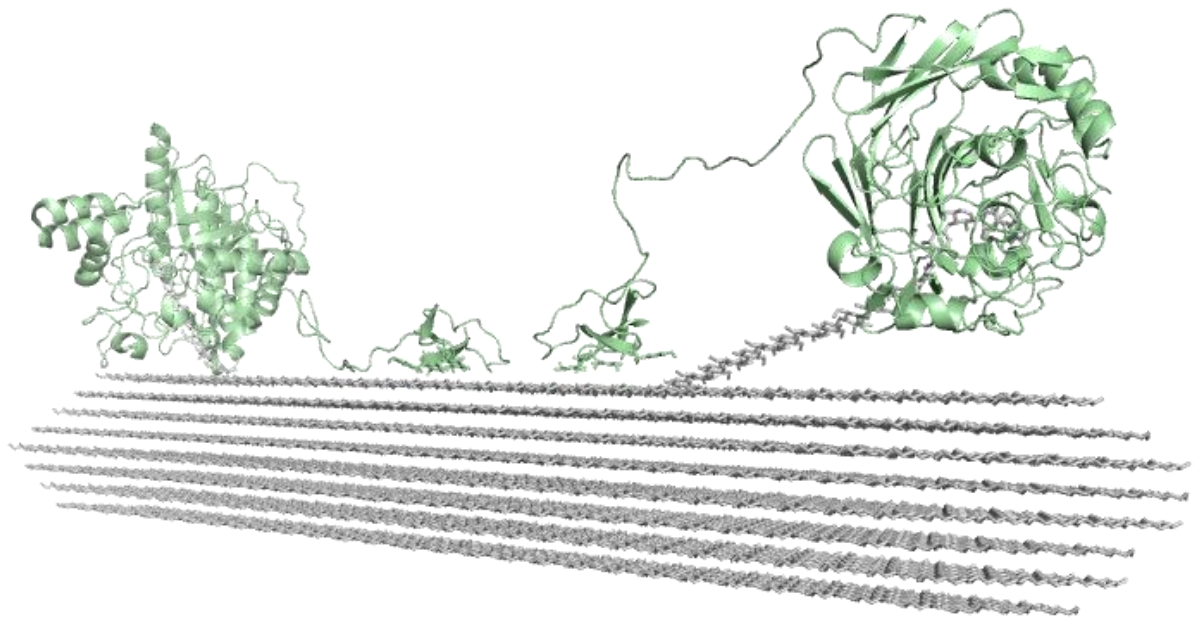
PhD Thesis

February 2017, Roskilde University  
Department of Science and Environment, INM

# Enzymatic Hydrolysis of Cellulose

---

A Kinetic Comparison of the two  
Cellobiohydrolases Cel6A and Cel7A from  
*Hypocrea jecorina*



Silke Flindt Badino

PhD thesis, Roskilde University

February 2017

## Summary

---

Climate changes are among the most severe present challenges and a transition to clean energy is crucial to reduce extensive global consequences. Lignocellulosic biomass is a massive energy resource and bioethanol generated from this source is predicted as a promising sustainable alternative to fossil fuels. One of the decisive and most challenging steps in the production of bioethanol from biomass is the degradation of cellulose into fermentable sugars. Cellulose is difficult to degrade, but some organisms such as the fungus *Hypocrea jecorina* are however able to hydrolyze cellulose into glucose units through secretion of different enzymes known as cellulases. Of the cellulases two cellobiohydrolases (CBHs) Cel6A and Cel7A are the most abundant and also the prominent components of industrial enzyme cocktails for saccharification of biomass. More insight into the catalytic behavior of these cellobiohydrolases is therefore informative in the design of new variants for commercial use.

The primary focus of this dissertation is a comparative kinetic characterization of Cel6A and Cel7A. Both enzymes are processive enzymes and they remain associated with the cellulose chain as they perform sequential catalytic cycles. Cel6A attacks non-reducing ends while Cel7A attacks reducing ends. The proof of the current work is to conduct direct comparisons of their properties. Most work pertains to the activities of these two enzymes, but we also present comparisons of stability. We postulate that comparative work under exact same experimental conditions is essential as the heterogeneous nature of the insoluble substrate has been shown to complicate comparisons between studies. At either substrate or enzyme excess we found widely diverse properties of the two cellobiohydrolases. By applying two different steady-state kinetic models we found that Cel6A was shown to be catalytic superior with a much higher maximal rate than Cel7A. Based on our results we further propose that Cel6A has high substrate specificity towards only limited substrate sites which seems to challenge the enzyme at low substrate concentration. In contrast Cel7A showed a very high ability to attack and hydrolyze many more sites resulting in a high activity at enzyme excess compared to Cel6A. In relation to this Cel7A showed higher binding capacity than Cel6A in adsorption studies. In addition, we found that the long term stability of Cel7A was high compared to the less stable Cel6A.



Both CBHs are multi-domain enzymes that besides a catalytic domain (core) also consist of a carbohydrate binding module (CBM) and a glycosylated linker that connects the CBM and core. We designed variants to investigate the role of these domains and we found that the CBM is essential for substrate adsorption and the ability to locate attack site, but that Cel6A and Cel7A without CBM and linker showed improved maximal rate. Our results further indicate that the CBM is highly optimized to interplay with the linker and core for each specific enzyme, since a CBM swap between Cel6A and Cel7A lowered the affinity towards cellulose despite high homology among the CBMs. Also some linker modifications were shown to reduce affinity for the substrate, but to increase the maximal rate. In the comparison of Cel6A and Cel7A and the characterized variants we found a general inverse relation between maximal catalytic rate and binding affinity. We suggest that at high substrate loads the hydrolysis is limited by the enzymes ability to dissociate. Contrary at low substrate load the ability to locate binding and attack sites becomes essential for the hydrolytic rate, where variants with high binding capacity are superior. Finally we studied the underlying interpretation of the strong synergy between Cel6A and Cel7A. We showed that the synergy is dependent on the presence of CBM and the experimental conditions. Based on our findings we suggest that substrate targeting and differences in specificity between Cel6A and Cel7A can explain the observed synergy, since the enzymes remove potential obstacles for each other and release new attack sites.

The present investigations of Cel6A and Cel7A have provided insights into their kinetics, adsorption behavior, stability, synergy, substrate interactions and the role of the different domains of the enzymes. These findings of the industrial relevant cellulases may be applicable in the rational engineering of new variants and contribute in the improvement of saccharification of biomass.

Klimaforandringer er en af vor tids mest alvorlige og omfattende udfordringer. For at reducere de vidt strækkende globale følgevirkninger, er overgangen til grøn energi altafgørende. Her har bioethanol produceret fra biomasse et enormt potentiale, da det er et bæredygtigt alternativ til fossile brændstoffer. En af de helt store udfordringer i produktionen af bioethanol er nedbrydningen af cellulose til sukker. Cellulose er svært genstridigt, men få organismer såsom svampen *Hypocrea jecorina* formår at nedbryde cellulose til glukose ved at udskille forskellige enzymer kaldet cellulaser. Her er særligt to cellulaser, de to cellobiohydrolaser (CBH'er), Cel6A og Cel7A dominerende og disse enzymer er også de mest forekommende i kommercielle enzym-cocktails til nedbrydelse af biomasse. Med henblik på design af nye og bedre CBH'er vil en bredere forståelse af deres katalyse og kinetiske egenskaber være informativ.

Denne afhandling har sit primære afsæt i en komparativ kinetisk karakterisering af Cel6A og Cel7A. Begge enzymer er processive, hvilket betyder at de forbliver bundet til cellulosekæden i hydrolysen af glykosidbindingerne. Cel6A angriber ikke-reducerende ender, mens Cel7A angriber reducerende ender. En stor styrke ved denne afhandling er at vi har benyttet en direkte sammenligning af Cel6A og Cel7A. Det overvejende fokus har været på enzymernes aktivitet, men vi har også sammenlignet deres stabilitet. Heterogeniteten i cellulosesubstrater har gjort det yderst vanskeligt at sammenligne forskellige kinetiske studier og vi hævder at en direkte kinetisk sammenligning under præcis samme eksperimentelle betingelser er essentiel. Ved at anvende to kinetiske steady-state modeller under forskellige eksperimentelle betingelser med enten substrat eller enzym overskud, fandt vi markante forskelle i de to CBH'ers kinetiske egenskaber. Cel6A viste sig at være katalytisk overlegen med en maksimal hastighed langt højere end Cel7A. Til gengæld tyder vores resultater på at Cel6A's høje substrat specificitet til limiterede områder er en ulempe under betingelser hvor kun begrænset substrat er tilgængeligt. Cel7A derimod var katalytisk underlegen, men viste en udpræget evne til at nedbryde svært tilgængeligt substrat. I relation til dette, viste Cel7A også en højere bindingskapacitet i adsorptionsstudier. Cel7A viste sig tilmed at være mere stabil end Cel6A.

Begge enzymer er multi-domæne enzymer og består af et katalytisk domæne (core), et 'carbohydrate binding module' (CBM) og en glukosyleret linker der forbinder CBM og core. Ved at designe og udtrykke forskellige varianter undersøgte vi betydningen af både CBM og linker. Her fandt vi at CBM'en er afgørende for enzymets adsorption til cellulose og dermed evnen til at finde celluloseender at angribe. Interessant nok viste varianter udtrykt uden linker og CBM en højere reaktionshastighed ved høj substrat koncentration. En ombytning af CBM'en mellem Cel6A og Cel7A reducerede deres affinitet til cellulose og vi foreslår, trods stor homologi mellem de to CBM'er, at de hver især er optimeret til samspil med tilhørende linker og katalytiske domæne. Ydermere fandt vi at ændringer i linkeren også havde direkte indflydelse på substrataffinitet og den lavere affinitet resulterede i højere maximal hastighed. I den komparative analyse af Cel6A og Cel7A samt diverse varianter fandt vi en generel sammenhæng mellem lav affinitet og høj maximal reaktionshastighed. Dette indikerer at enzymernes evne til at dissociere er hastighedsbegrænsende ved høj substrat koncentration. Derimod viste varianter med høj bindingskapacitet sig at have højere reaktionshastigheder ved lav substrat koncentration, sandsynligvis på grund af en forøget evne til at lokalisere celluloseender at angribe. Endelig undersøgte vi den markante synergi mellem Cel6A og Cel7A og observerede at synergien afhænger af de eksperimentelle betingelser, men mere interessant af tilstedeværelsen af CBM'er. Vi foreslår at forskelligheder i enzymernes substratspecificitet og targeting kan forklare deres synergi da de således frigør nye ender for hinanden og fjerner potentielle forhindringer.

De forskellige studier omhandlende Cel6A og Cel7A har givet indblik i enzymernes kinetik, adsorptions egenskaber, stabilitet, synergi, substrat interaktioner, samt de forskellige domæners rolle. Disse resultater kan være værdifulde i design af nye cellulaser og dermed bidrage til en optimering af nedbrydelsen af biomasse til sukker.

# Preface and Acknowledgement

---

This PhD dissertation is part of the RESAB<sup>1</sup> project run in the period from 2012-2017. The research project RESAB is a close collaboration between Roskilde University, Denmark and Novozymes A/S headed by Professor Peter Westh, Roskilde University and Science Director Kim Borch, Novozymes A/S. The project is partially funded by the Danish Council for Strategic Research and the Innovation Fund Denmark.

The major objective of the RESAB project is to improve cellulases for saccharification of biomass at industrial conditions. Since industrial conditions are far from conditions in nature we presume that cellulases have not evolved to adapt to these surroundings. Therefore rational engineering of cellulases together with a thorough understanding of the enzymes turn into a strong tool to develop improved cellulases. The work presented in this dissertation will mainly focus on already public known cellulases although a substantial and very motivating part of my work in the last 3 years has focused on engineering and characterization of more confidential cellulases. Part of that work resulted in patent WO/2016/138167.

The last 3 years have been inspiring, exciting, hardworking as well as joyful and when I look back, definitely essential for my personal development within the scientific field. For this I would like to express my gratitude.

Above all I will like to thanks my inspiring supervisor Professor Peter Westh. I feel that I have been very privileged to do research within your group. Your ability to provide excellent supervision, share your knowledge and new ideas and your enthusiastic involvement in the research has certainly impressed me and has functioned as a constantly driving force during my work. Next, I would like to thank my supervisor Science Director Kim Borch for likewise great supervision, where the opportunity to be involved in research more closely related to application has been very motivating. You have moreover demonstrated to me how to celebrate good results one day and how to handle disappointing results the day after.

---

<sup>1</sup> Rational Engineering of cellulases for improved SAccharification of Biomass

Thanks to both Peter and Kim for not just being great supervisors, but also for contributing to a great atmosphere where humor is always present and where social summer meetings among other events have been many.

Great thanks to all present and former members of the RESAB and TEMPEN project Nicolaj Cruys-Bagger, Trine Holst Sørensen, Johan Pelck Olsen, Jeppe Kari, Michael Skovbo Windahl, Nanna Sandager Røjel, Stefan Jarl Christensen, Corinna Schiano di Cola, Kadri Alasepp, Radina Tokin, Cynthia Segura Vesterager, Ana Mafalda de Almeida Cavaleiro and Eva Karlsen for collaboration, inspiring discussions and for being great colleagues that make life as a PhD pleasant. I have enjoyed working with you all in a happy atmosphere marked by great collaborations where individual competition is never present. I am especially very grateful to Trine for support and guidance from day one and throughout the last years. Your ability to care about others well-being is kindly appreciated especially in occasionally intense working periods. Also to Jeppe, Johan and Nicolaj whose prior work resulted in models, biosensors and a Quench Flow system that I have used in my studies and to Michael for generating and engineering an impressive number of interesting cellulase-variants.

Acknowledgements to all my colleagues at Novozymes especially to Ulla Rosenberg and Camilla Hindborg Kristensen for being very welcoming, always helpful and an invaluable part of the RESAB project. A special thanks to Kenneth Jensen for supervision in the generation of variants and also thanks to our collaborator Brett McBrayer from Novozymes, Davis for enthusiastic interest in the project and for getting our leading variants closer to application.

The final and warmest gratitude to those of you closest to me.

Silke Flindt Badino, February 2017

# Outline and Guide to the Reader

---

The work throughout this dissertation focuses on the two cellobiohydrolases Cel6A and Cel7A. Many different areas have been covered during the scientific work and the aim of this dissertation is to summarize a selection of the major findings that can provide information to a better understanding of the two enzymes. Thus, the current dissertation will not give an exhaustive survey of the last 3 years work and for details considering analysis, results, experimental procedures etc. the reader is referred to the appended manuscripts. All articles can somehow be related to the cellobiohydrolases Cel6A and/or Cel7A. Figure 1 visualizes how the appended papers are connected to the enzymes and their different domains.

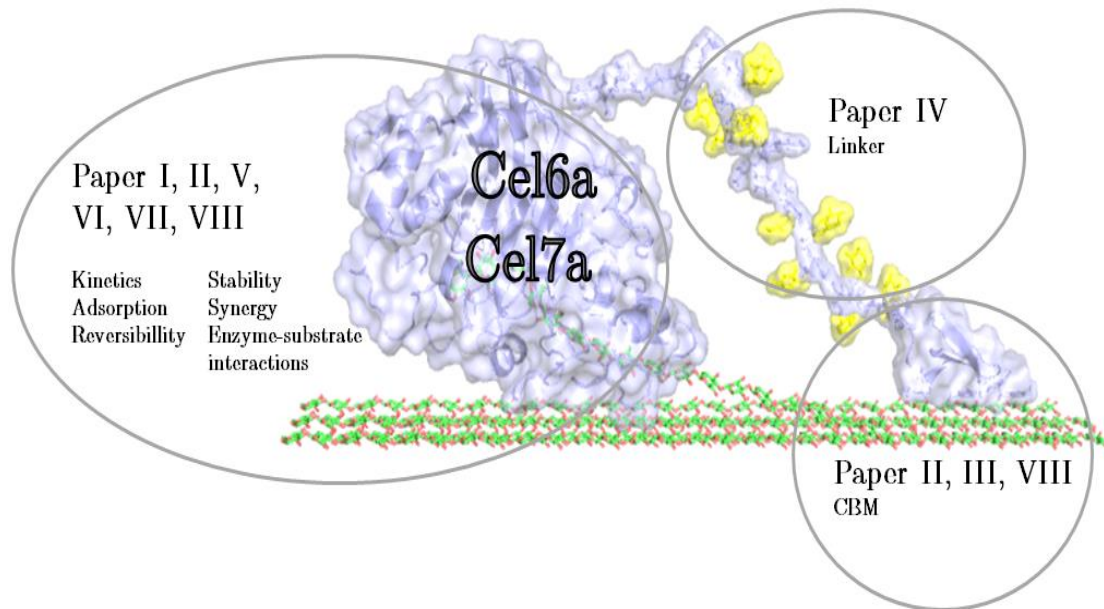


**Figure 1** An overview of the manuscripts including key words and how they are associated to the cellobiohydrolases.

The present work is divided into 4 chapters. Chapter 1 will provide a general introduction to the field primarily to the two enzymes and their different domains. The following three chapters will cover a selection of some experimental findings and discussions of these. Most of these new findings are also reported in the articles or manuscript drafts but some unpublished data will also be discussed. Chapter 2 is the central chapter where the overall theme is the kinetics of Cel6A and Cel7A, Chapter 3 will focus on enzyme-substrate interactions while Chapter 4 pertains to the synergy between the two enzymes.

All articles or manuscripts are appended and in the main text they will be referred to by their numeral letters. For simplicity they will all be referred to as articles through the text though some of them still appear as submitted manuscripts or manuscripts in preparation.

### **Disclaimer**

In the main text some data and figures will be copied or adapted from the appended manuscripts. In all cases this will be noticed in the figure legends. Data presented in Article VII was made prior to this PhD as part of my master thesis entitled *Rational Engineering of Cel6A from Trichoderma reesei*.

## List of Publications

---

Articles will be referred to by their roman numerals throughout the thesis. All articles are appended. All articles are reproduced with permission of the publisher.

- I. *Direct kinetic comparison of the two cellobiohydrolases Cel6A and Cel7A secreted by Hypocrea jecorina***  
Silke Flindt Badino, Stefan Jarl Christensen, Jeppe Kari, Kim Borch and Peter Westh  
(Accepted BBA- proteins and proteomics, In Press)
- II. *Exo-exo synergy between Cel6A and Cel7A from Hypocrea jecorina: role of CBM and the endo-lytic character of the enzymes***  
Silke Flindt Badino, Stefan Jarl Christensen, Jeppe Kari, Michael Skovbo Windahl, Søren Hvidt, Kim Borch & Peter Westh. *Biotechnol Bioeng*, 114 (8), 1639-1647, 2017
- III. *Exchanging carbohydrate binding modules between Cel6A and Cel7A from Hypocrea jecorina strongly influence the kinetics of the enzymes***  
Silke Flindt Badino, Michael Skovbo Windahl, Jeppe Kari, Kim Borch & Peter Westh  
(manuscript in preparation)
- IV. *The influence of different linker modifications on the catalytic activity and cellulose affinity of cellobiohydrolase Cel7A from Hypocrea jecorina***  
Silke Flindt Badino, Jenny Kim Bathke, Günther H. Peters, Trine Holst Sørensen, Kenneth Jensen, Michael Skovbo Windahl, Kim Borch and Peter Westh. *PEDS*, DOI:10.1093/protein/gzx036, pp1-7
- V. *In Situ Stability of Substrate-Associated Cellulases Studied by DSC***  
Kadri Alasepp, Kim Borch, Nicolaj Cruys-Bagger, Silke Badino, Kenneth Jensen, Trine H. Sørensen, Michael S. Windahl & Peter Westh. *Langmuir*, 30, 7134-42. 2014
- VI. *Reversibility of substrate adsorption for the cellulases Cel7A, Cel6A and Cel7B from Hypocrea jecorina***  
Vanessa O.A. Pellegrini, Nina lei, Madhuri Kyasaram, Johan P. Olsen, Silke F. Badino, Michael S. Windahl, Francieli Colussi, Nicolaj Cruys-Bagger, Kim Borch & Peter Westh. *Langmuir*, 30, 12602-09. 2014



**VII. *A pyranose dehydrogenase-based biosensor for kinetic analysis of enzymatic hydrolysis of cellulose by cellulases***

Nicolaj Cruys-Bagger, Silke Flindt Badino, Radina Tokin, Mark Gontsarik, Samin Fathalinejad, Kenneth Jensen, Miguel Duarte Toscano, Trine Holst Sørensen, Kim Borch, Hirosuke Tatsumi, Priit Väljamäe & Peter Westh. *Enzyme and Microbial Technology*, 58-59, 68-74, 2014

**VIII. *Temperature effects on kinetic parameters and substrate affinity of Cel7A cellobiohydrolases***

Trine Holst Sørensen, Nicolaj Cruys-Bagger, Michael Skovbo Windahl, Silke Flindt Badino, Kim Borch & Peter Westh *The journal of biological chemistry* 290: 22193-22202, 2015

**IX. *PATENT WO/2016/138167 CELLOBIOHYDROLASE VARIANTS AND POLYNUCLEOTIDES ENCODING SAME***

Brett McBrayer, Michael Skovbo Windahl, Peter Westh, Silke Flindt Badino, Kim Borch (date 01.09.2016)

## List of Abbreviations

---

|        |                                                                                |
|--------|--------------------------------------------------------------------------------|
| AA     | Amino acids                                                                    |
| AA9/10 | Auxiliary Activities family 9/10                                               |
| BC     | Bacterial cellulose                                                            |
| BG     | $\beta$ -glucosidase                                                           |
| BMCC   | Bacterial Micro Crystalline Cellulose                                          |
| CAZy   | Carbohydrate active enzymes database                                           |
| CBD    | Cellulose binding domain                                                       |
| CBM    | Carbohydrate binding module                                                    |
| CBH    | Cellobiohydrolase                                                              |
| CBH I  | Cellobiohydrolase I, same as Cel7A                                             |
| CBH II | Cellobiohydrolase II, same as Cel6A                                            |
| CD     | Circular Dichroism                                                             |
| CDH    | Cellobiose dehydrogenase                                                       |
| Cel6A  | Cellulase (cellobiohydrolase), glycoside hydrolase family 6                    |
| Cel7A  | Cellulase (cellobiohydrolase), glycoside hydrolase family 7                    |
| Cel7B  | Cellulase (endoglucanase), glycoside hydrolase family 7                        |
| Core   | Catalytic domain                                                               |
| COS    | Celooligosaccharide                                                            |
| CMC    | Carboxymethyl cellulose                                                        |
| DP     | Degree of polymerization                                                       |
| EG     | Endoglucanase                                                                  |
| EG I   | Endoglucanase I, same as Cel7B                                                 |
| GH     | Glycoside hydrolase                                                            |
| ICS    | Ion chromatography system                                                      |
| ITC    | Isothermal titration calorimetry                                               |
| LPMO   | Lytic polysaccharide monooxygenases                                            |
| MD     | Molecular Dynamics                                                             |
| MM     | Michaelis Menten                                                               |
| PAHBAH | 4-hydroxybenzoic acid hydrazide                                                |
| PDH    | Pyranose dehydrogenase                                                         |
| pNPL   | para-Nitrophenyl-lactopyranoside                                               |
| QF     | Quench Flow                                                                    |
| RAC    | Regenerated amorphous cellulose                                                |
| RESAB  | Rational Engineering of cellulases for improved<br>Saccharification of Biomass |
| SAXS   | Small-Angle X-ray Scattering                                                   |
| SHF    | Separate Hydrolysis and Fermentation                                           |
| SSF    | Simultaneous Saccharification and Fermentation                                 |
| QSSA   | Quasi steady state assumption                                                  |
| wt     | Wild-type                                                                      |

## Kinetic parameters and rate constants

|                             |                                                                                          |
|-----------------------------|------------------------------------------------------------------------------------------|
| $\Gamma_{max}$              | <i>Maximal adsorption capacity per gram of substrate</i>                                 |
| $^{kin}\Gamma_{max}$        | <i>Kinetic maximal adsorption capacity- amount of attack sites per gram of substrate</i> |
| $k_{cat}$                   | <i>Catalytic rate constant</i>                                                           |
| $\frac{pk_{cat}}{p}k_{cat}$ | <i>Catalytic rate constant (processive enzymes)</i>                                      |
| $\frac{pk_{cat}}{p}k_{cat}$ | <i>Average catalytic rate constant</i>                                                   |
| $K_B$                       | <i>Binding constant (equally to <math>1/K_d</math>)</i>                                  |
| $K_d$                       | <i>Dissociation constant</i>                                                             |
| $K_M$                       | <i>Michalis-Menten constant</i>                                                          |
| $^{conv}K_M$                | <i>Processive Michalis-Menten constant (in g/L)</i>                                      |
| $^{inv}K_M$                 | <i>Inverse Michalis-Menten constant</i>                                                  |
| $K_p$                       | <i>Partition coefficient</i>                                                             |
| $k_{off}$                   | <i>Rate constant for dissociation (off-rate)</i>                                         |
| $k_{on}$                    | <i>Rate constant for adsorption or association (on-rate)</i>                             |
| $n$                         | <i>Processivity</i>                                                                      |
| $^{conv}V_{max}$            | <i>The maximal rate at enzyme saturation</i>                                             |
| $^{inv}V_{max}$             | <i>The maximal rate at substrate saturation</i>                                          |

# Table of Contents

---

|                                       |      |
|---------------------------------------|------|
| Summary.....                          | I    |
| Resume .....                          | III  |
| Preface and Acknowledgement .....     | V    |
| Outline and Guide to the Reader ..... | VII  |
| List of Publications.....             | IX   |
| List of Abbreviations .....           | XI   |
| Table of Contents.....                | XIII |

## **Chapter 1 General Introduction.....1**

|                                          |    |
|------------------------------------------|----|
| Cellulose.....                           | 2  |
| Model substrates.....                    | 3  |
| Cellulases.....                          | 4  |
| Cellobiohydrolases Cel6A and Cel7A.....  | 6  |
| Catalytic core domain.....               | 7  |
| Catalytic Mechanism.....                 | 8  |
| Carbohydrate Binding Modules (CBM) ..... | 10 |
| Linkers.....                             | 14 |

## **Chapter 2 Cellobiohydrolase Kinetics .....17**

|                                                                     |    |
|---------------------------------------------------------------------|----|
| Part I - Non-linear Kinetics .....                                  | 18 |
| Enzyme related factors .....                                        | 18 |
| Substrate Related Factors .....                                     | 23 |
| Part II - Modelling Cellulase Kinetics.....                         | 23 |
| Traditional Enzyme Kinetics.....                                    | 24 |
| Modelling Processive Enzymes .....                                  | 25 |
| The Steady-State Model & the Inverse Michaelis Menten Approach..... | 27 |
| Part III - Kinetics of Cel6A and Cel7A.....                         | 31 |
| Cellulose consists of Good and Poor Attack Sites.....               | 35 |
| Not all Binding Sites are Attack Sites.....                         | 36 |
| Part IV - The Role of the CBM.....                                  | 38 |
| CBM Swap changed the Enzymes Kinetically.....                       | 43 |

|                                                               |           |
|---------------------------------------------------------------|-----------|
| Part V – The Role of the Linker.....                          | 46        |
| Part VI – Pre-steady State Kinetics .....                     | 47        |
| Exploring the Initial Kinetics using Quench Flow System ..... | 48        |
| <br>                                                          |           |
| <b>Chapter 3 Enzyme Substrate Interactions.....</b>           | <b>51</b> |
| What drives Processivity?.....                                | 56        |
| <br>                                                          |           |
| <b>Chapter 4 Cel6A and Cel7A in Synergy .....</b>             | <b>59</b> |
| Synergy depends on Experimental Conditions.....               | 59        |
| Exo-Exo Synergy is influenced by the Linker and CBM.....      | 61        |
| Endo-Character of Cel6A and Cel7A .....                       | 64        |
| Enzyme Specificity can explain Exo-Exo Synergy .....          | 66        |
| <br>                                                          |           |
| Concluding Remarks.....                                       | 69        |
| References.....                                               | 71        |

# General Introduction

---

Global warming and climate changes show that sustainable energy alternatives are crucial for the future. In order to accommodate the increasing energy demands on Earth and maintain our modern living standards the transition to green energy is essential. Recently, representatives of the World's countries managed to agree on a global Climate plan in Paris (UNTC, 2016) which indicates that long awaited political intentions are now present. Thus even though the incumbent most influential World leaders seem to avoid climate challenges as a political key issue the seriousness of the climate and our future is becoming a reality globally. Different sustainable solutions are necessary in the transition to green energy, where utilization of the enormous energy resource of lignocellulosic biomass is one important aspect. Bioethanol produced from biomass, such as biological waste products, can displace fossil fuels with a sustainable and renewable alternative. The bioethanol industry has great potential, but is still in the start-up phase worldwide, especially considering utilization of biological waste products and that even though the environmental and sustainable perspectives have been widespread (Lynd *et al.*, 1991, Himmel *et al.*, 1999, Farrell *et al.*, 2006). The current reduction in oil prices within the last few years (Nasdaq, 2016) might prolong the transition to biofuels even further since some investors keep away from the field. This additional challenge just emphasizes the importance of improving the production of bioethanol so this energy resource can be cost-competitive.

The process from lignocellulosic biomass to bioethanol includes different steps including pretreatment, enzymatic hydrolysis and fermentation (Himmel *et al.*, 2007, Payne *et al.*, 2015) as illustrated in Figure 2. After pretreatment, the hydrolysis and fermentation can be carried out in two steps known as separate hydrolysis and fermentation (SHF) or in a combined step known as simultaneous saccharification and fermentation (SSF) (Jørgensen *et al.*, 2007).

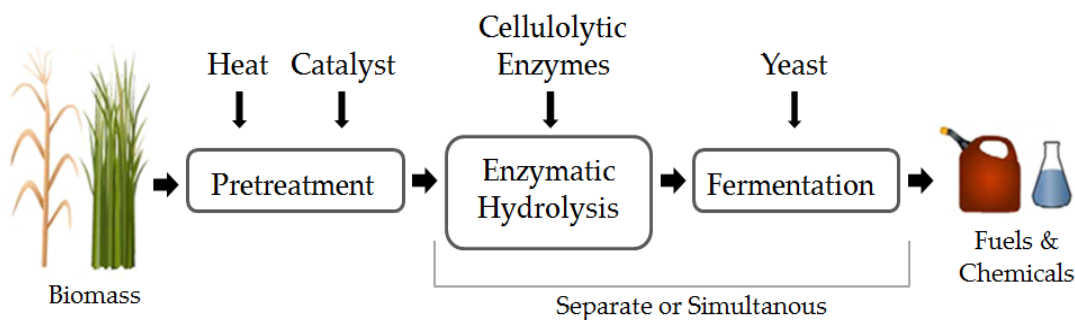


**Figure 2** The simplified process from lignocellulosic biomass for renewable fuels and chemicals. Based on (Payne *et al.*, 2015).

All steps in the production of bioethanol from biomass can be improved to enhance the production yield and decrease production costs. The focus within this dissertation is on the enzymatic hydrolysis of cellulose by cellulases.

## Cellulose

Cellulose is the most abundant renewable biological resource on Earth with an estimated annual biosynthesis of 100 billion dry tons per year (Percival Zhang *et al.*, 2006) which includes a huge resource of cellulosic biomass waste products from agriculture and other sources. Thus when solar energy is stored as carbon through photosynthesis in plants a substantial part is stored as cellulose. Cellulose is a simple polysaccharide consisting of  $\beta(1\rightarrow4)$  linked glucose units. The repeating unit of cellulose is the disaccharide cellobiose, where one of the glucose units is rotated  $180^\circ$ . Each cellulose chain has a reducing end and a non-reducing end, see Figure 3. The biosynthesis of cellulose is a condensation polymerization of glucose units. Cellulose is synthesized from cellulose synthase complexes in plant cell walls and from these “rosettes” complexes cellulose is synthesized into cellulose microfibrils or fibers (Klemm *et al.*, 2005, McFarlane *et al.*, 2014). These microfibrils typically consist of 36 or 24 cellulose chains (McFarlane *et al.*, 2014, Payne *et al.*, 2015) which are coupled together by hydrogen bonds and hydrophobic interactions. This complex crystalline

structure is extremely stable and the  $\beta(1,4)$  glycosidic bonds in cellulose has a predicted half-life of 5 million years (Wolfenden and Snider, 2001).

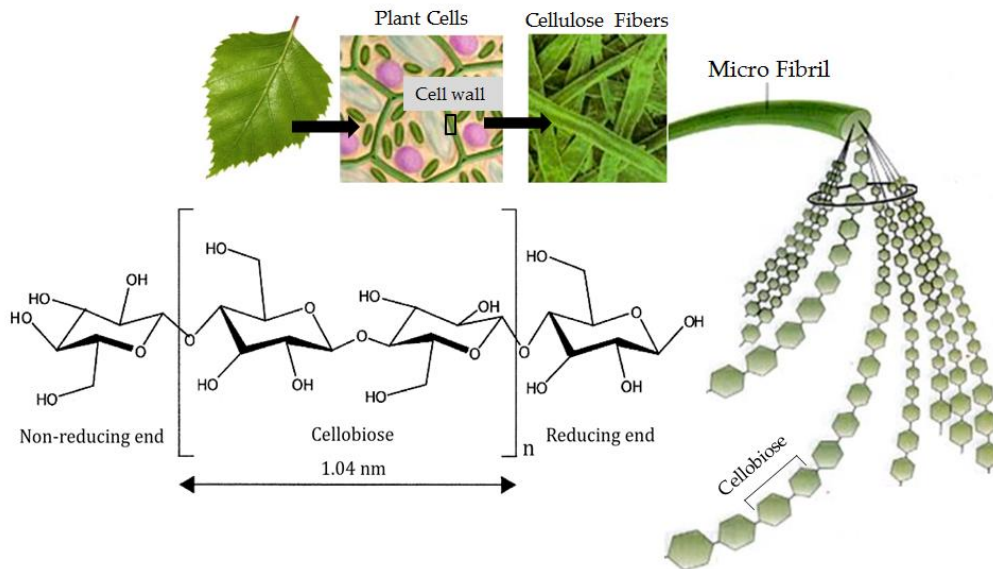


**Figure 3** Cellulose and the structure of a single cellulose chain with cellobiose as the repeating unit. Based on (Zhang and Lynd, 2004) and (Emaze, 2016).

### Model substrates

Different pure model cellulose substrates with less complexity than real biomass is often applied in experiments. In the studies presented here cellulose substrates such as Avicel, Regenerated Amorphous Cellulose (RAC), Bacterial Cellulose (BC), Bacterial Microcrystalline Cellulose (BMCC) and Carboxy Methyl Cellulose (CMC) were used. In addition, many other model substrates together with many soluble substrates exist.

In contrast to model substrates real biomass contains other components such as lignin and hemicellulose, which further complicate the degradation (Knowles *et al.*, 1987). Hence production of sustainable bioethanol from insoluble, highly heterogeneous and recalcitrant cellulosic biomass is clearly challenging, particularly the degradation of cellulose to fermentable soluble carbohydrates. Some organisms, such as fungi and bacteria are however able to degrade cellulose usually through expression of different enzymes named cellulases.



## Cellulases

In general, enzymes catalyze chemical reactions by increasing the rate of reaction by lowering the activation free energy. The reaction rate of many chemical reactions is increased several millions times in the presence of enzymes and numerous essential reactions would in principle 'not' or extremely rarely occur without these biological catalysts (Nelson and Cox, 2008). Hydrolysis of cellulose is clearly one such example. The most studied and industrially relevant cellulose-degrading catalysts are secreted by fungi. Here cellulases from the filamentous soft-rot fungus *Trichoderma reesei* are by far the most investigated (Martinez *et al.*, 2008). *Trichoderma reesei* was first discovered under World War II in tropical regions where the fungus started to degrade cotton tents and other materials from the army (Reese, 1976). The fungus was named after one of the discoverers E.T. Reese, but was later found to be an anamorph of the fungus *Hypocrea jecorina*<sup>2</sup>. The two cellobiohydrolases Cel7A and Cel6A, formerly known as CBHI and CBHII are the two most abundant cellulases secreted by *H. jecorina* and likewise the most prominent enzymes in commercial cellulase cocktails. Cel7A is reported to account for 40-60 % and Cel6A for 12-20% of the total protein level secreted (Teeri, 1997, Rosgaard *et al.*, 2007). Both Cel6A and Cel7A are processive cellobiohydrolases which means that they remain associated to the cellulose surface in between catalytic cycles. However, besides both being processive CBHs Cel6A and Cel7A differ in many aspects. Cel6A attacks the non-reducing ends while Cel7A attacks the reducing ends of cellulose (Barr *et al.*, 1996) and they use different catalytic mechanisms (Claeyssens *et al.*, 1990). Before focusing on the two cellobiohydrolases, we should mention that synergistic cooperation between different enzymes is essential for an efficient degradation of cellulose. By synergy we mean that the combined hydrolysis of different cellulases is more efficient than the sum of their individual activities. Already in the tentative beginning of the cellulase research field the first synergistic model was

---

<sup>2</sup> *Hypocrea jecorina* will be used consistently throughout the thesis

suggested (Reese *et al.*, 1950) and since that many studies have investigated the underlying mechanisms of cellulase synergism. One prominent type of synergy is between endoglucanases and cellobiohydrolases. The classical explanation for endo-exo synergy is that endoglucanases attack the cellulose surface randomly, but with preference for amorphous regions, thereby producing new chain ends for the cellobiohydrolases to attack (Teeri, 1997, Percival Zhang *et al.*, 2006, Payne *et al.*, 2015). The cellobiohydrolases are thus responsible for the primary hydrolysis, when degrading the more crystalline cellulose. Finally the  $\beta$ -glucosidase digests soluble sugars into glucose to reduce product inhibition. A more recent discovery of oxidative enzymes known as AA9, AA10, GH61 or LPMO (lytic polysaccharide monoxygenases) added a new mechanism for endo attack and a new aspect in the synergistic degradation of cellulose (Vaaje-Kolstad *et al.*, 2010, Lo Leggio *et al.*, 2012, Levasseur *et al.*, 2013, Kim *et al.*, 2014, Cannella *et al.*, 2016). The synergy between endoglucanases, cellobiohydrolases, LPMOs and  $\beta$ -glucosidases is illustrated in Figure 4.

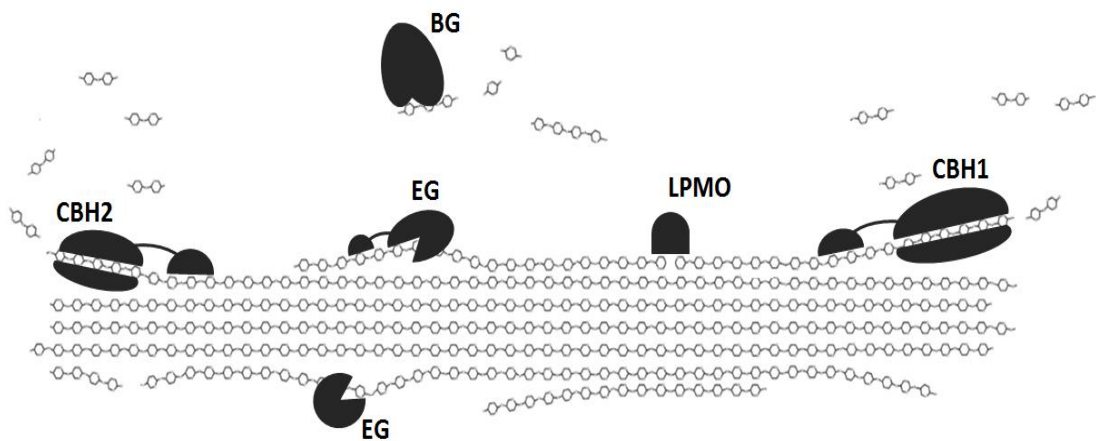


**Figure 4** Synergistic cooperation in degradation of cellulose. CBH1 (Cel7A) attacks reducing ends, CBH2 (Cel6A) attacks non-reducing ends. EGs (endoglucanases) are able to attack cellulose chains randomly with preference for amorphous region and LPMO (lytic polysaccharide mono-oxygenases) makes endo attack by oxidative degradation. Finally BG ( $\beta$ -glucosidase) digests soluble sugars into glucose.

Another conspicuous synergy occurs between exo-lytic enzymes such as Cel6A and Cel7A. The exo-exo synergy is studied in Article II and will be covered in Chapter 4.

The next section serves to give an introduction to the structural similarities and differences between the two cellobiohydrolases Cel6A and Cel7A.

## Cellobiohydrolases Cel6A and Cel7A

The cellobiohydrolases Cel6A and Cel7A are responsible for the primary hydrolysis of cellulose and the two CBHs have been major targets for enzyme engineering. Cel6A and Cel7A belong to glycoside hydrolase family 6 and 7 (GH6 and GH7), respectively. Both families represent a large number of characterized members (CAZy database) including both endoglucanases (EC 3.2.1.4 and EC 3.2.1.73) and cellobiohydrolases (EC 3.2.1.91 and EC 3.2.1.176). In this thesis we will merely focus on the two cellobiohydrolases Cel6A and Cel7A from the fungus *Hypocrea jecorina*. Both CBHs consists of a large catalytic domain (core), a linker and a carbohydrate binding module as shown in Figure 5 (Tomme *et al.*, 1988). We will now look closer into the structure, mechanism and function of the different domains.

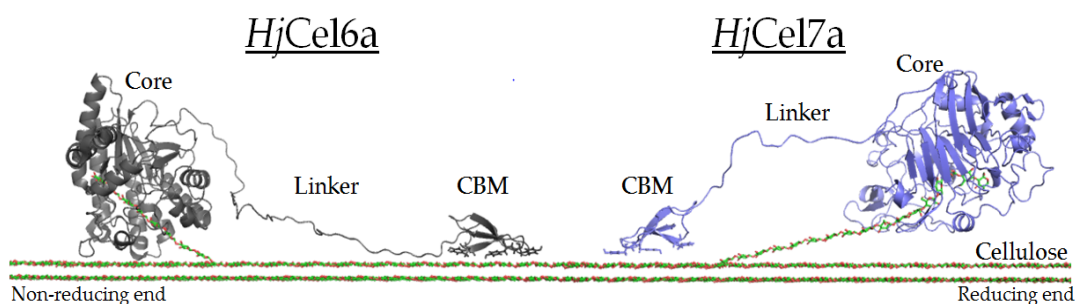


**Figure 5** The cellobiohydrolases *hjCel6A* and *hjCel7A* including core, linker and CBM. Constructed in PyMol using PDB (4C4C, 1QK2, 1CBH, linker sequences are added manually).

## Catalytic core domain

The first three-dimensional structure of a cellulase was solved for Cel6A from *H. jecorina* and the structure indicated that the active site was located inside a tunnel enclosed by 2 loops (Figure 6 (right)) (Rouvinen *et al.*, 1990). The large core domain (~40 kDa) is dominated by a central barrel connected by  $\alpha$ -helices. The tunnel shaped catalytic domain of Cel6A was first assumed to interact with the 4 glycosidic binding subsites -2,-1,+1,+2 but later suggested to interact with 6 glycosidic binding subsites instead, -2,-1,+1,+2,+3 and +4 (Figure 6 (left)) (Harjunpää *et al.*, 1996, Koivula *et al.*, 1998). The +4, and +3 sites are where the cellulose chain enters the tunnel and the -1 to -2 subsites are the position of the cellobiose unit cleaved off during hydrolysis. In general, glycosidic binding subsites in the catalytic core domains of glycosyl hydrolases are termed by numbers and the cleavage site in the catalytic domain is used as reference point (Davies *et al.*, 1997). Binding sites towards the reducing end of the cellulose chain are numbered positively +1,+2,+3... starting from the cleavage point and opposite binding sites towards the non-reducing end of the substrate are numbered negatively -1,-2,-3....

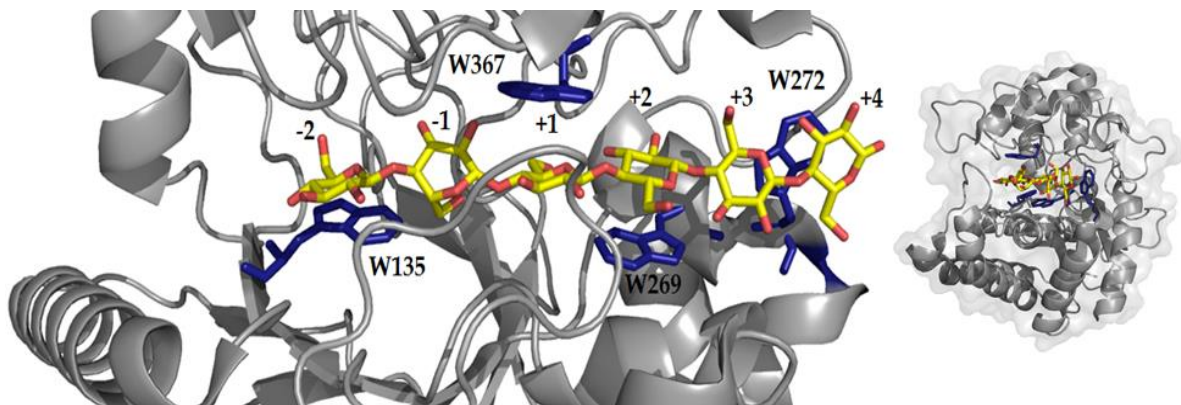


**Figure 6** The catalytic tunnel of Cel6A (left). The 6 glycosidic subsites on the glucan chain in yellow and the tryptophans contributing to the shape of the tunnel in blue. The -2 to -1 subsite is the cellobiose unit cleaved off during the hydrolysis. The entire core domain viewed from the entrance of the tunnel (right). Illustration constructed in PyMol using PDB 1QK2 and ligand from PDB 4AVO.

The structure of the core domain of Cel7A (~46 kDa) was solved in 1994 (PDB 1CEL) (Divne *et al.*, 1994). In contrast to Cel6A the catalytic tunnel of Cel7A does mainly consist of two opposing antiparallel  $\beta$ -sheets connected by loops forming a  $\beta$ -sandwich (Divne *et al.*, 1994). Like in Cel6A the active site of Cel7A is also located inside the tunnel and here the tunnel is more enclosed by several loops. The tunnel of Cel7A is suggested to interact with 9-10 glycosidic binding subsites, named -7, -6, -5, -4, -3, -2, -1, +1, +2, +3 (Figure 7)(Divne *et al.*, 1998).

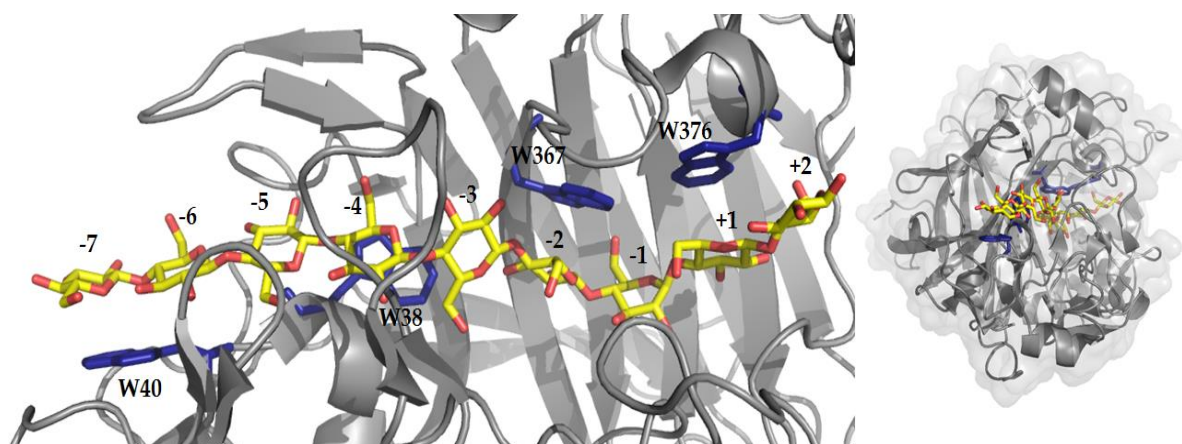


**Figure 7** The catalytic tunnel of Cel7A (left). The 10 glycosidic subsites on the glucan chain in yellow and the tryptophans contributing to the shape of the tunnel in blue. The +2 to +1 subsite is the cellobiose unit cleaved off. The entire core domain viewed from the entrance of the tunnel (right). Illustration constructed in PyMol using PDB 4C4C. The potential +3 subsite is not illustrated.

## Catalytic Mechanism

In general, the catalytic mechanism of Cel7A is a retaining mechanism whereas the mechanism of Cel6A is an inverting mechanism (Claeyssens *et al.*, 1990, Davies and Henrissat, 1995). This gives rise to an overall retention (retaining) or inversion (inverting) in the anomeric configuration. Like for other glycoside hydrolases the two hydrolysis reaction mechanisms involve proton donation to the leaving sugar by a carboxylic acid group (Golan, 2011). Besides the proton

donor a nucleophile or base which attacks the anomeric carbon either directly or through water molecules is also involved.

The catalytic mechanism of Cel7A is a so called two-step double displacement mechanism where the nucleophile Glu212 attacks the anomeric carbon forming the glycosyl-enzyme intermediate (Figure 8). Here Glu217 donates a proton to the leaving sugar. Secondly Glu217 deprotonates a water molecule which then attacks the anomeric carbon breaking the glycosyl-enzyme intermediate bond. The original stereochemistry is retained. Asp214 is also suggested to be involved in the catalysis with the role of coordinating the nucleophile in the right position and charge (Ståhlberg *et al.*, 1996, Knott *et al.*, 2014b).

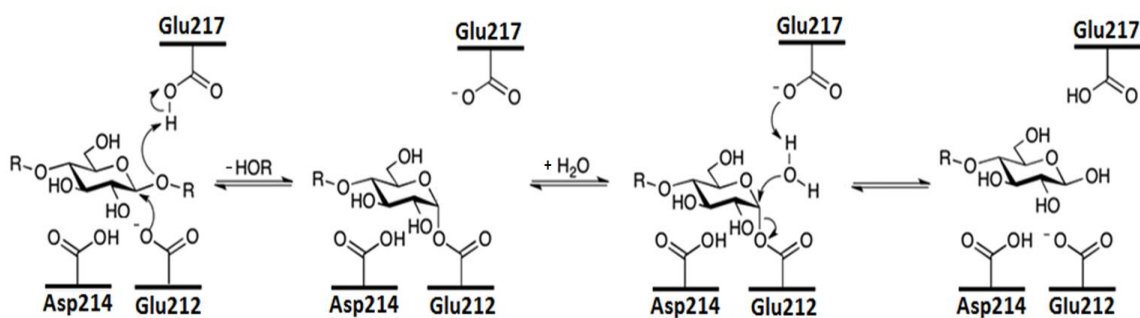
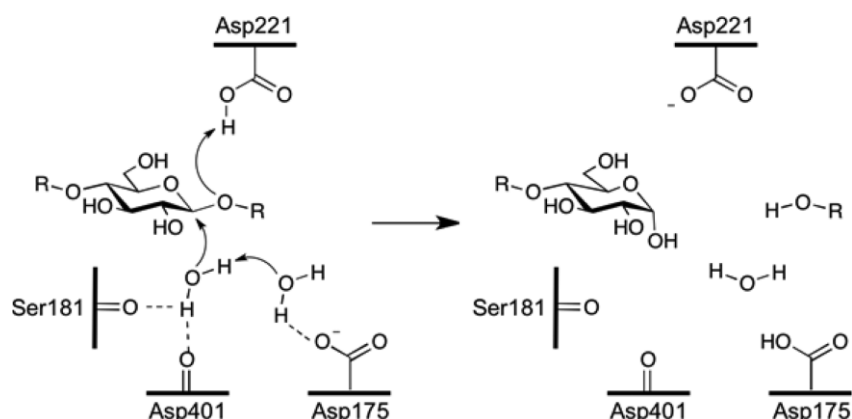


Figure 8 The catalytic mechanism of Cel7A from *H. jecorina*.

Modified from (Payne *et al.*, 2015)

There has been more discussion about the catalytic mechanism of Cel6A in particular identification of the nucleophile. The catalytic mechanism is a single displacement inverting mechanism and it works by a “water wire” or Grotthuss mechanism (Koivula *et al.*, 2002). Here Asp221 acts as the proton donor and Asp175 acts indirectly as the catalytic base, where the proton is transferred through two water molecules (Figure 9). Ser181 and the backbone carbonyl of Asp401 keep the water molecule in the right position (Payne *et al.*, 2015, Mayes *et al.*, 2016).



**Figure 9** The catalytic mechanism of Cel6A from *H. jecorina* (Payne *et al.*, 2015).

### Carbohydrate Binding Modules (CBM)

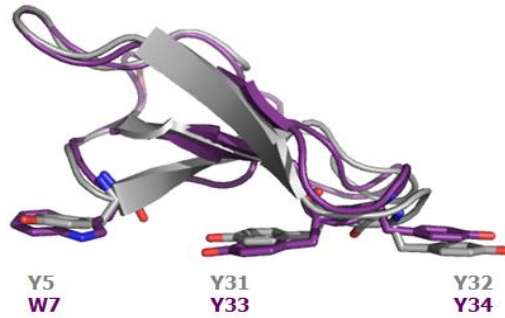
Cel7A has a C-terminal CBM whereas Cel6A has a N-terminal CBM (Van Tilbeurgh *et al.*, 1986, Tomme *et al.*, 1988). Both Cel7A and Cel6A have carbohydrate binding modules that belong to family 1 (CBM1) and henceforth they will be referred to as CBM<sub>Cel6A</sub> and CBM<sub>Cel7A</sub>. The family I CBM is the smallest CBM known and it is only found in fungal cellulases. CBM1 consist of 33-36 amino acids. The three-dimensional structure of the CBM<sub>Cel7A</sub> was solved by (Kraulis *et al.*, 1989) by NMR spectroscopy and they found that the CBM was organized into a wedge-shaped irregular  $\beta$ -sheet conformation. The planar face of the CBM dominated by three aromatic residues forms a hydrophobic surface that interacts with the cellulose surface (Kraulis *et al.*, 1989, Linder *et al.*, 1995a, Mattinen *et al.*, 1997b, Nimlos *et al.*, 2007). No three dimensional structure is solved for CBM<sub>Cel6A</sub> yet, but since the sequence is similar to CBM1 from Cel7A is it possible to predict a structural arrangement solely based on the amino acid sequence.

|           |                                                         |
|-----------|---------------------------------------------------------|
| CBM Cel7A | TQSH <b>Y</b> GQCGGIGYSGPTVCASGTTCQVLNP <b>YY</b> SQCL  |
| CBM Cel6A | QACSSV <b>W</b> GQCGGQNSGPTCCASGSTCVYSND <b>YY</b> SQCL |

**Figure 10** Alignment of the CBM protein sequence from *hj*Cel7A and *hj*Cel6A made with protein BLAST. The aromatic residues in the planar face are highlighted in bold.

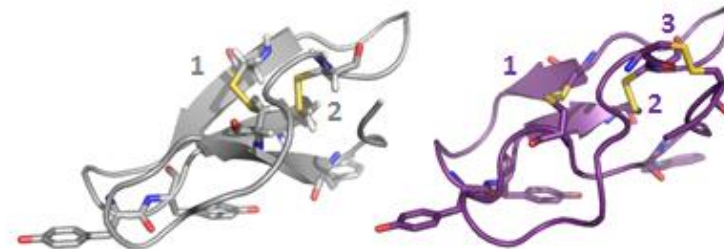


Figure 11 shows a predicted structure of CBM<sub>Cel6A</sub> in alignment with the structure of CBM<sub>Cel7A</sub> (PDB 1CBH). The aromatic residues in the planar face are highlighted.



**Figure 11** A predicted structure of CBM<sub>Cel6A</sub> (purple) modelled using Phyre2 in alignment with the structure of CBM<sub>Cel7A</sub> (grey) (PDB 1CBH). Aromatic residues (tryptophan W and tyrosines Y) in the planar face are highlighted.

From the structure of CBM<sub>Cel7A</sub> it is predicted that the CBM includes 2 disulfide bridges, whereas the CBM<sub>Cel6A</sub> might include 3 disulfide bridges. The N-terminus of CBM<sub>Cel6A</sub> is suggested to be covalently bond to the rest of the structure through a disulfide bond between Cys3 and Cys20 (Hoffrén *et al.*, 1995, Carrard and Linder, 1999).



**Figure 12** Left: Cel7A CBM with the two disulfide bonds 1) Cys8 - Cys25 and 2) Cys19 – Cys35. Right: Cel6A CBM with the three predicted disulfide bonds 1) Cys10-Cys27, 2) Cys21 – Cys37 and 3) Cys3 – Cys20. The third disulfide bond is constructed manually in PyMol and not part of the homology model made in Phyre2.

It is generally accepted that the function of the CBM is to increase affinity for the cellulose and to facilitate substrate binding (Tomme *et al.*, 1988, Ståhlberg



*et al.*, 1991, Boraston *et al.*, 2004, Várnai *et al.*, 2013, Payne *et al.*, 2015). Besides enhancing the affinity towards cellulose the CBM is also suggested to reduce the crystallinity of the substrate. The presence or pretreatment of isolated CBMs on crystalline cellulose have been shown to increase the enzymatic hydrolysis (Lemos *et al.*, 2003, Hall *et al.*, 2011). CBMs seem to be important for substrate affinity and the CBM has also been suggested to be essential for cellulose hydrolysis (Tomme *et al.*, 1988, Ståhlberg *et al.*, 1991). However, more recent studies suggest that the significance of the CBM depends on the experimental conditions (Le Costaouëc *et al.*, 2013, Várnai *et al.*, 2013, Pakarinen *et al.*, 2014). As we will see in Article III and VIII the CBM is catalytically advantageous at low substrate load but disadvantageous at high substrate loads. This finding seems to explain why some cellulases lack a CBM and it is speculated that the water content of the natural environment where the specific organisms live decides whether presence of CBMs is beneficial or not (Várnai *et al.*, 2013). In other words, the need for a CBM is dependent on the condition where the hydrolysis takes place.

Extensively research has been made to understand the role of CBMs. A collection of some essential articles that has investigated CBM1 are listed together with their major findings in Table 1. We will return to the role of the CBM of Cel6A and Cel7A later in Chapter 2.

**Table 1** Outline of a selection of essential articles that investigates CBM1 including some major conclusions

| Conclusion(s)                                                                                                                                                                                                 | Experimental conditions                             | Enzyme(s) from <i>H. jecorina</i>                      | Reference(s)                     |
|---------------------------------------------------------------------------------------------------------------------------------------------------------------------------------------------------------------|-----------------------------------------------------|--------------------------------------------------------|----------------------------------|
| Cleavage of the CBM strongly reduces the activity towards Avicel                                                                                                                                              | Endpoint, papain cleavage                           | Cel6A Cel7A                                            | (Tomme <i>et al.</i> , 1988)     |
| The structure of CBM1 is a wedge-shaped domain with a planar face and rough face                                                                                                                              | NMR                                                 | Cel7A                                                  | (Kraulis <i>et al.</i> , 1989)   |
| All CBMs show similar folding with a preserved binding surface, but different rigidity                                                                                                                        | MD simulations                                      | Cel7A, Cel6A EG1, EGII, EGV                            | (Hoffrén <i>et al.</i> , 1995)   |
| The difference in affinity between Cel7A and EG1 is mainly caused by Y/W in position 5                                                                                                                        | Binding isotherms                                   | Cel7A, EG1(Cel7B)                                      | (Linder <i>et al.</i> , 1995a)   |
| Changes in the planar face affect the binding affinity and cannot be explained solely by different fold of the peptide                                                                                        | Binding isotherms, NMR                              | Cel7A (synthetic CBM)                                  | (Linder <i>et al.</i> , 1995b)   |
| A double CBM exhibited much higher affinity on cellulose than either of the single CBMs indicating interplay between the two domains                                                                          | Binding isotherms                                   | Hybrid of CBM from Cel6A and linker and CBM from Cel7A | (Linder <i>et al.</i> , 1996)    |
| Tyrosine 5 has a structural and functional influence on the CBM, while Y31 and Y32 have only functional importance                                                                                            | NMR                                                 | CBM variants of Cel7A. Y5A, Y31A, Y32A                 | (Mattinen <i>et al.</i> , 1997a) |
| The three aromatic residues in the planar face interact with every second glucose moiety on celohexaose                                                                                                       | NMR                                                 | CBM from Cel7A, EG1 and Y→A variants                   | (Mattinen <i>et al.</i> , 1997b) |
| The binding of CBM <sub>Cel7A</sub> is reversible while the binding of CBM <sub>Cel6A</sub> is to some extent irreversible. Mutation W7Y and C3T+C20V made the binding reversible                             | Binding isotherms, <sup>3</sup> H-labelled CBM      | Cel6A, Cel7A                                           | (Carrard and Linder, 1999)       |
| Correlation of activity and affinity constants of Y→W combinations and some Y→F/G mutations in the planar face. WWY showed highest activity and affinity                                                      | Hydrophobic chromatography, endpoint, modelling     | Cel7A ( <i>Hypocrea grisea</i> )                       | (Takashima <i>et al.</i> , 2007) |
| The water content determine the benefits of CBMs. Reducing the amount of water favor cellulases without CBM                                                                                                   | Endpoint, free enzyme determination, sequence data. | Cel7A                                                  | (Várnai <i>et al.</i> , 2013)    |
| Variants with reduced affinity towards lignin, but unchanged or increased affinity against cellulose have improved activity (P30D, V27E together with glycosylated linker variant)                            | Endpoint activity and binding isotherms             | Cel7A                                                  | (Strobel <i>et al.</i> , 2015)   |
| Binding of CBM on cellulose is strongly dependent on the substrate (wood or bacterial cellulose) especially CBM-Cel7A seems to have different modes of binding. CBM Cel6A and Cel7A compete on binding sites. | Binding isotherms, <sup>3</sup> H-labelled CBM      | CBM-Cel6A, CBM-Cel7A, hybrid CBM complexes             | (Arola and Linder, 2016)         |

## Linkers

Extensively research has been done to understand the catalytic mechanism in the core domain of Cel7A and Cel6A and also the role of the CBM has been thoroughly investigated in the last decades. In contrast, only a limited amount of studies have so far focused on the role of the linker. The sequences of the Cel7A and Cel6A linker differ a lot (Figure 13) and none of the linkers are conserved throughout their families. Both linkers are, however, rich in proline, glycine, serine and threonine residues with a high degree of O-glycosylation on serines and threonines (Figure 13) (Srisodsuk *et al.*, 1993, Payne *et al.*, 2013b).



**Figure 13** The sequences of the linker region of Cel7A(top) and Cel6A(bottom) and the expected glycosylation pattern. Diamonds represents O-linked mannose residues. For Cel7A the threonines are heterogeneously mannosylated and here the predominant glycoform on each site is shown. In Cel6A the heterogeneity of the glycols is not shown. Modified from (Harrison *et al.*, 1998, Beckham *et al.*, 2010a, Sammond *et al.*, 2012)

The glycosylated linkers were originally reported simply to serve as a flexible connector between the catalytic domain and the CBM, but later different roles of the linker have been suggested. For instance, it has been shown that the O-glycosylation of the threonine and serine residues of the linker protect against proteolysis (Langsford *et al.*, 1987, Shen *et al.*, 1991). More recently Payne and colleagues (2013) proposed that the glycosylated linker binds dynamically and non-specifically to the cellulose surface and thereby play a more direct role in enzyme/substrate interactions. Table 2 summarizes a selection of articles that have focused on fungal cellulase linkers including their major conclusions.

**Table 2** Outline of essential linker articles including some major conclusions.

| Conclusion(s)                                                                                                                                                                                                                             | Experimental conditions                                           | Organism and enzyme(s)                                                                      | Reference                           |
|-------------------------------------------------------------------------------------------------------------------------------------------------------------------------------------------------------------------------------------------|-------------------------------------------------------------------|---------------------------------------------------------------------------------------------|-------------------------------------|
| O-glycosylation on linkers protects against proteolytic attack                                                                                                                                                                            | Western blotting and zymography                                   | <i>Cellulomonas fimi</i> , Exg, EngA                                                        | (Langsford <i>et al.</i> , 1987)    |
| Sufficient spatial separation between core and CBM is required for an efficient function of CBHI. Short linker deletion of hinge region did not affect the enzymatic activity while a long linker deletion dramatically reduced the rate. | Adsorption isotherms, activity                                    | <i>Hypocrea jecorina</i> Cel7A+ variants with shorter linkers                               | (Srisodsuk <i>et al.</i> , 1993)    |
| Linkers might perform caterpillar-like motions when cellulases move on the cellulose surface                                                                                                                                              | SAXS                                                              | <i>Humicola insolens</i> Cel45                                                              | (Receveur <i>et al.</i> , 2002)     |
| Linkers are flexible and adopt both extended and compact structures (In agreement with cater-pillar model)                                                                                                                                | SAXS                                                              | <i>Humicola insolens</i> Chimeric cellulase Cel6B-linker-linker-Cel6A                       | (von Ossowski <i>et al.</i> , 2005) |
| The linker is essential for adapting to cold environment for the psychrophilic Cel5G                                                                                                                                                      | Activity, fluorescence quenching, DSC, SAXS                       | <i>Pseudoalteromonas haloplanktis</i> , Cel5G + variants, <i>Erwinia chrysanthemi</i> Cel5A | (Sonan <i>et al.</i> , 2007)        |
| Optimal hydrolysis rate occurs at the transition from a compressed to an extended linker conformation.                                                                                                                                    | Modelling                                                         |                                                                                             | (Ting <i>et al.</i> , 2009)         |
| O-glycosylation does not influence flexibility or stiffness of the linker                                                                                                                                                                 | MD simulations                                                    | <i>Hypocrea jecorina</i> Cel7A                                                              | (Beckham <i>et al.</i> , 2010a)     |
| Fungal cellulases are rich in proline, glycine, serine and threonine residues, but no sequence homology is present.                                                                                                                       | Sequence alignment                                                | GH6 and GH7s                                                                                | (Sammond <i>et al.</i> , 2012)      |
| Glycosylated linkers bind dynamically to the cellulose surface                                                                                                                                                                            | MD simulations, binding isotherms w. linker-CBM and synthetic CBM | <i>Hypocrea jecorina</i> , Cel6A and Cel7A                                                  | (Payne <i>et al.</i> , 2013b)       |
| Changing the glycosylation pattern and charge of the linker can reduce lignin affinity and increase both affinity and activity against cellulose                                                                                          | Endpoint activity and binding isotherms                           | <i>Hypocrea jecorina</i> Cel7A                                                              | (Strobel <i>et al.</i> , 2015)      |
| Linker length, flexibility and rigidity influence the kinetics of a non-processive Cel5A. Stability and structure of CBM and core were not affected by the changes in the linker                                                          | Activity(DNS), SAXS, CD                                           | <i>Bacillus subtilis</i> , Cel5A                                                            | (Ruiz <i>et al.</i> , 2016)         |



## Cellobiohydrolase Kinetics

---

The kinetics of cellobiohydrolases is characterized by a dramatic slow-down in reaction rate over time. This kinetic behavior complicates the understanding of the enzymes and compared to many other enzymes the catalytic cycle of CBHs is slow (Nelson and Cox, 2008). However, in comparison with the uncatalyzed spontaneous hydrolysis of the  $\beta(1,4)$  glycosidic bonds in cellulose, cellulases are if anything remarkable. From a predicted half-life of  $\sim 5$  million years for the glycosidic bond to a hydrolysis rate of several cleavages per second they are among the most proficient catalysts (Zechel and Withers, 2000). The following chapter will focus on the kinetics of these enzymes. First we will summarize some of the enzyme and substrate related factors that can help to explain the characteristic rate decline in cellulose hydrolysis. Hereafter we will briefly introduce two different models that can be used to investigate the kinetics of cellulases. The models are based on previous work within the research group (Praestgaard *et al.*, 2011, Cruys-Bagger *et al.*, 2013a, Kari *et al.*, 2017). Finally a selection with kinetic results where these models are used will be presented.

For clarity and before focusing on cellobiohydrolase kinetics we should briefly examine the different possible states of cellobiohydrolases during hydrolysis. First the enzyme can be free in solution (not bound or associated to the substrate). Second the enzyme can be in the ES (enzyme-substrate) complex, where the CBM is associated with the substrate and a cellulose chain threaded into the tunnel. Then we have two modes in between; where the core is threaded without the CBM being associated and the CBM being associated without the core being threaded. The four different modes are illustrated in Figure 14.

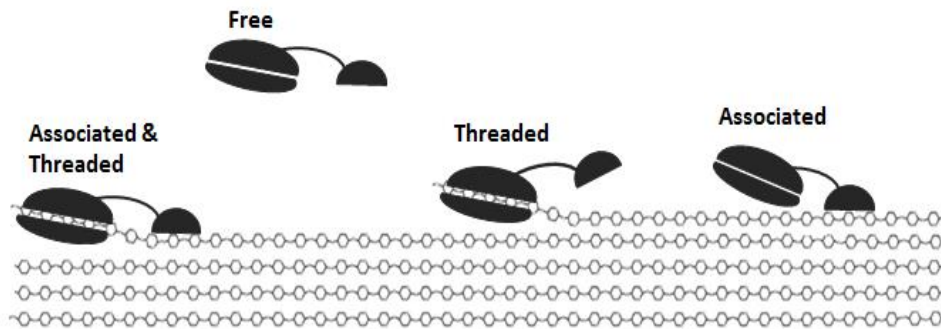


Figure 14 Four different states of a cellobiohydrolase: 1: Free, 2: Associated and Threaded, 3: Threaded and 4: Associated.

From the different modes of cellobiohydrolases it is obvious that only two situations are productive modes, namely where the enzyme is associated and threaded or where the enzyme is threaded. However as we will discuss later, cellobiohydrolases in these two states will not necessarily be productive.

## Part I - Non-linear Kinetics

Many different explanations have been suggested to explain the non-linear kinetics and one way to classify these interpretations is that they can either be assigned the enzyme or the substrate (Mansfield *et al.*, 1999, Yang *et al.*, 2006). Understanding the characteristic rate decline is complicated also because the slow-down occurs at different time-scales. The rate decline is most likely a combination of several factors where some of them will be presented here.

### Enzyme related factors

Examples of enzyme related factors that can slow down the reaction rate of cellobiohydrolases over time can be: instability of the enzymes, product inhibition, irreversible adsorption to cellulose, enzyme jamming or a slow dissociation rate.

### ***Binding Reversibility***

An enzyme-substrate complex can be formed without being productive for instance due to obstacles that prevent the processive movements of the enzymes. In this non-productive mode a reversible binding is critical in order to dissociate and then be able to reinitiate the catalytic cycle elsewhere. There have been controversies on whether the cellobiohydrolases Cel7A and Cel6A binds reversible to cellulose. Studies reporting full reversibility, irreversibility or partially reversibility all exist (Kyriacou *et al.*, 1989, Nidetzky *et al.*, 1994a, Palonen *et al.*, 1999, Zhang and Lynd, 2004). In Article VI the reversibility of Cel6A and Cel7A was investigated. To summarize we found fully dynamic equilibrium of both Cel6A and Cel7A in experiments where we released the enzymes by simple dilution. In contrast, experiments with centrifugation and resuspension of the pellet showed extensively irreversibility of the enzymes. Based on these results we speculate that centrifugation of cellulose could change the substrate somehow that these changes hinder or delay release of the CBHs. We imagine that some of the cellulases might be trapped in the cellulose crystal during centrifugation. The difference in the results between the two experimental procedures might explain some of the disagreement about reversibility of cellulases in the literature.

### ***Dissociation***

The binding of both Cel6A and Cel7A is reversible, but that does not mean that the dissociation of the enzymes is fast. In contrast, many previous studies suggest that the dissociation of the enzymes from the cellulose surface is rate-limiting for the overall hydrolytic reaction (Jalak and Våljamäe, 2010, Kurasin and Våljamäe, 2011, Praestgaard *et al.*, 2011, Cruys-Bagger *et al.*, 2013b). Unlike factors such as production inhibition and enzyme stability the slow dissociation rate can explain why the rate decline already takes place in the very early phase of hydrolysis. Results from Article I, II, III, IV, VIII strongly support this hypothesis, since



variants with lower affinity possess higher maximal catalytic activity, which is in agreement with other studies (Kari *et al.*, 2014, Sørensen *et al.*, 2017). The potentially increased dissociation rate of the variants has been suggested to explain the improved activity. This might appear counter intuitive since substrate affinity is essential in order to adsorb to the cellulose surface prior to hydrolysis. The underlying reason for this inverse correlation relies in the nature of the heterogeneous substrate and the processive behavior of the enzymes. A cellobiohydrolase moving along the cellulose chain during the processive cycle might encounter an obstacle for instance disordered cellulose chains. The enzyme is now stuck in an un-productive mode until dissociation (Eriksson *et al.*, 2002). After dissociation the free enzyme can reinitiate hydrolysis by attacking a new cellulose chain end. We will return to this reverse relation between activity and affinity in Part III. Another side effect of un-productive bound CBHs might be enzyme jams, where a stuck CBH block for the processive movement of other CBHs (Igarashi *et al.*, 2011, Bubner *et al.*, 2013).

### ***Product Inhibition***

Product inhibition of Cel6A and Cel7A is not covered in this work, but we would still like to address a few comments. Both Cel6A and Cel7A are inhibited by both cellobiose and glucose (Murphy *et al.*, 2013, Teugjas and Väljamäe, 2013). Cel7A is much more inhibited by cellobiose than Cel6A and conversely Cel6A is more inhibited by glucose than Cel7A. The cellobiose inhibition of cellulose hydrolysis of Cel7A has recently been suggested to be non-competitive inhibition (Kuusk *et al.*, 2015, Olsen *et al.*, 2015). Cellobiose inhibition can easily be prevented by addition of  $\beta$ -glucosidase. On the other hand the weaker inhibition of the end product glucose is more challenging to prevent, but can be reduced by simultaneous fermentation.

### *Enzyme Stability*

Inactivation of the cellulolytic enzymes makes up another potential reason for the observed slowdown. In Article V we investigated the stability of Cel6A and Cel7A using differential scanning calorimetry (DSC) and we found the method very effective for in situ stability. The transition temperature,  $T_T$ , for Cel7A is increased in the presence of substrate, while the  $T_T$  for Cel6A is unaffected in the presence of substrate, see Table 1. We speculate that this difference is caused by a stronger binding of Cel7A compared to Cel6A.

**Table 1** Transition Temperatures ( $T_T$ ) for Cel6A and Cel7A determined with and without substrate (data from Article V)

|              | Hydrolysis samples<br>(60 g/L Avicel) | Reference samples<br>(buffer) |
|--------------|---------------------------------------|-------------------------------|
| <b>Cel7A</b> | 70.5°C $\pm$ 0.3                      | 66.1°C $\pm$ 0.03             |
| <b>Cel6A</b> | 66.9°C $\pm$ 1.3                      | 66.5°C $\pm$ 0.2              |

In the same study we estimated long-term stability and we found that the stability depends on the thermal stress conditions and the presence of substrate (Figure 15). Interestingly, and contrary to the above observations, the loss of native enzymes was much higher in the presence of the substrate Avicel for both Cel6A and Cel7A. The experiments further showed a consistently higher gradual loss of native enzymes for Cel6A compared to Cel7A. In the most severe case Cel6A lost as much as 80% of the native enzymes after 53 hours incubation with Avicel at 49°C. Also Cel7A showed substantial loss of native enzymes under the same conditions as shown in Figure 15. Since the loss of enzymes is much higher in the presence of substrate the interactions with Avicel do somehow contribute to enzyme instability. These results can be explained by surface aggregation in the solid liquid interface. This observation is important since transition temperatures might be deceptive of enzyme stability. We expect that for industrial or commercial use the

long-term stability in the presence of biomass is critical and should be controlled for the cellulases that constitute commercial enzyme cocktails.

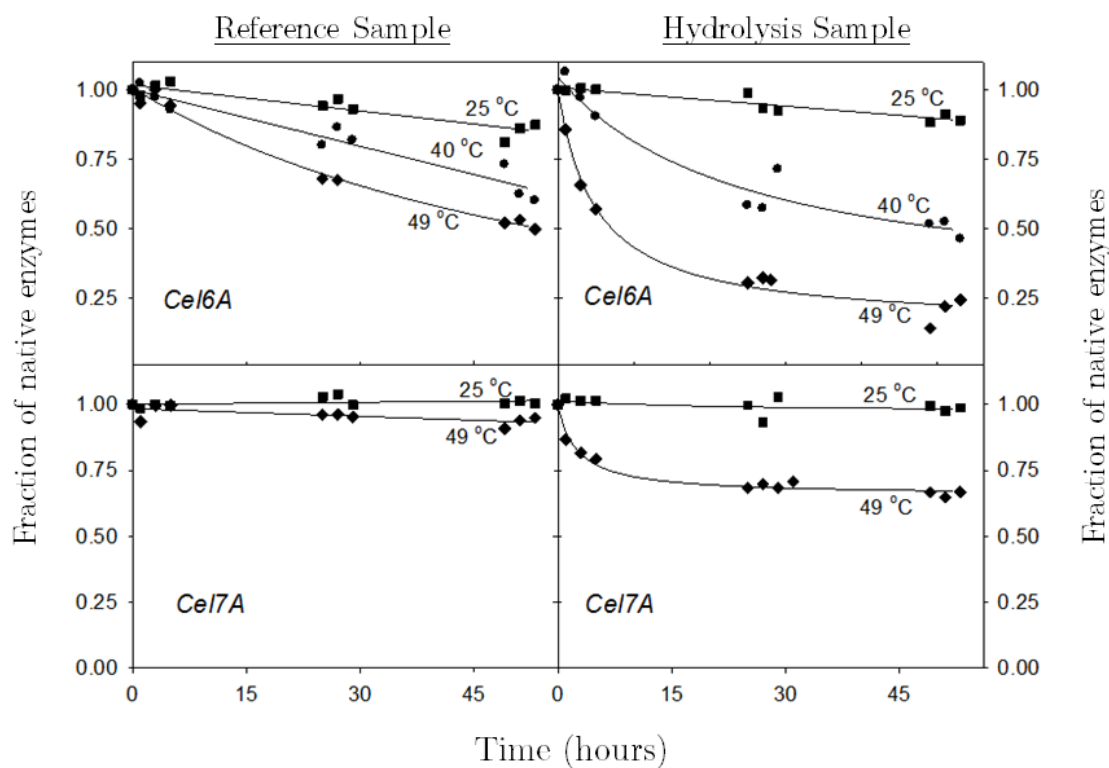


**Figure 15** The relative decrease in the fraction of native enzymes after thermal stress at different time scales, when incubated with buffer (reference sample) and with 60 g/L Avicel (hydrolysis sample) (Adapted from Article V).

Even though instability of Cel6A and Cel7A should be notified the dramatic slow-down in activity within the time scale of seconds or minutes at very low enzyme concentrations must additionally be caused by other factors. Besides enzyme related factors there are also other factors that can explain the pronounced slow-down in activity, which are more directly related to the substrate.

## Substrate Related Factors

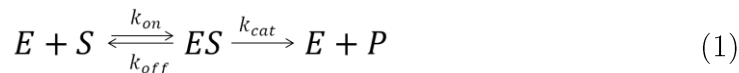
The deceptive simplicity of the repeating cellobiose unit in cellulose does not reflect the complexity of biomass. As mentioned earlier biomass is extremely complex and consists of many components including cellulose, but even within cellulose the heterogeneity is marked (Mansfield *et al.*, 1999). Common for substrate related factors that can influence the dramatic slow-down in activity is that they are somehow connected to the heterogeneity of the substrate. Substrate related factors that can affect the enzymatic hydrolysis are particle size, surface area, pretreatment including the effect of drying, crystallinity, substrate depletion, porosity and degree of polymerization (DP) (Mansfield *et al.*, 1999, Jeoh *et al.*, 2007). These factors are all connected to substrate accessibility. When focusing on cellulase action, we imagine that more easily accessible parts of the particle will be degraded first and the less accessible parts later. Potentially a rapid hydrolysis of more amorphous regions followed by a slower degradation of highly crystalline regions. The impact of substrate accessibility and substrate specificity on the kinetic behavior of Cel6A and Cel7A will be discussed later.

## Part II - Modelling Cellulase Kinetics

Many different models have been suggested to explain cellulase kinetics and many of them use different parameters and assumptions (Zhang and Lynd, 2004, Bansal *et al.*, 2009). It is clear that the different models depend on the experimental conditions, which is also the case for the models presented here. The two models used in this work will only be described briefly and for a more detailed description of the models is referred to their main articles (Cruys-Bagger *et al.*, 2013a, Kari *et al.*, 2017). Before focusing on the models we will briefly look at traditional enzyme kinetics.

## Traditional Enzyme Kinetics

The reaction scheme of a traditional reaction where an enzyme (E) converts a substrate (S) into a product (P) can be written as:



where ES is the enzyme substrate complex. The rate constant  $k_{cat}$  is often termed the turnover number, which is the maximum number of substrate molecules converted to product per second per enzyme molecule,  $k_{on}$  is the association constant in which the enzyme binds to the substrate to form the ES complex and  $k_{off}$  the dissociation constant in which the enzyme unbinds the substrate. If we consider quasi steady state assumption (QSSA) ( $\frac{d[ES]}{dt} \approx 0$ ) and that  $S_0 \gg E_0$  and thereby  $S_0 \approx [S]$  together with enzyme conservation  $E_0 = [E] + [ES]$ , where  $E_0$  and  $S_0$  are the initial enzyme and substrate concentration, respectively, we can use the widely used Michaelis Menten (MM) equation

$$v = \frac{V_{max}S_0}{K_M + S_0} \quad (2)$$

where  $v$  is the initial velocity of the reaction,  $V_{max}$  the maximal reaction velocity or reaction rate,  $K_M$  the Michaelis Menten constant, which is the substrate concentration at which the reaction rate is half  $V_{max}$ . The parameters  $V_{max}$  and  $K_M$  in the MM equation are defined as  $V_{max} = k_{cat}E_0$  and  $K_M = \frac{k_{cat} + k_{off}}{k_{on}}$  (Nelson and Cox, 2008). The MM relation between initial reaction rates and substrate concentration and the above kinetic parameters have contributed to a fundamental understanding of enzymatic systems where both enzyme and substrate are in solution.

Another and less widespread Michaelis Menten equation (3) is the inverse relation where  $E_0 \gg S_0$  and where a low substrate load is saturated with enzymes.

$$v = \frac{V_{max}E_0}{K_M + E_0} \quad (3)$$

here  $V_{max} = k_{cat}S_0$  and for homogenous enzymatic system both  $k_{cat}$  and  $K_M$  obtained from eq. (3) is identical to the parameters obtained from the conventional relation in eq. (2) (Bajzer and Strehler, 2012).

The degradation of cellulose by cellulases varies compared to traditional enzymatic reactions because the substrate is insoluble. This means that cellulases require adsorption to the substrate prior to the enzymatic reaction and that the hydrolysis of cellulose takes place in a solid-liquid interface. This heterogeneity complicates the understanding of cellulase kinetics especially because it is the substrate that is insoluble. Different kinetic models have been proposed to be valid for cellulase kinetics (Bansal *et al.*, 2009), but no generally accepted rate law is defined for surface active enzymes despite that many enzymatic reactions other than cellulases acting on cellulose take place in the solid-liquid interface.

## Modelling Processive Enzymes

As described earlier cellobiohydrolases are processive enzymes, which mean that they remain associated to the substrate in between each catalytic cycle. A simplified reaction scheme of processive cellulases can be written as in Figure 16 (Praestgaard *et al.*, 2011, Cruys-Bagger *et al.*, 2012a). Here the enzyme  $E$  adsorbs to the cellulose strand  $S_x$  forming the complex  $ES_x$ , where  $x$  describes the degree of polymerization (DP) of cellobiose units. This complex formation or association of enzyme and substrate is governed by the rate constant  ${}_p k_{on}$ . After the complex is formed the reaction can then proceed in two directions; either the enzyme makes a

catalytic cycle in which cellobiose ( $C$ ) is cleaved off governed by the catalytic rate constant  ${}_p k_{cat}$  or the enzyme dissociates governed by the rate constant  ${}_p k_{off}$ . The total number of steps  $n$ , reflects the processivity of the cellobiohydrolase.

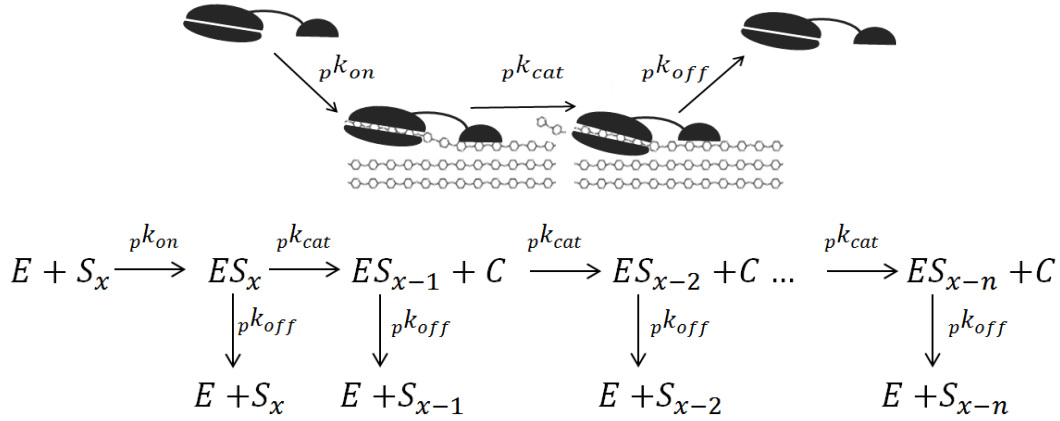


**Figure 16** The reaction scheme of processive cellulases as explained in the main text (bottom) together with a more simplified visual illustration of the meaning behind the rate constants  ${}_p k_{on}$ ,  ${}_p k_{cat}$  and  ${}_p k_{off}$  (top).

In the model developed by Praestgaard et al (2011) values of  ${}_p k_{cat}$ ,  ${}_p k_{on}$  and  ${}_p k_{off}$  can be estimated using pre-steady state kinetic measurements. Here the characteristic burst phase (Kipper *et al.*, 2005, Jalak and Våljamäe, 2010, Praestgaard *et al.*, 2011) where the reaction rate accelerates within a very short timeframe has to be captured. This requires advanced and very sensitive experimental set-up followed by a complicated mathematical analysis. Compared to simple endpoint measurements this procedure is inconvenient even though the development of sensitive amperometric biosensors with high time resolution (Cruys-Bagger *et al.*, 2012b) has shown to be a strong experimental tool. After the so called burst phase a steady rate appears. This steady-state rate can easily be approximated with use of simple endpoint measurements. Based on the same reaction scheme an alternative and more applicable steady-state model was developed (Cruys-Bagger *et al.*, 2013a). The steady-state model is created from traditional MM kinetics. As

indicated in the name the model is based on the QSSA, which means that all enzyme-substrate intermediate or complexes are in steady-state ( $\frac{d[ES_x]}{dt} = 0$ ) during the hydrolysis. Based on the same assumption an inverse steady-state MM approach was recently developed and found to be very valuable in the kinetic characterization of cellobiohydrolases (Kari *et al.*, 2017). Both steady-state models will now be introduced.

### The Steady-State Model & the Inverse Michaelis Menten Approach

Since cellulases show so called “double saturation” behavior where the hydrolysis rate levels off with either substrate or enzyme concentration (Sattler *et al.*, 1989, Bezerra and Dias, 2004) we have chosen to use two different kinetic models. The conventional steady-state model is based on substrate saturation with substrate excess  $S_0 \gg E_0$  like in the original MM equation while the inverse steady-state MM approach is based on enzyme saturation with enzyme excess  $E_0 \gg S_0$ . The simple concept behind the two models is illustrated in Figure 17.

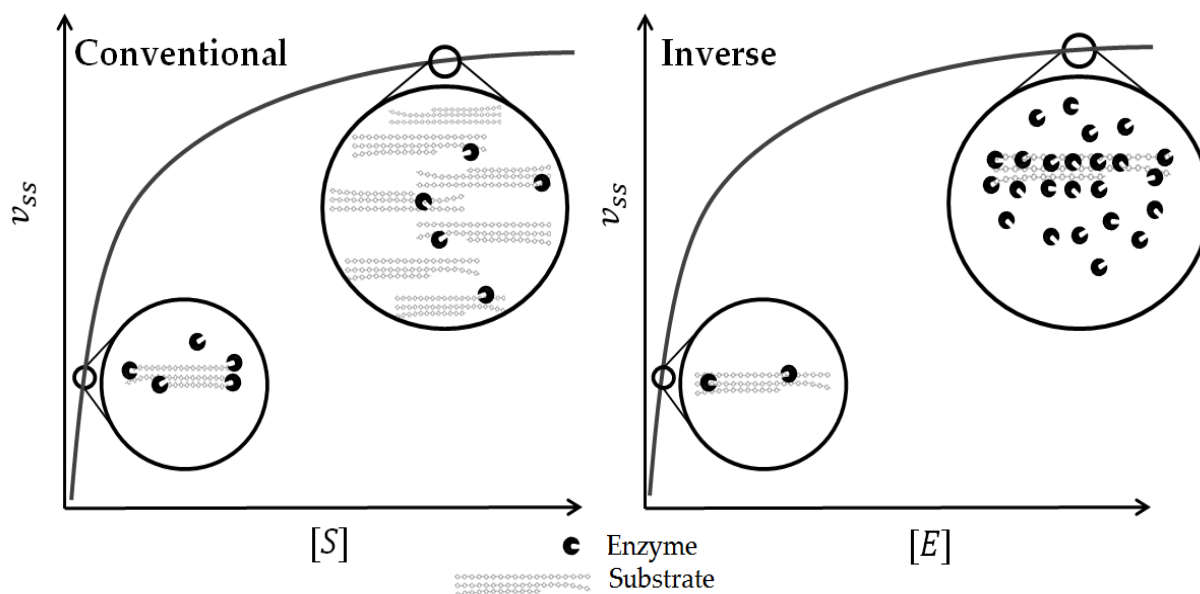


Figure 17 The simple concept behind the steady-state model (left) and the Inverse Michaelis Menten approach (right).



Here steady-state rates ( $v_{ss}$ ) are estimated after the characteristic burst phase, but before any noticeable changes in substrate concentration. The fundament of both steady-state models relies on traditional MM or inverse MM kinetics except that the maximal reaction velocity and the Michaelis Menten constant are defined differently. The essential equations that define the two models are listed in Table 3.

**Table 3** Outline of essential equations and definition of kinetic parameters in the processive steady-state model and the inverse MM approach

| Steady-State Model<br>(Conventional)                                      | Inverse MM Approach                                                              |
|---------------------------------------------------------------------------|----------------------------------------------------------------------------------|
| ${}^{conv}v_{ss} = \frac{{}^{conv}V_{max} \cdot S_0}{{}^{conv}K_M + S_0}$ | ${}^{inv}v_{ss} = \frac{{}^{inv}V_{max} \cdot E_0}{{}^{inv}K_M + E_0}$           |
| ${}^{conv}V_{max} = E_0 \cdot {}_p k_{cat}$                               | ${}^{inv}V_{max} = S_0 \cdot \overline{{}_p k_{cat}} \cdot {}^{kin}\Gamma_{max}$ |
| ${}^{conv}K_M \equiv \frac{{}_p k_{off}}{{}_p k_{on}}$                    | ${}^{inv}K_M = \frac{\overline{{}_p k_{cat}} + {}_p k_{off}}{{}_p k_{on}}$       |
| <p>Assumption:<br/> <math>S_0 + {}^{conv}K_M \gg E_0</math></p>           | <p>Assumption:<br/> <math>E_0^{inv} + K_M \gg S_0</math></p>                     |

From the equations in Table 3 two new parameters appear in the definition of  ${}^{kin}V_{max}$ . First  $\overline{{}_p k_{cat}}$  that differs from  ${}_p k_{cat}$  in which it is the average apparent catalytic rate constant. For clarity we define an attack site as a site where the CBH can associate to and generate products. In a condition with enzyme excess all

attack sites will be covered with enzymes both easily (good) and hardly (poor) accessible attack sites.  $\overline{p k_{cat}}$  is therefore an average catalytic rate constant of both good and bad sites. In contrast we expect that mainly easily accessible or good attack sites will be covered at substrate saturation in the conventional condition. Especially if we consider much higher specificity for good sites compared to poor sites. We therefore expect that the apparent processive catalytic constant  $p k_{cat}$  is higher than  $\overline{p k_{cat}}$ . The second parameter  $^{kin}\Gamma_{max}$  is somehow related to the common binding parameter  $\Gamma_{max}$ , which is the binding capacity or the amount of binding sites per substrate mass. As we will discuss later is a substrate binding site not necessarily also an attack site and the related parameter  $^{kin}\Gamma_{max}$  terms in this way the amount of attack sites per substrate mass.

### ***Assumptions for validity of the two models***

Cellulases have a characteristic burst phase which means that the reaction rate at pre-steady state accelerates fast followed by a steady-state rate. In other words the rate of hydrolysis reaches a plateau (steady-state) after this so called burst in activity. This steady-state rate ( $v_{ss}$ ) is a pseudo-steady state approximation, since the reaction rate continues to slow-down over time. Taken this into account the experimental reaction conditions were prudently chosen. We aimed to estimate the initial rate as the slope from  $t=0$  and the chosen reaction time. Here the optimal reaction time is where we have minimal impact from the activity burst and still are able to neglect impact from enzyme inactivation and product inhibition. Here a reaction time of 1 hour was shown to be competent. Another assumption is that the kinetics of the cellulase-cellulose system follows the fundamental laws of mass action, which means that the rate of reaction is proportional to the product of the concentration of the reactants ( $[E] \cdot [S_x]$ ). The substrate cellulose is insoluble which complicates a determination of the molar substrate concentration. The majority of the  $\beta(1,4)$  glycosidic bonds in cellulose is not accessible for CBHs. As CBHs predominantly attack chain ends a rough estimate of the number of attack sites

could potentially be estimated with information about DP, but since far from all chain ends will be accessible some chain ends will not appear as attack sites. Instead of using uncertain quantifications of the molar substrate concentration we assume that substrate dosage is proportional to attack sites as argued earlier (Cruys-Bagger *et al.*, 2013a). This means that the kinetic values, which are based on the substrate mass is strongly dependent on the specific substrate. Next we assume that the number of attack sites is maintained during hydrolysis at least at low conversion. We imagine that new attack-sites will appear with the same rate as the original ones depletes. When one cellulose layer is peeled off new attack sites will be accessible in the new layer. The assumption of substrate conservation correlates with the appearance of a binding-equilibrium (Medve *et al.*, 1998). Medve *et al* (1998) found that the fraction of bound enzymes remained constant within 1 hour of hydrolysis indicating that the number of binding sites (which might be proportional to attack sites) is maintained. The enzyme concentration is easier to handle and we also assume enzyme conservation  $E_0 = [E] + [ES]$ . This means that we neglect any effects of product inhibition and enzyme inactivation. In the following section we have therefore used short time hydrolysis (1 hour) and low temperature (25°C) to prevent enzyme denaturation or surface aggregation. The impact of product inhibition is also neglected, since only minor release of product accumulate within this time frame. As described earlier we showed in Article V that binding of both Cel6A and Cel7A is reversible at least within 1 hour of hydrolysis, which suggests that a dynamic equilibrium between cellulases and cellulose exist.

During the last decades several kinetics models have been developed and used to elucidate cellulase kinetics (Zhang and Lynd, 2004, Bansal *et al.*, 2009) and as mentioned earlier different kinetic models are strongly dependent on the experimental conditions. This complicates any comparative evaluation of kinetic parameters between studies since the experimental conditions most likely deviate. Based on this, the focus in the next chapter will not be to compare the

forthcoming estimated kinetic values with earlier kinetic studies. Instead the primary focus will be on what information we can subtract from a direct kinetic comparison of the two CBHs Cel6A and Cel7A.

### **Part III - Kinetics of Cel6A and Cel7A**

Cel6A and Cel7A are the two most abundant cellulases secreted from *H. jecorina* and the two only cellobiohydrolases. Besides attacking different chain ends, having diverse mechanism and structure one could argue that these enzymes are evolved to carry out similar efforts just working in different ends. Another interpretation of the dominance of the two CBHs in the secretome of the fungus is that differences in their specificity and activity help the organism to degrade the heterogeneous biomass. The appearance of a significant degree of synergy between Cel6A and Cel7A supports the latter. This exo-exo synergy is discussed in Chapter 4.

A direct biochemical comparison of Cel6A and Cel7A will now be presented to elucidate their roles and interrelationships in the degradation of cellulose. First we applied the two steady-state models visualized in Figure 17, where we either saturated the enzyme with substrate or oppositely saturated the substrate with enzyme. The experimental data together with the fit of the equations from the two models are shown in Figure 18.

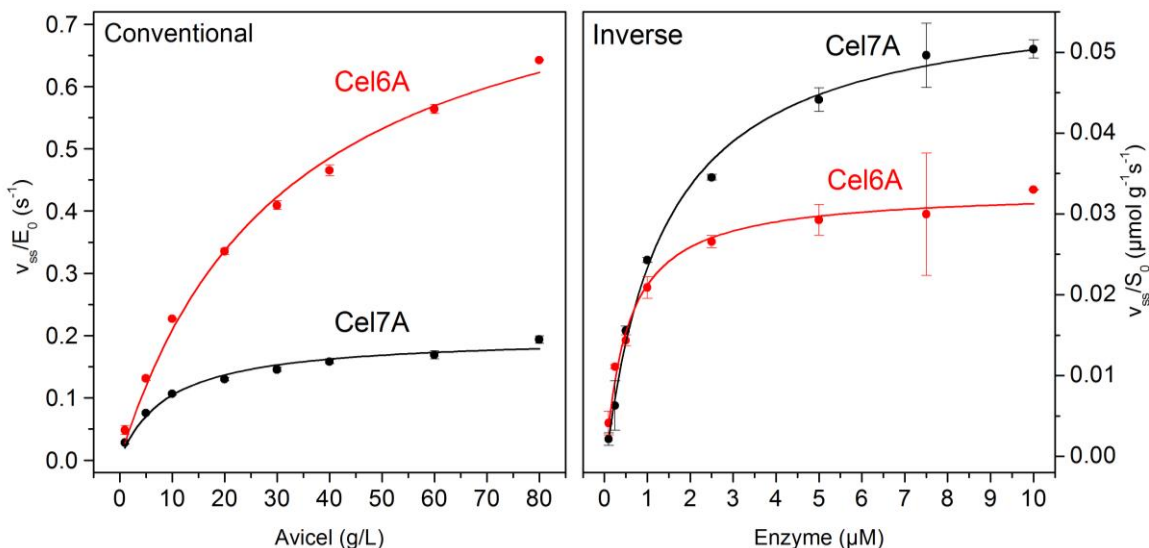


**Figure 18** Experimental data from Cel7A and Cel6A using the conventional steady-state approach where 200 nM enzyme were saturated with Avicel (left) and the inverse steady-state approach where 2 g/L Avicel was saturated with enzyme. Steady-state rates estimated after 1 hour hydrolysis. Since  $\beta$ -glucosidase was added rates are given as production of glucose. Figure adapted from Article I

If we first focus on the left (conventional) part of Figure 18, where we have measured the steady-state rate at different substrate loads of both enzymes, it is obvious that Cel6A is a much faster enzyme than Cel7A. The estimated kinetic parameter is listed in Table 5 in the next section and  $^{conv}V_{pmax}$  for Cel6A is 0.87 s<sup>-1</sup> compared to only 0.20 s<sup>-1</sup> for Cel7A. If we consider that the off-rate is a rate limiting factor one could speculate if Cel6A has a higher off-rate than Cel7A. Returning to the structure of their two catalytic domains the longer tunnel with more loops enclosing the tunnel in Cel7A might result in a reduced ability to dissociate. The higher value of  $^{conv}K_M$  for Cel6A (31.6 g/L vs 9.1 g/L for Cel7A) support this prospect of lower substrate affinity for Cel6A compared to Cel7A and does also indicate a higher  ${}_p k_{off}$ . A higher specific activity of Cel6A compared to Cel7A has previously been reported (Ståhlberg, 1993, Medve *et al.*,

1994, Nidetzky *et al.*, 1994a) and Medve *et al* (1994) also found a lower binding capacity of Cel6A compared to Cel7A.

Looking at the right part of Figure 18 the opposite relation appears. At enzyme loads higher than 1  $\mu\text{M}$  a higher steady-state rate is determined for Cel7A compared to Cel6A using low substrate load. According to Table 3 and Figure 17 the higher maximal rate of Cel7A under these conditions can be interpreted in two ways. Either is the average catalytic constant ( $\overline{p k_{cat}}$ ) higher for Cel7A or the number of attack sites on the surface ( $^{kin}\Gamma_{max}$ ) higher. Since Cel6A is much faster in the conventional plot and at pre-steady-state as we will see in part IV the first explanation is unlikely. Instead we assume that the attack sites density on the cellulose surface is higher for Cel7A compared to Cel6A. One could say that Cel6A is a picky cellobiohydrolase with only few attack sites, where Cel7A is more promiscuous and can attack a broader range of different sites. When only limited substrate is available it seems to be essential with a high ability to locate substrate sites. These data support the findings by Jeoh *et al.* (2007) who reported that higher cellulose accessibility is pivotal for a high cellulose conversion. At least on Avicel we find a similar relation and we speculate that this can explain why Cel7A is the major components in industrial enzyme cocktails though it has a relatively slow maximal reaction rate. One could argue that the high ability to locate attack sites must be related to binding affinity to the substrate. When comparing  $^{conv}K_M$  values this also indicates higher affinity towards Avicel for Cel7A (lower  $^{conv}K_M$ ). In order to elucidate this idea further we estimated binding affinity by traditional Langmuir binding isotherms where substrate is saturated with enzyme. After incubation the amount of free enzyme was determined by intrinsic fluorescence as described in Article VIII. From the values of free enzymes the amount of bound enzyme was estimated and plotted against free enzyme concentration,  $E_{free}$  as shown in Figure 19 and fitted to a standard Langmuir isotherm  $\Gamma = \Gamma_{max} \frac{E_{free}}{K_d + E_{free}}$ . Based

on the Langmuir parameters the partitioning coefficient,  $K_P = \Gamma_{max}/K_d$  was calculated as done elsewhere (Palonen et al., 1999).

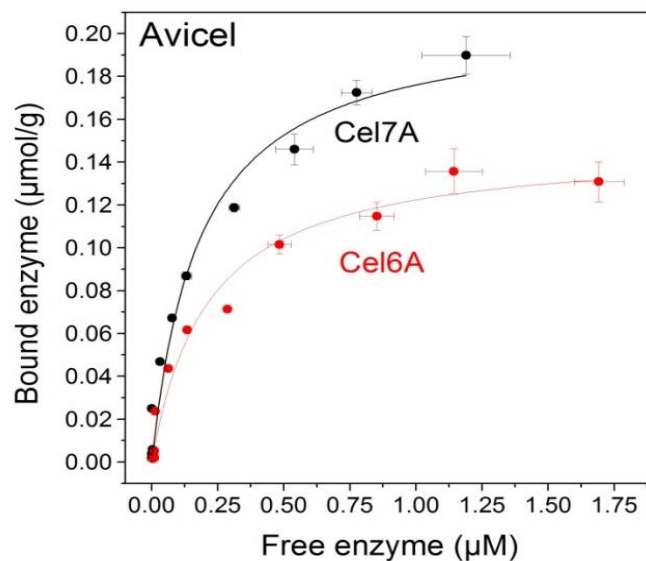


**Figure 19** A traditional Langmuir binding isotherm of Cel6A and Cel7A using 10 g/L avicel at 25°C.

We noticed that dissociation constant  $K_d$  is similar, between the two wild types, while a difference is observed when comparing the binding capacity  $\Gamma_{max}$ . This indicates that the affinity once bound is similar between the Cel6A and Cel7A, but that the ability to locate binding sites is higher for Cel7A.

**Table 4** Parameters extracted from the Langmuir binding isotherms

| <b>Binding isotherms</b> |                            |                   |                           |
|--------------------------|----------------------------|-------------------|---------------------------|
| <b>Avicel</b>            |                            |                   |                           |
|                          | $\Gamma_{max}$             | $K_d$             | $K_p$                     |
|                          | ( $\mu\text{mol g}^{-1}$ ) | ( $\mu\text{M}$ ) | ( $\text{liter g}^{-1}$ ) |
| <b>Cel6A</b>             | $0.148 \pm 0.008$          | $0.21 \pm 0.04$   | 0.704                     |
| <b>Cel7A</b>             | $0.208 \pm 0.014$          | $0.18 \pm 0.04$   | 1.148                     |

The Langmuir equation is widely used within this field although cellulase binding has been criticized not to comply with the underlying assumptions in the model. One of the challenges by using the Langmuir isotherm is that the heterogeneous nature of cellulose very likely consists of different binding or adsorption sites. Other alternative adsorption models have been suggested (Medve *et al.*, 1997, Zhang and Lynd, 2004), but we find the simple Langmuir isotherm useful in the comparison of the two cellobiohydrolases. We though agree that the use of traditional binding isotherms does not give varied or detailed insights in the substrate-enzyme interactions or the heterogeneity of cellulose.

### **Cellulose consists of Good and Poor Attack Sites**

The heterogeneity of cellulose is complex and we will now discuss how this can be relevant in the direct comparison of Cel6A and Cel7A. According to the heterogeneity of cellulose we suggest that the substrate consist of both good and poor binding and attack sites. Our results indicate than when plenty of good sites are available at high substrate load it is beneficial to have a low affinity and fast cellobiohydrolase such as Cel6A. Here it is the rate of dissociation that limits the overall reaction rate. Conversely if only few attack sites are available an improved dissociation rate will not be an advantage. Here it is more crucial to harness all available chain ends. Our findings together with previous work (Kari *et al.*, 2017) suggest that the inverse MM is valuable when investigating the enzymes ability to attack cellulose. We have seen when saturating a low substrate load with enzyme that the ability to find attack sites becomes essential. This is somehow related to the binding capacity of the enzyme, since the ability to associate to a broad range of binding sites is a prerequisite to attack these sites. From these results we suggest that Cel6A discriminate strongly against good and poor sites and Cel7A must be better to associate to and hydrolyze poor sites. Another aspect is if the number of good sites is simply



higher seen from Cel7A perspective compared to the perspective of the pickier Cel6A. When attack sites appear as poor sites for Cel6A similar attack sites might appear as good sites for Cel7A. This might be related to difference in substrate specificity between the two cellobiohydrolases. Cel6A has earlier been reported to have high activity on amorphous cellulose region and poor activity on highly crystalline regions, while Cel7A, on the other hand, is very efficient in degrading crystalline cellulose (Ståhlberg, 1993, Gruno *et al.*, 2004, Ganner *et al.*, 2012, Bubner *et al.*, 2013).

### Not all Binding Sites are Attack Sites

In Article I we also approximated a rough estimate of the attack density described by the parameter  $^{kin}\Gamma_{max}$ . Since the MM constants in the conventional and inverse plot both reflect half-saturation we argued that  $^{kin}\Gamma_{max} \approx \frac{invv_{max}/S_0}{convv_{max}/E_0}$ . By using this approach  $^{kin}\Gamma_{max} = 0.038 \mu\text{mol/g}$  for Cel6A and much higher  $0.29 \mu\text{mol/g}$  for Cel7A. When knowing  $^{kin}\Gamma_{max}$  and  $\Gamma_{max}$  from the binding isotherms we can estimate how big a fraction of the binding sites are actually also attack sites. From the binding isotherms in Article I we found  $\Gamma_{max}$  values of  $0.17 \mu\text{mol/g}$  for Cel6A and  $0.30 \mu\text{mol/g}$  for Cel7A. We note that these values are higher than those presented in Table 4 as enzyme adsorption continuous up to high enzyme concentrations as described by Jalak and colleagues (2014) (Jalak and Våljamäe, 2014). When using the  $\Gamma_{max}$  values covering the broader range of enzyme concentrations we found that for Cel7A  $\frac{^{kin}\Gamma_{max}}{\Gamma_{max}} = 0.97$  telling us that essentially all binding sites are also attack sites. For Cel6A, on the contrary,  $\frac{^{kin}\Gamma_{max}}{\Gamma_{max}} = 0.22$  indicating that for Cel6A the majority of the bound enzymes are just bound without being active.

To further test this hypothesis we tested if two enzyme injections upon each other gave rise to a similar activity response using biosensor real time measurements. With both Cel6A and Cel7A the second injection gave a smaller response than the first injection and apparently, from the inserts in Figure 20, we see that the relative size of the second activity response is lower for Cel6A compared to Cel7A. This result further support that when the best attack sites are already occupied the new injection of Cel6A enzymes find it more difficult to find new sites compared to the new injection of Cel7A molecules, Figure 20. In good agreement with our estimation of a higher attack site density on the cellulose surface for Cel7A compared to Cel6A.

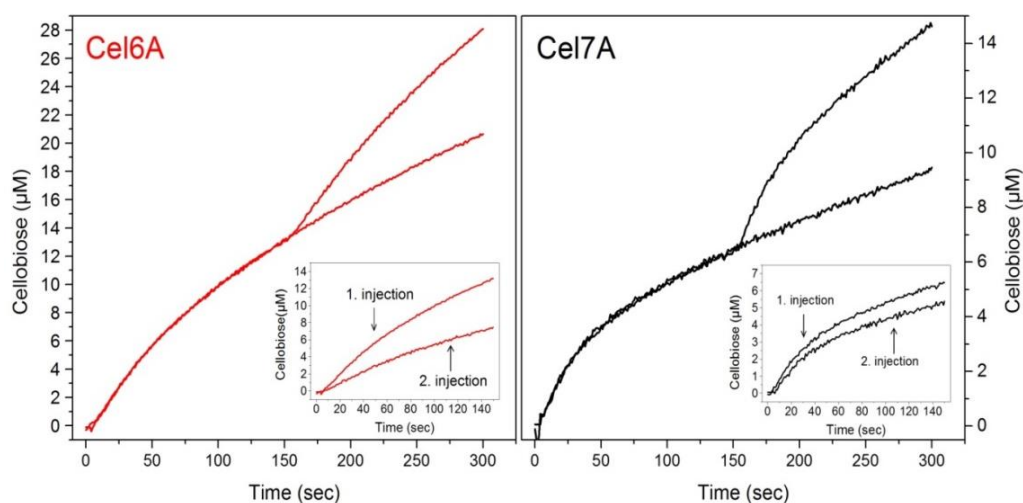


**Figure 20** Discovering the 1. and 2. burst using a real time biosensor with 40 g/L Avicel and 100 nM enzyme at each injection corresponding to 200 nM after 2. injection. The second injection was made after 150 sec of hydrolysis and the size of the second burst was determined simply by subtracting the signal from the run with only a single injection.

Figure from Article I.

To summarize the comparison of Cel6A and Cel7A showed us that Cel6A is a much faster cellobiohydrolase, but also much more “picky” than Cel7A. Cel7A is slower, but very promiscuous and able to attack most binding sites.

A last comment to this section is a notice on the importance of a comprehensive kinetic analysis of the enzymes instead of just single activity endpoint measurements. Obviously when comparing data and experimental conditions in the left and right part of Figure 18 two very distinct pictures appears. In a hypothetic situation where a single endpoint measurement was made to compare the hydrolytic activity of Cel7A and Cel6A two widely different conclusions could appear. In one case, we would hypothetically conclude >3 times higher activity of Cel6A compared to Cel7A and in the other extreme, opposite conclude  $\approx 1.5$  times higher activity of Cel7A compared to Cel6A.

## Part IV - The Role of the CBM

We know that both Cel6A and Cel7A are naturally expressed as multi-domain enzymes and in addition to the catalytic domain they also consist of a linker and CBM. First, we studied the role of these domains by expressing isolated core enzymes and compared them with the wt enzymes. These enzymes consist only of the catalytic domain (core) and hence lack both linker and CBM. The content of this section is mainly based on the findings in Article III.

Like earlier, the processive steady-state model and the inverse MM approach were applied on the core enzymes in comparison with their respective full-length enzymes as shown in Figure 21 and the extracted kinetic parameters collected in Table 5.

If we first focus on the conventional (left) part of Figure 21 interestingly it appears that both core enzymes have higher maximal specific rate ( ${}_pV_{max}/E_0$ ) than their wt enzymes. The two core variants established higher activity at high substrate loads, >15g/L Avicel for Cel7A core and >35g/L Avicel for Cel6A core. This contrary relation between affinity and activity was shown in the

previous section by comparing Cel6A and Cel7A, but also here by comparing Cel6A and Cel7A with their core enzymes.

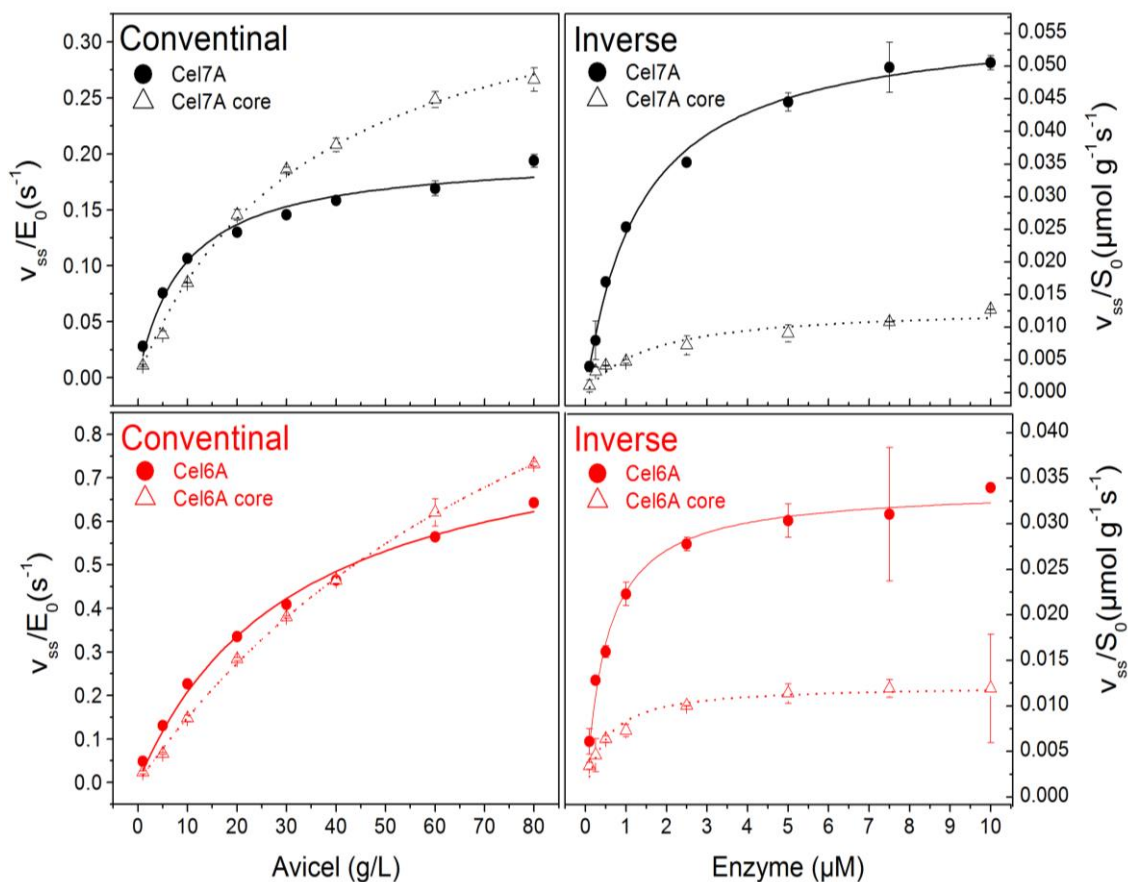


**Figure 21** A comparison of Cel6A and Cel7A with their corresponding core enzymes using the two models. The fit of the MM equation and the inverse MM equation is shown in solid lines for the wild types and in dotted lines for the core enzymes. Standard errors show deviation from triplicates or duplicates. The dataset for Cel6A and Cel7A is the same as presented in Figure 18. Data is adapted from Article III.

**Table 5** Kinetic parameters extracted from **Figure 21** using the conventional steady state model and the inverse Michaelis Menten approach.

|                   | Conventional MM plot              |                                  | Inverse MM plot                                    |                              |
|-------------------|-----------------------------------|----------------------------------|----------------------------------------------------|------------------------------|
|                   | ${}^pV_{max}/E_0$<br>( $s^{-1}$ ) | ${}^pK_M$<br>( $g\ liter^{-1}$ ) | ${}^{inv}V_{max}$<br>( $\mu mol\ g^{-1}\ s^{-1}$ ) | ${}^{inv}K_M$<br>( $\mu M$ ) |
| <b>Cel6A</b>      | $0.869 \pm 0.045$                 | $31.6 \pm 3.8$                   | $0.033 \pm 0.002$                                  | $0.506 \pm 0.050$            |
| <b>Cel6A core</b> | $1.657 \pm 0.071$                 | $100.9 \pm 6.7$                  | $0.012 \pm 0.001$                                  | $0.481 \pm 0.083$            |
| <b>Cel7A</b>      | $0.199 \pm 0.009$                 | $9.1 \pm 1.5$                    | $0.057 \pm 0.002$                                  | $1.343 \pm 0.112$            |
| <b>Cel7A core</b> | $0.388 \pm 0.015$                 | $34.5 \pm 3.0$                   | $0.013 \pm 0.002$                                  | $1.554 \pm 0.488$            |

This relation between core and wt has previously been shown for GH7 cellobiohydrolases (Le Costaouëc *et al.*, 2013, Várnai *et al.*, 2013, Pakarinen *et al.*, 2014, Sørensen *et al.*, 2015a, Sørensen *et al.*, 2015b), but apparently a similar relation is present for Cel6A. So even though we assume that the inherent dissociation is higher for Cel6A compared to Cel7A a decreased affinity still seems to improve the maximal rate at high substrate loads. Earlier we suggested that  $k_{off}$  must be higher for Cel6A compared to Cel7A, but the dissociation rate might still be rate-limiting since a further reduced affinity in the core enzyme resulted in higher activity. In Article VIII we discovered for two GH7 cellobiohydrolases that the catalytic advantage/disadvantage of a CBM is strongly influenced by temperature. The substrate concentration at which it becomes beneficial to lack the CBM increased with temperature. Thus at high temperature the presence of a CBM is an advantage for the hydrolytic activity in a larger substrate range. We explain this by the temperature induced enhanced ability to dissociate. Hence the off-rate is temperature dependent and increases with temperature. Since we expect the higher off-rate to be the force of the core enzymes this advantage is reduced when the temperature is increased.

The kinetic difference between wt and core enzymes is even more pronounced in the Inverse plot. Here the activity is strongly reduced for the core enzymes and it becomes clear that the presence of linker and CBM is essential at high E/S ratio. Referring back to the same metaphor as earlier both core enzymes must be extremely picky. The core enzymes only showed affinity and activity towards limited selected sites. We interpret these results and suggest that both the number of binding sites, but more important in the current context also the number of attack sites is much fewer for the core enzymes compared to the full length enzymes. Regarding the differences in cellulose adsorption between wt and core enzymes, many binding studies including results in Article III support that the CBM is essential for the adsorption to cellulose (Ståhlberg *et al.*, 1991, Ståhlberg, 1993, Nidetzky *et al.*, 1994a). More interestingly the lack of a CBM seems to obstruct the ability to find attack sites and we imagine that several attack sites can only be located with the aid from the CBM. This agrees with the finding that the need for a CBM increased with substrate conversion (Ståhlberg *et al.*, 1991). The concept of this idea is illustrated in Figure 22, where the wild type enzymes have many more attack sites than the core enzymes.

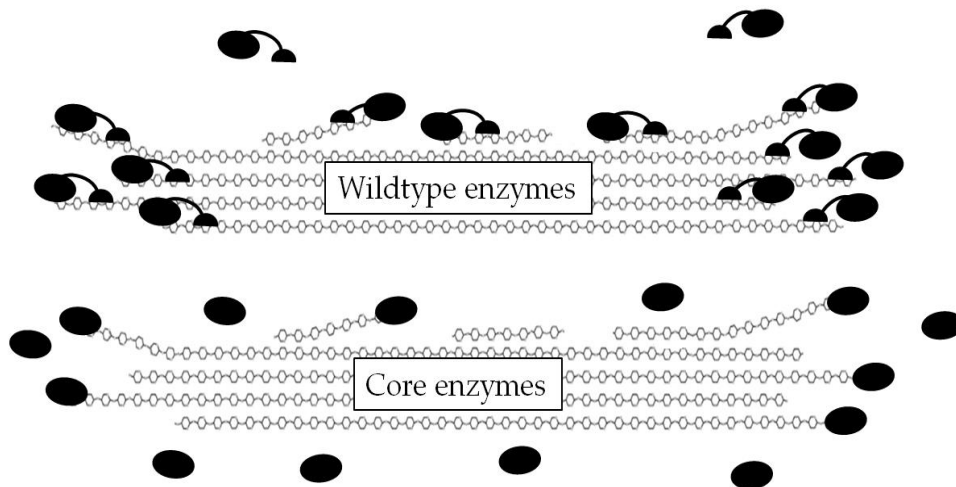


**Figure 22** An illustration that shows that wild type enzymes with linker and CBM (top) are much better to locate attack sites than the core enzymes (bottom). The black enzymes represent both Cel6A and Cel7A wild types and core enzymes.

Interestingly, when comparing the maximal rates in the inverse plot the two core enzymes have same maximal catalytic rate. We imagine that both core enzymes only can attack easily available sites. Recalling the suggestion that wt Cel7A has many more attack sites than wt Cel6A the linker and CBM of Cel7A enhanced the number of attack sites more than the linker and CBM in Cel6A. The maximal rate is 4.4 times higher for Cel7A compared to core, and only 2.8 times higher for Cel6A compared to core. This indicates that it is not just the differences in the enzymes catalytic domain that decide the degree of discrimination of good and bad sites, but also the interplay between the two different domains in the individual cellulase.

## CBM Swap changed the Enzymes Kinetically

In order to further investigate the role of the CBM we made two variants; one with the core domain and linker from Cel7A together with the CBM of Cel6A and opposite core and linker from Cel6A with the CBM of Cel7A as shown in Figure 23.

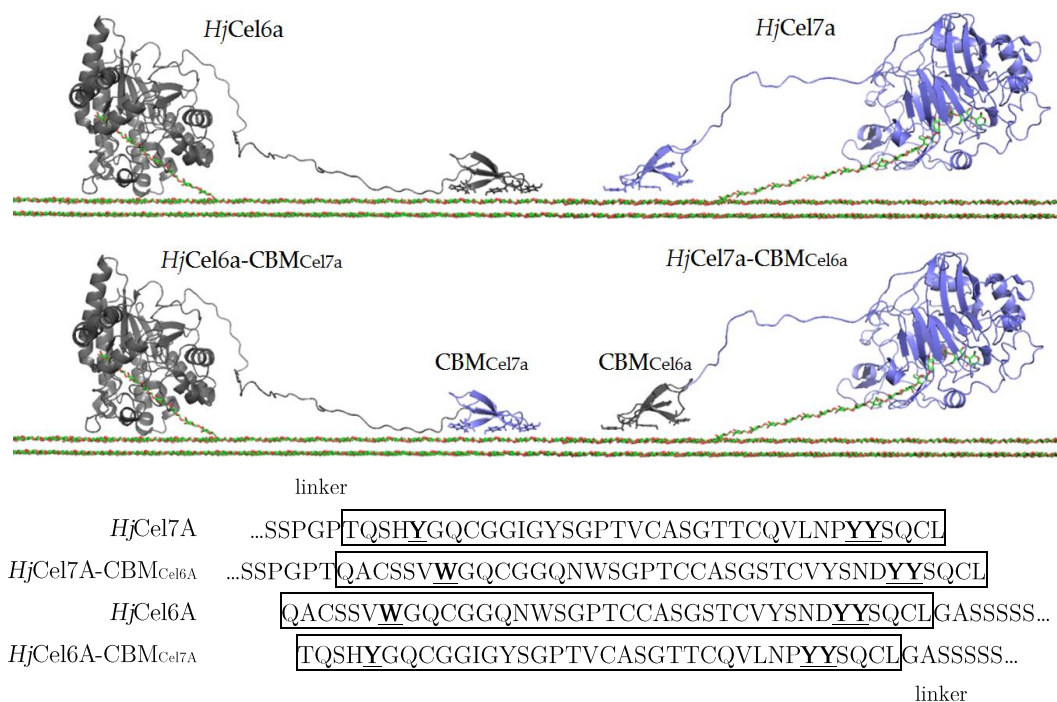


**Figure 23** An illustration of the concept of the two variants Cel6A<sub>CBM<sub>Cel7A</sub></sub> and Cel7A<sub>CBM<sub>Cel6A</sub></sub> together with amino acid sequences showing the CBMs (framed) and the transition to the linker. All sequences are written from the N-terminal. Figure copied from Article III.

Both CBMs from Cel6A and Cel7A belong to family 1 and from the comparable AA sequences a similar folding is predicted (Hoffrén *et al.*, 1995) as shown in Figure 11. With the planar face associated to the cellulose surface an isolated CBM1 is simulated to move along the cellulose chain without any favorable



direction and with thermodynamic energy minima with distances corresponding to the length scale of cellobiose (Beckham *et al.*, 2010b, Nimlos *et al.*, 2012). Same research group also simulated that a driving force makes the CBM translate away from the broken cellulose chain (Bu *et al.*, 2009). Together these studies indicate that the CBM most likely will slide away from the hydrolyzed bond in moves corresponding to the distance of a processive cycle, but that the CBM itself is not optimized to translate in the same direction as the processive movement of the core. Based on these findings CBM swap between two different GH families that attack either the reducing or non-reducing ends should be possible. The finding that isolated CBMs from Cel6A and Cel7A compete against the same binding sites (Arola and Linder, 2016) further support this.

Considering the many similarities between the two CBMs the kinetics of the enzymes was affected quite dramatically with the CBM swap as detailed in Article III. Both variants showed decreased binding capacity and higher maximal rate in the conventional MM approach. In the inverse plot both variants exhibited lower activity than Cel6A and Cel7A. The most drastic affect was seen for Cel6A<sub>CBMCel7A</sub> that behaved more similar to the isolated core domain than Cel6A. In an attempt to elucidate if the differences in the kinetics of the two variants were connected to a changed processivity we looked at the product profiles of the enzymes Figure 24. Processivity of cellobiohydrolases can be estimated in many ways including analysis of product profiles (Horn *et al.*, 2012). Considering that glucose and cellotriose will only be released in the initial cut (or in rare cases where the cellobiohydrolase reach an end) ratios between products can indicate processivity. Since some ambiguity occur about which product ratio that will give the best estimate of processivity (Horn *et al.*, 2012, Kari *et al.*, 2016) we simply just compared the relative ratio of glucose and cellotriose in between the variants instead. The different product profiles are shown in Figure 24.

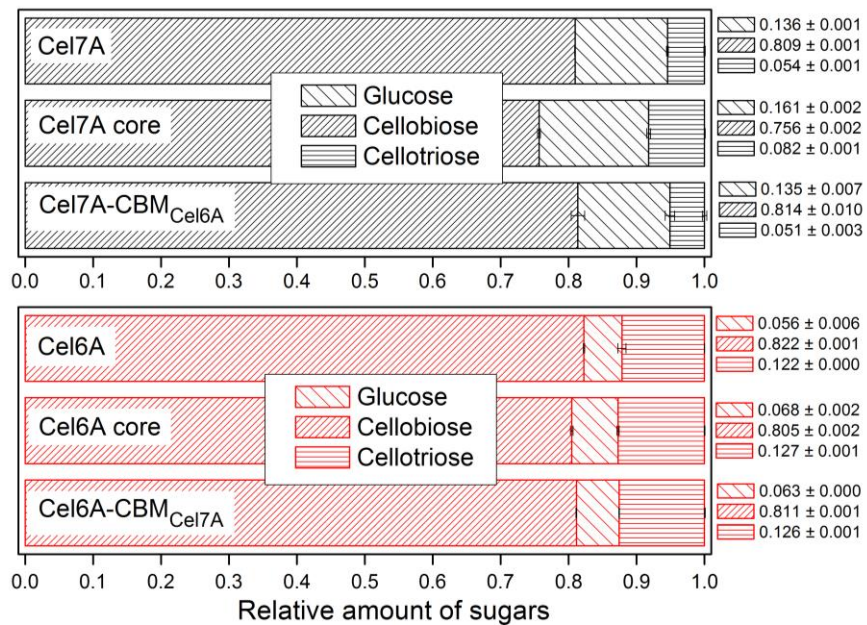


**Figure 24** Relative amount of glucose, cellobiose and cellotriose after 1 hour hydrolysis 0.1  $\mu$ M enzyme and 50 g/L Avicel. Figure adapted from Article III.

The product profile between Cel7A and the core were quite different indicating lower processivity of the core enzyme in agreement with earlier studies (Cruys-Bagger et al., 2013b, Sørensen et al., 2015a), but the product profile of Cel7ACBM<sub>Cel6A</sub> was very similar to the wt. This indicates that the processivity of Cel7ACBM<sub>Cel6A</sub> and the wt is alike. Unlike Cel7A the product profile was more similar between core and wt for Cel6A, but Cel6A<sub>CBM<sub>Cel7A</sub></sub> might have reduced processivity, since the product profile is more similar to the core domain than Cel6A. A disturbed processivity seems however not to explain the kinetic behavior of the CBM swapped variants, but exchanging the CBM seems somehow to affect the interplay between the core domain and the CBM.

The product profiles also showed us differences between Cel6A and Cel7A. From Figure 24 one could interpret that Cel7A will very often release glucose in the initial cut, where Cel6A more likely will release cellotriose. Considering that the

sum of glucose and celotriose is very equal for both enzymes this indicates a very similar processivity of both wild types on Avicel, but a different initial cut.

## Part V – The Role of the Linker

Compared to the extensive research on fungal cellulases have only few studies investigated the role of the linker domain. The content of this section is mainly based on the findings in Article IV and due to ongoing commercial interests this section will only briefly mention our major findings without any details about specific mutations. The role of the linker of Cel7A was investigated by construction of a few variants and in agreement with previous studies (Srisodsuk *et al.*, 1993, Payne *et al.*, 2013b, Strobel *et al.*, 2015, Ruiz *et al.*, 2016) we found that the linker has other functions than just connecting the CBM to the core domain. Very interestingly both a variant with shorter linker, longer linker and less glycosylation sites showed reduced affinity towards Avicel, which resulted in a higher velocity at high substrate loads. The benefits of the different linker modifications seem to be strongest at low temperatures in total agreement with the results in Article VIII where the kinetical advantages of being a low affinity variant (variant lacking a CBM) is very strong at low temperatures while we believe that at high temperature a stronger cellulose affinity becomes more essential because of the temperature induced ability to dissociate. Based on our study, the suggested attractive forces between cellulose and glucans on the linker (Payne *et al.*, 2013b) peptide appear to depend on location of glycosylation sites on the linker and not just the number of glycosylation sites. This is supported by previous findings (Strobel *et al.*, 2015). In general, it is difficult to decide whether the effect of the linker modifications is caused by an altered glycosylation pattern or changes in the linker length. The results from Article IV do however indicate that modification close to CBM seems to have a more dramatic impact on the function or kinetics of the enzyme while modifications in the so called hinge region close to the core seems to be less

dramatic in good agreement with (Srisodsuk) 1993. We suggest that the amino acids closely connected to the CBM are more directly associated to the cellulose surface. Regarding the inverse relationship of affinity and maximal rate that we also discovered with the linker variants we again argue that the high reaction rate at high substrate loads is an effect of dissociation controlled hydrolysis rate. Hence it seems not just to reflect properties of the linker or CBM, but seems to reflect a more generic relation between affinity and maximal rate.

## Part VI – Pre-steady State Kinetics

In industry real biomass is degraded by a cocktail of enzymes over a long period of time, usually several days, to reach the maximal conversion. Keeping that in mind one might question why we care about the kinetics of individual cellulases in the very early initial phase of hydrolysis? Even though conditions here are far from industrial conditions we believe that the information extracted from this kind of analysis is very useful in terms of understanding the behavior of the enzymes. Hydrolysis of insoluble cellulose by cellobiohydrolases is characterized by a high initial activity rate (pre-steady state rate) followed by a pronounced slow-down in activity over time and we have just discussed some of the factors that can explain this slow-down. Furthermore Cel7A has been shown to perform burst kinetics, which means that the reaction rates accelerate within seconds, followed by a dramatic slow-down. This burst behavior has earlier been explained by an accumulation of un-productive bound cellulases, where the underlying explanation is the dissociation limited reaction rate (Jalak and Våljamäe, 2010, Praestgaard *et al.*, 2011).

## Exploring the Initial Kinetics using Quench Flow System

Since pre-steady state kinetics is difficult to handle manually a Quench Flow (QF) system was recently developed (Olsen *et al.*, 2017). With a time resolution of 250 ms using insoluble substrate this system is a strong tool to explore transient kinetics. Here we applied the QF system to discover activity within the first 5 seconds of hydrolysis of both Cel6A and Cel7A. We used turraxed Avicel to homogenize the substrate and to reduce the risk of clogging of the QF system. After the samples were quenched we used an ion chromatography system (ICS) to determine the quantity of cellobiose as shown in Figure 25.

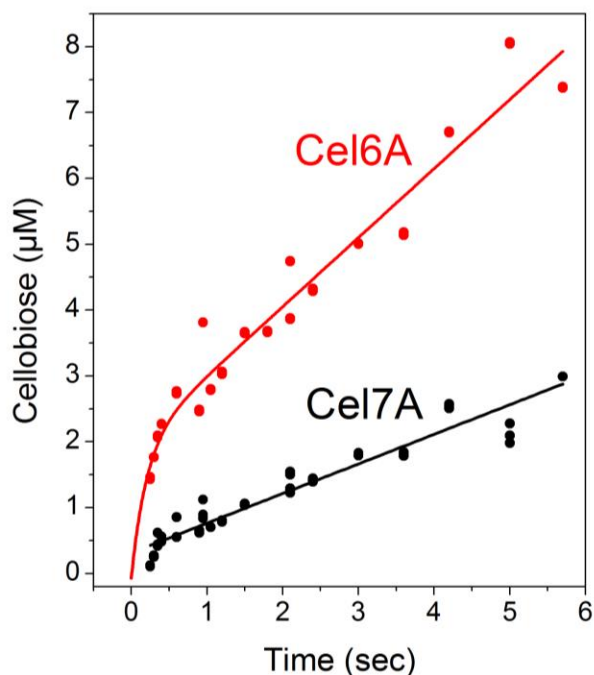


**Figure 25 A)** Quench flow data with hydrolysis using 0.5  $\mu\text{M}$  enzyme and 10 g/L turraxed Avicel. Fits are only made to guide the eye and have no theoretical function. Double exponential function for Cel6A (red) and linear regression for Cel7A (black). Data from Article I.

When looking at the very early kinetics of Cel6A and Cel7A on turraxed Avicel in comparison it is apparent that Cel6A is much faster at the very early phase than Cel7A. Using the slope up to 1 second we find a very high specific activity of  $\sim 10 \text{ s}^{-1}$  and after that an approximated specific rate of  $1.3 \text{ s}^{-1}$ . Data for Cel7A is more uncertain, but gives a specific steady state activity of approximate  $0.35 \text{ s}^{-1}$ , which is much lower than for Cel6A. The steady-state rate of Cel7A might however not have been reached within our timeframe and the actual steady state rate might be even lower. It has earlier been shown that the maximal rate it reach after approximately 5 seconds (Cruys-Bagger *et al.*, 2012a). The acceleration phase of Cel6A also seems to be very fast, even faster than the time limit of 250 ms. The highest rate is already obtained within 250 ms. The differences in the transient phase of hydrolysis might be explained by the two different catalytic mechanisms or maybe related to the different architecture of the core domain. We speculate that the more flexible and open structure of Cel6A compared to Cel7A facilitate the threading of the cellulose chain into the catalytic tunnel of Cel6A. Thus the architecture of the tunnel of Cel6A might not just contribute to a facilitated dissociation, but might also contribute to a faster threading or on-rate compared to Cel7A. If we recall similar dissociation constants ( $K_d$  values) for Cel6A and Cel7A and that  $K_d=k_{off}/k_{on}$  is it very likely that both the rate constant  $k_{off}$  and  $k_{on}$  are higher for Cel6A compared to Cel7A.

In this chapter we presented that Cel6A is a catalytic fast enzyme compared to Cel7A. In the pre-steady state regime and in conditions with substrate excess Cel6A was superior. The activity of Cel6A seems however to be more sensitive than Cel7A to small changes in the substrate governed by hydrolytic activity. At enzyme excess Cel7A showed higher activity than Cel6A and we propose that Cel7A is able to attack many more sites than Cel6A. Furthermore Cel7A has higher stability than Cel6A. Variants were made to investigate the role of both linker and CBM and both domains influence the kinetics and adsorption behavior of the enzymes. All our results support that dissociation limits the

overall reaction rate since all variants with lowered substrate affinity presented here showed higher maximal rate than the wild types. The improved ability to dissociate seems to be a drawback when only limited substrate is available since it additionally reduces the variants ability to locate and attack substrate sites.

## Enzyme Substrate Interactions

---

Until now we have concentrated on the kinetics of Cel7A and Cel6A without focusing on the catalytic tunnels where the enzymatic hydrolysis takes place. As described earlier CBHs are able to degrade crystalline cellulose by a processive mechanism, where a single strand need to be threaded inside the catalytic tunnel before the enzyme slides along the cellulose crystal releasing soluble sugars. Obviously, strong enzyme-cellulose interactions must occur in order to decrystallize the cellulose chain and to keep the enzyme bound through the sequential catalytic steps. The decrystallization of a cellulose chain from cellulose fibrils requires strong enough enzyme-substrate interactions to break the tight network of hydrogen bonds in the fibril (Beckham *et al.*, 2011). As described by Payne *et al.* (2013a) is the ability of an enzyme to decrystallize the polymer chain from a crystal dependent on the binding free energy of the enzyme to the cello-oligosaccharide (Payne *et al.*, 2013a). In this section we have investigated enzyme-substrate interactions in catalytic deficient variants of Cel6A using isothermal titration calorimetry (ITC). These results are unpublished and not part of any manuscript. The results are compared with a previous study with Cel7A (Colussi *et al.*, 2015). We also refer to Colussi (2015) for a detailed description of the experimental procedures.

We constructed 3 different catalytic deficient variants and the corresponding core variants. The 3 different inactive Cel6A variants and the positions of D221, D175 and S181 are shown in Figure 26.



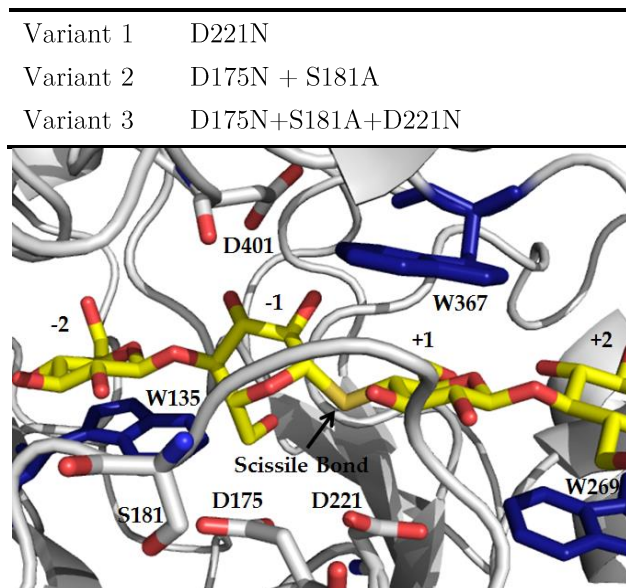


**Figure 26** The inactive variants and the position of the involved amino acids in the crystal structure (PDB 1QK2)

When changing the essential AA responsible for the catalysis we most likely also influence the enzyme-substrate interactions in the tunnel. Crystal structures with D221A (PDB 1HGY) and D175A (PDB 1HGW) have a very similar overall folding compared to the wild type (PDB 1QK2), but some differences occur (Koivula *et al.*, 2002). It is unknown what these small changes do to the COS-enzyme interactions. They might reduce the binding strength or even increased it if the ring distortion of the -1 site in Cel6A (Zou *et al.*, 1999) is changed. The D→N mutations made here are isosteric which could reduce potential changes in the structure, while the effect of S181A is unknown. Since no crystal structures of the exact variants exist, we notice that the results presented here should be interpreted with caution.

Figure 27 (left panel) shows an example of rawdata from the ITC experiments where the COS solution was injected every 120 sec. A model based on one set of thermodynamically equal binding sites was fitted to the integrated peaks to

estimate binding enthalpy ( $\Delta H$ ), stoichiometry ( $n$ ) and the binding constant ( $K_B$ ) as shown the right panel.

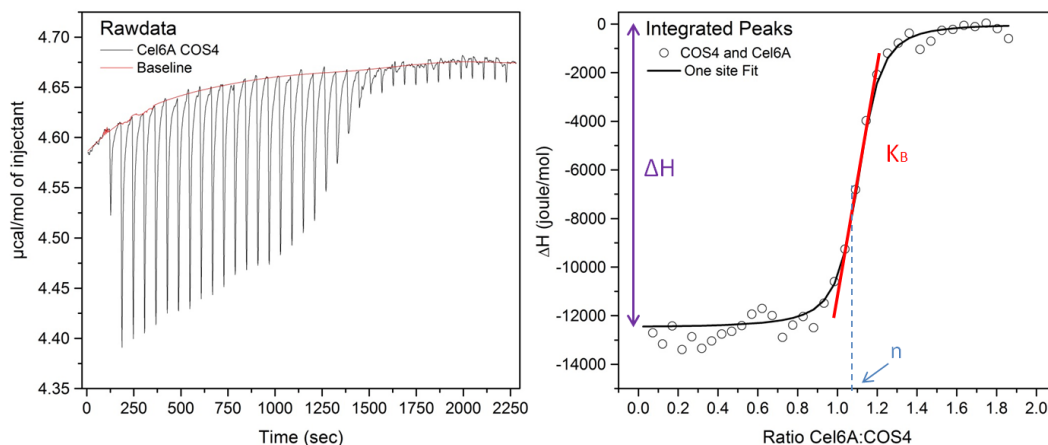


**Figure 27** ITC rawdata left at 10°C with titration injections every 120 sec including baseline (red). Right: Integrated rawdata peaks fitted to a one binding sites model. The binding enthalpy ( $\Delta H$ ), stoichiometry ( $n$ ) and the binding constant ( $K_B$ ) can be estimated from the fit as shown in the figure.  $K_B$  is not determined as the slope, but related to the gradient of the slope.

At first we tested whether the 3 variants including their inactive core variants gave rise to different COS-binding. All showed a similar binding to COS 4 and the estimated parameters from the ITC measurements are collected in Table 6. We found that the presence of the CBM and linker made no significant (or systematic) difference in the binding constant  $K_B$  and the stoichiometry ( $n$ ) was approximately 1 for all measurements indicating that the binding strength of any COS-CBM interactions that might occur is much lower than the strong interactions in the tunnel of the core domain. Furthermore unsystematic test-runs with selected inactive variants and COS of varying length were made to support that binding to COS of different DP was likewise similar (data not shown).

**Table 6** Results from isothermal titration where the calorimetric cell was loaded with 20  $\mu\text{M}$  enzyme and titrated with 200  $\mu\text{M}$  COS4 at 10°C. Parameters extracted from non-linear regression on data obtained on the three different catalytic deficient variants D221N, D175N S181A and D175N S181A D221N and the respective core enzymes. Errors indicate standard deviations for 2-3 independent experiments.

| DP | Enzyme                 | $\Delta\text{H}$<br>(kJ/mole) | n<br>(COS/Enzyme) | $\text{K}_\text{B}$ (1/ $\text{K}_\text{D}$ )<br>( $\text{M}^{-1}$ ) |
|----|------------------------|-------------------------------|-------------------|----------------------------------------------------------------------|
| 4  | D221N                  | $-12.0 \pm 0.0$               | $1.02 \pm 0.04$   | $(1.83 \pm 0.03) \cdot 10^7$                                         |
| 4  | D221N core             | $-12.2 \pm 0.1$               | $1.04 \pm 0.12$   | $(2.17 \pm 0.94) \cdot 10^7$                                         |
| 4  | D175N + S181A          | $-13.2 \pm 0.7$               | $0.99 \pm 0.08$   | $(1.38 \pm 0.01) \cdot 10^7$                                         |
| 4  | D175N + S181A core     | $-13.2 \pm 0.3$               | $1.03 \pm 0.00$   | $(1.65 \pm 0.24) \cdot 10^7$                                         |
| 4  | D175N+S181A+D221N      | $-12.9 \pm 0.6$               | $1.03 \pm 0.00$   | $(2.08 \pm 0.44) \cdot 10^7$                                         |
| 4  | D175N+S181A+D221N core | $-12.7 \pm 0.3$               | $1.08 \pm 0.01$   | $(1.69 \pm 0.09) \cdot 10^7$                                         |

A challenge was that all catalytic deficient variants remained some activity on the different COS (highest on COS6) especially at high temperatures. The variants D175N S181A D221N showed the lowest activity, but we still found a specific activity of  $0.03 \text{ min}^{-1}$  at 10°C on 100  $\mu\text{M}$  COS6 determined on the ICS after 1 hour of hydrolysis and even higher activity at higher temperatures. This result is in good agreement with the reported activity of the inactive D221A variants ( $0.04 \text{ min}^{-1}$  at 27°C on COS6) (Koivula *et al.*, 2002). All data presented in this chapter is therefore performed at 10°C to avoid large impact from the activity on the calorimetric signal. The core variant D175N S181A D221N was used to investigate the binding to the different COS molecules and the results are listed in Table 7.

The lower binding affinity of COS7 compared to COS6 imply that the length of the tunnel of Cel6A suits with 6 glycosidic subsites as suggested earlier and no strong enzyme-substrate interactions seem to occur in a potential -3 site or +5 site.

**Table 7** Results with the core variant D175N S181A D221N and COS molecules of different DP. Errors indicate standard deviations for 2-3 independent experiments. The calorimetric cell was loaded with 20  $\mu$ M enzyme and titrated with 200  $\mu$ M COS solution.

| DP | Enzyme                 | $\Delta H$<br>(kJ/mole) | n<br>(COS/Enzyme) | $K_B$ (1/ $K_D$ )<br>( $M^{-1}$ ) |
|----|------------------------|-------------------------|-------------------|-----------------------------------|
| 4  | D175N+S181A+D221N core | $-12.7 \pm 0.3$         | $1.08 \pm 0.01$   | $(1.69 \pm 0.09) \cdot 10^7$      |
| 5  | D175N+S181A+D221N core | $-13.5 \pm 0.0$         | $1.07 \pm 0.01$   | $(1.36 \pm 0.16) \cdot 10^8$      |
| 6  | D175N+S181A+D221N core | $-14.6 \pm 0.0$         | $0.99 \pm 0.01$   | $(3.05 \pm 1.34) \cdot 10^8$      |
| 7  | D175N+S181A+D221N core | $-13.1 \pm 0.1$         | $1.17 \pm 0.03$   | $(2.65 \pm 0.81) \cdot 10^7$      |

The ITC experiment within deficient Cel6A variants also estimated the stoichiometry to approximately 1 for all titration experiments. Thus unlike Cel7A, Cel6A seems only to bind one COS molecule at a time. Furthermore, this indicates only minor effects of any catalytic activity. The strongest interactions were between Cel6A and COS6  $K_B = 3.1 \cdot 10^8 M^{-1}$  which corresponds to the expected number of glycosidic subsites in the tunnel. Interestingly also Cel7A shows the strongest binding to COS6 with a  $K_B$  value of  $3.6 \cdot 10^7 M^{-1}$  (Colussi *et al.*, 2015) despite the longer and more closed tunnel of Cel7A. Surprisingly the  $K_B$  value of Cel6A of  $3 \cdot 10^8 M^{-1}$  for Cel6A indicates stronger enzyme-substrate interactions in the tunnel of Cel6A compared to Cel7A. This might be explained by the suggested low affinity sites around the -2 site in Cel7A (Colussi *et al.*, 2015) where the ligand is twisted (Divne *et al.*, 1998). We also noticed that  $\Delta H$  is quite similar for COS4-COS7 indicating that the interactions with the subsites covered by COS4 contribute most to the binding enthalpy. Compared to the  $\Delta H$  values from Colussi (2015) of approximately -35 kJ/mol the binding enthalpy found for the ligands in the tunnel of Cel6A is less exothermic. However, the binding affinity, in terms of  $K_B$ , is at least as strong.

The results presented here together with the thorough study of Colussi *et al* (2015) indicate that a binding strength of  $10^7$ - $10^8$  in the tunnel is optimal in order to be able to decrystallize a cellulose chain from the crystal and still allow the processive movement of the cellobiohydrolases.

## What drives Processivity?

The very strong interactions in the product- or expulsion site of Cel7A are thought to be the driving force that drives the processive movement of the enzyme (Knott *et al.*, 2014a) through an affinity gradient in the catalytic tunnel. Unlike Cel7A our results do not suggest that such strong interactions occur in the product site of Cel6A. Titrations with cellobiose gave no observable binding curve for any of the inactive variants and in comparison cellobiose binding to an inactive Cel7A gave a rather high binding constant of  $1.8 \cdot 10^5 \text{M}^{-1}$  (Colussi *et al.*, 2015) in good agreement with earlier estimates ( $5.4 \cdot 10^4 \text{M}^{-1}$ ) (Claeyssens *et al.*, 1989). A binding constant of  $5.4 \cdot 10^2 \text{M}^{-1}$  to cellobiose has earlier been reported for Cel6A (Claeyssens *et al.*, 1989), which is order of magnitudes lower than for Cel7A. This might be related to the lower cellobiose product inhibition of Cel6A compared to Cel7A (Murphy *et al.*, 2013, Teugas and Våljamäe, 2013). The ligand twist in the product site (-1 site) (Zou *et al.*, 1999) might also explain this weaker binding. To our knowledge no crystal structures in complex with cellobiose, cellotriose or cellopentaose is available for Cel6A and it is therefore difficult to predict the substrate affinity in the different subsites solely based on binding constants. The binding of a COS4 analog in subsite -1,-2,+1,+2 of Cel6A (PDB 1QK2) could indicate very strong interactions in the +1, +2 site in correlation with the high binding constant of  $2 \cdot 10^7 \text{M}^{-1}$  to COS4 found here. Compared to the low  $K_B$  of  $5.4 \cdot 10^2 \text{M}^{-1}$  to cellobiose (Claeyssens *et al.*, 1989) the binding to COS4 is really strong. Several substrate interactions are however predicted in the product site of Cel6A (-2

and -1) such as interactions to W135, K395, E399, D401 (Payne *et al.*, 2011, Mayes *et al.*, 2016), but we find it unlikely that these, in comparison to Cel7A weak interactions, are the major driving force of the processive movement of the enzyme. Instead we suggest that the dynamic architecture of the loops of Cel6A and the appearance of an open and closed form during the catalysis (Zou *et al.*, 1999, Payne *et al.*, 2015, Mayes *et al.*, 2016) is critical for the forward driving force when sliding on the cellulose chain. Hence based on our results we propose that a high affinity product site is not a premise for processive cellobiohydrolases.

The definition of Cel6A as a processive cellobiohydrolase is discussed in literature and some studies suggest that Cel6A is more likely an endo-processive cellobiohydrolase with a high capability of endo-initiation than a true exo-cellobiohydrolase like Cel7A (Boisset *et al.*, 2000, Poidevin *et al.*, 2013, Payne *et al.*, 2015). This proposed behavior of Cel6A is often used to explain the occurrence of synergy between Cel7A and Cel6A. The next chapter will focus on the synergy between the two cellobiohydrolases including the endo-character of the enzymes.



## Cel6A and Cel7A in Synergy

---

Cellulases work in synergy to degrade cellulose. One type of synergy is endo-exo synergy where endoglucanases attack the cellulose chains randomly generating new chain ends for cellobiohydrolases to attack as described earlier. It has also been suggested that degradation of the amorphous cellulose regions by endoglucanases prevent stalling of cellobiohydrolases and thereby leads to increased activity (Eriksson *et al.*, 2002, Jalak *et al.*, 2012). A more peculiar form of synergy is the synergy between Cel6A and Cel7A, the so called exo-exo synergy. Exo-exo synergy was first discovered in 1980 (Fägerstam and Pettersson, 1980). The extent of exo-exo synergy seems to depend on substrate properties including the degree of crystallinity (Henrissat *et al.*, 1985, Hoshino *et al.*, 1997). Moreover, it has been shown that exo-exo synergy may occur without simultaneous action of the cellobiohydrolases (Nidetzky *et al.*, 1994b, Våljamäe *et al.*, 1998), and this contradicts earlier suggestions that the synergy could rely on the formation of weakly bound Cel6A-Cel7A complexes (Tomme *et al.*, 1990).

The following chapter is based on Article II where we investigated the synergy between Cel6A and Cel7A and the corresponding core enzymes.

### Synergy depends on Experimental Conditions

For clarity we define that synergy occurs if combined hydrolysis of two enzymes is higher than the sum of their individual hydrolysis. The degree of synergy (DS) between Cel6A and Cel7A can be determine from Equation 4

$$DS = \frac{A_{Cel6A+Cel7A}}{A_{Cel6A} + A_{Cel7A}} \quad (4)$$



where  $A_{\text{Cel6A}+\text{Cel7A}}$  is the activity of the enzyme mixture, and  $A_{\text{Cel6A}}$  and  $A_{\text{Cel7A}}$  are the activities in the corresponding mono-component experiments. In the synergy experiments the enzyme concentration was maintained while the Cel6A: Cel7A ratio was changed.

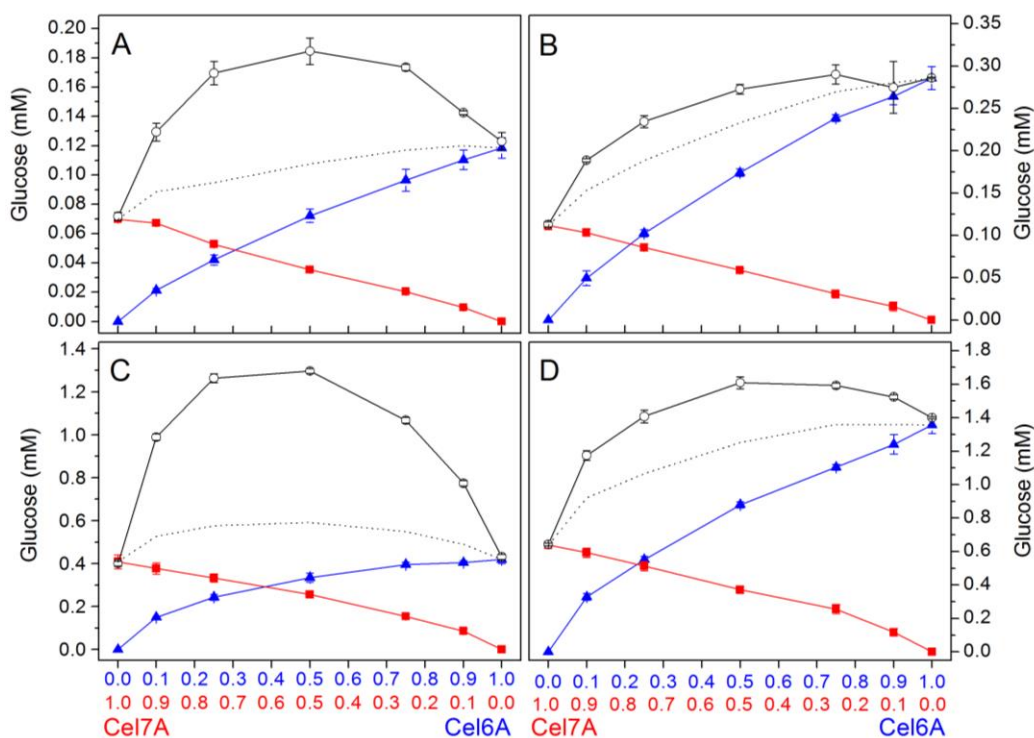


**Figure 28** Synergy between Cel6A and Cel7A in the presence of 10% β-glucosidase at four different conditions. A) 12 g/L Avicel [E]= 200 nM, B) 60 g/L Avicel [E]= 200 nM, C) 12 g/L Avicel [E]= 2 μM and D) 60 g/L Avicel [E]= 2 μM. Blue triangles: Cel6A in buffer, red squares: Cel7A in buffer, open circles: Mixtures of Cel6A and Cel7A in different enzyme ratios at constant enzyme concentration, dotted line: Theoretical sum of monocomponents. Errors bars indicate deviations from triplicates. Data from Article II.

Figure 28 shows an example of synergy experiments with mono-component dose activity of Cel6A (blue curve) and Cel7A (red curve), their theoretical sum (dotted lines) and the actual activity of both enzymes in different ratios (black curve)

under 4 different experimental conditions. If more glucose is produced in the black curve compared to the theoretical dotted line synergy is present. These results show that the synergy between Cel6A and Cel7A from *H. jecorina* is strongly dependent on enzyme and substrate concentrations. The highest degree of synergy was found at high enzyme concentration and low Avicel concentration (condition C). The synergy between Cel6A and Cel7A was increased when we lowered substrate concentration ( $B \rightarrow A$  or  $D \rightarrow C$ ) and also increased if we increased the enzyme concentration ( $A \rightarrow C$  or  $B \rightarrow D$ ). We suggest when the cellobiohydrolases are in a situation when easily accessible chain ends are available the exo-exo synergy becomes less beneficial. Furthermore the higher number of attack sites at high substrate loads do also minimize the probability that the enzymes work in the same area.

## **Exo-Exo Synergy is influenced by the Linker and CBM**

Synergy between the truncated cellobiohydrolases without CBM and linker was also determined. As presented earlier and in many previous studies the linker and CBM strongly influence the kinetics and adsorption of the cellobiohydrolases and apparently also on the exo-exo synergy between them. Here we found that notably more exo-exo synergy occurs between the full length enzymes compared to the isolated core enzymes under all conditions tested. We are aware that part of the difference in the synergy factor might simply be caused by higher degree of conversion for the wt enzymes compared to the core enzymes under some conditions, but the synergy is higher for the full length enzymes even at conditions where the overall conversion was higher for the core-core mixture. In Figure 29 the degree of synergy (DS) is summarized for the Cel6A-Cel7A mixtures and the core-core mixtures. To further investigate how the CBM influences the synergy, we also measured the synergy in wt-core combination. Both CBMs seem to contribute to

an increased synergy, but the presence of CBM on Cel7A seems to impact the synergy more than the CBM on Cel6A.

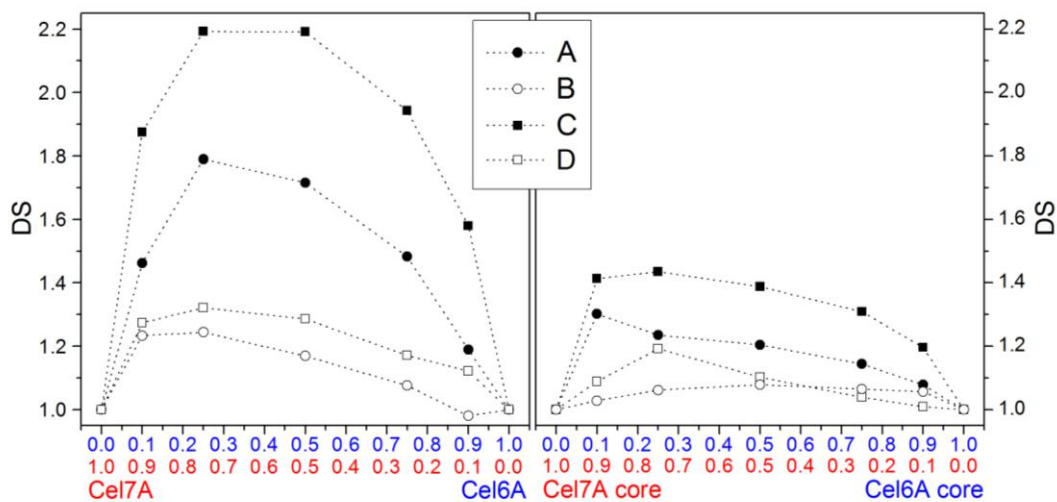


**Figure 29** The degree of synergy (DS) between Cel6A and Cel7A and between the two core enzymes at the different experimental conditions: A) 12 g/L Avicel [E]= 200 nM, B) 60 g/L Avicel [E]= 200 nM, C) 12 g/L Avicel [E]= 2 μM and D) 60 g/L Avicel [E]= 2 μM. Adapted from Article II.

Another important aspect of this work deal with the way DS is obtained experimentally. From our synergy data, like Figure 28, we noticed that the mono-component curves diluted in buffer are far from linear, especially with the highest enzyme loads. This non-linear relation between enzyme dose and activity is well established (Sattler *et al.*, 1989, Bezerra and Dias, 2004) likewise it is the fundament of enzyme saturation and the inverse MM approach covered in Chapter 2. However, in studies investigating exo-exo synergy the estimated DS is most often based on the assumption of linearity. Here the estimation of DS is based on only one mono-component activity at one enzyme concentration. We find this inappropriate since a simplified determination of the synergy by drawing a line from the two mono-component outer points would in many cases result in an

overestimation of the synergism. An illustration of this is shown in Figure 30 where the dashed blue and red lines assume linearity and the resulting sum of the two (dashed black line) shows the hypothetical estimated sum of the activity of the two core enzymes. From the actual sum of the experimental values (dotted line) it appears that the dashed line is a gross underestimate and that the DS calculated from this would give a maximal DS=1.6 even though only minor synergy actually occur (DS<1.1) in this particular experiment.

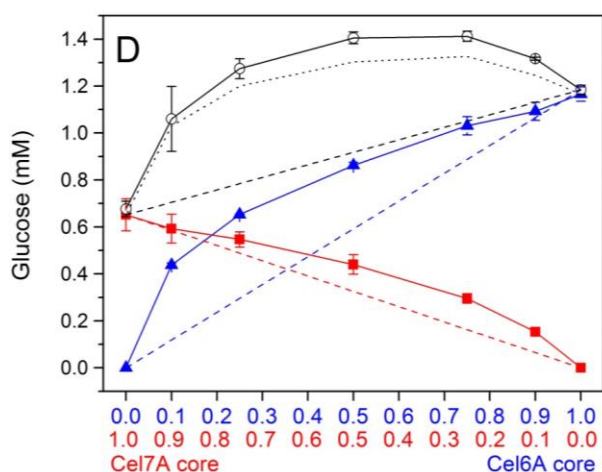


**Figure 30** Illustration of the consequence of assuming linear dose-activity relationships for monocomponent enzymes and its effect on synergy calculations. The experimental sum of monocomponent activities (dotted black line) appear much higher than the hypothetical sum (dashed black line). Synergy between core enzymes at condition D) 60 g/L Avicel [E]= 2  $\mu$ M. Based on data in Article II.

The widespread use of the linear dose-activity approximation in synergy measurements may be unacceptable under some conditions and we strongly recommend measuring several enzyme concentrations when performing such studies. We also notice that this type of hypothetical estimate would have hid the interesting difference in synergy between full length enzymes and catalytic domain enzymes in our study, corresponding to early results presented by Tomme *et al* (1988).

## Endo-Character of Cel6A and Cel7A

One of the dominant interpretations of exo-exo synergy is that the synergy occurs because of endo-activity of the cellobiohydrolases in particular Cel6A (Boisset *et al.*, 2000, Poidevin *et al.*, 2013, Payne *et al.*, 2015). This interpretation means that exo-exo synergy is actually a sort of endo-exo synergy. The more open tunnel with flexible loops of Cel6A (Figure 6) compared to the more closed tunnel of Cel7A support the idea of Cel6A as being an endo-processive CBH (Zou *et al.*, 1999). Our data support that both Cel6A and Cel7A have some degree of activity on for instance carboxymethyl cellulose (CMC) as shown in (Ståhlberg, 1993), but we find no results supporting that Cel6A has more endo-character than Cel7A. On the contrary all experiments presented in Article II illustrate higher endo-activity for Cel7A compared to Cel6A, which is supported by earlier findings (Henrissat *et al.*, 1985, Irwin *et al.*, 1993). We estimated endo-activity in 3 different ways. First we estimated activity on the substituted cellulose CMC that are often used for endo-activity. Then we measured the drop in viscosity of the same substrate, since viscosity correlates with the degree of polymerization (DP). Finally we measured the release of azurine from the insoluble azurine crosslinked cellulose (AZCL-HE-Cellulose). This is summarized in Table 8 where we have calculated the relative activity compared to the endoglucanase Cel7B.

**Table 8** Relative endo-activity of Cel7A and Cel6A compared to the endoglucanase Cel7B on carboxymethyl cellulose (CMC) and azurine crosslinked cellulose (AZCL-HE-Cellulose) (calculated from data presented in Article II)

|              | <b>AZCL-HE<br/>Cellulose Activity</b> | <b>CMC<br/>Drop in viscosity*</b> | <b>CMC<br/>Activity†</b> |
|--------------|---------------------------------------|-----------------------------------|--------------------------|
| <i>Cel7A</i> | $4.2 \cdot 10^{-4}$                   | $1.1 \cdot 10^{-3}$               | $5.7 \cdot 10^{-3}$      |
| <i>Cel6A</i> | $1.8 \cdot 10^{-4}$                   | $1.3 \cdot 10^{-4}$               | $4.8 \cdot 10^{-3}$      |
| <i>Cel7B</i> | 1                                     | 1                                 | 1                        |

\*Relative drop in viscosity ( $\mu\text{M}^{-1}$ ) after 60 min calculated from 0.01 $\mu\text{M}$  Cel7B

†Relative activity ( $\mu\text{M}^{-1}$  L/g) estimated after 10 min. We do also correlates for the 10 x lower CMC concentration compared to measurements with Cel6A and Cel7A.

The endo-lytic activity of both Cel6A and Cel7A is very small compared to the endoglucanase Cel7B as expected. In all three assays Cel7B showed  $10^3$ - $10^4$  times higher endo-activity than the two cellobiohydrolases. This minor endo-lytic activity of Cel6A and Cel7A agree with the observation that the cellobiohydrolases only produce a small amount or no new reducing ends on bacterial cellulose (BC) (Kipper et al., 2005, Kurasin and Våljamäe, 2011). Considering the natural habitat of the CBHs from *H. jecorina*, they are secreted together with numerous EGs (including Cel7B) (Vinzant et al., 2001, Martinez et al., 2008) and the evolutionary advantage or necessity of endo-lytic activity of the two CBHs might be questionable along with the many endo-specific enzyme. The minor endo-activity might instead be residual activity of common ancestors. Based on our findings in Table 8 we strongly doubt that the appearance of exo-exo synergy is caused by endo-attack of Cel6A. When focusing on the structure of Cel6A we suggest that the tunnel structure contribute to other purposes than the probability of endo-lytic cleavage. Instead we believe that the more open and flexible tunnel can explain the higher off and on-rate as argued earlier.

It has also been suggested that Cel6A has high preference for amorphous cellulose with only minor activity on crystalline regions, but that Cel7A prefer crystalline regions (Ståhlberg, 1993, Gruno *et al.*, 2004, Ganner *et al.*, 2012, Bubner *et al.*, 2013). Our results support that Cel6A has higher activity on amorphous cellulose compared to Cel7A illustrated by activity on RAC in Figure 31. On Avicel with both amorphous and crystalline regions also Cel6A show more activity compared to Cel7A and on the more crystalline cellulose substrate BMCC we found very similar activity. Comparable activity of the two CBHs on BMCC has earlier been reported (Våljamäe *et al.*, 1998, Palonen *et al.*, 1999), but in contrast to Ganner (2012) that reported very low activity of Cel6A on crystalline cellulose. Even though Cel6A and Cel7A seem to have similar activity towards crystalline cellulose within the short timescale presented here it is obviously that the two CBHs have different specificities towards cellulose.

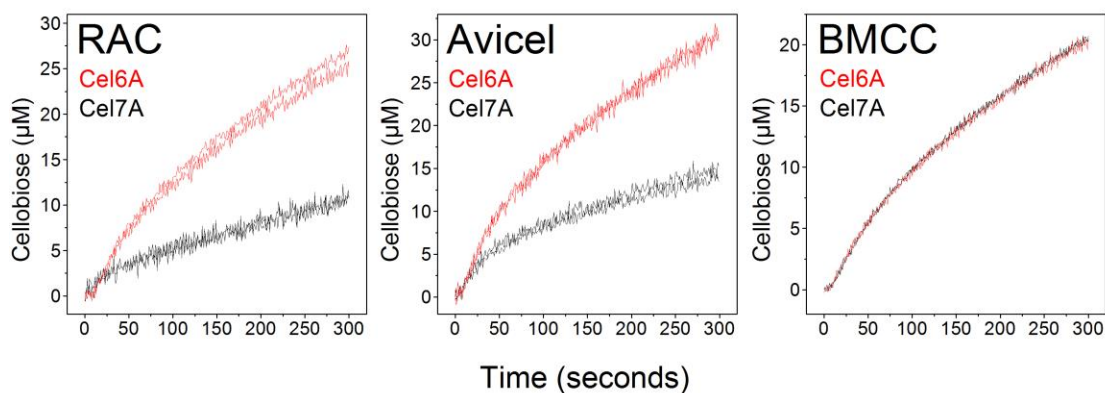


**Figure 31** Real time activity of Cel6A (red) and Cel7A (black) in the first 5 min of hydrolysis on the amorphous substrate RAC (1 g/L), the microcrystalline substrate Avicel (60 g/L) and the more highly crystalline substrate BMCC (1 g/L) using PDH-biosensors. The enzyme loads is 50 nM and in the graphs show duplicate measurements of each enzyme (unpublished data).

## Enzyme Specificity can explain Exo-Exo Synergy

Another explanation for the appearance of exo-exo synergy is enzyme specificity. At first the obvious difference in specificity is caused by Cel6A attacking non-reducing ends while Cel7A attacks reducing ends, which means that they don't compete against the same attack sites. Also, as we just described, that Cel6A has high activity on amorphous cellulose, while Cel7A prefer crystalline regions.

Cellulose is heterogeneous even in pure cellulose substrates such as Avicel, where both amorphous and crystalline regions are present. We imagine that new chain ends or better substrate will be exposed if one enzyme removes regions that are problematic for the other enzyme to convert. This will increase or facilitate targeting of the cellobiohydrolases and the ability to find new attack sites. In a crystal fibril a cellulose layer will probably also be removed faster and more easily because of the interplay between Cel6A and Cel7A working from each ends compared to just one of the CBHs working alone. This could result in a more

continuous flow of new exposed attack sites each time another layer is revealed. A related and probably more essential explanation for the observed synergy is clearance of each other's path by removal of obstacles. This is very important if we assume that many cellobiohydrolase are adsorbed to the cellulose surface without being active. This idea that one enzyme can reduce the amount of another unproductively bound enzyme and facilitate the processive hydrolysis of that enzyme has earlier been suggested to explain endo-exo synergy (Väljamäe *et al.*, 1998, Eriksson *et al.*, 2002, Jalak *et al.*, 2012). Considering the dissociation rate as rate limiting the synergistic effect facilitates the dissociation of the CBHs which will result in higher activity. One example could be that Cel6A degrade amorphous regions from the surface that otherwise will appear as obstacles for the processive movement of Cel7A. Instead of being stuck in front of the hindrance, in this case amorphous cellulose, Cel7A can now continue in the processive movement. This concept together with another hypothetic situation where structures in the crystal block for the processive movement of Cel6A is illustrated in Figure 32.

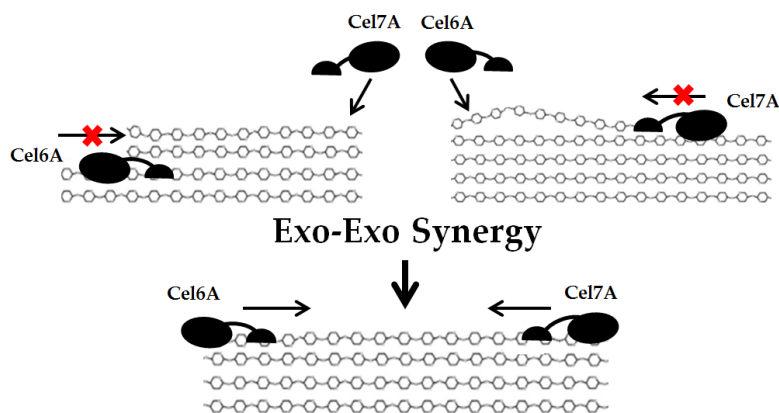


**Figure 32** A proposed concept behind exo-exo synergy where two cellobiohydrolases are non-productively bound, because of obstacles either crystal chain ends or amorphous cellulose. By exo-exo synergy the two CBHs provides better substrate for each other.

If we assume that exo-exo synergy is partly caused by a lower fraction of non-productively bound enzymes this also support why the synergy is much higher between wt enzymes compared to a pair of core enzymes. First the core enzymes



have already a higher inherent ability to dissociate from the cellulose surface compared to the wt enzymes and the benefits from the synergistic interplay become less pronounced. Another explanation is that the targeting of the core enzymes is reduced and they might not be able to clear obstacles for each other. From the significant differences between core enzymes and their wild types in the inverse MM plot with enzyme excess (Figure 21) we did earlier suggest that the isolated core domains have a reduce number of attack sites compared to their respective wild types. This could support that the core enzymes are less sufficient to clean the cellulose surface from obstacles.

To summarize we found that exo-exo synergy depend on the experimental conditions and the presence of linker and CBM. We suggest that differences in substrate targeting at least partly governed by the CBM are essential when understanding the phenomenon. The different targeting and substrate specificity of Cel6A and Cel7A results in clearance of each other's path which improve the overall hydrolysis. This means than at exo-exo synergy less cellobiohydrolases will be non-productive bound to cellulose. Even though these two enzymes are responsible for the primary hydrolysis we should remember that the fungus, in this case *Hypocrea jecorina* also secretes other enzymes such as endoglucanases. In the organism of the fungus and in industrial enzyme cocktails, where more cellulases and more diverse enzymes are present, this contributes to another and more complex level of the understanding of synergistic behavior. Also, when transfer from pure cellulose substrates to real biomass the complexity of synergy becomes even higher.

## Concluding Remarks

---

The work throughout this thesis is based on a direct kinetic comparison of the two cellobiohydrolases Cel6A and Cel7A from *H. jecorina*. These enzymes account for the majority of the enzymes expressed in cellulose degrading fungi as well as being the two major components of industrial enzyme cocktails. This clearly demonstrates that a better kinetic understanding of the two enzymes and especially their individual advantages and challenges can provide information for future enzyme engineering.

The present investigations of Cel6A and Cel7A has given us comparative insights about their kinetics, adsorption behavior, their synergy, their interactions with the substrate and the role of the different domains of the enzymes. To summarize we applied two different kinetic models where we either saturated the enzymes with substrate or opposite saturated substrate with enzymes. With this combined analysis we discovered very distinct kinetic properties of the two CBHs. We found that Cel6A is a much faster cellobiohydrolase than Cel7A and we suggest that the difference in activity is caused by an inherent ability of Cel6A to dissociate more rapidly. On the contrary Cel7A has a much higher ability to locate attack sites. Thus when Cel6A is a catalytically fast cellulase that discriminates strongly against good and poor sites Cel7A is on the other hand a slower cellulase that is able to degrade less accessible cellulose and in that way reach high cellulose conversion. We called Cel6A a fast, but picky enzyme, while Cel7A is a very promiscuous enzyme.

In order to investigate the role of the domains of the enzymes, different variants were made. Core enzymes without CBM and linker behaved kinetically different than their respective wild types. Interestingly both isolated core enzymes showed higher maximal rate, which can be explained by a higher rate of dissociation. At

substrate saturation the core enzymes lag behind indicating that they are very picky with very few binding and attack sites. CBM swap between Cel6A and Cel7A and also linker modifications of Cel7A seems to affect the behavior of the enzymes suggesting that all domains are directly involved in the hydrolysis of cellulose.

We found very strong enzyme-substrate interactions in the catalytic tunnel of Cel6A using isothermal titration calorimetry. At least as strong as those reported for Cel7A. Unlike Cel7A our results do not indicate a high affinity product site. We suggest therefore that the dynamic architecture of the catalytic domain of Cel6A might be the driving force for the forward processive movement of the enzyme.

When studying the two CBHs Cel6A and Cel7A we will naturally close with a few remarks on their strong synergistic interplay. The Exo-exo synergy depends on the experimental conditions and the presence of CBMs. The synergy was strongest between wt enzymes at high enzyme concentration and low substrate concentration. We found minor endo-lytic activity of both Cel6A and Cel7A, but suggest another interpretation to explain the current synergy. Instead we suggest that their different specificities for the substrate results in better substrate for each other by removing potential obstacles and by releasing new attack sites.

In conclusion we have provided insight into a better understanding of the two abundant cellobiohydrolases Cel6A and Cel7A by comparing them kinetically both mutual and by including selected variants. Even though industrial conditions vary from those presented here we believe that such information will be relevant when engineering cellulases for the production of sustainable bioethanol.

# References

---

- Arola, S. & Linder, M.B., 2016. Binding of cellulose binding modules reveal differences between cellulose substrates. *Scientific Reports*, 6, 35358.
- Bajzer, Ž. & Strehler, E.E., 2012. About and beyond the Henri-Michaelis–Menten rate equation for single-substrate enzyme kinetics. *Biochemical and Biophysical Research Communications*, 417, 982-985.
- Bansal, P., Hall, M., Realf, M.J., Lee, J.H. & Bommarius, A.S., 2009. Modeling cellulase kinetics on lignocellulosic substrates. *Biotechnol Adv*, 27, 833-48.
- Barr, B.K., Hsieh, Y.L., Ganem, B. & Wilson, D.B., 1996. Identification of two functionally different classes of exocellulases. *Biochemistry*, 35, 586-92.
- Beckham, G.T., Bomble, Y.J., Matthews, J.F., Taylor, C.B., Resch, M.G., Yarbrough, J.M., Decker, S.R., Bu, L., Zhao, X., McCabe, C., Wohler, J., Bergenstråhle, M., Brady, J.W., Adney, W.S., Himmel, M.E. & Crowley, M.F., 2010a. The O-glycosylated linker from the *Trichoderma reesei* Family 7 cellulase is a flexible, disordered protein. *Biophys J*, 99, 3773-81.
- Beckham, G.T., Matthews, J.F., Bomble, Y.J., Bu, L., Adney, W.S., Himmel, M.E., Nimlos, M.R. & Crowley, M.F., 2010b. Identification of Amino Acids Responsible for Processivity in a Family 1 Carbohydrate-Binding Module from a Fungal Cellulase. *The Journal of Physical Chemistry B*, 114, 1447-1453.
- Beckham, G.T., Matthews, J.F., Peters, B., Bomble, Y.J., Himmel, M.E. & Crowley, M.F., 2011. Molecular-level origins of biomass recalcitrance: decrystallization free energies for four common cellulose polymorphs. *J Phys Chem B*, 115, 4118-27.
- Bezerra, R.M. & Dias, A.A., 2004. Discrimination among eight modified michaelis-menten kinetics models of cellulose hydrolysis with a large range of substrate/enzyme ratios: inhibition by cellobiose. *Appl Biochem Biotechnol*, 112, 173-84.
- Boisset, C., Fraschini, C., Schüle, M., Henrissat, B. & Chanzy, H., 2000. Imaging the enzymatic digestion of bacterial cellulose ribbons reveals the endo character of the cellobiohydrolase Cel6A from *Humicola insolens* and its mode of synergy with cellobiohydrolase Cel7A. *Appl Environ Microbiol*, 66, 1444-52.
- Boraston, A.B., Bolam, D.N., Gilbert, H.J. & Davies, G.J., 2004. Carbohydrate-binding modules: fine-tuning polysaccharide recognition. *Biochem J*, 382, 769-81.
- Bu, L., Beckham, G.T., Crowley, M.F., Chang, C.H., Matthews, J.F., Bomble, Y.J., Adney, W.S., Himmel, M.E. & Nimlos, M.R., 2009. The Energy Landscape for the Interaction of the Family 1 Carbohydrate-Binding Module and the Cellulose Surface is Altered by Hydrolyzed Glycosidic Bonds. *The Journal of Physical Chemistry B*, 113, 10994-11002.
- Bubner, P., Plank, H. & Nidetzky, B., 2013. Visualizing cellulase activity. *Biotechnol Bioeng*, 110, 1529-49.

- Cannella, D., Möllers, K.B., Frigaard, N.U., Jensen, P.E., Bjerrum, M.J., Johansen, K.S. & Felby, C., 2016. Light-driven oxidation of polysaccharides by photosynthetic pigments and a metalloenzyme. *Nat Commun*, 7, 11134.
- Carrard, G. & Linder, M., 1999. Widely different off rates of two closely related cellulose-binding domains from *Trichoderma reesei*. *Eur J Biochem*, 262, 637-43.
- Claeysens, M., Tomme, P., Brewer, C.F. & Hehre, E.J., 1990. Stereochemical course of hydrolysis and hydration reactions catalysed by cellobiohydrolases I and II from *Trichoderma reesei*. *FEBS Lett*, 263, 89-92.
- Claeysens, M., Van Tilbeurgh, H., Tomme, P., Wood, T.M. & Mcrae, S.I., 1989. Fungal cellulase systems. Comparison of the specificities of the cellobiohydrolases isolated from *Penicillium pinophilum* and *Trichoderma reesei*. *Biochem J*, 261, 819-25.
- Colussi, F., Sørensen, T.H., Alasepp, K., Kari, J., Cruys-Bagger, N., Windahl, M.S., Olsen, J.P., Borch, K. & Westh, P., 2015. Probing substrate interactions in the active tunnel of a catalytically deficient cellobiohydrolase (Cel7). *J Biol Chem*, 290, 2444-54.
- Cruys-Bagger, N., Elmerdahl, J., Praestgaard, E., Borch, K. & Westh, P., 2013a. A steady-state theory for processive cellulases. *FEBS J*, 280, 3952-61.
- Cruys-Bagger, N., Elmerdahl, J., Praestgaard, E., Tatsumi, H., Spodsberg, N., Borch, K. & Westh, P., 2012a. Pre-steady-state kinetics for hydrolysis of insoluble cellulose by cellobiohydrolase Cel7A. *J Biol Chem*, 287, 18451-8.
- Cruys-Bagger, N., Ren, G., Tatsumi, H., Baumann, M.J., Spodsberg, N., Andersen, H.D., Gorton, L., Borch, K. & Westh, P., 2012b. An amperometric enzyme biosensor for real-time measurements of cellobiohydrolase activity on insoluble cellulose. *Biotechnol Bioeng*, 109, 3199-204.
- Cruys-Bagger, N., Tatsumi, H., Ren, G.R., Borch, K. & Westh, P., 2013b. Transient kinetics and rate-limiting steps for the processive cellobiohydrolase Cel7A: effects of substrate structure and carbohydrate binding domain. *Biochemistry*, 52, 8938-48.
- Davies, G. & Henrissat, B., 1995. Structures and mechanisms of glycosyl hydrolases. *Structure*, 3, 853-9.
- Davies, G.J., Wilson, K.S. & Henrissat, B., 1997. Nomenclature for sugar-binding subsites in glycosyl hydrolases. *Biochem J*, 321 ( Pt 2), 557-9.
- Divne, C., Ståhlberg, J., Reinikainen, T., Ruohonen, L., Pettersson, G., Knowles, J.K., Teeri, T.T. & Jones, T.A., 1994. The three-dimensional crystal structure of the catalytic core of cellobiohydrolase I from *Trichoderma reesei*. *Science*, 265, 524-8.
- Divne, C., Ståhlberg, J., Teeri, T.T. & Jones, T.A., 1998. High-resolution crystal structures reveal how a cellulose chain is bound in the 50 Å long tunnel of cellobiohydrolase I from *Trichoderma reesei*. *J Mol Biol*, 275, 309-25.
- Emaze, 2016. <https://www.emaze.com/@AWOLTCIT/Molecules-of-Life:-Cellulose-copy1-copy2> [online]. [Accessed Access Date 16th December 2016].
- Eriksson, T., Karlsson, J. & Tjerneld, F., 2002. A model explaining declining rate in hydrolysis of lignocellulose substrates with cellobiohydrolase I (Cel7A) and

- endoglucanase I (Cel7B) of *Trichoderma reesei*. *Applied Biochemistry and Biotechnology*, 101, 41-60.
- Farrell, A.E., Plevin, R.J., Turner, B.T., Jones, A.D., O'hare, M. & Kammen, D.M., 2006. Ethanol can contribute to energy and environmental goals. *Science*, 311, 506-8.
- Fägerstam, L.G. & Pettersson, G.L., 1980. The 1.4- $\beta$ glucan cellobiohydrolase of *Trichoderma reesei* QM 9414 - A new type of cellulolytic synergismThe 1.4- $\beta$ -glucan cellobiohydrolase of *Trichoderma reesei* QM 9414 - A new type of cellulolytic synergism. *FEBS LETTERS*, 119, 97-100.
- Ganner, T., Bubner, P., Eibinger, M., Mayrhofer, C., Plank, H. & Nidetzky, B., 2012. Dissecting and reconstructing synergism: in situ visualization of cooperativity among cellulases. *J Biol Chem*, 287, 43215-22.
- Golan, A.E., 2011. *Cellulase: Types, Actions, Mechanisms and Uses* New York: Nova Science Publishers, Inc.
- Gruno, M., Våljamäe, P., Pettersson, G. & Johansson, G., 2004. Inhibition of the *Trichoderma reesei* cellulases by cellobiose is strongly dependent on the nature of the substrate. *Biotechnol Bioeng*, 86, 503-11.
- Hall, M., Bansal, P., Lee, J.H., Reaff, M.J. & Bommaris, A.S., 2011. Biological pretreatment of cellulose: enhancing enzymatic hydrolysis rate using cellulose-binding domains from cellulases. *Bioresour Technol*, 102, 2910-5.
- Harjunpää, V., Teleman, A., Koivula, A., Ruohonen, L., Teeri, T.T., Teleman, O. & Drakenberg, T., 1996. Cello-oligosaccharide hydrolysis by cellobiohydrolase II from *Trichoderma reesei*. Association and rate constants derived from an analysis of progress curves. *Eur J Biochem*, 240, 584-91.
- Harrison, M.J., Nouwens, A.S., Jardine, D.R., Zachara, N.E., Gooley, A.A., Nevalainen, H. & Packer, N.H., 1998. Modified glycosylation of cellobiohydrolase I from a high cellulase-producing mutant strain of *Trichoderma reesei*. *Eur J Biochem*, 256, 119-27.
- Henrissat, B., Driguez, H., Viet, C. & Schülein, M., 1985. Synergism of Cellulases from *Trichoderma reesei* in the Degradation of Cellulose. *Nature Biotechnology*, 3, 722-726.
- Himmel, M.E., Ding, S.Y., Johnson, D.K., Adney, W.S., Nimlos, M.R., Brady, J.W. & Foust, T.D., 2007. Biomass recalcitrance: engineering plants and enzymes for biofuels production. *Science*, 315, 804-7.
- Himmel, M.E., Ruth, M.F. & Wyman, C.E., 1999. Cellulase for commodity products from cellulosic biomass. *Curr Opin Biotechnol*, 10, 358-64.
- Hoffrén, A.M., Teeri, T.T. & Teleman, O., 1995. Molecular dynamics simulation of fungal cellulose-binding domains: differences in molecular rigidity but a preserved cellulose binding surface. *Protein Eng*, 8, 443-50.
- Horn, S.J., Sørli, M., Vårum, K.M., Våljamäe, P. & Eijsink, V.G., 2012. Measuring processivity. *Methods Enzymol*, 510, 69-95.
- Hoshino, E., Shiroishi, M., Amano, Y., Nomura, M. & Kanda, T., 1997. Synergistic actions of exo-type cellulases in the hydrolysis of cellulose with different crystallinities. *Journal of Fermentation and Bioengineering*, 84, 300-306.

- Igarashi, K., Uchihashi, T., Koivula, A., Wada, M., Kimura, S., Okamoto, T., Penttilä, M., Ando, T. & Samejima, M., 2011. Traffic jams reduce hydrolytic efficiency of cellulase on cellulose surface. *Science*, 333, 1279-82.
- Irwin, D.C., Spezio, M., Walker, L.P. & Wilson, D.B., 1993. Activity studies of eight purified cellulases: Specificity, synergism, and binding domain effects. *Biotechnol Bioeng*, 42, 1002-13.
- Jalak, J., Kurasin, M., Teugjas, H. & Valjamae, P., 2012. Endo-exo Synergism in Cellulose Hydrolysis Revisited. *The Journal of Biological Chemistry*, 287, 28802-28815.
- Jalak, J. & Våljamäe, P., 2010. Mechanism of initial rapid rate retardation in cellobiohydrolase catalyzed cellulose hydrolysis. *Biotechnol Bioeng*, 106, 871-83.
- Jalak, J. & Våljamäe, P., 2014. Multi-Mode Binding of Cellobiohydrolase Cel7A from *Trichoderma reesei* to Cellulose. *PLoS One*, 9, e108181.
- Jeoh, T., Ishizawa, C.I., Davis, M.F., Himmel, M.E., Adney, W.S. & Johnson, D.K., 2007. Cellulase digestibility of pretreated biomass is limited by cellulose accessibility. *Biotechnol Bioeng*, 98, 112-22.
- Jørgensen, H., Bach Kristensen, J. & Felby, C., 2007. Enzymatic conversion of lignocellulose into fermentable sugars: challenges and opportunities. *Biofuels, Bioprod. Bioref*, 1, 119-134.
- Kari, J., Andersen, M., Borch, K. & Westh, P., 2017. An inverse Michaelis-Menten approach for interfacial enzyme kinetics. *Submitted catalysis*.
- Kari, J., Kont, R., Borch, K., Buskov, S., Olsen, J.P., Cruz-Bagger, N., Våljamäe, P. & Westh, P., 2016. Anomeric Selectivity and Product Profile of a Processive Cellulase. *Biochemistry*, 167-178.
- Kari, J., Olsen, J., Borch, K., Cruys-Bagger, N., Jensen, K. & Westh, P., 2014. Kinetics of cellobiohydrolase (Cel7A) variants with lowered substrate affinity. *J Biol Chem*, 289, 32459-68.
- Kim, I.J., Lee, H.J., Choi, I.G. & Kim, K.H., 2014. Synergistic proteins for the enhanced enzymatic hydrolysis of cellulose by cellulase. *Appl Microbiol Biotechnol*, 98, 8469-80.
- Kipper, K., Våljamäe, P. & Johansson, G., 2005. Processive action of cellobiohydrolase Cel7A from *Trichoderma reesei* is revealed as 'burst' kinetics on fluorescent polymeric model substrates. *Biochem J*, 385, 527-35.
- Klemm, D., Heublein, B., Fink, H.P. & Bohn, A., 2005. Cellulose: fascinating biopolymer and sustainable raw material. *Angew Chem Int Ed Engl*, 44, 3358-93.
- Knott, B.C., Crowley, M.F., Himmel, M.E., Ståhlberg, J. & Beckham, G.T., 2014a. Carbohydrate-Protein Interactions That Drive Processive Polysaccharide Translocation in Enzymes Revealed from a Computational Study of Cellobiohydrolase Processivity. *Journal of the American Chemical Society*, 136, 8810-8819.
- Knott, B.C., Haddad Momeni, M., Crowley, M.F., Mackenzie, L.F., Götz, A.W., Sandgren, M., Withers, S.G., Ståhlberg, J. & Beckham, G.T., 2014b. The mechanism of cellulose hydrolysis by a two-step, retaining cellobiohydrolase

- elucidated by structural and transition path sampling studies. *J Am Chem Soc*, 136, 321-9.
- Knowles, J., Lehtovaara, P. & Teeri, T., 1987. Cellulase families and their genes. *TIBTECH*, 5, 255-261.
- Koivula, A., Kinnari, T., Harjunpää, V., Ruohonen, L., Teleman, A., Drakenberg, T., Rouvinen, J., Jones, T.A. & Teeri, T.T., 1998. Tryptophan 272: an essential determinant of crystalline cellulose degradation by *Trichoderma reesei* cellobiohydrolase Cel6A. *FEBS Lett*, 429, 341-6.
- Koivula, A., Ruohonen, L., Wohlfahrt, G., Reinikainen, T., Teeri, T.T., Piens, K., Claeyssens, M., Weber, M., Vasella, A., Becker, D., Sinnott, M.L., Zou, J.Y., Kleywegt, G.J., Szardenings, M., Ståhlberg, J. & Jones, T.A., 2002. The active site of cellobiohydrolase Cel6A from *Trichoderma reesei*: the roles of aspartic acids D221 and D175. *J Am Chem Soc*, 124, 10015-24.
- Kraulis, J., Clore, G.M., Nilges, M., Jones, T.A., Pettersson, G., Knowles, J. & Gronenborn, A.M., 1989. Determination of the three-dimensional solution structure of the C-terminal domain of cellobiohydrolase I from *Trichoderma reesei*. A study using nuclear magnetic resonance and hybrid distance geometry-dynamical simulated annealing. *Biochemistry*, 28, 7241-57.
- Kurasin, M. & Väljamäe, P., 2011. Processivity of cellobiohydrolases is limited by the substrate. *J Biol Chem*, 286, 169-77.
- Kuusk, S., Sørli, M. & Väljamäe, P., 2015. The predominant molecular state of bound enzyme determines the strength and type of product inhibition in the hydrolysis of recalcitrant polysaccharides by processive enzymes. *J Biol Chem*, 290, 11678-91.
- Kyriacou, A., Neufeld, R.J. & Mackenzie, C.R., 1989. Reversibility and competition in the adsorption of *Trichoderma reesei* cellulase components. *Biotechnol Bioeng*, 33, 631-7.
- Langsford, M.L., Gilkes, N.R., Singh, B., Moser, B., Miller, R.C., Warren, R.A. & Kilburn, D.G., 1987. Glycosylation of bacterial cellulases prevents proteolytic cleavage between functional domains. *FEBS Lett*, 225, 163-7.
- Le Costaouëc, T., Pakarinen, A., Várnai, A., Puranen, T. & Viikari, L., 2013. The role of carbohydrate binding module (CBM) at high substrate consistency: comparison of *Trichoderma reesei* and *Thermoascus aurantiacus* Cel7A (CBHI) and Cel5A (EGII). *Bioresour Technol*, 143, 196-203.
- Lemos, M.A., Teixeira, J.A., Domingues, M.R.M., Mota, M. & Gama, F.M., 2003. The enhancement of the cellulolytic activity of cellobiohydrolase I and endoglucanase by the addition of cellulose binding domains derived from *Trichoderma reesei*. *Enzyme Microb Technol*, 32, 35-40.
- Levasseur, A., Drula, E., Lombard, V., Coutinho, P.M. & Henrissat, B., 2013. Expansion of the enzymatic repertoire of the CAZy database to integrate auxiliary redox enzymes. *Biotechnol Biofuels*, 6, 41.
- Linder, M., Lindeberg, G., Reinikainen, T., Teeri, T.T. & Pettersson, G., 1995a. The difference in affinity between two fungal cellulose-binding domains is dominated by a single amino acid substitution. *FEBS Lett*, 372, 96-8.



- Linder, M., Mattinen, M.L., Kontteli, M., Lindeberg, G., Ståhlberg, J., Drakenberg, T., Reinikainen, T., Pettersson, G. & Annila, A., 1995b. Identification of functionally important amino acids in the cellulose-binding domain of *Trichoderma reesei* cellobiohydrolase I. *Protein Sci*, 4, 1056-64.
- Linder, M., Salovuori, I., Ruohonen, L. & Teeri, T.T., 1996. Characterization of a double cellulose-binding domain. Synergistic high affinity binding to crystalline cellulose. *J Biol Chem*, 271, 21268-72.
- Lo Leggio, L., Welner, D. & De Maria, L., 2012. A structural overview of GH61 proteins - fungal cellulose degrading polysaccharide monooxygenases. *Comput Struct Biotechnol J*, 2, e201209019.
- Lynd, L.R., Cushman, J.H., Nichols, R.J. & Wyman, C.E., 1991. Fuel ethanol from cellulosic biomass. *Science*, 251, 1318-23.
- Mansfield, S.D., Mooney, C. & Saddler, J.N., 1999. Substrate and Enzyme Characteristics that Limit Cellulose Hydrolysis. *Biotechnol Prog*, 15, 804-816.
- Martinez, D., Berka, R.M., Henrissat, B., Saloheimo, M., Arvas, M., Baker, S.E., Chapman, J., Chertkov, O., Coutinho, P.M., Cullen, D., Danchin, E.G., Grigoriev, I.V., Harris, P., Jackson, M., Kubicek, C.P., Han, C.S., Ho, I., Larrondo, L.F., De Leon, A.L., Magnuson, J.K., Merino, S., Misra, M., Nelson, B., Putnam, N., Robbertse, B., Salamov, A.A., Schmoll, M., Terry, A., Thayer, N., Westerholm-Parvinen, A., Schoch, C.L., Yao, J., Barabote, R., Barbote, R., Nelson, M.A., Detter, C., Bruce, D., Kuske, C.R., Xie, G., Richardson, P., Rokhsar, D.S., Lucas, S.M., Rubin, E.M., Dunn-Coleman, N., Ward, M. & Brettin, T.S., 2008. Genome sequencing and analysis of the biomass-degrading fungus *Trichoderma reesei* (syn. *Hypocrea jecorina*). *Nat Biotechnol*, 26, 553-60.
- Mattinen, M.L., Kontteli, M., Kerovuo, J., Linder, M., Annila, A., Lindeberg, G., Reinikainen, T. & Drakenberg, T., 1997a. Three-dimensional structures of three engineered cellulose-binding domains of cellobiohydrolase I from *Trichoderma reesei*. *Protein Sci*, 6, 294-303.
- Mattinen, M.L., Linder, M., Teleman, A. & Annila, A., 1997b. Interaction between cellobiohydrolase and cellulose binding domains from *Trichoderma reesei* cellulases. *FEBS Lett*, 407, 291-6.
- Mayes, H.B., Knott, B.C., Crowley, M.F., Broadbelt, L.J., Stahlberg, J. & Beckham, G.T., 2016. Who's on base? Revealing the catalytic mechanism of inverting family 6 glycoside hydrolases. *Chemical Science*, 7, 5955-5968.
- Mcfarlane, H.E., Döring, A. & Persson, S., 2014. The cell biology of cellulose synthesis. *Annu Rev Plant Biol*, 65, 69-94.
- Medve, J., Karlsson, J., Lee, D. & Tjerneld, F., 1998. Hydrolysis of microcrystalline cellulose by cellobiohydrolase I and endoglucanase II from *Trichoderma reesei*: adsorption, sugar production pattern, and synergism of the enzymes. *Biotechnol Bioeng*, 59, 621-34.
- Medve, J., Ståhlberg, J. & Tjerneld, F., 1994. Adsorption and synergism of cellobiohydrolase I and II of *Trichoderma reesei* during hydrolysis of microcrystalline cellulose. *Biotechnol Bioeng*, 44, 1064-73.

- Medve, J., Ståhlberg, J. & Tjerneld, F., 1997. Isotherms for adsorption of cellobiohydrolase I and II from *Trichoderma reesei* on microcrystalline cellulose. *Appl Biochem Biotechnol*, 66, 39-56.
- Murphy, L., Bohlin, C., Baumann, M.J., Olsen, S.N., Sørensen, T.H., Anderson, L., Borch, K. & Westh, P., 2013. Product inhibition of five *Hypocrea jecorina* cellulases. *Enzyme Microb Technol*, 52, 163-9.
- Nasdaq, 2016. <http://www.nasdaq.com/markets/crude-oil.aspx?timeframe=3y>. visited 27 th December 2016.
- Nelson & Cox, 2008. *Lehninger principles of biochemistry*, 5. ed. New York: W.H.Freeman.
- Nidetzky, B., Steiner, W. & Claeyssens, M., 1994a. Cellulose hydrolysis by the cellulases from *Trichoderma reesei*: adsorptions of two cellobiohydrolases, two endocellulases and their core proteins on filter paper and their relation to hydrolysis. *Biochem J*, 303 ( Pt 3), 817-23.
- Nidetzky, B., Steiner, W., Hayn, M. & Claeyssens, M., 1994b. Cellulose hydrolysis by the cellulases from *Trichoderma reesei*: a new model for synergistic interaction. *Biochem J*, 298 Pt 3, 705-10.
- Nimlos, M.R., Beckham, G.T., Matthews, J.F., Bu, L., Himmel, M.E. & Crowley, M.F., 2012. Binding preferences, surface attachment, diffusivity, and orientation of a family 1 carbohydrate-binding module on cellulose. *J Biol Chem*, 287, 20603-12.
- Nimlos, M.R., Matthews, J.F., Crowley, M.F., Walker, R.C., Chukkapalli, G., Brady, J.W., Adney, W.S., Cleary, J.M., Zhong, L. & Himmel, M.E., 2007. Molecular modeling suggests induced fit of Family I carbohydrate-binding modules with a broken-chain cellulose surface. *Protein Eng Des Sel*, 20, 179-87.
- Olsen, J.P., Alasepp, K., Kari, J., Cruys-Bagger, N., Borch, K. & Westh, P., 2015. Mechanism of product inhibition for cellobiohydrolase Cel7A during hydrolysis of insoluble cellulose. *Biotechnol Bioeng*.
- Olsen, J.P., Kari, J., Borch, K. & Westh, P., 2017. A quenched-flow system for measuring heterogeneous enzyme kinetics with sub-second time resolution. *Microbial Technology submitted*.
- Pakarinen, A., Haven, M.O., Djajadi, D.T., Várnai, A., Puranen, T. & Viikari, L., 2014. Cellulases without carbohydrate-binding modules in high consistency ethanol production process. *Biotechnol Biofuels*, 7, 27.
- Palonen, H., Tenkanen, M. & Linder, M., 1999. Dynamic interaction of *Trichoderma reesei* cellobiohydrolases Cel6A and Cel7A and cellulose at equilibrium and during hydrolysis. *Appl Environ Microbiol*, 65, 5229-33.
- Payne, C.M., Bomble, Y.J., Taylor, C.B., McCabe, C., Himmel, M.E., Crowley, M.F. & Beckham, G.T., 2011. Multiple functions of aromatic-carbohydrate interactions in a processive cellulase examined with molecular simulation. *J Biol Chem*, 286, 41028-35.
- Payne, C.M., Jiang, W., Shirts, M.R., Himmel, M.E., Crowley, M.F. & Beckham, G.T., 2013a. Glycoside hydrolase processivity is directly related to oligosaccharide binding free energy. *J Am Chem Soc*, 135, 18831-9.

- Payne, C.M., Knott, B.C., Mayes, H.B., Hansson, H., Himmel, M.E., Sandgren, M., Ståhlberg, J. & Beckham, G.T., 2015. Fungal Cellulases. *Chem Rev*.
- Payne, C.M., Resch, M.G., Chen, L., Crowley, M.F., Himmel, M.E., Taylor, L.E., Sandgren, M., Ståhlberg, J., Stals, I., Tan, Z. & Beckham, G.T., 2013b. Glycosylated linkers in multimodular lignocellulose-degrading enzymes dynamically bind to cellulose. *Proc Natl Acad Sci U S A*, 110, 14646-51.
- Percival Zhang, Y.H., Himmel, M.E. & Mielenz, J.R., 2006. Outlook for cellulase improvement: screening and selection strategies. *Biotechnol Adv*, 24, 452-81.
- Poidevin, L., Feliu, J., Doan, A., Berrin, J.G., Bey, M., Coutinho, P.M., Henrissat, B., Record, E. & Heiss-Blanquet, S., 2013. Insights into exo- and endoglucanase activities of family 6 glycoside hydrolases from *Podospora anserina*. *Appl Environ Microbiol*, 79, 4220-9.
- Praestgaard, E., Elmerdahl, J., Murphy, L., Nymand, S., Mcfarland, K.C., Borch, K. & Westh, P., 2011. A kinetic model for the burst phase of processive cellulases. *FEBS J*, 278, 1547-60.
- Receveur, V., Czjzek, M., Schülein, M., Panine, P. & Henrissat, B., 2002. Dimension, shape, and conformational flexibility of a two domain fungal cellulase in solution probed by small angle X-ray scattering. *J Biol Chem*, 277, 40887-92.
- Reese, E.T., 1976. History of the cellulase program at the U.S. army Natick Development Center. *Biotechnol Bioeng Symp*, 9-20.
- Reese, E.T., Siu, R.G. & Levinson, H.S., 1950. The biological degradation of soluble cellulose derivatives and its relationship to the mechanism of cellulose hydrolysis. *J Bacteriol*, 59, 485-97.
- Rosgaard, L., Pedersen, S., Langston, J., Akerhielm, D., Cherry, J.R. & Meyer, A.S., 2007. Evaluation of minimal *Trichoderma reesei* cellulase mixtures on differently pretreated Barley straw substrates. *Biotechnol Prog*, 23, 1270-6.
- Rouvinen, J., Bergfors, T., Teeri, T., Knowles, J.K. & Jones, T.A., 1990. Three-dimensional structure of cellobiohydrolase II from *Trichoderma reesei*. *Science*, 249, 380-6.
- Ruiz, D.M., Turowski, V.R. & Murakami, M.T., 2016. Effects of the linker region on the structure and function of modular GH5 cellulases. *Sci Rep*, 6, 28504.
- Sammond, D.W., Payne, C.M., Brunecky, R., Himmel, M.E., Crowley, M.F. & Beckham, G.T., 2012. Cellulase linkers are optimized based on domain type and function: insights from sequence analysis, biophysical measurements, and molecular simulation. *PLoS One*, 7, e48615.
- Sattler, W., Esterbauer, H., Glatter, O. & Steiner, W., 1989. The effect of enzyme concentration on the rate of the hydrolysis of cellulose. *Biotechnol Bioeng*, 33, 1221-34.
- Shen, H., Schmuck, M., Pilz, I., Gilkes, N.R., Kilburn, D.G., Miller, R.C. & Warren, R.A., 1991. Deletion of the linker connecting the catalytic and cellulose-binding domains of endoglucanase A (CenA) of *Cellulomonas fimi* alters its conformation and catalytic activity. *J Biol Chem*, 266, 11335-40.

- Sonan, G.K., Receveur-Brechot, V., Duez, C., Aghajari, N., Czjzek, M., Haser, R. & Gerday, C., 2007. The linker region plays a key role in the adaptation to cold of the cellulase from an Antarctic bacterium. *Biochem J*, 407, 293-302.
- Srisodsuk, M., Reinikainen, T., Penttilä, M. & Teeri, T.T., 1993. Role of the interdomain linker peptide of *Trichoderma reesei* cellobiohydrolase I in its interaction with crystalline cellulose. *J Biol Chem*, 268, 20756-61.
- Strobel, K.L., Pfeiffer, K.A., Blanch, H.W. & Clark, D.S., 2015. Engineering Cel7A Carbohydrate Binding Module and Linker for Reduced Lignin Inhibition. *Biotechnol Bioeng*.
- Ståhlberg, J., 1993. *Trichoderma reesei* has no true exo-cellulase: all intact and truncated cellulases produce new reducing end groups on cellulose. *Biochimica et biophysica acta. General subjects. - Amsterdam*, 1157, 107-113.
- Ståhlberg, J., Divne, C., Koivula, A., Piens, K., Claeysens, M., Teeri, T.T. & Jones, T.A., 1996. Activity studies and crystal structures of catalytically deficient mutants of cellobiohydrolase I from *Trichoderma reesei*. *J Mol Biol*, 264, 337-49.
- Ståhlberg, J., Johansson, G. & Pettersson, G., 1991. A New Model For Enzymatic Hydrolysis of Cellulose Based on the Two-Domain Structure of Cellobiohydrolase I. *Nat Biotech*, 9, 286-290.
- Sørensen, T.H., Cruys-Bagger, N., Borch, K. & Westh, P., 2015a. Free Energy Diagram for the Heterogeneous Enzymatic Hydrolysis of Glycosidic Bonds in Cellulose. *J Biol Chem*, 290, 22203-11.
- Sørensen, T.H., Cruys-Bagger, N., Windahl, M.S., Badino, S.F., Borch, K. & Westh, P., 2015b. Temperature Effects on Kinetic Parameters and Substrate Affinity of Cel7A Cellobiohydrolases. *J Biol Chem*, 290, 22193-202.
- Sørensen, T.H., Windahl, M.S., Mcbrayer, B., Kari, J., Olsen, J.P., Borch, K. & Westh, P., 2017. Loop variants of the thermophile *Rasamsonia emersonii* Cel7A with improved activity against cellulose. *Biotechnol Bioeng*, 114, 53-62.
- Takashima, S., Ohno, M., Hidaka, M., Nakamura, A., Masaki, H. & Uozumi, T., 2007. Correlation between cellulose binding and activity of cellulose-binding domain mutants of *Humicola grisea* cellobiohydrolase 1. *FEBS Letters*, 581, 5891-5896.
- Teeri, T.T., 1997. Crystalline cellulose degradation: new insight into the function of cellobiohydrolases. *Trends in Biotechnology*, 15, 160-167.
- Teugjas, H. & Väljamäe, P., 2013. Product inhibition of cellulases studied with <sup>14</sup>C-labeled cellulose substrates. *Biotechnol Biofuels*, 6, 104.
- Ting, C.L., Makarov, D.E. & Wang, Z.G., 2009. A kinetic model for the enzymatic action of cellulase. *J Phys Chem B*, 113, 4970-7.
- Tomme, P., Heriban, V. & Claeysens, M., 1990. ADSORPTION OF 2 CELLOBIOHYDROLASES FROM TRICHODERMA-REESEI TO AVICEL - EVIDENCE FOR EXO-EXO SYNERGISM AND POSSIBLE LOOSE COMPLEX-FORMATION. *Biotechnology Letters*, 12, 525-530.
- Tomme, P., Van Tilbeurgh, H., Pettersson, G., Van Damme, J., Vandekerckhove, J., Knowles, J., Teeri, T. & Claeysens, M., 1988. Studies of the cellulolytic system of *Trichoderma reesei* QM 9414. Analysis of domain function in two cellobiohydrolases by limited proteolysis. *Eur J Biochem*, 170, 575-81.

- Untc, 2016. Paris Agreement:  
[https://treaties.un.org/pages/ViewDetails.aspx?src=TREATY&mtdsg\\_no=XXVII-7-d&chapter=27&clang=en](https://treaties.un.org/pages/ViewDetails.aspx?src=TREATY&mtdsg_no=XXVII-7-d&chapter=27&clang=en). Visited 26th January 2017.
- Vaaje-Kolstad, G., Westereng, B., Horn, S.J., Liu, Z., Zhai, H., Sørli, M. & Eijsink, V.G., 2010. An oxidative enzyme boosting the enzymatic conversion of recalcitrant polysaccharides. *Science*, 330, 219-22.
- Van Tilbeurgh, H., Tomme, P., Claeyssens, M., Bhikhabhai, R. & Pettersson, G., 1986. Limited proteolysis of the cellobiohydrolase I from *Trichoderma reesei*. *FEBS Letters*, 204, 223-227.
- Vinzant, T.B., Adney, W.S., Decker, S.R., Baker, J.O., Kinter, M.T., Sherman, N.E., Fox, J.W. & Himmel, M.E., 2001. Fingerprinting *Trichoderma reesei* hydrolases in a commercial cellulase preparation. *Appl Biochem Biotechnol*, 91-93, 99-107.
- Von Ossowski, I., Eaton, J.T., Czjzek, M., Perkins, S.J., Frandsen, T.P., Schülein, M., Panine, P., Henrissat, B. & Receveur-Bréchet, V., 2005. Protein disorder: conformational distribution of the flexible linker in a chimeric double cellulase. *Biophys J*, 88, 2823-32.
- Várnai, A., Siika-Aho, M. & Viikari, L., 2013. Carbohydrate-binding modules (CBMs) revisited: reduced amount of water counterbalances the need for CBMs. *Biotechnol Biofuels*, 6, 30.
- Väljamäe, P., Sild, V., Pettersson, G. & Johansson, G., 1998. The initial kinetics of hydrolysis by cellobiohydrolases I and II is consistent with a cellulose surface-erosion model. *Eur J Biochem*, 253, 469-75.
- Wolfenden, R. & Snider, M.J., 2001. The depth of chemical time and the power of enzymes as catalysts. *Acc Chem Res*, 34, 938-45.
- Yang, B., Willies, D.M. & Wyman, C.E., 2006. Changes in the enzymatic hydrolysis rate of Avicel cellulose with conversion. *Biotechnol Bioeng*, 94, 1122-8.
- Zechel, D.L. & Withers, S.G., 2000. Glycosidase Mechanisms: Anatomy of a Finely Tuned Catalyst. *Accounts of Chemical Research*, 33, 11-18.
- Zhang, Y.H. & Lynd, L.R., 2004. Toward an aggregated understanding of enzymatic hydrolysis of cellulose: noncomplexed cellulase systems. *Biotechnol Bioeng*, 88, 797-824.
- Zou, J., Kleywegt, G.J., Ståhlberg, J., Driguez, H., Nerinckx, W., Claeyssens, M., Koivula, A., Teeri, T.T. & Jones, T.A., 1999. Crystallographic evidence for substrate ring distortion and protein conformational changes during catalysis in cellobiohydrolase Ce16A from *trichoderma reesei*. *Structure*, 7, 1035-45.

Direct Kinetic Comparison of the two  
Cellobiohydrolases Cel6A and Cel7A from  
*Hypocrea jecorina*

---

*Accepted for publication, In press*

I



## Accepted Manuscript

Direct kinetic comparison of the two cellobiohydrolases Cel6A and Cel7A from *Hypocrea jecorina*

Silke Flindt Badino, Jeppe Kari, Stefan Jarl Christensen, Kim Borch, Peter Westh



PII: S1570-9639(17)30196-6  
DOI: doi: [10.1016/j.bbapap.2017.08.013](https://doi.org/10.1016/j.bbapap.2017.08.013)  
Reference: BBAPAP 39998

To appear in:

Received date: 12 April 2017  
Revised date: 25 July 2017  
Accepted date: 14 August 2017

Please cite this article as: Silke Flindt Badino, Jeppe Kari, Stefan Jarl Christensen, Kim Borch, Peter Westh, Direct kinetic comparison of the two cellobiohydrolases Cel6A and Cel7A from *Hypocrea jecorina*, (2017), doi: [10.1016/j.bbapap.2017.08.013](https://doi.org/10.1016/j.bbapap.2017.08.013)

This is a PDF file of an unedited manuscript that has been accepted for publication. As a service to our customers we are providing this early version of the manuscript. The manuscript will undergo copyediting, typesetting, and review of the resulting proof before it is published in its final form. Please note that during the production process errors may be discovered which could affect the content, and all legal disclaimers that apply to the journal pertain.



# Direct kinetic comparison of the two cellobiohydrolases Cel6A and Cel7A from *Hypocrea jecorina*

Silke Flindt Badino<sup>1</sup>, Jeppe Kari<sup>1</sup>, Stefan Jarl Christensen<sup>1</sup>, Kim Borch<sup>2</sup> and Peter Westh<sup>1\*</sup>

1. Research Unit for Functional Biomaterials, Department of Science and Environment, Roskilde University. 1 Universitetsvej, Build. 28.C, DK-4000, Roskilde, Denmark. Email: sbadino@ruc.dk , jkari@ruc.dk , sjarlc@ruc.dk , pwesth@ruc.dk
2. Novozymes A/S, Krogshøjvej 36, DK-2880, Bagsværd, Denmark. E-mail: kimb@novozymes.com

\*Corresponding author: Email: pwesth@ruc.dk ; Telephone: +45 4674 2879; Fax: +45 4674 3011

ACCEPTED MANUSCRIPT

**Abstract**

Cellulose degrading fungi such as *Hypocrea jecorina* secrete several cellulases including the two cellobiohydrolases (CBHs) Cel6A and Cel7A. The two CBHs differ in catalytic mechanism, attack different ends, belong to different families, but are both processive multi-domain enzymes that are essential in the hydrolysis of cellulose. Here we present a direct kinetic comparison of these two enzymes acting on insoluble cellulose. We used both continuous- and end-point assays under either enzyme- or substrate excess, and found distinct kinetic differences between the two CBHs. Cel6A was catalytically superior with a maximal rate over four times higher than Cel7A. Conversely, the ability of Cel6A to attack diverse structures on the cellulose surface was inferior to Cel7A. This latter difference was pronounced as the density of attack sites for Cel7A was almost an order of magnitude higher compared to Cel6A. We conclude that Cel6A is a fast but selective enzyme and that Cel7A is slower, but promiscuous. One consequence of this is that Cel6A is more effective when substrate is plentiful, while Cel7A excels when substrate is limiting. These diverse kinetic properties of Cel6A and Cel7A might elucidate why both cellobiohydrolases are prominent in cellulolytic degrading fungi.

## 1. Introduction

Cel6A and Cel7A are the two most abundant cellulases secreted from *Hypocrea jecorina* (teleomorph of *Trichoderma reesei*) [1-3] and these cellobiohydrolases (CBHs) are essential for an efficient cellulose degradation. They are both multi domain enzymes [4, 5] composed by a large catalytic domain (CD) and a small carbohydrate binding domain (CBM) connected by a flexible and glycosylated linker. They also share the properties of primarily attacking the cellulose chain from the end, and processively hydrolyzing one cellulose strand, which is bound in a long catalytic tunnel [4, 5]. The two enzymes differ in several other aspects. They have different overall folds and belong to different GH families. They also have different mechanisms as Cel7A attacks reducing ends of cellulose strands and performs a retaining hydrolytic reaction. Conversely, Cel6A attacks non-reducing ends and utilizes an inverting mechanism [6, 7]. The overall arrangements of domains are opposite in the sense that the CBM makes up the C-terminal for Cel7A, while it is the N-terminal in Cel6A. Another difference, which may be particularly important from a kinetic point of view, is the design of the substrate binding region. Cel7A has a 50 Å long cleft in the CD, which is covered by 4 pairs of loops that protrude from each side of the cleft [4, 8]. Although these peripheral loops are not connected by any covalent bonds, they essentially cover the cleft and hence give rise to a tunnel shaped binding region with the active site towards the product end. Cel6A, on the other hand, has a shorter binding cleft, which is covered by 2 loops that are proposed to be more flexible [5, 8-12], and this more open and dynamic structure may be associated with a faster and facilitated substrate binding and dissociation from the substrate for Cel6A [13].

One appealing interpretation of the prevalence of Cel6-Cel7 mixtures in the secretome of *H. jecorina* and other cellulose degrading fungi is that differences in their activities and specificities help the organisms degrade diverse structures of cellulose in plant biomass. This idea is supported by the observation of a significant degree of synergy between Cel7A and Cel6A during the break-down of pure cellulose [14-17]. The level of kinetic understanding for the two types of CBHs varies. Hence, kinetic aspects of a number of fungal Cel7 enzymes, in particular Cel7A from *H. jecorina*, has been studied quite comprehensively (see [18] for a review), and this has made Cel7A-kinetics the best understood among cellulases. Cel6A, on the other hand, is less investigated although important progress has been made [12, 13, 19]. Direct kinetic comparisons of the two enzymes have not been made, and this hampers discussions of their roles and interrelationships in the cellulolytic process. Particularly so as cellulase kinetics is notorious for its dependence on substrate properties and experimental conditions, thus making kinetic parameters from different studies hard to compare. Here, we report a thorough kinetic characterization using methods that allow direct comparison of Cel6A and Cel7A. The results unveiled distinctive kinetic differences between the enzymes. In particular we found that Cel6A is a much faster enzyme with a maximal initial rate about four times higher than

Cel7A. Conversely, Cel6A is far inferior with respect to the ability to attack diverse sites on the substrate surface. Thus, Cel6A only recognized comparably few sites for enzymatic attack, while Cel7A was able to initiate catalysis on most of its adsorption sites. We speculate that these differences could be important for the efficacy of Cel6A-Cel7A mixtures against complex lignocellulosic biomass.

## 2. Materials and Methods

### 2.1 Enzymes and substrate

Enzymes were expressed heterologously in *Aspergillus oryzae* and purified as described elsewhere [20, 21]. Concentrations were determined by UV absorption at 280 nm using theoretical [22] extinction coefficients of 97,790 M<sup>-1</sup>cm<sup>-1</sup> (Cel6A), 86,760 M<sup>-1</sup>cm<sup>-1</sup> (Cel7A) and 177,880 M<sup>-1</sup>cm<sup>-1</sup> ( $\beta$ -glucosidase). All experiments were performed in 50 mM NaAcetate pH 5.0 at 25°C and Avicel (PH101, Sigma Aldrich 11365), that had initially been washed and precipitated five times in buffer, was used as substrate. Avicel consists of microcrystalline cellulose, and the product used here has a typical particle size of 10-50  $\mu$ m [23]. The quenched flow instruments works better with smaller particles, and the substrate used here was dispersed for 10 min with an ultra Turrax T25 Basic (IKA, Staufen, Germany) coaxial homogenizer with a nominal final particle size of 5  $\mu$ m. Earlier work has shown that the crystallinity of the dispersed Avicel was not changed [24].

### 2.2 Reducing Sugar Activity Assays

Activity assays were based on quantification of reducing sugars using the *para*-hydroxybenzoic acid hydrazide (PAHBAH) method [25] following an experimental procedure described elsewhere [21]. We used 0.2  $\mu$ M of enzyme and substrate loads ranged from 1 g/L to 80 g/L Avicel (including controls with no substrate). After 1 h hydrolysis, the reaction was quenched by centrifugation at 2000 g, and 11  $\mu$ l 1  $\mu$ M  $\beta$ -glucosidase from *Aspergillus oryzae* was added to 100  $\mu$ l supernatant. This mixture was allowed to react for 1 h at room temperature to convert all soluble sugars to glucose. After the PAHBAH reaction, concentrations were determined in a plate reader (Spectra Max 3, Molecular Devices, Sunnyvale, Ca) using absorption at 405 nm and a glucose standard series from 0-500  $\mu$ M. In the inverse MM approach a constant substrate load of 2 g/L Avicel was used with varying enzyme concentrations ranging from 0.1  $\mu$ M to 10  $\mu$ M all in the presence of 0.1  $\mu$ M  $\beta$ -glucosidase. All experiments were carried out in triplicates.

### 2.3 Binding isotherms

Binding isotherms were made with different enzyme concentrations ranging from 0.1-6  $\mu\text{M}$  on Avicel. On Thurax dispersed Avicel the enzyme concentration range was 0.05-8  $\mu\text{M}$ . In both cases, standards with the same enzyme concentrations in buffer were also made. After 30 min equilibration time, the Avicel samples were centrifuged at 2000 g and the concentration of enzyme in the supernatant was determined from the intrinsic fluorescence as described previously [21]. In addition to the 100  $\mu\text{L}$  supernatant we added another 50  $\mu\text{L}$  buffer to each well before measuring the intrinsic fluorescence, since the larger volume resulted in less noisy fluorescence measurement. 10 g/L washed Avicel or 10 g/L washed and turraxed Avicel was used as substrate.

#### 2.4 Real time activity

Real time hydrolysis was measured using a pyranose dehydrogenase (PDH) biosensor, which detects both  $\alpha$ - and  $\beta$ -anomers of soluble sugars. PDH biosensors were prepared according to a previously published protocol [26] except that benzoquinone was used as mediator. In the hydrolysis experiments we used 40 g/L Avicel and doses of 100 nM enzyme (final concentration). Progress curves at 25°C were followed over 5 min in experiments with either one dosage at  $t=0$  or two dosages at  $t=0$  and  $t=150$  s (the latter giving a total enzyme concentration of 200 nM). Comparisons of single and double dose experiments were used to elucidate the enzymes' sensitivity to small substrate modifications. The sensors were calibrated with cellobiose solutions ranging from 0-50  $\mu\text{M}$  as described in detail elsewhere [26].

#### 2.5 Quench flow

Quenched flow measurements were made on a system recently developed for enzyme reactions on solid substrates catalysis [27], and used to estimate the specific activity at the initial rapid phase. We used 10 g/L turraxed Avicel and 0.5  $\mu\text{M}$  of enzyme in this assay, where a flow of enzyme and substrate generated by a peristaltic pump are mixed in a mixing tee and subsequently "aged" by passing through loops of tubing of different length [27]. By using different flow rates and different loops the enzyme substrate solution was quenched with 0.1 M NaOH giving a hydrolysis time resolution ranging from 250 ms to 3000 ms. All samples were run in triplicate (three separate experiments through the same loop). Samples were collected in a deepwell plate and supernatants were isolated from the insoluble Avicel by centrifugation (1000 g, 3 min). Hereafter analyzed by High-Performance Anion-Exchange Chromatography with Pulsed Amperometric Detection (HPAEC-PAD) using a Dionex ICS-5000 instrument fitted with a CarboPac PA10 column (Thermo Scientific, Waltham, MA). Cellobiose contents were calculated against an 8-point external standard. Blanks were subtracted the samples and carried out as the samples except that the enzymes were quenched with NaOH prior to the experiments.

### 3. Results and data analysis

The initial hydrolysis rate for cellulases generally levels off towards a constant value when either the substrate load or the enzyme concentration is increased [28-31]. This is sometimes called “double saturation” [32] and it implies that a saturation curve for the initial rate can be acquired from two types of experiments. The first is the conventional Michaelis Menten approach, where experiments are set up with a low, constant *enzyme* concentration and the initial, steady state rates is measured for gradually increasing substrate loads (see [33-35] for examples with cellulases). Alternatively, one may strive for the opposite limit and conduct the experiments at a constant and low *substrate* load and excess of enzyme. In this latter case, initial rates are measured and plotted as a function of the enzyme concentration (*c.f.* Fig. 1B). This idea of using enzyme excess is unusual, but has nevertheless been suggested within different areas of enzymology [36-40]. We have recently argued [41] that both experimental conditions (enzyme excess and substrate excess) may be analyzed by a simple steady-state treatment, and that combined interpretation of the kinetic parameters from each of these two approaches provide particular insights into a given cellulase-substrate system. In the current work we will use this combined analysis to highlight differences between Cel7A and Cel6A.

Initial steady-state rates measured under substrate excess were plotted against the substrate load in Fig. 1C and analyzed with respect to eq. (1).

$${}^{conv}v = \frac{{}^{conv}V_{\max}S_0}{{}^{conv}K_M + S_0} \quad (1)$$

Henceforth, we will call eq. (1) *the conventional Michaelis Menten (MM-) equation* and identify its parameters by the superscript *conv*. In eq. (1),  ${}^{conv}v$  is the rate measured under substrate excess, and  $S_0$  is the load of substrate in g/L. It follows that  ${}^{conv}K_M$ , the substrate load at half-saturation, also has units of mass per volume (*c.f.* Fig. 1A). The validity of this simple MM equation for processive enzymes (like Cel7A or Cel6A) has been discussed earlier [33]. This work showed that the steady state rate could be expressed by eq. (1), although there were some differences in the meaning of the kinetic parameters compared to simple MM theory. These differences are discussed in detail elsewhere [33], but they are not important for the comparative analysis presented here.

Steady-state rates measured under enzyme excess were plotted against the enzyme concentration in Fig. 1D, and analyzed with respect to eq. (2), which we will call the *inverse MM equation* [41],

$${}^{inv}v = \frac{{}^{inv}V_{max} E_0}{{}^{inv}K_M + E_0} \quad (2)$$

In eq. (2),  $E_0$  is the total enzyme concentration in  $\mu\text{M}$ , and  ${}^{inv}K_M$  is the concentration ( $\mu\text{M}$ ) required to reach half saturation (*c.f.* Fig. 1B). Lines in panels with experimental data represent non-linear regression with respect to eq. (1) (Fig. 1C) or eq. (2) (Fig. 1D), and the kinetic parameters  ${}^{conv}V_{max}/E_0$ ,  ${}^{conv}K_M$ ,  ${}^{inv}V_{max}/S_0$  and  ${}^{inv}K_M$  derived from the regression analyses are listed in Tab. 1.

Figure1

**Figure 1** Principles of interpretation and experimental data for conventional and inverse Michaelis Menten analysis. The top panel shows a simplified illustration of how we interpret results by respectively the conventional (panel A) and inverse (Panel B) Michaelis Menten (MM) equation. The substrate is depicted as flakes with a chess-board pattern representing the reaction points or attack sites for the enzyme. Two types of saturation are considered. In the conventional approach, addition of high loads of substrate eventually binds all enzymes, and this situation parallels MM-saturation in normal bulk reactions. For the inverse approach, addition of high enzyme concentrations (to a low load of substrate) leads to the saturation of all attack sites, while free enzyme builds up in the aqueous bulk. The lower panels shows experimental data for Cel7A and Cel6A using the conventional steady-state approach where 200 nM enzyme were saturated with Avicel (Panel C) and the inverse steady-state approach where 2 g/L Avicel was saturated with enzyme (panel D).

|              | Conventional MM plot                          |                                             | Inverse MM plot                                               |                                    |
|--------------|-----------------------------------------------|---------------------------------------------|---------------------------------------------------------------|------------------------------------|
|              | ${}^{conv}V_{max}/E_0$<br>( $\text{s}^{-1}$ ) | ${}^{conv}K_M$<br>( $\text{g liter}^{-1}$ ) | ${}^{inv}V_{max}$<br>( $\mu\text{mol g}^{-1} \text{s}^{-1}$ ) | ${}^{inv}K_M$<br>( $\mu\text{M}$ ) |
| <b>Cel6A</b> | $0.87 \pm 0.05$                               | $32 \pm 4$                                  | $0.033 \pm 0.001$                                             | $0.51 \pm 0.05$                    |
| <b>Cel7A</b> | $0.20 \pm 0.01$                               | $9 \pm 2$                                   | $0.057 \pm 0.001$                                             | $1.34 \pm 0.11$                    |

**Table 1** Kinetic parameters from the conventional- and inverse Michaelis Menten analysis. Standard errors are from the the fit of eq. 1 and eq. 2 to the experimental data.

In the conventional MM plot (Fig 1C) Cel6A showed higher steady-state rates at all substrate loads, and the specific maximal rate  ${}^{conv}V_{max}/E_0$  was > 4 times higher for Cel6A ( $0.87 \text{ s}^{-1}$ ) compared to Cel7A ( $0.20 \text{ s}^{-1}$ ). The conventional Michaelis constant,  ${}^{conv}K_M$ , was approximately 3 times higher for Cel6A indicating lower substrate affinity. In the inverse analysis, on the other hand, Cel7A showed higher activity, and the maximal specific rate,  ${}^{inv}V_{max}/S_0$ , was  $0.057 \mu\text{mol g}^{-1} \text{s}^{-1}$  for Cel7A compared to  $0.033 \mu\text{mol g}^{-1} \text{s}^{-1}$  for Cel6A.

The kinetic response to two sequential enzyme doses was tested by biosensor measurements. Results in Fig. 2 show that the cellobiose production by Cel6A over 150 s was about two-fold higher than for Cel7A (100 nM enzyme and 40 g/L Avicel in both cases).

When a second enzyme dose was added after 150 s (raising the total concentration to 200 nM) we found a significant reduction in the kinetic response for Cel6A (see insert). In other words the specific activity of the enzymes in the second dose was lower compared to the enzymes in the first dose (the second dose generated about 57% of the cellobiose produced by the first dose over the 150 s course). It is worth noticing that this reduction in specific activity happened although the degree of substrate conversion (about 0.01 %) and enzyme coverage of the substrate (about 2% of saturation, *c.f.* Fig. 4 below) were both very low. For Cel7A, which had similar low conversion and coverage, we observed a smaller difference between the first and second dose of enzyme. Here the product made by the second dose was 83% of the first dose. We conclude that Cel6A is more sensitive than Cel7A to changes brought about as the reaction progresses. The distinctive reduction in specific activity even for very low coverage and degree of conversion suggests that high Avicel conversion will be hard to attain even in prolonged reactions with these mono-component enzymes. This, in turn, may be related to the pronounced synergy of Cel6A and Cel7A (so-called exo-exo synergy), which probably reflects specificity for different types of surface structures and hence the ability of one enzyme to exhumate good attack sites for the other [42, 43], but we will not pursue this topic further in the current work.

Figure 2

**Figure 2** Kinetic response to two sequential enzyme dosages of Cel6A and Cel7A. Both panels show data for two biosensor measurements. In the first measurement 100 nM enzyme was added to 40 g/L Avicel at  $t=0$  and the progress curve was recorded for 300 s. The second experiment was started in the same way (and hence the curves are initially superimposed), but at  $t=150$  s a second enzyme dosage was added (total concentration now 200 nM enzyme). The effect of the second dosage (from  $t=150$  s to  $t=300$  s) was calculated as the difference between the two curves and plotted together with the first 150 s of the progress curve in the insert. It appears that the second dosage has less effect on the progress curve for Cel7A compared to Cel6A.

We used quenched-flow measurements to elucidate the initial substrate attack and the activity at extremely low degrees of substrate conversion. Results in Fig. 3 show that Cel6A initiated hydrolysis much faster than Cel7A. Thus, the slope over the first second for Cel6A corresponded to a turnover of over  $10\text{ s}^{-1}$ , while the rate for Cel7A was an order of magnitude lower. After the pronounced initial burst in Cel6A activity, which lasted about 0.8 s, the progress curve for this enzyme became near-linear with a slope corresponding to a specific rate of  $1.3\text{ s}^{-1}$ . Cel7A also showed signs of an early burst for  $t < 0.5$  s, but the amplitude of this effect was very low ( $0.5\text{ }\mu\text{M}$ ), and comparable to the experimental scatter. Earlier work has shown a strong burst in Cel7A activity with a maximum rate after 5-10 s [27, 44], *i.e.* later than the highest times considered in Fig. 3. More work including the use of higher dilutions and lower temperatures (to slow down the reaction) will be required to elucidate this possible rapid phase in Cel7A activity. Here we just note that to within the



experimental scatter, the progress curve for Cel7A was linear over the 6 s time interval covered in Fig. 3. The slope suggested a specific activity of about  $0.35 \text{ s}^{-1}$  for Cel7A.

Figure 3

**Figure 3** Quenched- flow data for the initial kinetics of Cel6A and Cel7A. In both cases, the final concentration was  $0.5 \text{ }\mu\text{M}$  enzyme and  $10 \text{ g/L}$  turraxed Avicel.

To enable comparisons of the kinetic data and the extent of surface coverage we measured the concentration of free enzyme,  $E_{free}$ , in  $10 \text{ g/L}$  Avicel suspensions as a function of the total enzyme concentration. We calculated the surface coverage,  $\Gamma = \frac{(E_0 - E_{free})}{S_0}$  in  $\mu\text{mol/g}$  cellulose and plotted this parameter against  $E_{free}$  in Fig. 4. As often seen for cellulases [45], a simple Langmuir isotherm,  $\Gamma = \Gamma_{max} \frac{E_{free}}{K_d + E_{free}}$ , where  $\Gamma_{max}$  and  $K_d$  are respectively saturation coverage and dissociation constant, accounted reasonably for the binding data in this range of  $E_{free}$ . We emphasize that a simple Langmuir isotherm, which relies on the assumption that all sites are equal, only provides a coarse description of the adsorption process. Thus, several earlier studies [46, 47] have shown that sites with widely differing affinities can be identified on the surface of cellulose. It follows that parameters derived from the simplified treatment used here are only apparent values that may not be valid outside the range of experimental conditions under which they are measured. However, in accord with earlier work [45], we suggest that the partitioning coefficient,  $K_p = \Gamma_{max}/K_d$  may be used as a gauge of cellulase-substrate affinity; at least in comparative discussions of related enzymes. This is because  $K_p$  signifies the distribution of bound and free enzyme at very low substrate coverage where the population of weakly-binding sites can be neglected.

The kinetic data was obtained on either unmodified Avicel (PAHBAH-assay and biosensor measurements) or Avicel that had been dispersed by a Thurax coaxial homogenizer (quenched-flow measurements). The particle size of the Thurax-dispersed Avicel was lower and it consequently had a larger surface area for enzyme adsorption. Earlier studies have shown that the adsorption capacity of typical cellulases approximately doubles after Thurax treatment of Avicel [24]. Therefore, adsorption isotherms were obtained on both unmodified Avicel and dispersed Avicel, and Langmuir parameters are listed in Tab. 2.

Figure 4

**Figure 4** Binding isotherms for Cel6A (red) and Cel7A (black). Circles represents measurements on unmodified Avicel ( $10 \text{ g/L}$ ), and the solid lines are best fits of the Langmuir equation (see main text). Triangles and dotted lines are the analogous data for Avicel ( $10 \text{ g/L}$ ) that had been dispersed by a

Thurax homogenizer. The latter substrate was used in the quenched-flow measurements while the former was used in other activity assays.

|              | Binding isotherms<br>Avicel                  |                                    | Binding isotherms<br>Thuraxed Avicel         |                                    |
|--------------|----------------------------------------------|------------------------------------|----------------------------------------------|------------------------------------|
|              | $\Gamma_{max}$<br>( $\mu\text{mol g}^{-1}$ ) | $K_p$<br>( $\text{liter g}^{-1}$ ) | $\Gamma_{max}$<br>( $\mu\text{mol g}^{-1}$ ) | $K_p$<br>( $\text{liter g}^{-1}$ ) |
| <b>Cel6A</b> | 0.17 $\pm$ 0.01                              | 0.23                               | 0.49 $\pm$ 0.01                              | 1.01                               |
| <b>Cel7A</b> | 0.30 $\pm$ 0.03                              | 0.28                               | 0.75 $\pm$ 0.02                              | 1.77                               |

**Table 2** Parameters extracted from the binding isotherms made with 10 g/L Avicel and 10 g/L thuraxed Avicel.

From the binding isotherms we found a higher saturation coverage ( $\Gamma_{max}$ ) for Cel7A compared to Cel6A, and this is in line with earlier reports [45, 48, 49]. Also, the affinity for Avicel, as indicated by the partitioning constant,  $K_p$ , was moderately higher for Cel7A as seen previously [45, 48]. For both Cel6A and Cel7A the saturation coverage increased after the substrate was homogenized (Thuraxed), probably as a result of a larger specific surface area in the dispersed samples.

#### 4. Discussion

Many cellulose degrading fungi have secretomes that are dominated by mixtures of cellobiohydrolases (CBHs) from respectively Glucoside Hydrolase family 6 and 7. CBHs from both families are processive and primarily exo-lytic enzymes [4-6, 42, 50, 51] although they both show a small auxiliary endo-activity [14, 42, 52, 53]. They are structurally rather different and utilize respectively the retaining (GH7) and inverting (GH6) hydrolytic mechanism. The two CBHs have also been reported to have quite different specificities with respect to the physical properties of the cellulose surface they attack [54], and perhaps for this reason, they can show a significant degree of synergy, when they act simultaneously or sequentially on the same substrate [14-17]. The kinetics of both CBHs has been studied separately and especially the kinetics of Cel7A has been exposed to comprehensive investigations. However, direct biochemical comparisons of the two cellobiohydrolases have not been presented. This limits appraisals of their differences because kinetic studies of cellulases acting on insoluble substrates tend to give quite variable parameters in different trials, possibly as a result of subtle differences in the physical properties of the insoluble cellulose (c.f. Fig. 4) and complications associated with homogenizing the two-phase reaction system. In the current work we report kinetic measurements for Cel7A and Cel6A from *H. jecorina* under equal conditions and use this information to highlight kinetic similarities and differences. We used the standard substrate, Avicel, which is purified from wood and composed of

microcrystalline- and amorphous cellulose [55, 56]. Avicel particles have a complex structure with a high degree of roughness [23], which probably present a diversity of attack sites for the enzymes.

As illustrated in Fig. 1A, saturation in the conventional MM-approach implies that all enzyme is complexed, and in analogy with the usual MM-treatment, we may consider the maximal specific rate, ( $^{conv}V_{max}/E_0$ ) listed in Tab. 1 as a measure of the rate constant,  $k_{cat}$  at steady-state, governing the release of product from such complexes. Interestingly, this turnover number is over four-fold faster for Cel6A ( $k_{cat} = 0.87 \text{ s}^{-1}$ ) compared to Cel7A ( $k_{cat} = 0.20 \text{ s}^{-1}$ ), and we deduce that the former enzyme is superior with respect to catalytic efficacy. Turning to the inverse maximal rates we found the opposite picture with almost twice as high a value for Cel7A (respectively  $0.057 \text{ } \mu\text{molg}^{-1}\text{s}^{-1}$  and  $0.033 \text{ } \mu\text{molg}^{-1}\text{s}^{-1}$  for Cel7A and Cel6A, see Tab. 1). To illustrate the meaning of this, we first introduce a parameter,  $^{kin}\Gamma_{max}$  in units of  $\mu\text{mol}/(\text{g cellulose})$ , which enumerates accessible attack sites on the surface of the substrate. These attack sites represents loci where the enzyme can bind and initiate hydrolysis, and they are indicated by the small grey-and-white squares in the cartoons in Fig. 1.  $^{kin}\Gamma_{max}$  is related to the adsorption saturation  $\Gamma_{max}$  (Tab 2), and we will discuss this below, but for now we just emphasize that these two parameters are different as not all adsorption sites are necessarily competent for catalysis. When kinetic saturation occurs in inverse MM-experiments (*i.e.* with a large excess of enzyme, see Fig. 1B) all attack sites are complexed. Hence, we may say that the molar concentration of enzyme-substrate complexes is  $^{kin}\Gamma_{max}S_0$ , and as the rate of product formation is governed by  $k_{cat}$ , the hydrolytic rate may be written

$$^{inv}V_{max} = k_{cat} \ ^{kin}\Gamma_{max} S_0 \quad (3)$$

As  $^{inv}V_{max}/S_0$  and  $k_{cat} = ^{conv}V_{max}/E_0$  are known from the experiments (Tab. 1), Eq. (3) provides a convenient way to an experimental value for  $^{kin}\Gamma_{max}$ . Thus, rearrangement gives

$$^{kin}\Gamma_{max} = \frac{^{inv}V_{max}/S_0}{k_{cat}} \quad (4)$$

Insertion of the data from Tab. 1 into eq. (4) gives  $^{kin}\Gamma_{max}$  values of  $0.29 \pm 0.02 \text{ } \mu\text{mol/g}$  and  $0.038 \pm 0.003 \text{ } \mu\text{mol/g}$  for Cel7A and Cel6A respectively, and these numbers reveal another central difference between these enzymes. Thus, Cel7A is able to locate almost an order of magnitude more attack sites on Avicel compared to Cel6A. This means that the higher inverse maximal rate for Cel7A (Fig. 1D) occurs in spite of the lower catalytic rate of this enzyme. We interpret this as Cel7A being more efficient in attacking a broad range of structures on the cellulose surface. One way to perceive this disparity between Cel7A and Cel6A is in terms of substrate specificity. Typically, specificity describes the relative activity of an enzyme against chemically distinct substrates. In the current context, we are considering substrate (*i.e.* attack sites) of the same chemical composition, but with physical (structural) differences. With this proviso, we may say that Cel6A showed high specificity and only hydrolyzed a small subset of the available surface sites. Conversely, Cel7A was a promiscuous cellulase that hydrolyzed

almost any site it associated with. This may be further illustrated by comparing  $k_{in}\Gamma_{max}$  and the adsorption saturation parameter,  $\Gamma_{max}$  (Tab 2). For Cel7A these parameters were equal whereas for Cel6A binding saturation (0.17  $\mu\text{mol/g}$ ) much exceeded the density of attack sites (0.038  $\mu\text{mol/g}$ ). This again suggests that Cel7A initiates hydrolysis on essentially all sites to which it binds while Cel6A is unable to attack the majority of its adsorption sites, and hence shows a larger degree of unproductive binding. Thus Cel6A has a high catalytic speed, but a poor ability to locate attack sites on Avicel compared to Cel7A. The suggestion that Cel6A is superior with respect to catalytic speed is corroborated by the quenched flow measurements in Fig. 3. Hence, the specific rate of Cel6A at very low reaction times ( $t < 1$  s), exceeded  $10 \text{ s}^{-1}$ , and to our knowledge this is the fastest room-temperature rate reported hitherto for a CBH acting on insoluble cellulose. One possible origin of the higher catalytic rate for Cel6A could be the inverting (one-step) catalytic mechanism of this enzyme, but the current results support another interpretation. Thus, the transient specific rate over the first second is an order of magnitude higher than  $k_{cat}$  at steady state ( $^{\text{conv}}V_{\text{max}}/E_0 = 0.87 \text{ s}^{-1}$ ; see above). This behavior with an initial burst followed by a much slower steady state rate parallels the kinetics of Cel7A, and implies that the rate of enzyme-substrate dissociation at the end of a processive sweep determines the overall rate at steady state [44, 57-59]. In light of that, the high catalytic efficacy of Cel6A may reflect weaker interactions with the substrate, which leads to faster dissociation rate and short residence time of unproductive enzyme-substrate complexes. Faster dissociation would appear likely for Cel6A as its substrate-binding cleft is less covered compared to Cel7A [4, 5, 9].

A weaker binding of Cel6A could also be related to the lower (structural) specificity of this enzyme (discussed above). This is because transfer of a piece of cellulose strand from its crystal to the substrate-binding site of the enzyme requires strong interactions to compensate for the loss of crystal lattice energy [60, 61]. If such interactions are weaker in Cel6A compared to Cel7A, there will be fewer sites, where this transfer can occur spontaneously for Cel6A. The kinetic measurements suggested an order of magnitude fewer sites for Cel6A and insufficient binding energy (low substrate affinity) could potentially underlie this observation. It could also rely on differences in glycosylation. Thus, *in silico* studies [62] have suggested attractive forces between O-glycans on the linker of Cel7A and cellulose, and this could clearly also influence substrate affinity and dissociation rates. Further progress in these structural interpretations awaits direct investigations of structure and kinetics of enzyme variants. With respect to substrate affinity, it is interesting to note that higher temperatures induces a significant release of Cel7A from the substrate surface [21]. This may suggest that an enzyme with weaker substrate affinity such as Cel6A becomes less efficient as temperature raises, and this is relevant in industrial application that usually involves high temperatures.

The limited ability of Cel6A to find appropriate attack sites means that this enzyme experiences a comparably lower molar concentration of substrate. This interpretation can be further assessed by the double injection data in Fig. 3. Here it appeared that a second dose of Cel6A was much less productive than the first dose. This difference between first and second dose was smaller for Cel7A, and we suggest that this reflect the onset of substrate depletion

(reduction in number of attack sites) either because the sites are occupied or already hydrolyzed.

To summarize, the combined analysis of conventional- and inverse MM-measurements revealed complementary kinetic properties of Cel7A and Cel6A. Cel6A is catalytically superior, and able to release cellobiose at a much higher rate than Cel7A, when substrate is plentiful. However, Cel6A is inferior in the sense that it is only capable of attacking a limited number of sites on the cellulose surface. One may say that the effective (molar) substrate concentration experienced by Cel6A at a given mass load of cellulose is much lower than the concentration experienced by Cel7A. For the substrate investigated here (Avicel) this difference was quite noticeable with an eight-fold higher number of attack sites for Cel7A, and this may be interpreted as a disparity in the (structural) specificity of the two enzymes. It appears relevant to further study how these kinetic properties are related to enzyme structure, and whether the differences are significant for the synergy between Cel6 and Cel7 enzymes. If indeed so, these differences may be important for the common occurrence of Cel6 and Cel7 CBHs in the secretome of cellulose degrading fungi.

#### **Acknowledgement**

Funding: This work was supported by the Innovation Fund Denmark [grant number 0603-00496B] and Carlsbergfondet [grant number 2013-01-0208].

Conflicts of interest

Kim Borch works for Novozymes A/S, a major manufacturer of industrial enzymes

ACCEPTED MANUSCRIPT

## References

- 1 Rosgaard L, Pedersen S, Langston J, Akerhielm D, Cherry JR, Meyer AS. Evaluation of minimal *Trichoderma reesei* cellulase mixtures on differently pretreated Barley straw substrates. *Biotechnol Prog* 2007, 23: 1270-1276
- 2 Teeri TT. Crystalline cellulose degradation: new insight into the function of cellobiohydrolases. *Trends in Biotechnology* 1997, 15: 160-167
- 3 Nidetzky B, Claeysens M. Specific quantification of *Trichoderma reesei* cellulases in reconstituted mixtures and its application to cellulase-cellulose binding studies. *Biotechnology and bioengineering* 1994: 961-966
- 4 Divne C, Ståhlberg J, Reinikainen T, Ruohonen L, Pettersson G, Knowles JK, Teeri TT, *et al.* The three-dimensional crystal structure of the catalytic core of cellobiohydrolase I from *Trichoderma reesei*. *Science* 1994, 265: 524-528
- 5 Rouvinen J, Bergfors T, Teeri T, Knowles JK, Jones TA. Three-dimensional structure of cellobiohydrolase II from *Trichoderma reesei*. *Science* 1990, 249: 380-386
- 6 Claeysens M, Tomme P, Brewer CF, Hehre EJ. Stereochemical course of hydrolysis and hydration reactions catalysed by cellobiohydrolases I and II from *Trichoderma reesei*. *FEBS Lett* 1990, 263: 89-92
- 7 Davies G, Henrissat B. Structures and Mechanisms of Glycosyl Hydrolases. *Structure* 1995, 3: 853-859
- 8 Divne C, Ståhlberg J, Teeri TT, Jones TA. High-resolution crystal structures reveal how a cellulose chain is bound in the 50 Å long tunnel of cellobiohydrolase I from *Trichoderma reesei*. *J Mol Biol* 1998, 275: 309-325
- 9 Zou J, Kleywegt GJ, Ståhlberg J, Driguez H, Nerinckx W, Claeysens M, Koivula A, *et al.* Crystallographic evidence for substrate ring distortion and protein conformational changes during catalysis in cellobiohydrolase Cel6A from *Trichoderma reesei*. *Structure* 1999, 7: 1035-1045
- 10 Mayes HB, Knott BC, Crowley MF, Broadbelt LJ, Stahlberg J, Beckham GT. Who's on base? Revealing the catalytic mechanism of inverting family 6 glycoside hydrolases. *Chemical Science* 2016, 7: 5955-5968
- 11 Koivula A, Kinnari T, Harjunpää V, Ruohonen L, Teleman A, Drakenberg T, Rouvinen J, *et al.* Tryptophan 272: an essential determinant of crystalline cellulose degradation by *Trichoderma reesei* cellobiohydrolase Cel6A. *FEBS Lett* 1998, 429: 341-346
- 12 Harjunpää V, Teleman A, Koivula A, Ruohonen L, Teeri TT, Teleman O, Drakenberg T. Cello-oligosaccharide hydrolysis by cellobiohydrolase II from *Trichoderma reesei*. Association and rate constants derived from an analysis of progress curves. *Eur J Biochem* 1996, 240: 584-591
- 13 Nakamura A, Tasaki T, Ishiwata D, Yamamoto M, Okuni Y, Visootsat A, Maximilien M, *et al.* Single-molecule imaging analysis of binding, processive movement, and dissociation of cellobiohydrolase *Trichoderma reesei* Cel6A and its domains on crystalline cellulose. *J Biol Chem* 2016,
- 14 Henrissat B, Driguez H, Viet C, Schülein M. Synergism of Cellulases from *Trichoderma reesei* in the Degradation of Cellulose. *Nature Biotechnology* 1985, 3: 722-726
- 15 Tomme P, Heriban V, Claeysens M. Adsorption of two cellobiohydrolases from *Trichoderma reesei* to Avicel: Evidence for "exo-exo" synergism and possible "loose complex" formation. *Biotechnology Letters* 1990, 12: 525-530
- 16 Igarashi K, Uchihashi T, Koivula A, Wada M, Kimura S, Okamoto T, Penttilä M, *et al.* Traffic Jams Reduce Hydrolytic Efficiency of Cellulase on Cellulose Surface. *Science* 2011, 333: 1279-1282
- 17 Boisset C, Fraschini C, Schülein M, Henrissat B, Chanzy H. Imaging the enzymatic digestion of bacterial cellulose ribbons reveals the endo character of the cellobiohydrolase Cel6A from *Humicola insolens* and its mode of synergy with cellobiohydrolase Cel7A. *Appl Environ Microbiol* 2000, 66: 1444-1452

- 18 Payne CM, Knott BC, Mayes HB, Hansson H, Himmel ME, Sandgren M, Stahlberg J, *et al.* Fungal Cellulases. *Chem Rev* 2015, 115: 1308-1448
- 19 Koivula A, Ruohonen L, Wohlfahrt G, Reinikainen T, Teeri TT, Piens K, Claeysens M, *et al.* The active site of cellobiohydrolase Cel6A from *Trichoderma reesei*: the roles of aspartic acids D221 and D175. *J Am Chem Soc* 2002, 124: 10015-10024
- 20 Borch K, Jensen K, Krogh K, McBrayer B, Westh P, Kari J, Olsen J, *et al.* WO2014138672 A1 Cellobiohydrolase variants and polynucleotides encoding same. 2014,
- 21 Sørensen TH, Cruys-Bagger N, Windahl MS, Badino SF, Borch K, Westh P. Temperature Effects on Kinetic Parameters and Substrate Affinity of Cel7A Cellobiohydrolases. *J Biol Chem* 2015, 290: 22193-22202
- 22 Gasteiger E, Hoogland C, Gattiker A, Duvaud S, Wilkins MR, Appel RD, Bairoch A. Protein Identification and Analysis Tools on the Expasy Server. In: Walker JM ed. *The Proteomics Protocols Handbook* Totowa, New Jersey: Humana Press 2005: 571-607
- 23 Olsen JP, Donohoe BS, Borch K, Westh P, Resch MG. Interrelationships between cellulase activity and cellulose particle morphology. *Cellulose* 2016, 23: 2349-2361
- 24 Pellegrini VO, Lei N, Kyasaram M, Olsen JP, Badino SF, Windahl MS, Colussi F, *et al.* Reversibility of substrate adsorption for the cellulases Cel7A, Cel6A, and Cel7B from *Hypocrea jecorina*. *Langmuir* 2014, 30: 12602-12609
- 25 Lever M. Colorimetric and fluorometric carbohydrate determination with p-hydroxybenzoic acid hydrazide. *Biochem Med* 1973, 7: 274-281
- 26 Cruys-Bagger N, Badino SF, Tokin R, Gontsarik M, Fathalinejad S, Jensen K, Toscano MD, *et al.* A pyranose dehydrogenase-based biosensor for kinetic analysis of enzymatic hydrolysis of cellulose by cellulases. *Enzyme Microb Technol* 2014, 58-59: 68-74
- 27 Olsen JP, Kari J, Borch K, Westh P. A quenched-flow system for measuring heterogeneous enzyme kinetics with sub-second time resolution. *Enzyme and Microbial Technology* 2017, 105: 45-50
- 28 Bezerra RMF, Dias AA. Discrimination among eight modified Michaelis-Menten kinetics models of cellulose hydrolysis with a large range of substrate/enzyme ratios. *Appl Biochem Biotechnol* 2004, 112: 173-184
- 29 Nidetzky B, Steiner W, Hayn M, Claeysens M. Cellulose Hydrolysis by the Cellulases from *Trichoderma-Reesei* - a New Model for Synergistic Interaction. *Biochem J* 1994, 298: 705-710
- 30 Steiner W, Sattler W, Esterbauer H. ADSORPTION OF TRICHODERMA-REESEI CELLULASE ON CELLULOSE - EXPERIMENTAL-DATA AND THEIR ANALYSIS BY DIFFERENT EQUATIONS. *Biotechnol Bioeng* 1988, 32: 853-865
- 31 Valjamae P, Sild V, Pettersson G, Johansson G. The initial kinetics of hydrolysis by cellobiohydrolases I and II is consistent with a cellulose surface - erosion model. *Eur J Biochem* 1998, 253: 469-475
- 32 Lynd L, Weimer P, van Zyl W, Pretorius I. Microbial cellulose utilization: fundamentals and biotechnology. *Microbiol Mol Biol Rev* 2002, 66
- 33 Cruys-Bagger N, Elmerdahl J, Praestgaard E, Borch K, Westh P. A steady-state theory for processive cellulases. *FEBS J* 2013, 280: 3952-3961
- 34 Sørensen TH, Cruys-Bagger N, Windahl MS, Badino S, Borch K, Westh P. Temperature effects on kinetic parameters and substrate affinity of Cel7A cellobiohydrolases. *J Biol Chem* 2015, 290: 22193-22202
- 35 Gruno M, Valjamae P, Pettersson G, Johansson G. Inhibition of the *Trichoderma reesei* cellulases by cellobiose is strongly dependent on the nature of the substrate. *Biotechnol Bioeng* 2004, 86: 503-511
- 36 Bailey CJ. ENZYME-KINETICS OF CELLULOSE HYDROLYSIS. *Biochem J* 1989, 262: 1001-1001
- 37 Bajzer Z, Strehler EE. About and beyond the Henri-Michaelis-Menten rate equation for single-substrate enzyme kinetics. *Biochem Biophys Res Commun* 2012, 417: 982-985



- 38 Kartal O, Ebenhoh O. A generic rate law for surface-active enzymes. *FEBS Lett* 2013, 587: 2882-2890
- 39 McLaren AD, Packer L. Some aspects of enzyme reactions in heterogenous systems. *Adv Enzymol Relat Areas Mol Biol* 1970, 33: 245-308
- 40 Wang GS, Post WM. A note on the reverse Michaelis-Menten kinetics. *Soil Biol Biochem* 2013, 57: 946-949
- 41 Kari J, Andersen M, Borch K, Westh P. An inverse Michaelis-Menten approach for interfacial enzyme kinetics. *ACS Catalysis* 2017, 7: 4904-4914
- 42 Badino SF, Christensen SJ, Kari J, Windahl MS, Hvidt S, Borch K, Westh P. Exo-exo synergy between Cel6A and Cel7A from *Hypocrea jecorina*: Role of carbohydrate binding module and the endo-lytic character of the enzymes. *Biotechnol Bioeng* 2017, 114: 1639-1647
- 43 Våljamäe P, Sild V, Pettersson G, Johansson G. The initial kinetics of hydrolysis by cellobiohydrolases I and II is consistent with a cellulose surface-erosion model. *Eur J Biochem* 1998, 253: 469-475
- 44 Cruys-Bagger N, Elmerdahl J, Praestgaard E, Tatsumi H, Spodsberg N, Borch K, Westh P. Pre-steady-state kinetics for hydrolysis of insoluble cellulose by cellobiohydrolase Cel7A. *J Biol Chem* 2012, 287: 18451-18458
- 45 Palonen H, Tenkanen M, Linder M. Dynamic interaction of *Trichoderma reesei* cellobiohydrolases Cel6A and Cel7A and cellulose at equilibrium and during hydrolysis. *Appl Environ Microbiol* 1999, 65: 5229-5233
- 46 Jalak J, Valjamae P. Multi-Mode Binding of Cellobiohydrolase Cel7A from *Trichoderma reesei* to Cellulose. *PLoS One* 2014, 9: e108181
- 47 Stahlberg J, Johansson G, Pettersson G. A NEW MODEL FOR ENZYMATIC-HYDROLYSIS OF CELLULOSE BASED ON THE 2-DOMAIN STRUCTURE OF CELLOBIOHYDROLASE-I. *Bio-Technology* 1991, 9: 286-290
- 48 Medve J, Ståhlberg J, Tjerneld F. Adsorption and synergism of cellobiohydrolase I and II of *Trichoderma reesei* during hydrolysis of microcrystalline cellulose. *Biotechnol Bioeng* 1994, 44: 1064-1073
- 49 Medve J, Ståhlberg J, Tjerneld F. Isotherms for adsorption of cellobiohydrolase I and II from *Trichoderma reesei* on microcrystalline cellulose. *Appl Biochem Biotechnol* 1997, 66: 39-56
- 50 Davies G, Henrissat B. Structures and mechanisms of glycosyl hydrolases. *Structure* 1995, 3: 853-859
- 51 Payne CM, Knott BC, Mayes HB, Hansson H, Himmel ME, Sandgren M, Ståhlberg J, *et al.* Fungal Cellulases. *Chem Rev* 2015,
- 52 Ståhlberg J. *Trichoderma reesei* has no true exo-cellulase: all intact and truncated cellulases produce new reducing end groups on cellulose. *Biochimica et biophysica acta General subjects - Amsterdam* 1993, 1157: 107-113
- 53 Irwin DC, Spezio M, Walker LP, Wilson DB. Activity studies of eight purified cellulases: Specificity, synergism, and binding domain effects. *Biotechnol Bioeng* 1993, 42: 1002-1013
- 54 Ganner T, Bubner P, Eibinger M, Mayrhofer C, Plank H, Nidetzky B. Dissecting and reconstructing synergism: in situ visualization of cooperativity among cellulases. *J Biol Chem* 2012, 287: 43215-43222
- 55 Zhang YH, Lynd LR. Toward an aggregated understanding of enzymatic hydrolysis of cellulose: noncomplexed cellulase systems. *Biotechnol Bioeng* 2004, 88: 797-824
- 56 Kabindra K, Heenae S, Christopher ML, Sunkyu P, Seong HK. Progressive structural changes of Avicel, bleached softwood, and bacterial cellulose during enzymatic hydrolysis. *Scientific Reports* 2015, 5
- 57 Kurašin M, Kuusk S, Kuusk P, Sørliie M, Våljamäe P. Slow Off-rates and Strong Product Binding Are Required for Processivity and Efficient Degradation of Recalcitrant Chitin by Family 18 Chitinases. *J Biol Chem* 2015, 290: 29074-29085

- 58 Jalak J, Väljamäe P. Mechanism of initial rapid rate retardation in cellobiohydrolase catalyzed cellulose hydrolysis. *Biotechnol Bioeng* 2010, 106: 871-883
- 59 Praestgaard E, Elmerdahl J, Murphy L, Nyman S, McFarland KC, Borch K, Westh P. A kinetic model for the burst phase of processive cellulases. *FEBS J* 2011, 278: 1547-1560
- 60 Payne CM, Jiang W, Shirts MR, Himmel ME, Crowley MF, Beckham GT. Glycoside hydrolase processivity is directly related to oligosaccharide binding free energy. *J Am Chem Soc* 2013, 135: 18831-18839
- 61 Beckham GT, Matthews JF, Peters B, Bomble YJ, Himmel ME, Crowley MF. Molecular-level origins of biomass recalcitrance: decrystallization free energies for four common cellulose polymorphs. *J Phys Chem B* 2011, 115: 4118-4127
- 62 Payne CM, Resch MG, Chen L, Crowley MF, Himmel ME, Taylor LE, Sandgren M, *et al.* Glycosylated linkers in multimodular lignocellulose-degrading enzymes dynamically bind to cellulose. *Proc Natl Acad Sci U S A* 2013, 110: 14646-14651

ACCEPTED MANUSCRIPT

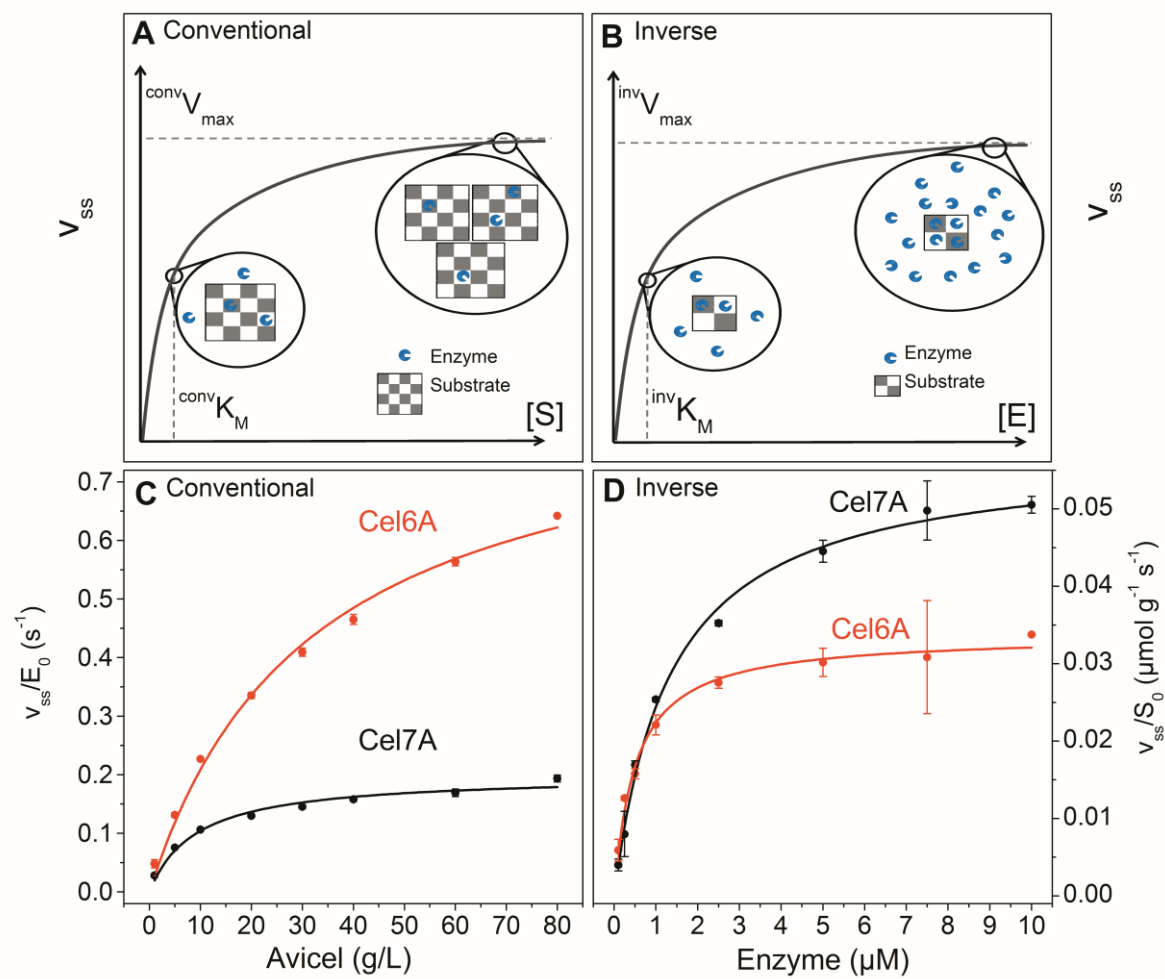


Fig. 1

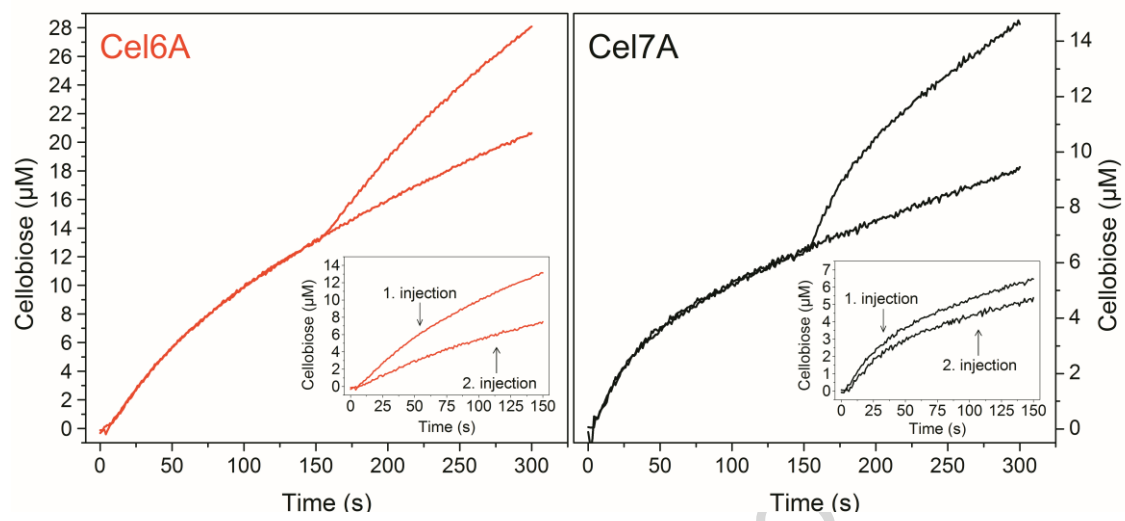


Fig. 2

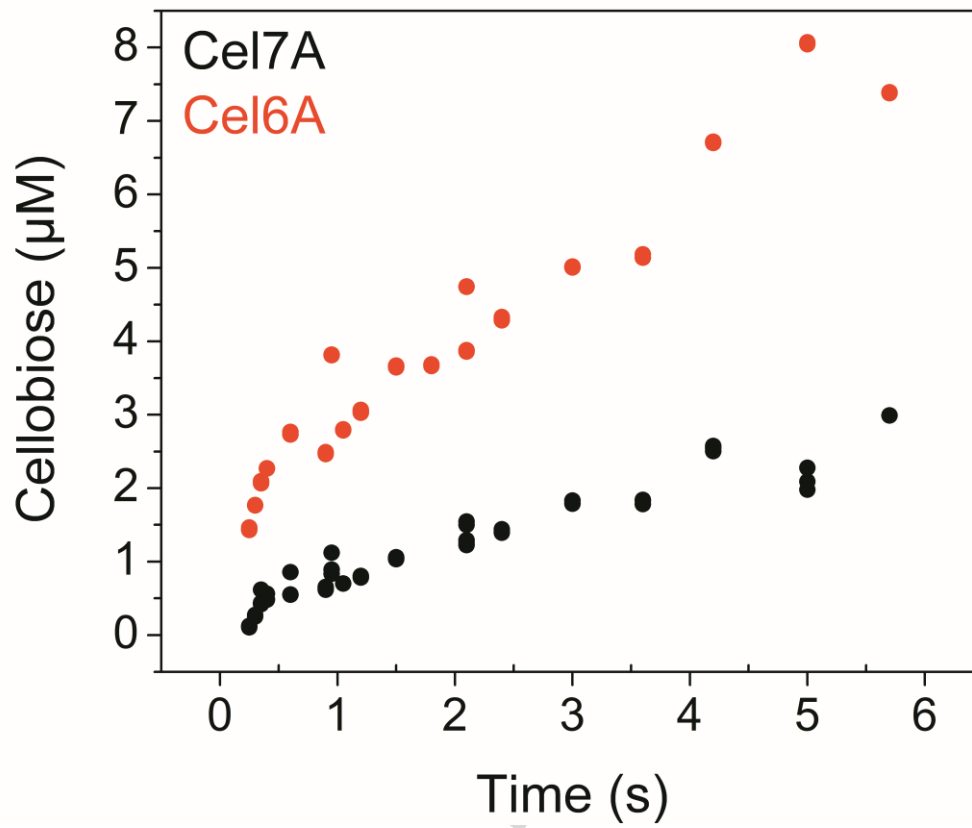


Fig. 3

ACCEPTED

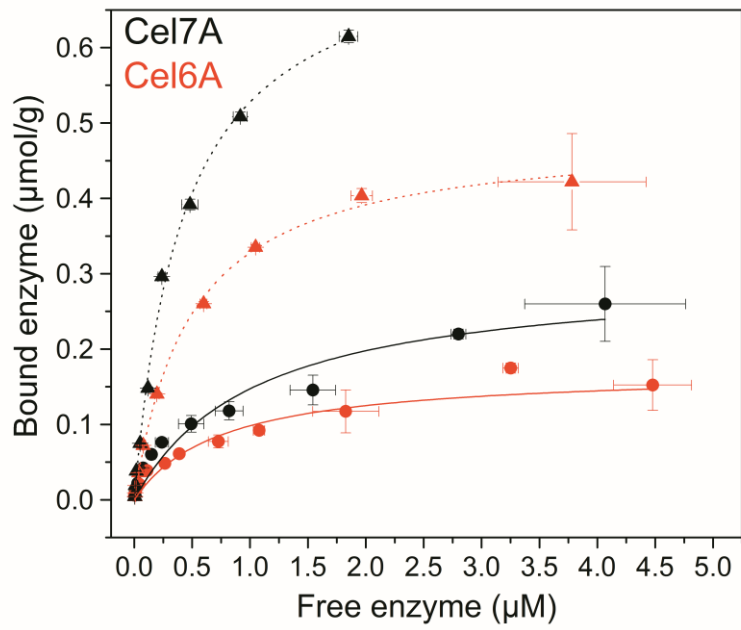
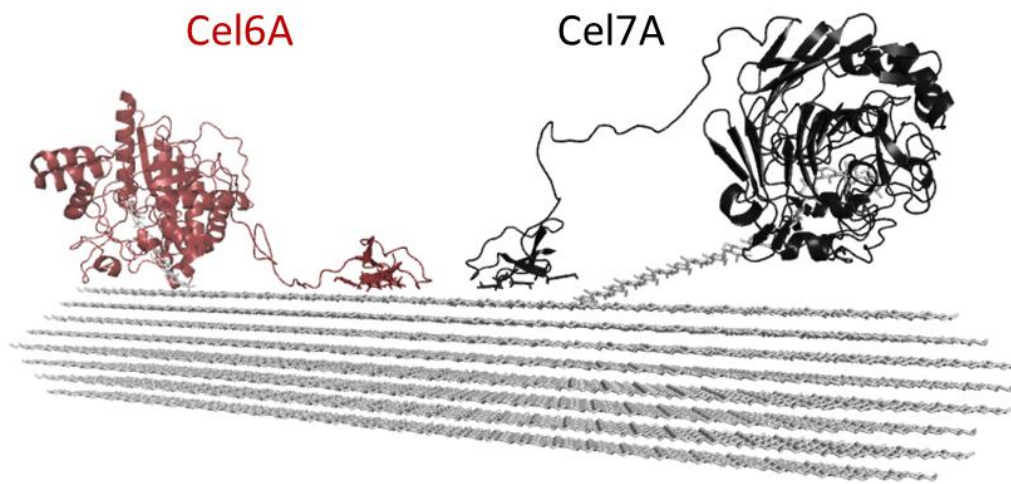


Fig. 4

ACCEPTED MANUSCRIPT



Graphical abstract

ACCEPTED

## Highlights BBA

- A direct kinetic comparison of Cel6A and Cel7A elucidates their differences
- A conventional and an inverse Michaelis Menten approach were applied
- The cellobiohydrolase Cel6A was catalytically superior compared to Cel7A
- Cel7A is able to locate many more attack sites on the cellulose surface than Cel6A

ACCEPTED MANUSCRIPT





Exo-exo Synergy between Cel6A and Cel7A  
from *Hypocrea jecorina*: Role of CBM and the  
Endo-lytic Character of the Enzymes

---

II



### ■ Insights Into Exo–Exo Synergy

Synergy between different cellulases is essential for efficient industrial breakdown of biomass, and has therefore attracted extensive research interest. The most commonly studied type occurs from the interplay of endo- and exo-lytic enzymes, but an equally strong synergy has been observed for pairs of exo-lytic enzymes (so-called exo–exo synergy). Earlier suggestions to the molecular underpinnings of exo–exo synergy rely on auxiliary endo-lytic activity or differences in substrate specificity. Westh and coworkers address this by investigating the synergy between two exo-lytic enzymes. They considered both wild types and variants without the carbohydrate binding module (CBM), and the results showed that the degree of synergy was much lower for CBM-less enzymes. Very little endo-activity could be detected for any of the enzymes, and it was suggested that the pronounced exo–exo synergy observed for this system reflects different substrate targeting for the two enzymes, which at least in part relies on the CBM. *Page 1639*

DOI 10.1002/bit.26145

### ■ Hyperosmolality on Protein Glycosylation in CHO Cells

Hyperosmolality, which is induced by repeated feeding of medium concentrates and/or the addition of a base to maintain optimal pH during fed-batch culture, often negatively affects protein glycosylation in recombinant CHO (rCHO) cells. However, the mechanism behind such osmolality-dependent glycosylation variations in rCHO cells remains unclear. In this work, the Lee group studies a comprehensive correlation between protein glycosylation and glycosylation-related gene expression in Fc-fusion protein-producing rCHO cells under hyperosmotic conditions.

Their study demonstrates that hyperosmolality decreases the sialylation of Fc-fusion proteins through reducing the highly sialylated and tetra-antennary *N*-linked glycans. Thus, decreased expression of the genes with roles in the *N*-glycan biosynthesis pathway correlates with reduced sialic acid content of Fc-fusion protein caused by hyperosmotic conditions. Further work is ongoing in the Lee lab to engineer rCHO cells to overcome the detrimental effect of hyperosmolality on glycoprotein sialylation. *Page 1721*

DOI 10.1002/bit.26146

### ■ Microfluidic-Based Process to Sort Cells Efficiently Secreting a Protein

Stable gene transfer in mammalian cells remains an unreliable process, demanding lengthy screening to find a cell clone that stably expresses the recombinant protein of interest and secretes it at high levels. A high-throughput and efficient solution to this issue is still lacking, which has been hampering both research and the pharmaceutical development of therapeutic proteins. In this paper, Droz, Harraghy, Lançon et al. report a novel microfluidic-based process relying on a mix of remanent and non-remanent magnetic microparticles to sort cells that efficiently secrete a protein of interest at high speed. Using approaches bridging physics, biology, and engineering, they design a device and methods that can be used to sort CHO cells secreting efficiently a therapeutic protein, and this at frequencies unseen with current state of the art approaches. *Page 1791*

DOI 10.1002/bit.26144

### ■ A Novel, High Fidelity Site-Specific Integration System for CHO Expression

Development of stable cell lines for expression of large molecule therapeutics represents a significant portion of the time and effort required to advance a molecule to clinical studies. Previously, the cell line development group at Pfizer developed a site-specific integration system based on Flp recombinase mediated cassette exchange (RMCE) to specifically target transgene expression to a pre-determined locus in the CHO genome. The system has proven to be effective in developing recombinant cell lines with predictable performance, shortening the development timeline and reducing effort from molecule selection to initiation of the manufacturing campaign. To further improve the targeting efficiency and develop additional CHO host engineering tools for the production of complex therapeutic modalities, in this issue, the authors developed a novel RMCE system based on the highly efficient Bxb1 recombinase. The authors inserted genetic constructs flanked by the recognition sites of either Bxb1 or Flp in a specific locus in the CHO-S genome using CRISPR technology and created Bxb1- or Flp-RMCE host cell lines. They then demonstrated the superior precision of the Bxb1-RMCE system in delivering targeting expression vector for monoclonal antibody production. *Page 1837*

DOI 10.1002/bit.26147



# Exo-Exo Synergy Between Cel6A and Cel7A From *Hypocrea jecorina*: Role of Carbohydrate Binding Module and the Endo-Lytic Character of the Enzymes

Silke F. Badino <sup>1</sup>, Stefan J. Christensen <sup>1</sup>, Jeppe Kari <sup>1</sup>, Michael S. Windahl,<sup>1,2</sup> Søren Hvidt <sup>1</sup>, Kim Borch,<sup>2</sup> Peter Westh <sup>1</sup>

<sup>1</sup>Research Unit for Functional Biomaterials, Department of Science and Environment, INM, Roskilde University, 1 Universitetsvej, Build. 28C, DK-4000, Roskilde, Denmark; telephone: +45 4674 2879; fax: +45 4674 3011; e-mail: pwesth@ruc.dk

<sup>2</sup>Novozymes A/S, Bagsværd, Denmark

**ABSTRACT:** Synergy between cellulolytic enzymes is essential in both natural and industrial breakdown of biomass. In addition to synergy between endo- and exo-lytic enzymes, a lesser known but equally conspicuous synergy occurs among exo-acting, processive cellobiohydrolases (CBHs) such as Cel7A and Cel6A from *Hypocrea jecorina*. We studied this system using microcrystalline cellulose as substrate and found a degree of synergy between 1.3 and 2.2 depending on the experimental conditions. Synergy between enzyme variants without the carbohydrate binding module (CBM) and its linker was strongly reduced compared to the wild types. One plausible interpretation of this is that exo-exo synergy depends on the targeting role of the CBM. Many earlier works have proposed that exo-exo synergy was caused by an auxiliary endo-lytic activity of Cel6A. However, biochemical data from different assays suggested that the endo-lytic activity of both Cel6A and Cel7A were  $10^3$ – $10^4$  times lower than the common endoglucanase, Cel7B, from the same organism. Moreover, the endo-lytic activity of Cel7A was 2–3-fold higher than for Cel6A, and we suggest that endo-like activity of Cel6A cannot be the main cause for the observed synergy. Rather, we suggest the exo-exo synergy found here depends on different specificities of the enzymes possibly governed by their CBMs. *Biotechnol. Bioeng.* 2017;114: 1639–1647.

© 2017 Wiley Periodicals, Inc.

**KEYWORDS:** exo-exo synergy; Cel6A; Cel7A; CBM; cellulose; cellobiohydrolase

## Introduction

Mixtures of different cellulolytic enzymes usually show higher activity than the sum of the constituent enzymes assayed separately. This synergy between cellulases was discovered already in 1950 (Reese et al., 1950), and interest in the phenomenon has greatly increased as it has become clear that it is crucially important for industrial degradation of biomass to soluble sugars. Cellulase synergy has commonly been ascribed to the combined effect of endo-lytic enzymes such as endoglucanases (EG) or lytic polysaccharide monooxygenases (LPMO) on one hand, and processive, exo-lytic cellobiohydrolases (CBH) on the other (Eibinger et al., 2014; Henrissat et al., 1985; Kostylev and Wilson, 2012; Vaaje-Kolstad et al., 2010; Woodward, 1991). This so-called endo-exo synergy may arise as the EG or LPMO attack the chain internally and thus produce new chain ends for CBH attacks. This mechanism, however, does not seem to explain all observations of cellulase synergy, particularly the commonly observed synergy between exo-lytic CBHs such as Cel6A and Cel7A. This so-called exo-exo synergy was first reported by Fägerstam and Pettersson (1980) and has subsequently been observed for a range of systems and conditions (Boisset et al., 2000, 2001; Henrissat et al., 1985; Hoshino et al., 1997; Igarashi et al., 2011; Nidetzky et al., 1994; Tomme et al., 1988; Våljamäe et al., 1998). The extent of the synergistic effect (the so-called degree of synergy defined below) is typically quite similar for both exo-exo and endo-exo synergies (Henrissat et al., 1985; Igarashi et al., 2011; Nidetzky et al., 1994), and this obviously points toward a significant role of both modes.

Current suggestions regarding the molecular underpinnings of exo-exo synergy focus on two main ideas. One interpretation is based on a potential endo-lytic activity of CBHs; particularly Cel6A (Boisset et al., 2000, 2001; Divne et al., 1994; Medve et al., 1994; Poidevin et al., 2013; Ståhlberg, 1993). Thus, if indeed Cel6A conducts frequent internal attacks on the cellulose strand,

Michael S. Windahl's present address is Bioneer A/S, Kogle Allé 2, DK-2970 Hørsholm, Denmark.

Conflict of interest: KB works at Novozymes A/S, a major manufacturer of industrial enzymes.

Correspondence to: P. Westh

Contract grant sponsor: Carlsbergfondet

Contract grant number: 2013-01-0208

Contract grant sponsor: Innovation Fund Denmark

Contract grant numbers: 0603-00496B; 5150-00020A

Received 30 November 2016; Revision received 17 February 2017; Accepted 21 February 2017

Accepted manuscript online 28 February 2017;

Article first published online 16 March 2017 in Wiley Online Library

(<http://onlinelibrary.wiley.com/doi/10.1002/bit.26276/abstract>).

DOI 10.1002/bit.26276

synergy between Cel7A and Cel6A could simply be a special case of conventional endo-exo synergy, where Cel6A played the role of the EG. Alternatively, exo-exo synergy could rely on differences in enzyme specificity. In this case, synergy could be envisioned if one enzyme removes certain regions or patches, and hence reveals a new surface that makes up a better substrate for the other enzyme. This idea that one enzyme can remove structures that are problematic to convert for the other, has also been put forward as an alternative explanation for conventional endo-exo synergy (Eriksson et al., 2002; Fox et al., 2012; Jalak et al., 2012; Våljamäe et al., 1998).

The suggestion of an (auxiliary) endolytic activity of Cel6A is generally linked to the architecture of its active site region, which is more open and dynamic than the analogous region in Cel7A (Divne et al., 1994; Rouvinen et al., 1990; Varrot et al., 2003; Zou et al., 1999). This is thought to facilitate internal association with the cellulose strand and hence endo-lytic catalysis. This interpretation was used for example by Boisset et al. (2000), who studied Cel7A and Cel6A from *Humicola insolens*. This work used TEM images to elucidate structural changes in cellulose particles during hydrolysis and concluded that Cel6A was an endo-processive CBH. Many subsequent studies have used this classification to rationalize different types of activity data for Cel6A (see Payne et al., 2015 for a review). Direct biochemical evidence for endo-lytic activity of both Cel6A and Cel7A was provided in a ground breaking study by Ståhlberg (1993), but otherwise both qualitative and quantitative measurements of the endo-lytic activity of CBHs remain sparse and it appears that further insights into this is necessary for a better understanding of the catalytic interplay of Cel7A and Cel6A. Turning to substrate specificity, the second plausible cause of exo-exo synergy, some conspicuous disparities in the preference of respectively Cel6A and Cel7A has been identified. Firstly, Cel7A attacks the reducing end of the cellulose strand whereas Cel6A is specific for the non-reducing end (Claeysens et al., 1990; Davies and Henrissat, 1995). Secondly, Cel6A has been reported to preferentially hydrolyse amorphous cellulose, while Cel7A is superior on crystalline substrates (Bubner et al., 2013; Ganner et al., 2012; Gruno et al., 2004; Ståhlberg, 1993).

To elucidate the importance of these two mechanisms, we have conducted a comprehensive biochemical investigation of mixtures of Cel7A and Cel6A from *Hypocrea jecorina*. The work covered a range of enzyme- and substrate concentrations, and used both wild type enzymes and truncated variants, where the carbohydrate binding module (CBM) and linker had been removed from one or both enzymes. Based on the synergy data and three independent assays for the endo-lytic activity we suggest that substrate specificity, probably governed by the targeting role of the CBM is the main reason for synergy between Cel7A and Cel6A.

## Materials and Methods

Enzymes were expressed in *Aspergillus oryzae* and purified as described elsewhere (Borch et al., 2014; Sørensen et al., 2015b) and truncated core enzymes were expressed without

linker and CBM. Enzyme concentrations were determined by UV absorption at 280 nm using theoretical extinction coefficients (Gasteiger et al., 2003) of 97,790 M<sup>-1</sup>cm<sup>-1</sup> (Cel6A), 82,195 M<sup>-1</sup>cm<sup>-1</sup> (Cel6A core), 86,760 M<sup>-1</sup>cm<sup>-1</sup> (Cel7A), 80,550 M<sup>-1</sup>cm<sup>-1</sup> (Cel7A core), 74,145 M<sup>-1</sup>cm<sup>-1</sup> (Cel7B), and 177,880 M<sup>-1</sup>cm<sup>-1</sup> (β-glucosidase). Enzyme activity was determined from the end-point concentration of reducing ends in 1 h trials. The substrate was Avicel PH-101 (Sigma–Aldrich St. Louis, MO) and we used loads of either 12 g/L Avicel (low substrate) or 60 g/L Avicel (high substrate). In all experiments with mixtures of Cel6A and Cel7A the total enzyme concentration of CBH was either 0.2 or 2 μM (while the ratio of the two components was varied systematically). In the reference experiments with only one CBH, we used concentrations between either 0 and 0.2 μM or 0 and 2 μM. The concentrations in these mono-component measurements were chosen to match the concentration of the component in the corresponding synergy mixture. All samples contained 10% β-glucosidase (mol βG/mol total enzyme) from *Aspergillus fumigatus*, and all experiments were made in 50 mM sodium acetate pH 5.0 at 25°C. Activity was quantified by the *para*-hydroxybenzoic acid hydrazide (PAHBAH) method (Lever, 1973) and experiments were performed, and quenched as described elsewhere (Sørensen et al., 2015b).

Endo-lytic activity was estimated by real-time measurements with a pyranose dehydrogenase (PDH) biosensor. PDH biosensors were prepared according to a previously published protocol (Cruys-Bagger et al., 2014) except that benzoquinone was used as mediator (instead of 2,6-dichlorophenolindophenol). The substrate used for the PDH measurements was carboxymethylated cellulose (CMC) 90 kDa (9004-32-4 Sigma–Aldrich) with an average molecular mass and degree of substitution of respectively, 90 kDa and 0.7 carboxymethyl substituent per pyranose ring. Sensors were calibrated several times daily in CMC against cellobiose solutions ranging from 0 to 100 μM. Experiments with Cel6A and Cel7A were made with 5 g/L CMC and 1 μM enzyme while for Cel7B, we used 0.5 g/L CMC and 0.2 μM enzyme. These differences in conditions were necessary as the production of cellobiose by Cel7B was otherwise too high and rapid to be captured by the biosensor in real time.

Endo activity was further determined in a simple colorimetric assay using the insoluble substrate azurine crosslinked cellulose; AZCL-HE-Cellulose (Megazyme, Bray, Ireland), which has previously been used to quantify endo-lytic activity (Kračun et al., 2015; Li et al., 2011). For Cel6A and Cel7A we used 10 μM while the enzyme concentration for Cel7B was 0.10 μM. We used 5 g/L AZCL-HE in all measurements and the reaction was allowed to progress for 1 h at pH 5.0 at 25°C in a thermomixer operating at 1100 rpm. Reactions were terminated by centrifugation and the endo-lytic activity was specified as the absorbance in the supernatant at 595 nm per μM enzyme.

Finally, endo-lytic activity was monitored on the basis of changes in the viscosity of CMC semi-dilute solutions, for which the viscosity depends very strongly on molar mass. Steady shear viscosities were measured in a Bohlin VOR

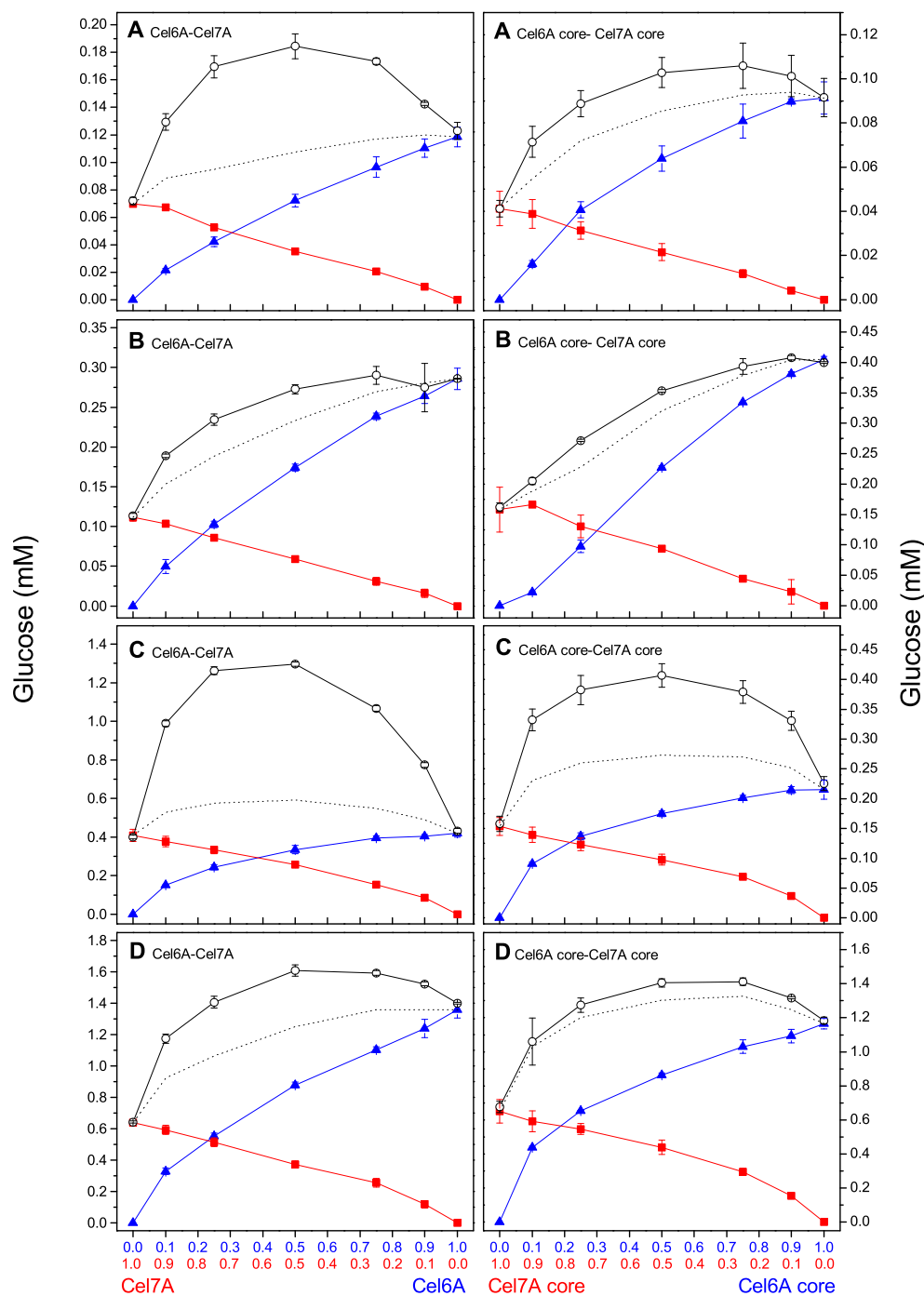


**Figure 1.** Activity data (formation of glucose) for Cel6A, Cel7A and their mixtures (left column), and for Cel6A core, Cel7A core, and their mixtures (right column). All experiments had 10%  $\beta$ -glucosidase (mol  $\beta$ G/mol CBH). Condition (A) 12 g/L Avicel and total [CBH] = 0.2  $\mu$ M, (B) 60 g/L Avicel and total [CBH] = 0.2  $\mu$ M, (C) 12 g/L Avicel and total [CBH] = 2  $\mu$ M, and (D) 60 g/L avicel and total [CBH] = 2  $\mu$ M. Blue triangles: Cel6A (or Cel6A core) in buffer. Red squares: Cel7A (or Cel7A core) in buffer. Dotted line indicates theoretical sum of the mono-components. Open circles: activity of mixtures of Cel6A and Cel7A or Cel6A core, and Cel7A core in different enzyme ratios with a constant enzyme concentration. Symbols are averages of triplicate measurements and error bars represent SD. All activities are plotted as function of fraction of Cel6A/Cel6A core and Cel7A/Cel7A core.

rheometer using a C14 couette system with a constant steady shear rate of 14.6  $s^{-1}$  at 25°C (Pedersen et al., 2016). The viscosity changes of 50 g/L CMC were monitored following addition of 5  $\mu$ M enzyme for Cel6A and Cel7A and 1, 0.1, and

0.01  $\mu$ M for Cel7B. The volume added were 240  $\mu$ L for all runs. The effect of dilution on the viscosity was determined by addition of 240  $\mu$ L buffer and subtracted the drop in viscosity caused by the enzymes.



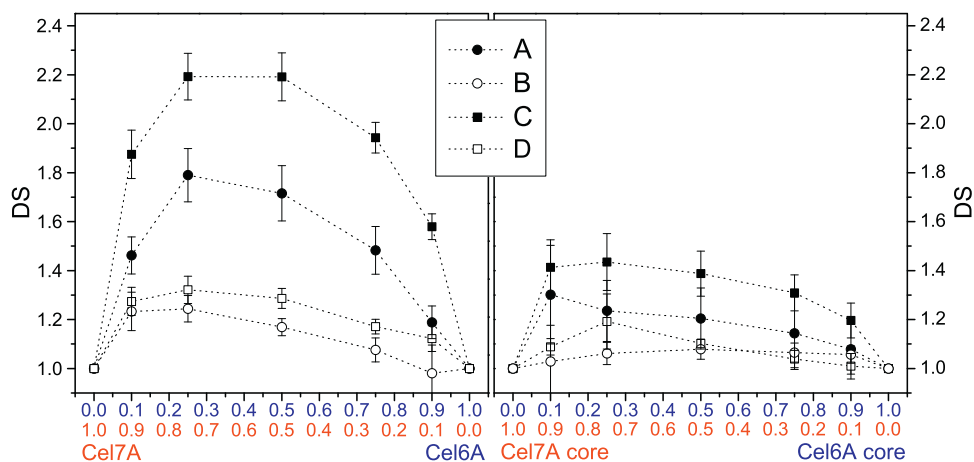


**Figure 2.** Degree of synergy (DS) calculated according to eq. (1) for pairs of wild-type enzymes (left) and pairs of core variants (right), and plotted as function of enzyme composition. The different curves in each panel refer to the experimental conditions (A, B, C, or D) specified in Fig. 1). Error bars are SD propagated forward from original SD in Figure 1.

## Results

### Synergy Measurements

The activity of Cel6A, Cel7A, and their mixtures (both wild-types and truncated core enzymes) was assessed from 1 h end-point measurements. Four different types of experiments were conducted for each pair of enzymes. These were high enzyme (total

concentration of cellulases 2 and 0.2  $\mu\text{M}$   $\beta\text{G}$ ), low enzyme (0.2  $\mu\text{M}$  cellulase plus 0.02  $\mu\text{M}$   $\beta\text{G}$ ), high substrate (60 g/L Avicel), and low substrate (12 g/L). Results for enzyme mixtures are given by black symbols in Figure 1. To calculate the degree of synergy, the activity of the enzyme mixtures must be compared with the activity of each component in isolation. To this end we measured the glucose concentration in experiments with only one component. These reference experiments were conducted for both enzymes and at

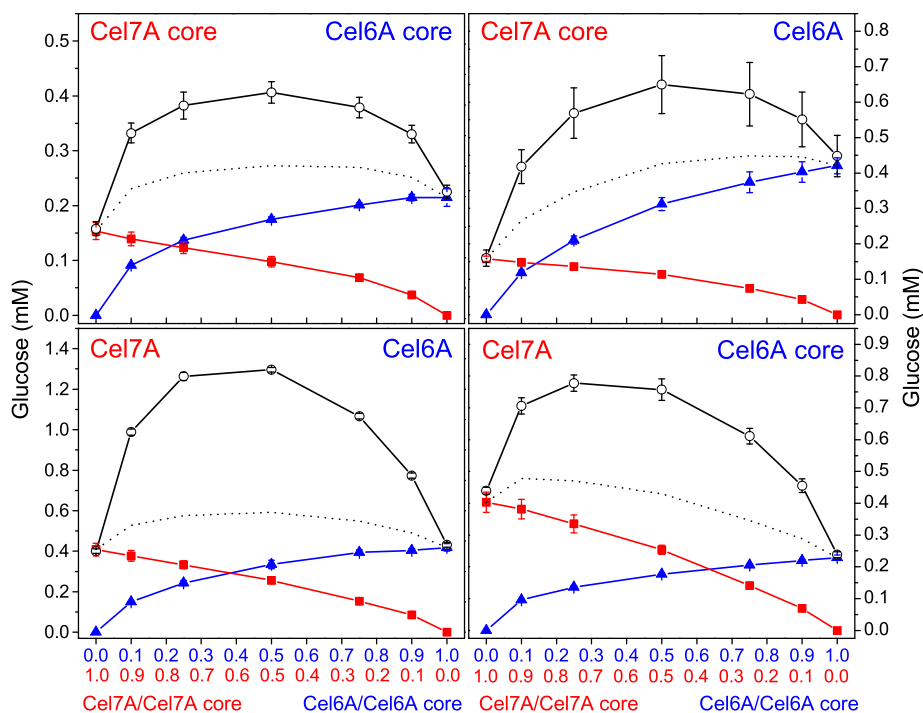


**Figure 3.** Activity data (formation of glucose) for Cel6A and Cel7A, Cel6A and Cel7A core, Cel6A core and Cel7A, Cel6A core and Cel7A core, and their mixtures at 12 g/L Avicel and  $[\text{CBH}] = 2 \mu\text{M}$  in the presence of 10%  $\beta$ -glucosidase. Blue triangles: Cel6A or Cel6A core in buffer. Red squares: Cel7A or Cel7A core in buffer. Dotted line indicates theoretical sum of the mono-components. Open circles represent activity of mixtures at different enzyme ratios. Error bars indicate SD from triplicates.

all seven mono-component concentrations that occurred in the enzyme mixture measurements. Results for the reference experiments are given in respectively blue (Cel6A) and red (Cel7A) in Figure 1. The apparent activities of the enzyme mixtures (black lines) were consistently higher than the sum of the mono-components (dashed lines) and this is a hallmark of exo-exo synergy. The extent of this synergy varied strongly among the tested systems, but it was always higher for pairs of wild-type enzymes compared to pairs of core variants. To assess this quantitatively, we calculated the degree of synergy, DS

$$DS = \frac{A_{\text{Cel6A}+\text{Cel7A}}}{A_{\text{Cel6A}} + A_{\text{Cel7A}}} \quad (1)$$

where,  $A_{\text{Cel6A}+\text{Cel7A}}$  is the apparent activity of the enzyme mixture, and  $A_{\text{Cel6A}}$  and  $A_{\text{Cel7A}}$  are the apparent activities in the corresponding mono-component experiments (i.e., the two separate experiments with the same mono-component concentrations as in the mixture). Values of DS are plotted as a function of the enzyme composition in Figure 2, and these results underscore that synergy is much stronger for pairs of wild types (both having a CBM) than for pairs of core variants. Regardless of whether the enzymes have a CBM (Fig. 2 left) or not (Fig. 2 right), condition C with low substrate load (12 g/L) and high enzyme concentration (2  $\mu\text{M}$ ) gives rise to the strongest synergy. Conversely, synergy for conditions B and D (with high substrate load) consistently showed low DS, and under these conditions synergy between the two core variants could only just be singled out against the experimental scatter.

To further study the role of the CBM for exo-exo synergy, we tested Cel6A-Cel7A enzyme pairs composed of one wild type and one core variant (e.g., Cel6A and Cel7A core). These measurements were all done under condition C (2  $\mu\text{M}$  cellulase and 12 g/L Avicel), where DS had been shown (Fig. 2) to be strongest. Results are presented in Figures 3 and 4, which are designed analogously to Figures 1 and 2. The results for asymmetric pairs of core-wild type enzymes reiterate the general picture for the symmetric enzyme pairs in Figure 2. Thus, the overall trend was that DS decreased when one of the enzymes had no CBM. Closer

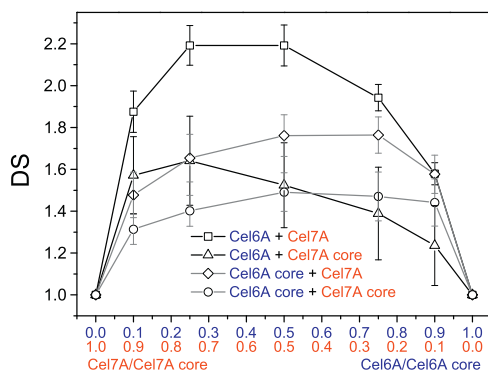


**Figure 4.** Degree of synergy (DS) calculated according to eq. (1) for the wt-core combinations at condition C (2  $\mu\text{M}$  [CBH] and 12 g/L Avicel). Error bars are SD propagated forward from original SD in Figure 3.

inspection of Figure 4 suggests that the loss of the CBM from Cel7A had a stronger negative effect on synergy than the loss of the CBM from Cel6A.

## Endo-Lytic Activity

Existing biochemical methods for the distinction of endo- and exolytic cellulase activity have different shortcomings, and we therefore conducted three independent assays to assess the endo-lytic activity of the wild-type CBHs. Two of the experimental approaches were based on CMC, which is the standard substrate used to identify endo-lytic cellulase activity (McCleary et al., 2012). In the first of these assays we followed the enzymatic release of soluble sugars in real time by a PDH biosensor (Cruys-Bagger et al., 2014). Results in Figure 5A show an initial phase of rapid hydrolysis followed by a much slower, almost constant reaction rate. The slope in the rapid phase (first 10–20 s in Fig. 5A) is about 10-fold higher than in the slow phase (after 250 s) for both enzymes. The transition between the fast- and slow phase occurs at 5–10  $\mu\text{M}$  cellobiose,

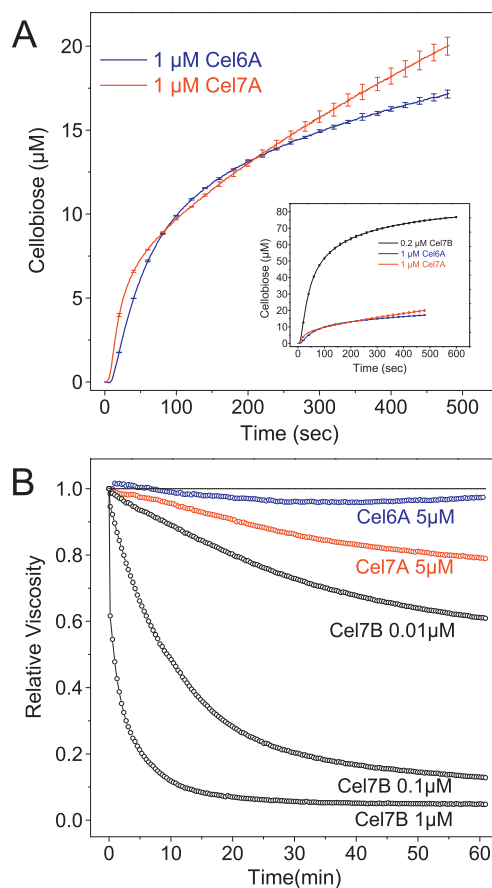


**Figure 5.** Endolytic activity of Cel6A and Cel7A on carboxymethyl cellulose (CMC) (A) Real-time recording of hydrolytic activity. The blue and red trace represent hydrolysis of 5 g/L CMC by respectively, 1  $\mu\text{M}$  Cel6A and 1  $\mu\text{M}$  Cel7A. The black curve in the inset shows the activity of 0.2  $\mu\text{M}$  Cel7B against 0.5 g/L CMC. Error bars (shown at every 20 s) indicate SD from duplicates. (B) Relative changes in viscosity of 50 g/L CMC upon enzymatic attack at 25°C, Cel6A (blue), Cel7A (red), and the endoglucanase Cel7B (black).

which corresponds to the conversion of less than 0.1% of the CMC, and we deduce that this small population of CMC is readily available as substrate for the CBHs, possibly through exo-attack. This interpretation is in accord with both the viscosimetric measurements (see Fig. 5B) and estimates based on the degree of substitution of the CMC. Thus, we estimated the concentration of unlabeled stretches of pyranose rings at the end of the CMC molecule that the CBHs could realistically attack on the basis of the average molecular mass and degree of substitution (see Materials and Methods section). Unlabeled stretches of four pyranose units, for example, statistically occurred at a concentration of about 4  $\mu\text{M}$  for the samples used in Figure 5A, while the analogous number for stretches of six unlabeled pyranose moieties was about 1  $\mu\text{M}$ . These concentrations compare well to the location of the transition in Figure 5A, and we conclude that the degree of substitution of the CMC does not contradict the above interpretation of the transition point. Another possible reason for the transition in Figure 5A is product inhibition, but firstly this would not be expected to show a discrete change as in the figure and secondly the inhibition constant for cellobiose of Cel7A acting on polymeric substrate is hundredths of  $\mu\text{M}$  (Gruno et al., 2004; Olsen et al., 2016; Teugjas and Våljamäe, 2013), and product inhibition would therefore only induce insignificant effects on the overall rates in Figure 5A. The inhibition of Cel6A by cellobiose is still lower (Murphy et al., 2013; Teugjas and Våljamäe, 2013), and it appears that product inhibition is an unlikely cause for the sharp change of trace in Figure 5A. After this exo-attack available substrate has been degraded, the biosensor trace reflects endo-lytic activity of the enzyme. Interestingly, this interpretation implies about twice as high endo-lytic activity of Cel7A compared to Cel6A. As a control, the activity against CMC of *H. jecorina* Cel7B, which is traditionally categorized as an endoglucanase, was also measured with the biosensor. Results in the inset of Figure 5A show much higher activity for this enzyme (note that both enzyme and substrate concentrations are strongly reduced compared to the CBH measurements).

We also assessed the endo-lytic activity on the basis of the reduction in the viscosity of CMC solutions. This approach has been used extensively (see McCleary et al., 2012 for a review) and its main advantage is that exo-lytic attacks are essentially mute with respect to viscosity changes. The analysis applied here has been described elsewhere (Pedersen et al., 2016). Results in Figure 5B show that high concentrations (5  $\mu\text{M}$ ) of either Cel7A or Cel6A bring about a moderate reduction in the viscosity of a 50 g/L CMC solution over the time scale studied here. Cel7B, on the other hand, reduces viscosity dramatically and normalization of the initial slope in Figure 5B with respect to the enzyme concentration suggests  $10^3$ – $10^4$  times higher endo-lytic activity of Cel7B compared to the CBHs. These results support the above interpretation of the biosensor measurements inasmuch as the high initial activity of Cel6A and Cel7A on CMC (Fig. 5A) did not lead to detectable viscosity changes in the same systems (Fig. 5B). This behavior is expected if the initial activity burst in Figure 5A reflects exo-lytic hydrolysis of a small population of the CMC, which has accessible strand ends (this reaction would essentially not change the viscosity). More importantly, the results in Figure 5B are also congruent in the sense that Cel7A shows 2–3-fold higher endo-lytic activity than Cel6A.

**Table I.** Endo-activity of Cel7A, Cel6A, and Cel7B on the endo cellulose-substrate azurine crosslinked cellulose (AZCL-HE-Cellulose) estimated from absorption  $A_{595}/\mu\text{M}$  enzyme after 1 h hydrolysis. We used 5 g/L AZCL-HE-Cellulose and 10  $\mu\text{M}$  [E] for Cel7A and Cel6A, and 0.1  $\mu\text{M}$  for Cel7B.

|       | AZCL-HE cellulose activity $A_{595}/\mu\text{M}$ | Relative activity     |
|-------|--------------------------------------------------|-----------------------|
| Cel7A | $0.0133 \pm 0.0001$                              | $4.23 \times 10^{-4}$ |
| Cel6A | $0.0058 \pm 0.0003$                              | $1.84 \times 10^{-4}$ |
| Cel7B | $31.300 \pm 0.2498$                              | 1                     |

In the third assay for endolytic activity we measured the release of azurine from azurine crosslinked cellulose (AZCL-HE-Cellulose). Results in Table I confirm the interpretation of Figure 5. Thus, we found a 2–3-fold higher endo-lytic activity for Cel7A compared to Cel6A and a  $10^3$ – $10^4$  times higher activity for Cel7B. In conclusion, we consistently found that the endo-lytic activity of Cel7A was 2–3 times higher than Cel6A, and that these two CBH are at least 1,000 times less endo-active than Cel7B. As the endo-lytic activity of the CBHs is so low, we cannot rule out that the results can be influenced by a slight EG contamination in our samples (a contamination in the order of  $1:10^4$  by Cel7B, e.g. would influence the results, but be essentially impossible to detect by standard methods). Therefore, our relative endo-lytic activities of the CBHs ( $10^3$ – $10^4$  times less than Cel7B) are upper limits, and the true endo-activity of the CBHs could be even lower. Furthermore we cannot eliminate that differences in EG contamination could influence the relative endo-activity of the two CBHs, but since both CBHs are expressed and purified by exactly the same protocol we find this unlikely.

## Discussion

Enzymatic conversion of biomass to fermentable sugars is a key process in emerging industries that produce sustainable fuels and alternatives to petrochemicals from lignocellulosic feedstocks. This conversion (so-called saccharification) requires quite large enzyme doses and minimization of enzyme consumption is therefore vitally important for the economic feasibility of the industry. One important avenue toward lower enzyme consumption is design of enzyme cocktails with a higher degree of synergy. However, the degree of synergy has been shown to depend quite markedly on a range of parameters including surface density of bound enzyme (Medve et al., 1994; Woodward et al., 1988), physical properties of the substrate (Hoshino et al., 1997; Valjamae et al., 1999), hydrolysis time (Boisset et al., 2001; Medve et al., 1998), cellulase mole fraction and substrate conversion (Jeoh et al., 2006; Olsen et al., 2017), and this complex behavior has challenged attempts to elucidate molecular origins of the measured synergy. As a result, discovery of cellulase cocktails with a high degree of synergy remains primarily an empirical endeavor. Clearly, better understanding of the underlying mechanisms would be desirable as it could gradually promote rational elements in the development of enzyme cocktails with more efficient synergy. In the current work we have zoomed in on the origin of the less extensively studied exo-exo synergy.

One central molecular interpretation of exo-exo synergy between Cel7A and Cel6A has been an auxiliary endo-lytic activity of the latter

(Boisset et al., 2000; Poidevin et al., 2013), and this understanding has been mainly based on structural evidence (see Introduction section and Payne et al., 2015 for a review). However, this explanation was not supported by the biochemical data presented here. We found a low endo-lytic activity of both wild types, but Cel7A was more endo-active compared to Cel6A. Our results on the endo-lytic activity of the CBHs were consistent among the three assays types and also congruent to some earlier studies. For example, both Cel7A and Cel6A have been shown to have low activity against CMC (Ståhlberg, 1993), and an earlier work also found that Cel7A was slightly more active than Cel6A on this substrate (Irwin et al., 1993). Our experiments with both CMC and AZCL-HE cellulose indicated a relative endo-lytic activity of the two CBHs, which was  $10^3$ – $10^4$  times lower than an EG (Cel7B) from the same organism. This minor endo-lytic activity is in line with the observation that Cel7A only produce a small amount of new reducing ends on bacterial cellulose (BC) (Kurasin and Våljamäe, 2011). Overall these results suggest that generation of new chain ends by the CBHs, in particular Cel6A, is of limited importance and hence not the main mechanism behind exo-exo synergy. Finally, we note that in light of the higher endo-lytic activity of Cel7A found here, the assignment of *H. jecorina* Cel6A as an endo-processive enzyme (Boisset et al., 2000) may need further examination.

In search for an interpretation that is more consistent with the current observations we note that the CBM promoted exo-exo synergy under all conditions studied here (Figs. 2 and 4). Thus, the highest DS (about 2.2, Fig. 2) was found for mixtures of the two wild type enzymes and removal of one or both CBMs gradually lowered DS. Mixtures of two core variants on high substrate load (60 g/L) showed limited or no synergy (DS < 1.2). Results from the asymmetric mixtures (one core and one wild type, Fig. 4) further suggested that the CBM on Cel7A was more important for DS than Cel6A's CBM. This behavior is in line with the interpretation that synergy is connected to the targeting function of the CBM (Carrard et al., 2000; Fox et al., 2013; Herve et al., 2010; Liu et al., 2011; McLean et al., 2002). Different targeting of two enzymes may cause synergy if one enzyme hydrolyzes certain surface structures, crystalline or amorphous regions, and hence expose better substrate for the other. This molecular origin of synergy is independent of whether the enzymes utilize exo- or endo lytic mechanisms, and it has indeed previously been proposed to underlie some cases of endo-exo synergy (Eriksson et al., 2002; Fox et al., 2012; Igarashi et al., 2011; Jalak et al., 2012). In particular, Jalak et al. (2012) suggested that endo-exo synergy reflected a preference of the EG for amorphous sections of BC because sparse amorphous segments make obstacles for the processive movement of Cel7A. In accordance with this, Fox et al. (2012) found that presence of EG increased the processive length of Cel7A. As Cel6A has been suggested to be particularly active on amorphous cellulose (Ganner et al., 2012), an analogous mechanisms could be responsible for the exo-exo synergy observed here. This interpretation is further supported by Igarashi et al. (2011) who showed that presence of Cel6A improved the mobility of Cel7A enzymes and thereby reduced enzyme "traffic jams." This conclusion would also be in line with the reported preference of Cel7A's CBM for the hydrophobic surface of crystalline cellulose (McLean et al., 2002), as well as an earlier observation that

sequential exo-exo synergy is observed with pretreatment of Cel6A before action of Cel7A (Våljamäe et al., 1998).

Some studies have suggested that in addition to its role in binding and targeting, the CBM directly assists the catalytic process (Beckham et al., 2010; Din et al., 1991; Guillen et al., 2010; Hall et al., 2011; Lemos et al., 2003; Mulakala and Reilly, 2005; Teeri et al., 1992), and if indeed so, this could also lead to synergy in mixtures of enzymes with different CBMs. We note, however, that a clear positive role of the CBM for activity does not appear from the current results. Looking, for example, at the data in Figure 1B and D, we find that at high substrate loads, the pair of core variants had a comparable or higher activity than the pair of wild types with CBMs. Synergy, on the other hand, was consistently low in these high-solid experiments (see Fig. 2). High activity of CBM-free enzymes in concentrated substrate suspensions, as observed here, has been reported earlier (Le Costaouec et al., 2013; Pakarinen et al., 2014; Várnai et al., 2013), and interpreted as a sign of an off-rate controlled reaction (Sørensen et al., 2015a,b). Thus, if enzyme-substrate dissociation is the rate limiting step, the weaker association of core-variants will speed up the overall reaction at high loads of substrate (increase  $V_{max}$ ) (Sørensen et al., 2015a,b). More importantly in the current context, comparison of results for wild types and core variants in Figures 1 and 2 shows that high apparent activity and high synergy may occur independently. This observation is consistent with the mechanism of synergy suggested by Jalak et al. (2012) (see the Introduction section). These workers noted that if slow dissociation of enzyme that was stalled in front of obstacles on the cellulose surface was rate limiting, synergy could occur if another enzyme specifically removed such obstacle structures. Jalak et al. (2012) suggested that the obstacles were amorphous regions of cellulose, but the same argument could be valid for other putative structures that obstruct the processive movement of the CBH. For the core variants with higher rates of dissociation, stalling in front of obstacles is likely to be less important, and it follows that removal of such obstacles would not generate the same degree of synergy.

One last aspect of this work concerns the way DS is obtained experimentally. Thus, many earlier studies have measured mono-component activity only at one enzyme concentration, typically corresponding to the total enzyme concentration in the mixtures (see, e.g., Boisset et al., 2000, 2001; Henrissat et al., 1985; Olsen et al., 2017; Tomme et al., 1988). The contribution at other mono-component concentrations that occurred in mixtures was then estimated based on the assumption of a linear dose-activity relationship. However, some of the mono-component dose-activity curves in Figure 1 (red and blue lines) were highly non-linear. This non-linearity is common for cellulases (Bezerra and Dias, 2004; Sattler et al., 1989), and neglect of this will severely influence the calculated value of DS. An extreme example of this can be seen in Figure 1D, where the core enzymes show essentially no synergy (black and dashed curves are almost superimposed). This result, however, is very dependent on the non-linearity of the mono-component activity curves (Fig. 1D), and for these specific results, a linear approximation would give (erroneous) DS values up to 1.6. We strongly suggest that future work includes mono-component activity measurements at several concentrations as it was recently done by Igarashi et al. (2011).

In conclusion we have found that Cel6A and Cel7A from *H. jecorina* show distinct synergy with DS values exceeding two under some conditions. The auxiliary endo-lytic activity of both enzymes was extremely small compared to an endoglucanase from the same organism, and we suggest that an endo-like activity of the CBH is not the cause of the synergy observed here. The extent of the exo-exo synergy gradually decreased if one or both enzymes did not have a CBM. This observation is consistent with the hypothesis put forward for conventional exo-endo synergy (Eriksson et al., 2002; Jalak et al., 2012) that targeting toward different structures on the cellulose surface can cause synergy. We speculate that the well-known targeting role of the CBM could be the primary cause of exo-exo synergy for Cel7A and Cel6A.

This work was supported by Innovation Fund Denmark and Carlsberg Foundation. We are grateful for the technical assistance of Cynthia Segura Vesterager.

## References

- Beckham GT, Matthews JF, Bomble YJ, Bu LT, Adney WS, Himmel ME, Nimlos MR, Crowley MF. 2010. Identification of amino acids responsible for processivity in a family 1 carbohydrate-binding module from a fungal cellulase. *J Phys Chem B* 114(3):1447–1453.
- Bezerra RM, Dias AA. 2004. Discrimination among eight modified michaelis-menten kinetics models of cellulose hydrolysis with a large range of substrate/enzyme ratios: Inhibition by cellobiose. *Appl Biochem Biotechnol* 112(3):173–184.
- Boisset C, Frascini C, Schülein M, Henrissat B, Chanzy H. 2000. Imaging the enzymatic digestion of bacterial cellulose ribbons reveals the endo character of the cellobiohydrolase Cel6A from *Humicola insolens* and its mode of synergy with cellobiohydrolase Cel7A. *Appl Environ Microbiol* 66(4):1444–1452.
- Boisset C, Pétrequin C, Chanzy H, Henrissat B, Schülein M. 2001. Optimized mixtures of recombinant *Humicola insolens* cellulases for the biodegradation of crystalline cellulose. *Biotechnol Bioeng* 72(3):339–345.
- Borch K, Jensen K, Krogh K, McBrayer B, Westh P, Kari J, Olsen J, Sørensen T, Windahl M, Xu H. 2014. W02014138672 A1 Cellobiohydrolase variants and polynucleotides encoding same.
- Bubner P, Plank H, Nidetzky B. 2013. Visualizing cellulase activity. *Biotechnol Bioeng* 110(6):1529–1549.
- Carrard G, Koivula A, Soderlund H, Beguin P. 2000. Cellulose-binding domains promote hydrolysis of different sites on crystalline cellulose. *Proc Natl Acad Sci USA* 97(19):10342–10347.
- Claeyssens M, Tomme P, Brewer CF, Hehre EJ. 1990. Stereochemical course of hydrolysis and hydration reactions catalysed by cellobiohydrolases I and II from *Trichoderma reesei*. *FEBS Lett* 263(1):89–92.
- Cruys-Bagger N, Badino SE, Tokin R, Gontsarik M, Fathalinejad S, Jensen K, Toscano MD, Sørensen TH, Borch K, Tatsumi H, Våljamäe P, Westh P. 2014. A pyranose dehydrogenase-based biosensor for kinetic analysis of enzymatic hydrolysis of cellulose by cellulases. *Enzyme Microb Technol* 58–59:68–74.
- Davies G, Henrissat B. 1995. Structures and mechanisms of glycosyl hydrolases. *Structure* 3(9):853–859.
- Din N, Gilkes NR, Tekant B, Miller RC, Warren RAJ, Kilburn DG. 1991. Non-Hydrolytic disruption of cellulose fibres by the binding domain of a bacterial cellulase. *Nat Biotech* 9(11):1096–1099.
- Divne C, Ståhlberg J, Reinikainen T, Ruohonen L, Pettersson G, Knowles JK, Teeri TT, Jones TA. 1994. The three-dimensional crystal structure of the catalytic core of cellobiohydrolase I from *Trichoderma reesei*. *Science* 265(5171):524–528.
- Eibinger M, Ganner T, Bubner P, Rosker S, Kracher D, Haltrich D, Ludwig R, Plank H, Nidetzky B. 2014. Cellulose surface degradation by a lytic polysaccharide monoxygenase and its effect on cellulase hydrolytic efficiency. *J Biol Chem* 289(52):35929–35938.
- Eriksson T, Karlsson J, Tjerneld F. 2002. A model explaining declining rate in hydrolysis of lignocellulose substrates with cellobiohydrolase I (Cel7A) and endoglucanase I (Cel7B) of *Trichoderma reesei*. *Appl Biochem Biotechnol* 101(1):41–60.
- Fox JM, Jess P, Jambusaria RB, Moo GM, Liphardt J, Clark DS, Blanch HW. 2013. A single-molecule analysis reveals morphological targets for cellulase synergy. *Nat Chem Biol* 9(6):356–361.
- Fox JM, Levine SE, Clark DS, Blanch HW. 2012. Initial- and processive-cut products reveal cellobiohydrolase rate limitations and the role of companion enzymes. *Biochemistry* 51(1):442–452.
- Fägerstam LG, Pettersson GL. 1980. The 1,4-β-glucan cellobiohydrolase of *Trichoderma reesei* QM 9414—a new type of cellulolytic synergism The 1,4-β-glucan cellobiohydrolase of *Trichoderma reesei* QM 9414—a new type of cellulolytic synergism. *FEBS Lett* 119(1):97–100.
- Ganner T, Bubner P, Eibinger M, Mayrhofer C, Plank H, Nidetzky B. 2012. Dissecting and reconstructing synergism: In situ visualization of cooperativity among cellulases. *J Biol Chem* 287(52):43215–43222.
- Gasteiger E, Gattiker A, Hoogland C, Ivanyi I, Appel RD, Bairoch A. 2003. ExPASy: The proteomics server for in-depth protein knowledge and analysis. *Nucl Acids Res* 31(13):3784–3788.
- Gruno M, Våljamäe P, Pettersson G, Johansson G. 2004. Inhibition of the *Trichoderma reesei* cellulases by cellobiose is strongly dependent on the nature of the substrate. *Biotechnol Bioeng* 86(5):503–511.
- Guillen D, Sanchez S, Rodriguez-Sanoja R. 2010. Carbohydrate-binding domains: Multiplicity of biological roles. *Appl Microbiol Biotechnol* 85(5):1241–1249.
- Hall M, Bansal P, Lee JH, Realf MJ, Bommarius AS. 2011. Biological pretreatment of cellulose: Enhancing enzymatic hydrolysis rate using cellulose-binding domains from cellulases. *Bioresour Technol* 102(3):2910–2915.
- Henrissat B, Driguez H, Viet C, Schülein M. 1985. Synergism of cellulases from *Trichoderma reesei* in the degradation of cellulose. *Nat Biotechnol* 3:722–726.
- Herve C, Rogowski A, Blake AW, Marcus SE, Gilbert HJ, Knox JP. 2010. Carbohydrate-binding modules promote the enzymatic deconstruction of intact plant cell walls by targeting and proximity effects. *Proc Natl Acad Sci USA* 107(34):15293–15298.
- Hoshino E, Shiroishi M, Amano Y, Nomura M, Kanda T. 1997. Synergistic actions of exo-type cellulases in the hydrolysis of cellulose with different crystallinities. *J Ferment Bioeng* 84(4):300–306.
- Igarashi K, Uchihashi T, Koivula A, Wada M, Kimura S, Okamoto T, Penttilä M, Ando T, Samejima M. 2011. Traffic jams reduce hydrolytic efficiency of cellulase on cellulose surface. *Science* 333(6047):1279–1282.
- Irwin DC, Spezio M, Walker LP, Wilson DB. 1993. Activity studies of eight purified cellulases: Specificity, synergism, and binding domain effects. *Biotechnol Bioeng* 42(8):1002–1013.
- Jalak J, Kurasin M, Teugias H, Valjamae P. 2012. Endo-exo synergism in cellulose hydrolysis revisited. *J Biol Chem* 287(34):28802–28815.
- Jeoh T, Wilson DB, Walker LP. 2006. Effect of cellulase mole fraction and cellulose recalcitrance on synergism in cellulose hydrolysis and binding. *Biotechnol Prog* 22(1):270–277.
- Kostylev M, Wilson D. 2012. Synergistic interactions in cellulose hydrolysis. *Biofuels* 3(1):61–70.
- Kračun SK, Schückel J, Westereng B, Thygesen LG, Monrad RN, Eijsink VG, Willats WG. 2015. A new generation of versatile chromogenic substrates for high-throughput analysis of biomass-degrading enzymes. *Biotechnol Biofuels* 8:70.
- Kurasin M, Våljamäe P. 2011. Processivity of cellobiohydrolases is limited by the substrate. *J Biol Chem* 286(1):169–177.
- Le Costaouec T, Pakarinen A, Várnai A, Puranen T, Viikari L. 2013. The role of carbohydrate binding module (CBM) at high substrate consistency: Comparison of *Trichoderma reesei* and thermoascus aurantiacus Cel7A (CBHI) and Cel5A (EGII). *Bioresour Technol* 143:196–203.
- Lemos MA, Teixeira JA, Domingues MRM, Mota M, Gama FM. 2003. The enhancement of the cellulolytic activity of cellobiohydrolase I and endoglucanase by the addition of cellulose bindingdomains derived from *Trichoderma reesei*. *Enzyme Microb Technol* 32:35–40.
- Lever M. 1973. Colorimetric and fluorometric carbohydrate determination with p-hydroxybenzoic acid hydrazide. *Biochem Med* 7(2):274–281.
- Li LL, Taghavi S, McCorkle SM, Zhang YB, Blewitt MG, Brunecky R, Adney WS, Himmel ME, Brumm P, Drinkwater C, Mead DA, Tringe SG, Lelie D. 2011. Bioprospecting metagenomics of decaying wood: Mining for new glycoside hydrolases. *Biotechnol Biofuels* 4(1):23.

- Liu YS, Baker JO, Zeng YN, Himmel ME, Haas T, Ding SY. 2011. Cellobiohydrolase hydrolyzes crystalline cellulose on hydrophobic faces. *J Biol Chem* 286(13):11195–11201.
- McCleary BV, McKie V, Draga A. 2012. Measurement of endo-1, 4-beta-glucanase. *Methods Enzymol* 510:1–17.
- McLean BW, Boraston AB, Brouwer D, Sanaie N, Fyfe CA, Warren RAJ, Kilburn DG, Haynes CA. 2002. Carbohydrate-binding modules recognize fine substructures of cellulose. *J Biol Chem* 277(52):50245–50254.
- Medve J, Karlsson J, Lee D, Tjerneld F. 1998. Hydrolysis of microcrystalline cellulose by cellobiohydrolase I and endoglucanase II from *Trichoderma reesei*: Adsorption, sugar production pattern, and synergism of the enzymes. *Biotechnol Bioeng* 59(5):621–634.
- Medve J, Ståhlberg J, Tjerneld F. 1994. Adsorption and synergism of cellobiohydrolase I and II of *Trichoderma reesei* during hydrolysis of microcrystalline cellulose. *Biotechnol Bioeng* 44(9):1064–1073.
- Mulakala C, Reilly PJ. 2005. *Hypocrea jecorina* (*Trichoderma reesei*) Cel7A as a molecular machine: A docking study. *Proteins* 60(4):598–605.
- Murphy L, Bohlin C, Baumann MJ, Olsen SN, Sørensen TH, Anderson L, Borch K, Westh P. 2013. Product inhibition of five *Hypocrea jecorina* cellulases. *Enzyme Microb Technol* 52(3):163–169.
- Nidetzky B, Steiner W, Hayn M, Claeysens M. 1994. Cellulose hydrolysis by the cellulases from *Trichoderma reesei*: A new model for synergistic interaction. *Biochem J* 298(Pt 3):705–710.
- Olsen JP, Alasepp K, Kari J, Cruys-Bagger N, Borch K, Westh P. 2016. Mechanism of product inhibition for cellobiohydrolase Cel7A during hydrolysis of insoluble cellulose. *Biotechnol Bioeng* 113(6):1178–1186.
- Olsen JP, Borch K, Westh P. 2017. Endo/exo-synergism of cellulases increases with substrate conversion. *Biotechnol Bioeng* 114(3):696–700.
- Pakarinen A, Haven MO, Djajadi DT, Várnai A, Puranen T, Viikari L. 2014. Cellulases without carbohydrate-binding modules in high consistency ethanol production process. *Biotechnol Biofuels* 7(1):27–38.
- Payne CM, Knott BC, Mayes HB, Hansson H, Himmel ME, Sandgren M, Stahlberg J, Beckham GT. 2015. Fungal cellulases. *Chem Rev* 115(3):1308–1448.
- Pedersen KJ, Elsalhi HA, Thorsted PA, Khoury R, Vestager CS, Hvidt S. 2016. Rapid discrimination of endo- and exo-cellulases. *Nordic Rheology Society. Annu Trans* 24:103–109.
- Poidevin L, Feliu J, Doan A, Berrin JG, Bey M, Coutinho PM, Henrissat B, Record E, Heiss-Blanquet S. 2013. Insights into exo- and endoglucanase activities of family 6 glycoside hydrolases from *Podospora anserina*. *Appl Environ Microbiol* 79(14):4220–4229.
- Reese ET, Siu RG, Levinson HS. 1950. The biological degradation of soluble cellulose derivatives and its relationship to the mechanism of cellulose hydrolysis. *J Bacteriol* 59(4):485–497.
- Rouvinen J, Bergfors T, Teeri T, Knowles JK, Jones TA. 1990. Three-dimensional structure of cellobiohydrolase II from *Trichoderma reesei*. *Science* 249(4967):380–386.
- Sattler W, Esterbauer H, Glatter O, Steiner W. 1989. The effect of enzyme concentration on the rate of the hydrolysis of cellulose. *Biotechnol Bioeng* 33(10):1221–1234.
- Ståhlberg J. 1993. *Trichoderma reesei* has no true exo-cellulase: All intact and truncated cellulases produce new reducing end groups on cellulose. *Biochim Biophys Acta. General subjects.* —Amsterdam 1157(1):107–113.
- Sørensen TH, Cruys-Bagger N, Borch K, Westh P. 2015. Free energy diagram for the heterogeneous enzymatic hydrolysis of glycosidic bonds in cellulose. *J Biol Chem* 290(36):22203–22211.
- Sørensen TH, Cruys-Bagger N, Windahl MS, Badino SF, Borch K, Westh P. 2015. Temperature effects on kinetic parameters and substrate affinity of Cel7A cellobiohydrolases. *J Biol Chem* 290(36):22193–22202.
- Teeri TT, Reinikainen T, Ruohonen L, Jones TA, Knowles JKC. 1992. Industrial applications of natural, modified and artificial enzymes domain function in *trichoderma reesei* cellobiohydrolases. *J Biotechnol* 24(2):169–176.
- Teugjas H, Våljamäe P. 2013. Product inhibition of cellulases studied with 14C-labeled cellulose substrates. *Biotechnol Biofuels* 6(1):104.
- Tomme P, Van Tilbeurgh H, Pettersson G, Van Damme J, Vandekerckhove J, Knowles J, Teeri T, Claeysens M. 1988. Studies of the cellulolytic system of *Trichoderma reesei* QM 9414. Analysis of domain function in two cellobiohydrolases by limited proteolysis. *Eur J Biochem* 170(3):575–581.
- Vaaje-Kolstad G, Westereng B, Horn SJ, Liu Z, Zhai H, Sorlie M, Eijsink VG. 2010. An oxidative enzyme boosting the enzymatic conversion of recalcitrant polysaccharides. *Science* 330(6001):219–222.
- Våljamäe P, Sild V, Nutt A, Pettersson G, Johansson G. 1999. Acid hydrolysis of bacterial cellulose reveals different modes of synergistic action between cellobiohydrolase I and endoglucanase I. *Eur J Biochem* 266(2):327–334.
- Varrot A, Frandsen TP, von Ossowski I, Boyer V, Cottaz S, Driguez H, Schülein M, Davies GJ. 2003. Structural basis for ligand binding and processivity in cellobiohydrolase Cel6A from *Humicola insolens*. *Structure* 11(7): 855–864.
- Várnai A, Siika-Aho M, Viikari L. 2013. Carbohydrate-binding modules (CBMs) revisited: Reduced amount of water counterbalances the need for CBMs. *Biotechnol Biofuels* 6(1):30.
- Våljamäe P, Sild V, Pettersson G, Johansson G. 1998. The initial kinetics of hydrolysis by cellobiohydrolases I and II is consistent with a cellulose surface-erosion model. *Eur J Biochem* 253(2):469–475.
- Woodward J. 1991. Enzymatic hydrolysis of cellulose synergism in cellulase systems. *Bioresour Technol* 36(1):67–75.
- Woodward J, Hayes MK, Lee NE. 1988. Hydrolysis of cellulose by saturating and non-saturating concentrations of cellulase: Implications for synergism. *Nat Biotech* 6(3):301–304.
- Zou J, Kleywegt GJ, Ståhlberg J, Driguez H, Nerinckx W, Claeysens M, Koivula A, Teeri TT, Jones TA. 1999. Crystallographic evidence for substrate ring distortion and protein conformational changes during catalysis in cellobiohydrolase Cel6A from *trichoderma reesei*. *Structure* 7(9):1035–1045.



Exchanging Carbohydrate Binding  
Modules between Cel6A and Cel7A from  
*Hypocrea jecorina* strongly Influence the  
Kinetics of the Enzymes

---

*Manuscript in preparation*

III





## *Manuscript in preparation*

# Exchanging carbohydrate binding modules between Cel6A and Cel7A from *Hypocrea jecorina* strongly influence the kinetics of the enzymes

Silke Flindt Badino<sup>1</sup>, Michael Skovbo Windahl<sup>3</sup>, Jeppe Kari<sup>1</sup>, Kim Borch<sup>2</sup> & Peter Westh<sup>1</sup>

1. Research Unit for Functional Biomaterials, Department of Science and Environment, Roskilde University. 1 Universitetsvej, Build. 28.C, DK-4000, Roskilde Denmark.
2. Novozymes A/S, Krogshøjvej 36, DK-2880, Bagsværd, Denmark
3. Bioneer A/S, Kogle Allé 2, DK-2970 Hørsholm, Denmark

\*Corresponding author. Email: [pwesth@ruc.dk](mailto:pwesth@ruc.dk)

## **Abstract**

Hydrolysis of insoluble cellulose occurs in a solid-liquid interface where enzymes in solution associate to the substrate before catalysis. Many cellulases consist of a non-catalytic carbohydrate binding module (CBM) besides the catalytic domain (core). *Hypocrea jecorina* secretes two processive cellobiohydrolases (CBHs) Cel7A and Cel6A that attack reducing and non-reducing chain ends and they both contain a very similar CBM. Here we constructed two variants Cel6A<sub>Cel7ACBM</sub> and Cel7A<sub>Cel6ACBM</sub> where the CBM between Cel6A and Cel7A were exchanged. We applied two different kinetic analysis in comparison with their wildtypes and isolated core domains in order to investigate how the CBM swap changed the kinetics of the enzymes. Surprisingly, both variants exhibited significant reduction in the adsorption to Avicel and very interestingly an increased maximal catalytic rate at high substrate loads. The inverse relation between affinity and maximal activity was even more pronounced in wt core comparison of both Cel6A and Cel7A, but a dramatic change was also observed for Cel6A<sub>Cel7ACBM</sub> which performed more similar to the isolated core domain than Cel6A. Contrariwise at low substrate load and high enzyme concentrations the CBM exchange decreased the activity of Cel6A<sub>Cel7ACBM</sub> and Cel7A<sub>Cel6ACBM</sub> compared to the wildtypes indicating that both number of binding sites, but also the number of attack sites were reduced by the CBM swap. We speculate if a disrupted interplay between core, linker and CBM in Cel6A<sub>Cel7ACBM</sub> and Cel7A<sub>Cel6ACBM</sub> can explain the observed kinetic behavior.

## **Introduction**

Cellulase kinetics differs from traditional enzyme kinetics in which the substrate, cellulose, is an insoluble polymer. This means that cellulases need to associate or bind to the substrate before

catalysis. Many cellulases are multi-domain enzymes that consist of a catalytic core domain and a non-catalytic carbohydrate binding module (CBM) has been shown to be essential in the adsorption to cellulose [1-4]. CBMs are a diverse group of domains divided into different families where family 1 CBM (CBM1) is the smallest among them. All two-domain cellulases, including cellobiohydrolases and endoglucanases, secreted from *Hypocrea jecorina* (formerly known as *Trichoderma reesei*) have a CBM1. The structure of CBM1 of Cel7A was solved by NMR [5] and the CBM was shown to consist of two faces; a planar face formed by three aromatic tyrosines and a more rough face. Based on sequence homology the CBM from Cel6A were suggested a similar structure [6] with an additional disulfide bond in Cel6A. Several studies have investigated the role of the different amino acids (aa) in the CBM through site-directed mutagenesis and chemically synthetic CBM peptides [7-15], where especially the aromatic residues in the planar face have been addressed to be essential for substrate binding. The arrangement of the domains is mirror images in Cel6A and Cel7A in which the CBM is attached to the N-terminal of Cel6A and C-terminal of Cel7A. CBM1 has been exposed to extensive research, but studies with CBM exchange in between different GH families remain sparse. Many previous studies have shown that isolated core domains behave kinetically different from the full length enzymes, but how does CBM exchange affect the enzymes? To investigate this we made two variants; one with the core domain and linker from Cel7A together with the CBM of Cel6A and opposite core and linker from Cel6A with the CBM of Cel7A to investigate how this CBM exchange influence the enzymes. The concept of the two variants together with the protein sequence covering the linker-CBM transition is shown in Figure 1.

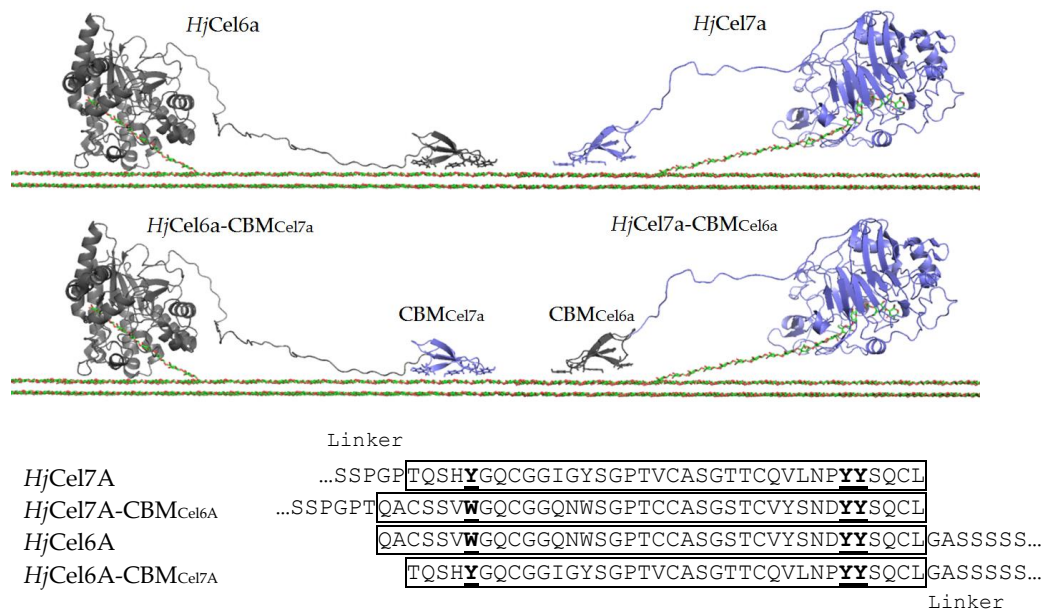


**Figure 1** An illustration of the concept of variants  $Cel6A_{CBM_{Cel7A}}$  and  $Cel7A_{CBM_{Cel6A}}$  together with the sequence covering the CBM and the linker transition. CBM sequences are framed and the three aromatic amino acids from the planar face highlighted. In  $HjCel7A-CBM_{Cel6A}$  an extra threonine (T) is inserted between linker and CBM in order to approximate the original transition from  $HjCel7A$ .

## Experimental Procedures and Kinetic Analysis

*Enzymes* were expressed in *Aspergillus oryzae* and purified as described elsewhere [16, 17] and UV absorption at 280nm and theoretical extinction coefficients were used to determine enzyme concentrations: 97,790 M<sup>-1</sup>cm<sup>-1</sup> (Cel6A), 82,195 M<sup>-1</sup>cm<sup>-1</sup> (Cel6A-core), 93,655 M<sup>-1</sup>cm<sup>-1</sup> (Cel6A<sub>Cel7ACBM</sub>), 86,760 M<sup>-1</sup>cm<sup>-1</sup> (Cel7A) and 80,550 M<sup>-1</sup>cm<sup>-1</sup> (Cel7A-core), 90,895 M<sup>-1</sup>cm<sup>-1</sup> (Cel6A<sub>Cel7ACBM</sub>). All experiments were performed in 50 mM NaAcetate pH 5.0 at 25°C and washed Avicel was used as substrate.

*Activity assays* where the amount of soluble reducing sugars produced during hydrolysis was quantified using the *para*-hydroxybenzoic acid hydrazide method [18] following the experimental procedure described in [17]. We used 0.2 μM of enzyme and substrate concentrations ranging from 1g/L to 80g/L Avicel. After hydrolysis we added 0.1 μM β-glucosidase from *Aspergillus oryzae* to increase the signal and we used a glucose standard from 0-500 μM. Absorption at 405 nm was determined. In the inverse MM approach a constant substrate load of 2g/L Avicel was used with varying enzyme concentrations ranging from 0.1 μM to 10 μM all in the presence of 0.1 μM β-glucosidase to prevent product inhibition of the enzymes in particular Cel7A [19, 20]. All experiments were carried out in triplicates.

*Binding isotherms* were made with different enzyme concentrations ranging from 0.1-3 μM. Standard curves ranging from 0.1-3 μM enzyme in buffer were made for all enzymes. The amount of free enzymes was determined by intrinsic fluorescence as described previously [17] using a plate reader (SpectraMax M2). In addition to the 100 μL supernatant we added another 50 μL buffer to each well before measuring the intrinsic fluorescence. 25 g/L Avicel was used as substrate.

*Product profiles* were determined on a Dionex ICS-5000 ion chromatograph using a CarboPac PA10 column. Samples were eluted with 190 mM NaOH and 425 mM sodium acetate. The product profiles were determined after 1 hour hydrolysis 50 g/L Avicel and 0.1 μM enzyme at 25°C. The reaction was terminated by adding NaOH to a final concentration of 0.1 M followed by centrifugation. Products were quantified using glucose, cellobiose and cellotriose standards and diluted 10 times prior to chromatography.

*Kinetic analysis* We investigated enzyme kinetics in two different steady state regimes at either enzyme or substrate excess. Detailed descriptions of the underlying kinetic analysis and derivation of relevant rate equations have been given elsewhere [21-24]. Here we provide a brief overview to facilitate assessment of the parameters derived in this work. The concept of respectively enzyme- and substrate saturation on a heterogeneous, insoluble substrate is illustrated in Fig. 2. The former behavior is well-known from traditional MM theory, and reflects a gradual saturation of all

enzyme molecules with substrate. The latter reflects the opposite situation, where a high concentration of enzyme eventually saturates all attack sites on the substrate surface, and hence prevents further increase in reaction rate.

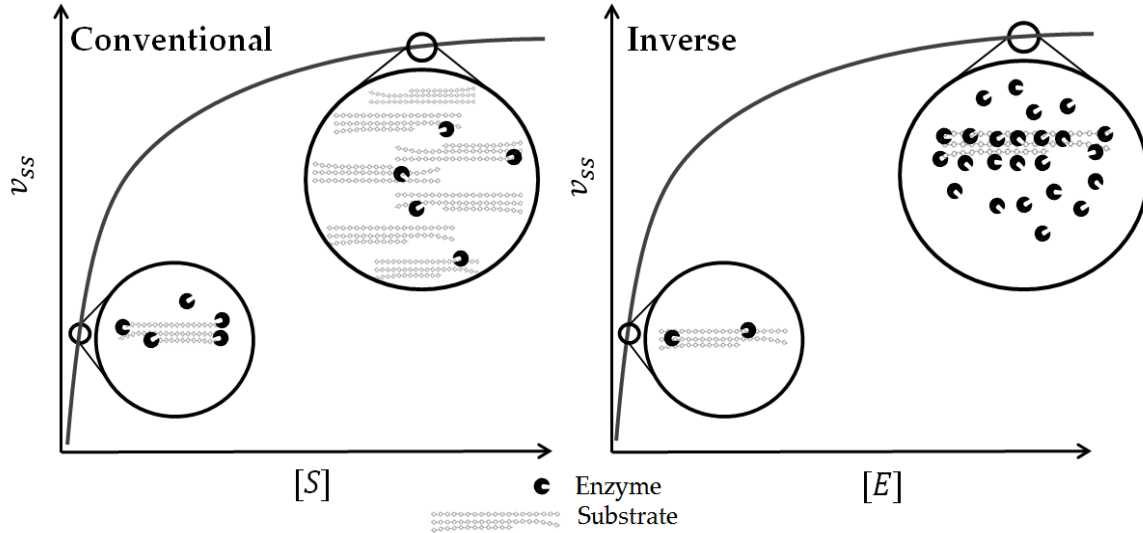


**Figure 2** The concept of substrate saturation (conventional) and enzyme saturation (inverse)

Under the assumption that all enzyme-substrate (ES) intermediates are at steady state and the substrate is in large excess, the expression for steady-state rate reduces into an analog to the conventional Michaelis Menten (MM) equation [21]

$${}^{conv}v_{ss} = \frac{{}^{conv}V_{max} \cdot S_0}{{}^{conv}K_M + S_0} \quad (1)$$

where  $S_0$  is the (total) load of substrate,  ${}^{conv}V_{max}$  the maximal rate and  ${}^{conv}K_M$  the Michaelis constant. This can be readily applied in comparative analysis of processive cellulases [25] simply by plotting the steady-state reaction rate (at a low and constant  $E_0$ ) against the load of substrate in g/L as visualized in Fig. 2 (analogously to conventional MM analysis for homogenous systems).

Cellulases show so-called “double saturation” [26, 27] where the rate of reaction levels off at either increasing substrate load (as described in eq. (1)) or enzyme concentration. This opens a possibility of steady-state analysis under the unusual condition of enzyme excess. We have recently discussed this possibility [24] and suggested an “inverse MM equation”, where the roles of E and S have been swapped

$${}^{inv}v_{ss} = \frac{{}^{inv}V_{max} \cdot E_0}{{}^{inv}K_M + E_0} \quad (2)$$

where  $E_0$  is the (total) load of substrate,  $^{inv}V_{max}$  the maximal rate and  $^{inv}K_M$  the Michaelis constant.

In this work we will apply both the conventional MM-equation and the inverse MM-equation. The former will be used to analyze initial rates in trials with a constant and low enzyme concentration (here 200nM) and gradually increasing loads of substrate. Conversely, the inverse MM-equation will be applied to data obtained at a constant and low load of substrate (here 2g/L Avicel) and gradually increasing enzyme concentrations.

## Results

In the conventional analog MM regime steady-state rates were determined at varying substrate concentrations ranging from 1 g/L to 80 g/L and a low enzyme concentration of 0.2  $\mu$ M. Eq. 1 was used to extract values of the processive analogs of  $V_{max}$  and  $K_M$ ,  $^pV_{max}$  and  $^pK_M$ . Interestingly for both CBM shifted variants we found a higher  $^pV_{max}$  and  $^pK_M$  compared to their wt which indicate lower substrate affinity, but higher maximal catalytic rate. Both core enzymes showed specific steady-state rates higher than the wt at substrate loads higher than 15 g/L for Cel7A core and higher than 45 g/L Avicel for Cel6A core resulting in an even higher maximal rate than the CBM swapped variants. From the results it appears that Cel7A<sub>CBM-Cel6A</sub> behaves most similar to Cel7A while Cel6A<sub>CBM-Cel7A</sub> behaves more like Cel6A core.

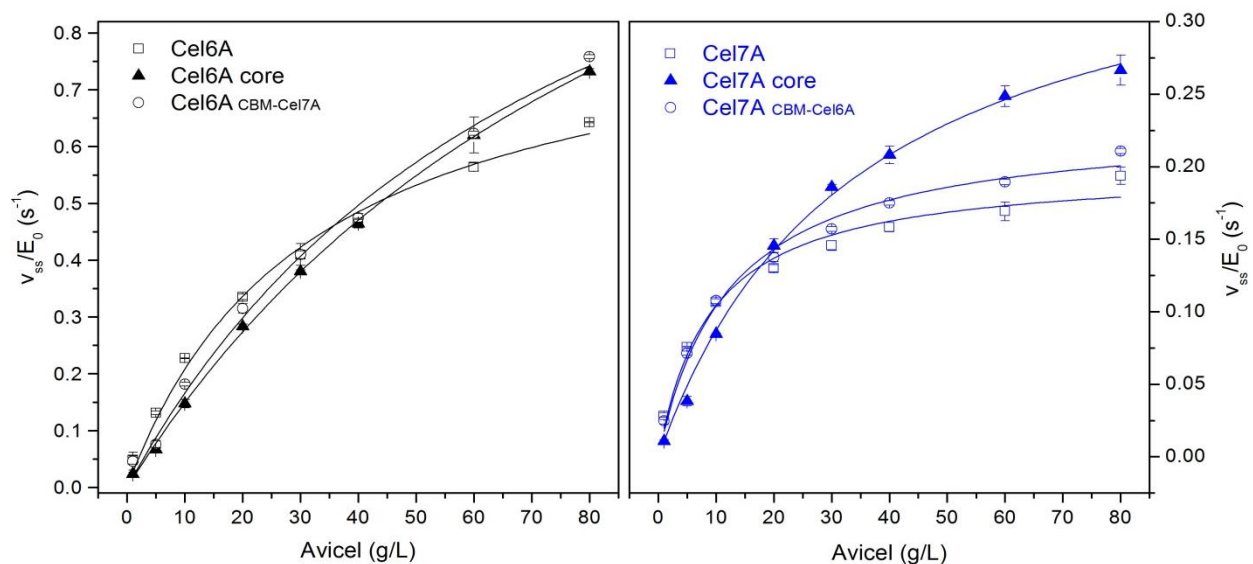


**Figure 3** Steady-state rates were determined at different substrate loads from 1-80 g/L with 0.2  $\mu$ M enzyme. Errorbars show standard deviations from triplicates.

We also applied the inverse MM kinetics saturating a low substrate concentration of 2 g/L washed Avicel with enzymes. Kinetic parameters extracted from the fitted curves in Figure 3 and Figure 4 are collected in Table 1. In contrast to the conventional regime the two wildtypes showed the

highest activity in the group of Cel6A and Cel7A variants. The differences between core enzymes and wt enzymes were even more pronounced in the inverse plot and again Cel6A<sub>CBM</sub>Cel7A behaved almost as poor as the isolated core domain. Also Cel7A<sub>CBM</sub>Cel6A showed a reduced rate compared to the wt, but still much higher than Cel7A core.

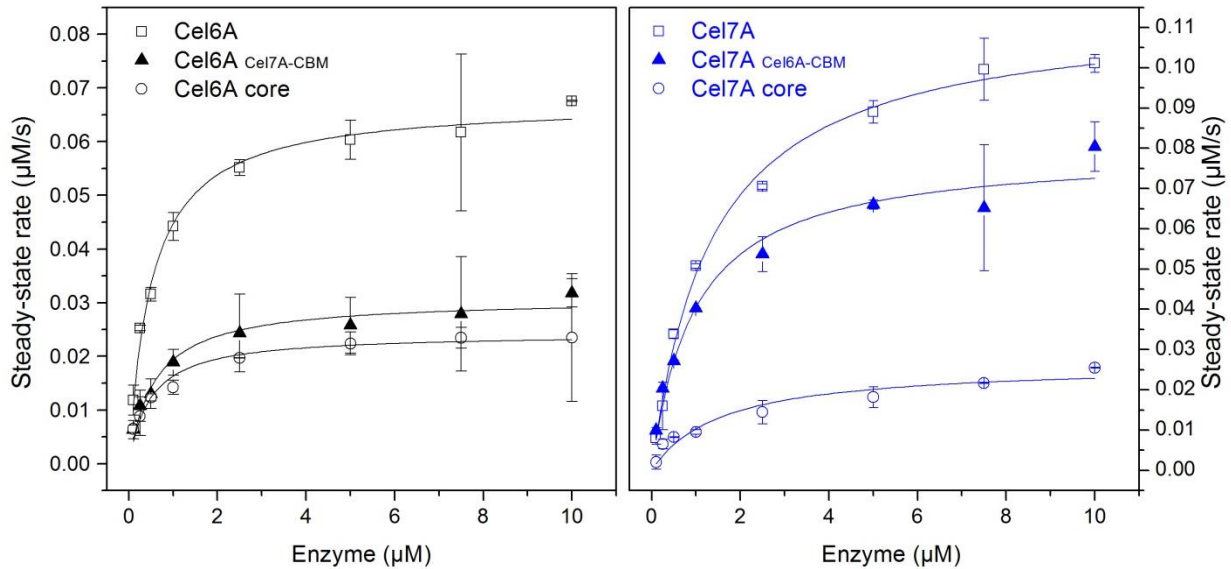


**Figure 4** Steady-state rates was determined with different enzyme loads ranging from 0.1  $\mu\text{M}$  to 10  $\mu\text{M}$ . Errors bars show standard deviations from duplicates.

**Table 1** Kinetic parameters extracted from the conventional steady state model and the inverse Michaelis Menten approach. Parameters from the two wild types are published elsewhere [28].

|                                  | Conventional MM plot              |                                  | Inverse MM plot                          |                              |
|----------------------------------|-----------------------------------|----------------------------------|------------------------------------------|------------------------------|
|                                  | ${}^pV_{max}/E_0$<br>( $s^{-1}$ ) | ${}^pK_M$<br>( $g\ liter^{-1}$ ) | ${}^{inv}V_{max}$<br>( $\mu M\ s^{-1}$ ) | ${}^{inv}K_M$<br>( $\mu M$ ) |
| <b>Cel6A</b>                     | $0.869 \pm 0.045$                 | $31.6 \pm 3.8$                   | $0.067 \pm 0.002$                        | $0.506 \pm 0.050$            |
| <b>Cel6A<sub>CBM</sub>-Cel7A</b> | $1.468 \pm 0.136$                 | $78.2 \pm 12.8$                  | $0.031 \pm 0.001$                        | $0.581 \pm 0.104$            |
| <b>Cel6A core</b>                | $1.657 \pm 0.071$                 | $100.9 \pm 6.7$                  | $0.024 \pm 0.001$                        | $0.481 \pm 0.083$            |
| <b>Cel7A</b>                     | $0.199 \pm 0.009$                 | $9.1 \pm 1.5$                    | $0.114 \pm 0.002$                        | $1.343 \pm 0.112$            |
| <b>Cel7A<sub>CBM</sub>-Cel6A</b> | $0.231 \pm 0.008$                 | $12.3 \pm 1.5$                   | $0.080 \pm 0.004$                        | $0.960 \pm 0.188$            |
| <b>Cel7A core</b>                | $0.388 \pm 0.015$                 | $34.5 \pm 3.0$                   | $0.026 \pm 0.002$                        | $1.554 \pm 0.488$            |

Finally binding isotherms of the variants with 25g/L Avicel (Figure 5) and varying enzyme concentrations enable us to estimate  $\Gamma_{max}$  and  $K_d$  using the standard Langmuir isotherm  $\Gamma = \Gamma_{max} \frac{E_{free}}{K_d + E_{free}}$ . Based on the Langmuir parameters the partitioning coefficient,  $K_P = \Gamma_{max}/K_d$ , which is traditionally used as a measure of cellulase-substrate affinity [29] was determined. First we visualized the drastic effect of the lack of CBM on  $K_P$  and thereby the adsorption behavior of both

Cel6A and Cel7A. Next we found that both CBM swapped variants showed reduced binding capacity ( $\Gamma_{max}$ ) towards Avicel and Cel6A<sub>Cel7ACBM</sub> showed also lower binding affinity in terms of a higher  $K_d$ . Also on the adsorption behavior Cel6A<sub>Cel7ACBM</sub> looked more than the core enzyme than Cel6A. Based on the kinetic and adsorption behavior of Cel6A<sub>Cel7ACBM</sub> we suspected that the CBM might have been lost in the specific variant. Ingel analysis of the amino acids sequence and SDS-PAGE could however disprove this suspicion (supplemental material).

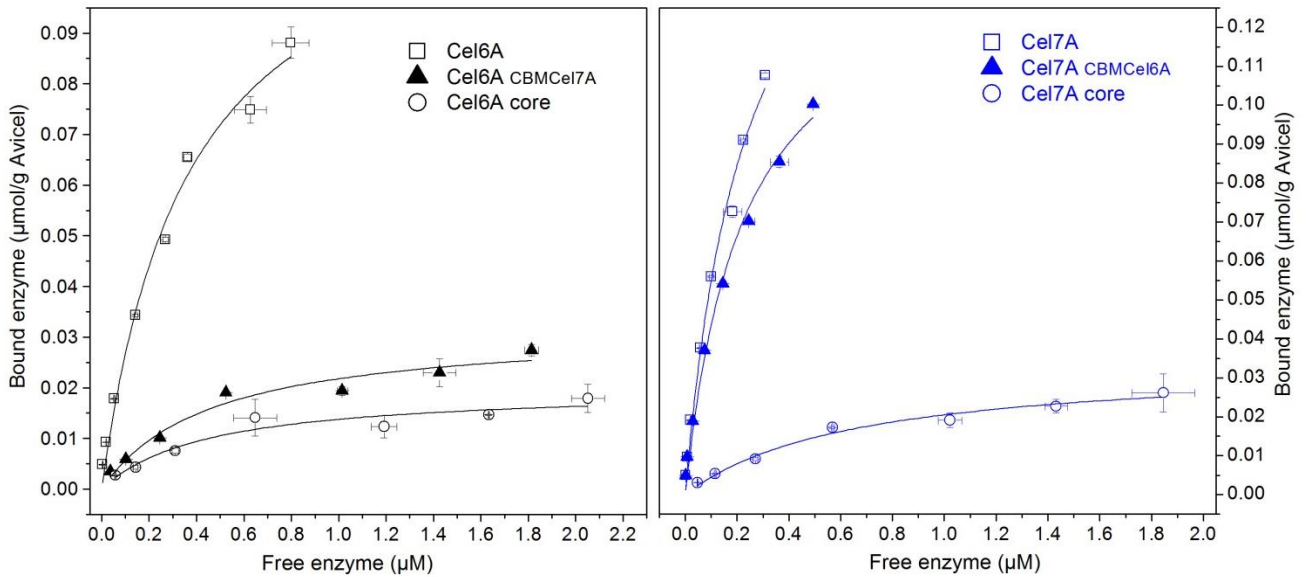


**Figure 5** Binding isotherms with 25g/L Avicel and 0.1-3μM enzyme.

**Table 2** Parameters extracted from the binding isotherms.

| Binding isotherms                |                                              |                            |                                    |
|----------------------------------|----------------------------------------------|----------------------------|------------------------------------|
|                                  | $\Gamma_{max}$<br>( $\mu\text{mol g}^{-1}$ ) | $K_d$<br>( $\mu\text{M}$ ) | $K_p$<br>( $\text{liter g}^{-1}$ ) |
| <b>Cel6A</b>                     | $0.124 \pm 0.010$                            | $0.364 \pm 0.068$          | 0.341                              |
| <b>Cel6A<sub>CBM-Cel7A</sub></b> | $0.032 \pm 0.003$                            | $0.460 \pm 0.135$          | 0.069                              |
| <b>Cel6A core</b>                | $0.020 \pm 0.002$                            | $0.444 \pm 0.170$          | 0.045                              |
| <b>Cel7A</b>                     | $0.184 \pm 0.024$                            | $0.235 \pm 0.057$          | 0.782                              |
| <b>Cel7A<sub>CBM-Cel6A</sub></b> | $0.141 \pm 0.011$                            | $0.223 \pm 0.038$          | 0.630                              |
| <b>Cel7A core</b>                | $0.034 \pm 0.002$                            | $0.655 \pm 0.139$          | 0.052                              |

From chromatographic measurements we determined the product profile after 1 hour hydrolysis, to see if the CBM exchange also influenced the ratio of glucose, cellobiose and cellotriose. In Figure 6, the relative fractions of the three soluble products are shown. At first, we found a clear difference between Cel6A variants compared to the group of Cel7A variants. In general Cel7A variants produce much more glucose than Cel6A variants and opposite Cel6A variants produce



more cellotriose than Cel7A variants. Besides Cel7A core the fraction of cellobiose was similar among all other variants. The product profile of Cel7A<sub>CBM-Cel6A</sub> is very similar to the product profile of Cel7A. The difference in the product profile between Cel6A and Cel6A core is not that pronounced and the product profile of Cel6A<sub>CBM-Cel7A</sub> seems to be somewhere in between core and wildtypes, but most comparable to the product profile of the core variant.

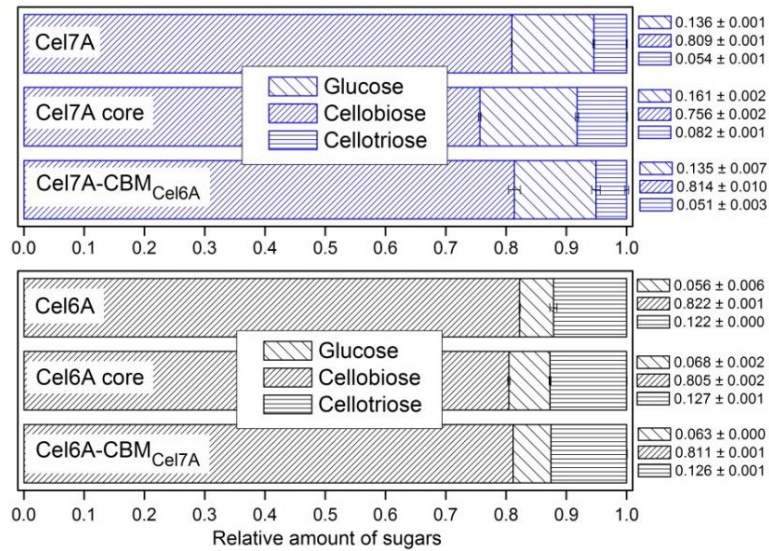


**Figure 6** Relative amount of glucose, cellobiose and cellotriose after 1 hour hydrolysis 0.1 $\mu$ M enzyme and 50 g/L Avicel.

We also experienced that the CBM exchange lowered the melting temperature ( $T_m$ ) of both enzymes with 2°C (data not shown). We suggest that this reduced stability could result from a destabilized or weaker transition between linker and CBM. Since all experiments are performed at 25°C this small reduction in stability is however not given any more attention.

## Discussion

The diversity within CBMs is enormous while CBMs belonging to family 1 are quite conserved. CBM1 from Cel7A is simulated to translate along the hydrophobic surface of cellulose in both forward and backward direction with equal probability [30] indicating that the CBM is not optimized to move in the same direction as the processive enzyme it is attached to, but seems to translate along the cellulose chains. Likewise a CBM2 was also shown to exhibit a linear motion along the cellulose crystal [31]. Beckham and colleagues (2010) probed with a fully atomistic model the molecular-level behavior of Cel7A CBM1 on cellulose chains. They found thermodynamic energy minima with distances corresponding to the length of cellobiose units along the hydrophobic face of cellulose, which equals the catalytic length scale of processive cellobiohydrolases [32]. Furthermore, the same group found that there is a driving force for the

CBM to translate away from a hydrolyzed or broken cellulose chain [33] indicating that the cellulose interactions of the CBM is optimized to follow the processive movement of the core enzyme. These studies all agree that CBM1 translate along cellulose chains, but without any favorable direction, thus both CBMs from Cel6A and Cel7A should be able to translate from reducing towards non-reducing ends and from non-reducing towards reducing ends. Arola and Linder (2016) further discovered that the two different CBMs fully compete on binding sites on both bacterial microcrystalline cellulose (BMCC) and cellulose nanofibrils (CNF) [34] indicating that the binding specificity is not unique for the two isolated CBM domains. Based on earlier studies the CBM exchange constructed here could point towards conserved changes in the kinetics of the two variants Cel6A<sub>Cel7A-CBM</sub> and Cel7A<sub>Cel6A-CBM</sub> compared to their wildtypes. Nevertheless quite strong changes were observed in this study. From the steady-state processive model and the conventional type of the MM plot we found that both Cel6A<sub>CBM-Cel7A</sub> and Cel7A<sub>CBM-Cel6A</sub> variants exhibited different kinetics than their wildtypes, where both  $pV_{max}$  and  $pK_m$  were increased. Interestingly, as illustrated in Figure 3 this means that the two variants established higher activity at high substrate loads, >15g/L Avicel for Cel7A<sub>CBM-Cel6A</sub> and >35g/L Avicel for Cel6A<sub>CBM-Cel7A</sub>. If we compare the core enzymes with the wildtype enzymes this tendency is even more pronounced. Earlier studies have shown that GH7 core enzymes show higher activity at high substrate loads [17, 35-37] and also low affinity variants of Cel7A has been shown to enhance the maximal rate [38, 39](Article IV). Interestingly this inverse relationship between affinity and maximal rate seems also to be valid for the other cellobiohydrolase Cel6A indicating a more generic trend of a dissociation limited catalysis. When comparing the two wildtypes Cel6A has a much higher rate in the conventional regime while Cel7A performs much better in the inverse regime. The underlying understanding of the differences between Cel6A and Cel7A is however discussed elsewhere (Article I) and will not be covered in this study. Focusing on the group of Cel6A and Cel7A variants strong differences were also observed in the inverse MM approach where the substrate is saturated with enzymes. If we first focus on the relationship between core enzymes and the wildtypes it is very noticeable that both Cel6A and Cel7A (with linker and CBM) show much higher activity than their respective core enzymes. This result might be explained by the much higher binding capacity of the wildtypes (Figure 5). At very low substrate load a strong binding affinity seems essential. In the presence of linker and CBM the possibility to associate to the substrate and locate an attack site becomes rate limiting. We have earlier used the term a picky cellulase (Article I) of a fast enzyme with high maximal rate, but with a poor ability to find attack sites at low substrate load. Here the core enzymes acting on the heterogeneous cellulose surface look very picky compared to the wt. Full length Cel6A and Cel7A are on the other hand more promiscuous and able to locate more binding and attack sites. Surprisingly Cel6A<sub>CBM-Cel7A</sub> performed almost as poor as the isolated core enzyme in the inverse approach indicating that the new CBM did not function as the original CBM. Also Cel7A<sub>CBM-Cel6A</sub> showed reduces activity compared to Cel7A however not as drastically as for Cel6A<sub>CBM-Cel7A</sub>. From our binding isotherms we found that both variants lost affinity to Avicel compared to their respective wildtypes. Also

here Cel6A<sub>CBM-Cel7A</sub> showed a much more drastically loss than Cel7A<sub>CBM-Cel6A</sub>. Thus exchanging the CBM with a CBM from another enzyme class seems to affect the interplay between the core domain and the CBM in the adsorption to cellulose. We speculate if the less substantial effect of the CBM exchange on Cel7A can be explained by differences in the two CBMs. Isolated CBMs of Cel6A and Cel7A have previously been investigated and the CBM Cel6A was reported to show higher affinity towards Avicel and BMCC [13, 40], while other studies reports a stronger binding of CBM Cel7A [29, 34]. If we assume that CBM-Cel6A has higher binding affinity and binding capacity on Avicel this might neutralize the effect of the CBM exchange on Cel7A, since the new CBM itself has a stronger binding to Avicel. Thus even though the binding interplay between the two domains might be reduced, the more sticky CBM somehow compensate for that. On the contrary we assume that the enormous difference in binding affinity of the Cel6A variants can only partly be explained by the addition of a low affinity CBM. The results more likely indicate that the function of the CBM in Cel6A<sub>CBM-Cel7A</sub> is disappeared or reduced to a minimum. According to **Figure 1** the linker-CBM transition in Cel6A and Cel6A<sub>CBM-Cel7A</sub> looks very similar, but differences in glycosylation pattern might affect the interplay between the domains. Differences in the glycosylation could also explain the variation in size of the bands on the SDS-PAGE in supplemental info.

There is true agreement about that it is the planar face of the CBM that interacts with the cellulose surface and preferentially it binds along the cellulose chain. If we look upon a perfect cellulose crystal the binding orientation of the CBM in terms of whether the tip of the wedge-shaped CBM points towards the reducing end or non-reducing ends should be totally random due to the symmetry of cellulose. Based on this it is unlikely to believe that CBMs of Cel6A and Cel7A are tuned to move in one direction corresponding to the processive movement of the cellobiohydrolases, so that CBM-Cel7A solely moves from reducing towards non-reducing ends and CBM-Cel6A opposite only moves from non-reducing towards the reducing ends. But regarding a more disturbed or imperfect cellulose surface, such as the surface of Avicel we cannot exclude that the two different CBMs will prefer to bind in the same orientation as the sliding of its original core domain. Since the CBM is connected to the C-terminal of Cel7A and N-terminal of Cel6A this could change the distance between core and CBM, the processivity of the enzymes and maybe more importantly the CBM-linker transition. A wrong orientation of the two CBMs of Cel6A<sub>CBM-Cel7A</sub> and Cel7A<sub>CBM-Cel6A</sub> could result in changes in the processive movement even though the CBMs themselves have no preferred directional movement. The inappropriate domain orientation was recently suggested to explain results with CelEcc fusions with CBM22 and CBM30 [41]. In an attempt to elucidate this aspect we looked at the product profiles of the enzymes. Processivity of cellobiohydrolases can be estimated in many ways [42], where product profiles is one tool. Considering that glucose and cellotriose can only be released during the first catalytic step, while cellobiose is released during the processive cycle, the ratio of the products can predict the processivity of the enzymes. Since different ways of estimating processivity from the product

profiles is available we simply just compare the relative ratio of glucose and cellobiose in between variants here. For the group of Cel7A variants the product profile is unchanged between Cel7A and Cel7A<sub>CBM<sub>Cel6A</sub></sub>, while the relative amount of glucose and cellobiose is higher for Cel7A core. This indicates lower processivity for the core variant, which is in accordance with earlier estimates [35, 43]. The difference in product profile between Cel6A and Cel6A core is not very pronounced compared to Cel7A, but there is a tendency that the product profile of Cel6A<sub>CBM<sub>Cel7A</sub></sub> is more comparable to the core enzyme than the wildtypes. This indicates that the processivity of Cel6A<sub>CBM<sub>Cel7A</sub></sub> is reduced. Based on this study we cannot exclude that the drastically effect of the CBM exchange is somehow connected to the differences in the linker-CBM transition and not just caused by another CBM. Since the two CBMs are attached to the two different terminals it is likely that the linker somehow can collide with the CBM cellulose surface interactions and thereby decrease the overall affinity, which is the case in both Cel7A<sub>CBM<sub>Cel6A</sub></sub> and more markedly in Cel6A<sub>CBM<sub>Cel7A</sub></sub>. Since both the affinity and kinetics are strongly influenced in Cel6A<sub>CBM<sub>Cel7A</sub></sub> we cannot exclude that the CBM does not function as a CBM in this particular variant.

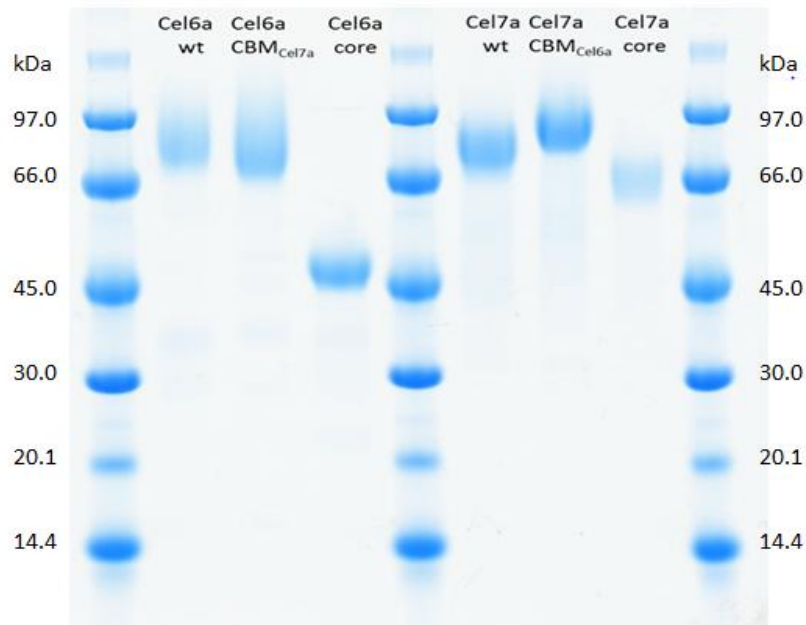
In conclusion, we found that the CBM-exchange of the two cellobiohydrolases Cel6A and Cel7A strongly influence the kinetic behavior of the enzymes. The CBM exchange seems to reduce the affinity towards Avicel which results in higher activity of both variants at high substrate loads. In conditions with enzyme excess the wt enzymes with the original CBMs performed better, which indicate that when the number of attack sites are low a strong interplay between CBM and core domain becomes essential. The most dramatic difference is found for Cel6A<sub>CBM<sub>Cel7A</sub></sub> that behaves more like the isolated core-domain while the differences between Cel7A<sub>CBM<sub>Cel6A</sub></sub> and wt are more conserved. Even though the presence of the CBM in Cel6A<sub>CBM<sub>Cel7A</sub></sub> was confirmed the different transition or differences in glycosylation pattern might minimize the function of the swapped CBM. Based on this study, the molecular understanding of the differences between wt and the CBM exchanged variants can only be imagined, but our findings suggest that the interplay between the different domains are optimized and unique in both Cel6A and Cel7A.

## Acknowledgements

We are grateful to the MS-EDMAN group at Novozymes AS/, Bagsværd for analysis confirming that CBM was present in the Cel6A<sub>CBM<sub>Cel7A</sub></sub> variant.

## Supplemental Materials

Proteins were analyzed by SDS-PAGE and the bands of Cel6A<sub>CBM<sub>Cel7A</sub></sub> excised. The protein was digested using chymotrypsin and the released peptides were analyzed by LC-MS



The purified enzymes were loaded on a SDS-PAGE using 12-well NuPAGE®4-12%Bis-Tris gel (GE Healthcare). We suggest that the observed differences in the band size of Cel6A<sub>CBM<sub>Cel7A</sub></sub> and Cel6A and between Cel7A<sub>CBM<sub>Cel6A</sub></sub> and Cel7A is caused by a different glycosylation pattern of the CBM. Before InGel digest the band of Cel6A<sub>CBM<sub>Cel7A</sub></sub> was cut out of the gel and washed 3x30 min at RT with 150  $\mu$ L 50% EtOH/50 mM  $\text{NH}_4\text{HCO}_3$ . 50  $\mu$ L MeCN was added to shrink the gel piece. Solvent was removed after 15 min and the gel piece dried in speedvac 10 min. The gel piece was Re-swelled in 15  $\mu$ L 25 mM  $\text{NH}_4\text{HCO}_3$  containing Chymotrypsin. After 15 min we added 25  $\mu$ L 25 mM  $\text{NH}_4\text{HCO}_3$  and the plate was incubated overnight at 37°C. After incubation we added 50  $\mu$ L 70% MeCN +0.1%TFA and the sample was incubating for 15 min at R.T. The supernatant was saved. The extraction was repeated twice. The extracts and speedvac was combined to dryness and reconstituted in 50  $\mu$ L 5 % FA.

*Mass spectrometry:* 1-10  $\mu$ L of the sample was injected. The experiment was performed as an nth order double play with MS/MS analysis of the top 3 peaks using HCD activation. The MS scan was performed in the Orbitrap using a resolution of 30000 and a scan range, 300-2000 m/z.

Results from Ingel analysis. Sequences covering 56% of the protein (red AA) were identified including most of the expected N-terminal CBM (marked with grey).

|     |                   |                    |                   |                   |                    |
|-----|-------------------|--------------------|-------------------|-------------------|--------------------|
| 1   | <b>QSHYGQCGGI</b> | <b>GYSGPTVCAS</b>  | <b>GTTCQVLNPY</b> | YSQCLPGAAS        | SSSSTRAAST         |
| 51  | TSRVSEPTTSR       | SSSATPPPGS         | TTTRVPPVGS        | GTATYSGNPF        | VGVTPWANAY         |
| 101 | YASEVSSLAI        | PSLTGAMATA         | AAAVAKVPSF        | MWLDTLDKTP        | LMEQTL <b>ADIR</b> |
| 151 | <b>TANKNGGNYA</b> | GQFVVY <b>DLPD</b> | <b>RDCAALASNG</b> | <b>EYSIADGGVA</b> | <b>KYKNYIDTIR</b>  |
| 201 | <b>QIVVEYSDIR</b> | <b>TLLVIEPDSL</b>  | <b>ANLVTNLGTP</b> | <b>KCANAQSAYL</b> | ECINYAVT <b>QL</b> |
| 251 | <b>NLPNVAMYLD</b> | <b>AGHAGWLGWP</b>  | <b>ANQDPAAQLF</b> | ANVYKNASSP        | <b>RALRGLATNV</b>  |
| 301 | <b>ANYNGWNITS</b> | PPSYTQGNV          | <b>YNEKLYIHAI</b> | <b>GPLLANHGWS</b> | <b>NAFFITDQGR</b>  |
| 351 | <b>SGKQPTGQQQ</b> | <b>WGDWCNVIGT</b>  | <b>GFGIRPSANT</b> | <b>GDSLDSFVW</b>  | VKPGGECDGT         |
| 401 | SDSSAPRFDS        | HCALPDALQP         | APQAGAWFQA        | <b>YFVQLLTNAN</b> | <b>PSFL</b>        |

## References

- 1 Nidetzky B, Steiner W, Claeysens M. Cellulose hydrolysis by the cellulases from *Trichoderma reesei*: adsorptions of two cellobiohydrolases, two endocellulases and their core proteins on filter paper and their relation to hydrolysis. *Biochem J* 1994, 303 ( Pt 3): 817-823
- 2 Ståhlberg J. *Trichoderma reesei* has no true exo-cellulase: all intact and truncated cellulases produce new reducing end groups on cellulose. *Biochimica et biophysica acta General subjects - Amsterdam* 1993, 1157: 107-113
- 3 Ståhlberg J, Johansson G, Pettersson G. A New Model For Enzymatic Hydrolysis of Cellulose Based on the Two-Domain Structure of Cellobiohydrolase I. *Nat Biotech* 1991, 9: 286-290
- 4 Tomme P, Van Tilbeurgh H, Pettersson G, Van Damme J, Vandekerckhove J, Knowles J, Teeri T, *et al.* Studies of the cellulolytic system of *Trichoderma reesei* QM 9414. Analysis of domain function in two cellobiohydrolases by limited proteolysis. *Eur J Biochem* 1988, 170: 575-581
- 5 Kraulis J, Clore GM, Nilges M, Jones TA, Pettersson G, Knowles J, Gronenborn AM. Determination of the three-dimensional solution structure of the C-terminal domain of cellobiohydrolase I from *Trichoderma reesei*. A study using nuclear magnetic resonance and hybrid distance geometry-dynamical simulated annealing. *Biochemistry* 1989, 28: 7241-7257
- 6 Hoffrén AM, Teeri TT, Teleman O. Molecular dynamics simulation of fungal cellulose-binding domains: differences in molecular rigidity but a preserved cellulose binding surface. *Protein Eng* 1995, 8: 443-450
- 7 Linder M, Lindeberg G, Reinikainen T, Teeri TT, Pettersson G. The difference in affinity between two fungal cellulose-binding domains is dominated by a single amino acid substitution. *FEBS Lett* 1995, 372: 96-98
- 8 Strobel KL, Pfeiffer KA, Blanch HW, Clark DS. Engineering Cel7A Carbohydrate Binding Module and Linker for Reduced Lignin Inhibition. *Biotechnol Bioeng* 2015,
- 9 Carrard G, Linder M. Widely different off rates of two closely related cellulose-binding domains from *Trichoderma reesei*. *Eur J Biochem* 1999, 262: 637-643
- 10 Linder M, Mattinen ML, Kontteli M, Lindeberg G, Ståhlberg J, Drakenberg T, Reinikainen T, *et al.* Identification of functionally important amino acids in the cellulose-binding domain of *Trichoderma reesei* cellobiohydrolase I. *Protein Sci* 1995, 4: 1056-1064
- 11 Mattinen ML, Kontteli M, Kerovuo J, Linder M, Annala A, Lindeberg G, Reinikainen T, *et al.* Three-dimensional structures of three engineered cellulose-binding domains of cellobiohydrolase I from *Trichoderma reesei*. *Protein Sci* 1997, 6: 294-303
- 12 Mattinen ML, Linder M, Teleman A, Annala A. Interaction between cellohexaose and cellulose binding domains from *Trichoderma reesei* cellulases. *FEBS Lett* 1997, 407: 291-296
- 13 Guo J, Catchmark JM. Binding specificity and thermodynamics of cellulose-binding modules from *Trichoderma reesei* Cel7A and Cel6A. *Biomacromolecules* 2013, 14: 1268-1277
- 14 Linder M, Teeri TT. The cellulose-binding domain of the major cellobiohydrolase of *Trichoderma reesei* exhibits true reversibility and a high exchange rate on crystalline cellulose. *Proc Natl Acad Sci U S A* 1996, 93: 12251-12255
- 15 Takashima S, Ohno M, Hidaka M, Nakamura A, Masaki H, Uozumi T. Correlation between cellulose binding and activity of cellulose-binding domain mutants of *Humicola grisea* cellobiohydrolase 1. *FEBS Letters* 2007, 581: 5891-5896
- 16 Borch K, Jensen K, Krogh K, McBrayer B, Westh P, Kari J, Olsen J, *et al.* WO2014138672 A1 Cellobiohydrolase variants and polynucleotides encoding same. 2014,

- 17 Sørensen TH, Cruys-Bagger N, Windahl MS, Badino SF, Borch K, Westh P. Temperature Effects on Kinetic Parameters and Substrate Affinity of Cel7A Cellobiohydrolases. *J Biol Chem* 2015, 290: 22193-22202
- 18 Lever M. Colorimetric and fluorometric carbohydrate determination with p-hydroxybenzoic acid hydrazide. *Biochem Med* 1973, 7: 274-281
- 19 Olsen JP, Alasepp K, Kari J, Cruys-Bagger N, Borch K, Westh P. Mechanism of product inhibition for cellobiohydrolase Cel7A during hydrolysis of insoluble cellulose. *Biotechnol Bioeng* 2016, 113: 1178-1186
- 20 Murphy L, Bohlin C, Baumann MJ, Olsen SN, Sørensen TH, Anderson L, Borch K, *et al.* Product inhibition of five *Hypocrea jecorina* cellulases. *Enzyme Microb Technol* 2013, 52: 163-169
- 21 Cruys-Bagger N, Elmerdahl J, Praestgaard E, Borch K, Westh P. A steady-state theory for processive cellulases. *FEBS J* 2013, 280: 3952-3961
- 22 Cruys-Bagger N, Elmerdahl J, Praestgaard E, Tatsumi H, Spodsberg N, Borch K, Westh P. Pre-steady state kinetics for the hydrolysis of insoluble cellulose by *Trichoderma reesei* Cel7A. *J Biol Chem* 2012, 287: 18451-18458
- 23 Praestgaard E, Elmerdahl J, Murphy L, Nymand S, McFarland KC, Borch K, Westh P. A kinetic model for the burst phase of processive cellulases. *FEBS J* 2011, 278: 1547-1560
- 24 Kari J, Andersen M, Borch K, Westh P. An Inverse Michaelis Menten Approach for General Description of Interfacial Enzyme Kinetics. manuscript in preparation,
- 25 Sørensen TH, Cruys-Bagger N, Windahl MS, Badino S, Borch K, Westh P. Temperature effects on kinetic parameters and substrate affinity of Cel7A cellobiohydrolases. *J Biol Chem* 2015, 290: 22193-22202
- 26 Sattler W, Esterbauer H, Glatter O, Steiner W. THE EFFECT OF ENZYME CONCENTRATION ON THE RATE OF THE HYDROLYSIS OF CELLULOSE. *Biotechnol Bioeng* 1989, 33: 1221-1234
- 27 Bezerra RMF, Dias AA. Discrimination among eight modified Michaelis-Menten kinetics models of cellulose hydrolysis with a large range of substrate/enzyme ratios. *Appl Biochem Biotechnol* 2004, 112: 173-184
- 28 Badino SF, Kari J, Christensen SJ, Borch K, Westh P. Direct kinetic comparison of the two cellobiohydrolases Cel6A and Cel7A from *Hypocrea jecorina*. submitted to PEDS 2017,
- 29 Palonen H, Tenkanen M, Linder M. Dynamic interaction of *Trichoderma reesei* cellobiohydrolases Cel6A and Cel7A and cellulose at equilibrium and during hydrolysis. *Appl Environ Microbiol* 1999, 65: 5229-5233
- 30 Nimlos MR, Beckham GT, Matthews JF, Bu L, Himmel ME, Crowley MF. Binding preferences, surface attachment, diffusivity, and orientation of a family 1 carbohydrate-binding module on cellulose. *J Biol Chem* 2012, 287: 20603-20612
- 31 Liu Y-S, Zeng Y, Luo Y, Xu Q, Himmel ME, Smith SJ, Ding S-Y. Does the cellulose-binding module move on the cellulose surface? *Cellulose* 2009, 16: 587-597
- 32 Beckham GT, Matthews JF, Bomble YJ, Bu L, Adney WS, Himmel ME, Nimlos MR, *et al.* Identification of amino acids responsible for processivity in a Family 1 carbohydrate-binding module from a fungal cellulase. *J Phys Chem B* 2010, 114: 1447-1453
- 33 Bu L, Beckham GT, Crowley MF, Chang CH, Matthews JF, Bomble YJ, Adney WS, *et al.* The Energy Landscape for the Interaction of the Family 1 Carbohydrate-Binding Module and the Cellulose Surface is Altered by Hydrolyzed Glycosidic Bonds. *The Journal of Physical Chemistry B* 2009, 113: 10994-11002



- 34 Arola S, Linder MB. Binding of cellulose binding modules reveal differences between cellulose substrates. *Scientific Reports* 2016, 6: 35358
- 35 Sørensen TH, Cruys-Bagger N, Borch K, Westh P. Free Energy Diagram for the Heterogeneous Enzymatic Hydrolysis of Glycosidic Bonds in Cellulose. *J Biol Chem* 2015, 290: 22203-22211
- 36 Várnai A, Siika-Aho M, Viikari L. Carbohydrate-binding modules (CBMs) revisited: reduced amount of water counterbalances the need for CBMs. *Biotechnol Biofuels* 2013, 6: 30
- 37 Pakarinen A, Haven MO, Djajadi DT, Várnai A, Puranen T, Viikari L. Cellulases without carbohydrate-binding modules in high consistency ethanol production process. *Biotechnol Biofuels* 2014, 7: 27
- 38 Kari J, Olsen J, Borch K, Cruys-Bagger N, Jensen K, Westh P. Kinetics of cellobiohydrolase (Cel7A) variants with lowered substrate affinity. *J Biol Chem* 2014, 289: 32459-32468
- 39 Sørensen TH, Windahl MS, McBrayer B, Kari J, Olsen JP, Borch K, Westh P. Loop variants of the thermophile *Rasamsonia emersonii* Cel7A with improved activity against cellulose. *Biotechnol Bioeng* 2017, 114: 53-62
- 40 Lehtiö J, Sugiyama J, Gustavsson M, Fransson L, Linder M, Teeri TT. The binding specificity and affinity determinants of family 1 and family 3 cellulose binding modules. *Proc Natl Acad Sci U S A* 2003, 100: 484-489
- 41 Walker JA, Takasuka TE, Deng K, Bianchetti CM, Udell HS, Prom BM, Kim H, *et al.* Multifunctional cellulase catalysis targeted by fusion to different carbohydrate-binding modules. *Biotechnol Biofuels* 2015, 8: 220
- 42 Horn SJ, Sørli M, Vårum KM, Väljamäe P, Eijsink VG. Measuring processivity. *Methods Enzymol* 2012, 510: 69-95
- 43 Cruys-Bagger N, Tatsumi H, Ren GR, Borch K, Westh P. Transient kinetics and rate-limiting steps for the processive cellobiohydrolase Cel7A: effects of substrate structure and carbohydrate binding domain. *Biochemistry* 2013, 52: 8938-8948

The Influence of different Linker Modifications  
on the Catalytic Activity and Cellulose  
Affinity of Cellobiohydrolase Cel7A from  
*Hypocrea jecorina*

---

IV



## Original Article

# The influence of different linker modifications on the catalytic activity and cellulose affinity of cellobiohydrolase Cel7A from *Hypocrea jecorina*

Silke Flindt Badino<sup>1</sup>, Jenny Kim Bathke<sup>2,4</sup>, Trine Holst Sørensen<sup>1</sup>, Michael Skovbo Windahl<sup>1,5</sup>, Kenneth Jensen<sup>3</sup>, Günther H.J. Peters<sup>2</sup>, Kim Borch<sup>3</sup>, and Peter Westh<sup>1,\*</sup>

<sup>1</sup>Research Unit for Functional Biomaterials, Department of Science and Environment, INM, Roskilde University, 1 Universitetsvej, Build. 28 C, DK-4000, Roskilde, Denmark, <sup>2</sup>Department of Chemistry, Technical University of Denmark, Kemitorvet, Build. 207, DK-2800 Kgs. Lyngby, Denmark, and <sup>3</sup>Novozymes A/S, Krogshøjvej 36, DK-2880, Bagsværd, Denmark

\*To whom correspondence should be addressed. E-mail: pwesth@ruc.dk

Edited by Daniel Otzen

<sup>4</sup>Present address: Novo Nordisk A/S, Vandtårnsvej 114, DK-2860 Søborg, Denmark

<sup>5</sup>Present address: Bioneer A/S, Kogle Allé 2, DK-2970 Hørsholm, Denmark

Received 21 March 2017; Revised 30 June 2017; Editorial Decision 2 July 2017; Accepted 4 July 2017

## Abstract

Various cellulases consist of a catalytic domain connected to a carbohydrate-binding module (CBM) by a flexible linker peptide. The linker is often strongly O-glycosylated and typically has a length of 20–50 amino acid residues. Functional roles, other than connecting the two folded domains, of the linker and its glycans, have been widely discussed, but experimental evidence remains sparse. One of the most studied cellulose degrading enzymes is the multi-domain cellobiohydrolase Cel7A from *Hypocrea jecorina*. Here, we designed variants of Cel7A with mutations in the linker region to elucidate the role of the linker. We found that moderate modification of the linker could result in significant changes in substrate affinity and catalytic efficacy. These changes were quite different for different linker variants. Thus, deletion of six residues near the catalytic domain had essentially no effects on enzyme function. Conversely, a substitution of four glycosylation sites near the middle of the linker reduced substrate affinity and increased maximal turnover. The observation of weaker binding provides some support of recent suggestions that linker glycans may be directly involved in substrate interactions. However, a variant with several inserted glycosylation sites near the CBM also showed lower affinity for the substrate compared to the wild-type, and we suggest that substrate interactions of the glycans depend on their exact location as well as other factors such as changes in structure and dynamics of the linker peptide.

**Key words:** affinity, cellobiohydrolase, glycosylation, hydrolysis, linker

## Introduction

Many cellulases are multi-domain enzymes consisting of a catalytic domain (henceforth denoted ‘core’) and a carbohydrate-binding module (CBM) connected by a glycosylated linker. Linkers from different

cellulases show little or no sequence homology even within the same family, but linkers from fungal cellulases are in general rich in glycine, proline, serine and threonine (Sammond *et al.*, 2012). Besides the function to serve as a connector between CBM and core different

roles of the linker have been hypothesized. One idea is that the linker functions as a caterpillar or spring which accumulates and dissipates energy and hence helps the processive movement of the enzyme along the cellulose chain (Receveur et al., 2002; von Ossowski et al., 2005). Another more recent suggestion of a direct role in the catalytic process is that the linker adsorbs to the cellulose surface and hence contributes to substrate affinity and dampen fluctuations in the complexed enzyme (Payne et al., 2013). Only few experimental studies have addressed functional roles of the linker, but Shen et al. (1991) reported that activity of the endoglucanase CenA from the bacterium *Cellulomonas fimi* was ~2-fold reduced in a variant with dramatically reduced linker length. Interestingly, these changes in CenA activity did not appear to be related to substrate affinity as the binding isotherms of variant and wild-type (wt) enzymes were identical. Recently, Ruiz et al. (2016) found that linker length of the endoglucanase Cel5A from *Bacillus subtilis* influenced the flexibility, rigidity and interestingly also the kinetics of the non-processive endoglucanase. Srisodsuk et al. (1993) studied activity and affinity of linker variants of the processive cellobiohydrolase (CBH) Cel7A from *Trichoderma reesei* (anamorph of the fungus *Hypocrea jecorina*). They found that deletion of about one third of the linker near the core reduced affinity, but did not change activity against crystalline cellulose. Truncation of almost the entire linker, on the other hand, significantly reduced both affinity and activity. Based on this, it was suggested that the Cel7A linker includes a flexible hinge region close to the core and a more stiff region with O-glycosylation near to the CBM (Srisodsuk et al., 1993). More recent computational work (Beckham et al., 2010) found that the linker of Cel7A was an intrinsically disordered protein, and that presence of glycans did not seem to decrease the flexibility. Other discussions of linker functional roles have also focused on the high extent of O-glycosylation in fungal cellulases with at least a single O-mannose moiety on every serine and threonine in the linker (Harrison et al., 1998). This glycosylation has long been suggested to confer resistance against protease attack (Langsford et al., 1987; Shen et al., 1991) and more recently, it has also been shown to reduce adsorption to lignin and hence reduce cellulase inhibition by lignin during hydrolysis of lignocellulosic plant material (Strobel et al., 2015).

Molecular dynamics simulations have shown that the glycosylated linker from both Cel7A and Cel6A binds dynamically to cellulose surfaces and hence potentially play a direct role in cellulase-substrate interactions (Payne et al., 2013). The same study also provided experimental evidence for direct interactions of the natively glycosylated linker from Cel7A and bacterial cellulose. It was suggested that this interaction could rely on glycan-cellulose contacts, and the general idea of attractive forces between O-linked glycans and cellulose has been confirmed in extensive studies of CBM-variants (Chen et al., 2014; Guan et al., 2015). This possible role of glycans for substrate affinity raises interesting questions regarding their role for catalytic efficacy. Thus, a number of reports (Wilson, 2009; Kurasin and Valjamae, 2011; Praestgaard et al., 2011; Fox et al., 2012; Maurer et al., 2012; Cruys-Bagger et al., 2013b) starting with work by Zhang and Wilson (1997); Zhang et al. (2000), have proposed that the overall rate of hydrolysis for processive cellulases is governed not by bond cleavage, but the rate the enzyme binds and/or unbinds the insoluble substrate. If indeed so, attractive forces between the linker and substrate could play a direct role for the overall rate of catalysis. Relationships of affinity and activity have recently been elucidated in comprehensive comparisons of Cel7A with linker and CBM and core variants where both the linker

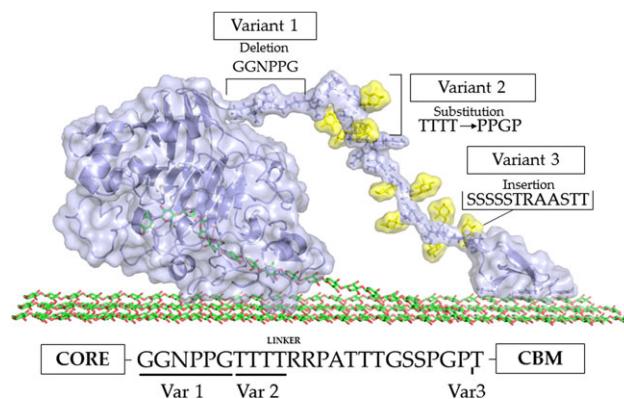


**Fig. 1** Design of linker variants. Variant 1: Deletion of six residues close to core domain (G439\*G440\*N441\*P442\*P443\*G444\*), Variant 2: Substitution of four O-glycosylation sites near the middle of the linker (T445P T446P T447G T448P), Variant 3: Elongation of the linker near the CBM through insertion (462aS\*462bS\*462cS\*462dS\*462eS\*462fT\*462gR\*462hA\*462iA\*462jS\*462kT\*462lT\*). Besides making the linker longer this change introduces nine new potential sites for O-glycosylation. In addition to these three variants we studied the wt and a core variant where both linker and CBM had been truncated. Figure constructed in PyMol from (PDB 4C4C) (Knott et al., 2014) and (PDB 1CBH) (Kraulis et al., 1989), where cellulose surface (green) and the linker with single glycans on potential glycosylation sites (yellow) are added manually.

and CBM have been truncated. Interestingly, this work has consistently shown that core variants (with comparably lower affinity) are faster at high substrate loads while enzymes variants with linker and CBM (high affinity) are the most active in dilute substrate suspension (Le Costaouéc et al., 2013; Pakarinen et al., 2014; Sørensen et al., 2015b). These earlier studies cannot distinguish between contributions to substrate affinity arising from either CBM or linker, but they underscore that any investigation of affinity-activity relationships must include assays over a broad range of substrate loads, and preferably also separate adsorption measurements to provide direct information on affinity. In the present study we pursue this idea for Cel7A variants with moderate changes in the linker. The design of variants is specified in Fig. 1 and was chosen to investigate effects of length and glycosylation. We aimed to reduce or increase the linker length (Variants 1 and 3) and to decrease or enlarge the number of glycosylation sites (Variants 2 and 3). The different modifications were furthermore made in three different regions of the linker. Our main findings were that some modifications of the linker led to distinctive changes in the kinetic parameters, while others did not. We did not find a correlation between the kinetic effect of linker modifications and the overall degree of linker glycosylation, but it appeared that linker variants with lower substrate affinity showed a higher saturation rate.

## Materials and Methods

### Enzymes

The linker modifications were introduced by mutagenesis with the following primers: Variant 1: fw-CCTCCGGTGGAAACCCTCCTACA ACTACAACACGACGGCCTG and rv- AGGAGG GTTCCACCG GAGGGGTTGCCGGT, Variant 2: fw -CTGGCGGAAACCCTCCT GGCCCTCCTGGA CCTCGACGGCCTGCGACTACAAC and rv-GCCAG GAGGGTTCCGCCAGGAGGGTTTCCA and Variant 3:

fw-GTTCGTCCTCCCTGGACCGACCTCCTCCTCCTCCTCCACCAG GGCAGCATCCACCACCCAGTCCCCTACTACGGACAGTGT and rv-GGTCCGGTCCAGGGGACGAAACCCGTTGTAGTC. All variants were expressed in *Aspergillus oryzae* and fermented as described earlier (Borch *et al.*, 2014).

Enzymes were purified using three steps; hydrophobic interaction chromatography (HIC), desalting and ion exchange chromatography. We used the ÄKTA system (GE Healthcare) and the 3 columns: 150 ml-phenyl Sepharose® 6 FastFlow column XK50 (GE Healthcare) equilibrated with 1.8 M (NH<sub>4</sub>)<sub>2</sub>SO<sub>4</sub> 25 mM HEPES, pH 7.0, 540 ml Sephadex™ G-25 (medium) column (GE Healthcare) and 60 ml SOURCE™ 15Q column (GE Healthcare) both equilibrated with 25 mM MES, pH 6.0. The HIC column was eluted by a step gradient with 30% 25 mM HEPES pH 7.0 followed by 100% HEPES pH 7.0. After desalting the enzymes were finally eluted with a linear gradient from 50 to 300 mM NaCl in MES pH 6.0 for 3 column volumes.

The enzyme concentrations were determined by absorbance at 280 nm using calculated (Gasteiger *et al.*, 2005) molar extinction coefficient of respectively 86.8 mM<sup>-1</sup> cm<sup>-1</sup> for Cel7A wt and linker variants and 80.6 mM<sup>-1</sup> cm<sup>-1</sup> for the core domain alone. The purified enzymes were loaded on a SDS-PAGE using 12-well NuPAGE® 4–12% Bis-Tris gel (GE Healthcare).

### Hydrolysis

The activity assay was run for 1 h at 25 and 50°C at different substrate loads ranging from 1 to 80 g/l Avicel and an enzyme concentration of 400 nM. The amount of cellobiose produced were quantified by the *p*-hydroxybenzoic acid hydrazide (PAHBAH) method (Lever, 1973) using a procedure detailed elsewhere (Sørensen *et al.*, 2015b). Absorption at 405 nm was determined and the soluble reducing sugars were quantified based on standards with 0–0.5 mM cellobiose. All experiments were performed in 50 mM Acetate 2 mM CaCl<sub>2</sub>, pH 5.0 buffer and carried out in triplicates. After centrifugation and before the PAHBAH reaction 100 µl of the supernatant was transferred to a black microtiter plate (Greiner Bio one 655079). The amount of free enzyme was determined by intrinsic protein fluorescence at 345 nm in a plate reader (Molecular Devices SpectraMax M2) using an excitation wavelength of 280 nm. Standards curves ranging from 0 to 2 µM in 50 mM Acetate 2 mM CaCl<sub>2</sub>, pH 5.0 buffer were made for all individual enzymes to translate the fluorescence signal to a concentration. Fractions of bound enzyme were estimated from the measured free- and the known total enzyme. Activity against the soluble substrate para-nitrophenyl-lactopyranoside (pNPL) was further measured at 25°C and 15 min hydrolysis with pNPL concentrations ranged from 0.1 to 5 mM and an enzyme concentration of 400 nM as detailed elsewhere (Olsen *et al.*, 2015).

### Binding isotherms

Samples with 20 g/l Avicel and total enzyme concentrations of respectively 0, 0.125, 0.25, 0.5, 0.75, 1, 1.5, 2 and 2.5 µM were allowed to equilibrate for 30 min. Subsequently, the substrate was separated by centrifugation and the free enzyme concentration quantified by intrinsic fluorescence as described above.

### Results

Enzyme purity was assessed by SDS-PAGE as shown in Fig. 2, and these results also provided information on the degree of glycosylation. Thus, comparison of the relative migration of Cel7A WT and markers suggested a molecular weight about 83 kDa. This is well

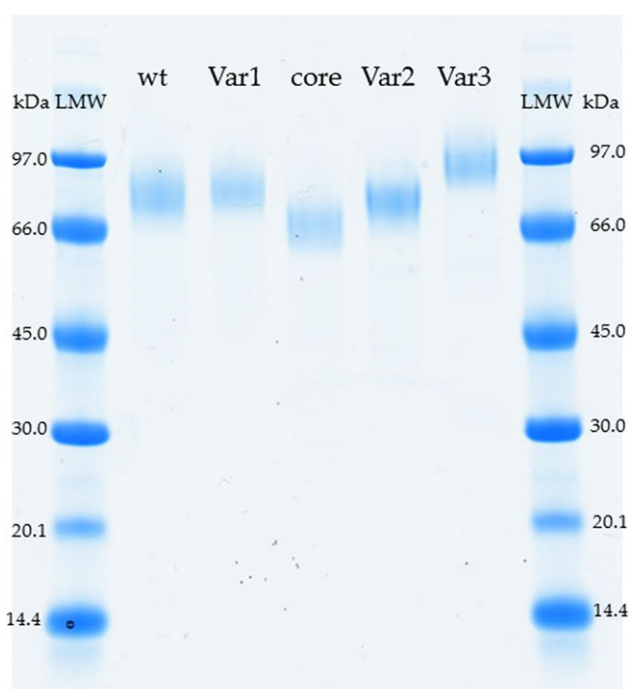


**Fig. 2** SDS-PAGE for wt and variants. In addition to confirming the purity, this figure provides some insight into the glycosylation of the variants as discussed in the main text.

above the MW of the Cel7A peptide (52 kDa), and this discrepancy is in line with a significant degree of glycosylation. More importantly, we observed changes in the migration of the variants. Var2 migrated further than the wt although these two enzymes had essentially the same peptide MW. We interpret this as evidence that the four Thr-residues, which had been substituted in Var2, indeed had some degree of O-glycosylation in the wt enzyme. Analogously, we interpret the reduced migration of Var3 as evidence of some glycosylation of the six Thr and three Ser inserted in the linker of this variant. This conclusion for Var3 was further supported by mass spectrometry type MAXIS II electrospray (data not shown). Finally, no detectable change in the migration of Var1 was observed, and this is in accord with the expectations for the deletion of 6 amino acids without any glycosylation sites.

We measured both steady-state hydrolytic rates,  $v_{ss}$ , and free enzyme concentrations,  $E_{free}$  for all variants in samples with a total enzyme concentration  $E_0 = 400$  nM and eight different Avicel loads ranging from 0 to 80 g/l. While the exact meaning of steady-state rates for cellulases acting on their insoluble substrate remains controversial (Bansal *et al.*, 2009), we have argued that average rates measured in short experiments are useful approximations for  $v_{ss}$ , at least for comparative purposes (Cruys-Bagger *et al.*, 2013a; Sørensen *et al.*, 2015a). Here, the steady-state rate was approximated simply as the amount of soluble sugar measured by the PAHBAH method divided by the contact time (1 h). The specific steady-state rates,  $v_{ss}/E_0$ , in units of s<sup>-1</sup>, are plotted as a function of the substrate load in Fig. 3. The concentration of bound enzyme in the samples was calculated from the measured values of free enzyme at the end of the hydrolysis experiments and also plotted against the Avicel load in Fig. 3. Direct comparisons of binding (lower panels) and kinetics (upper panels) reveal that the former consistently saturates before the latter. Looking at Cel7A wt at 50°C, as an example,

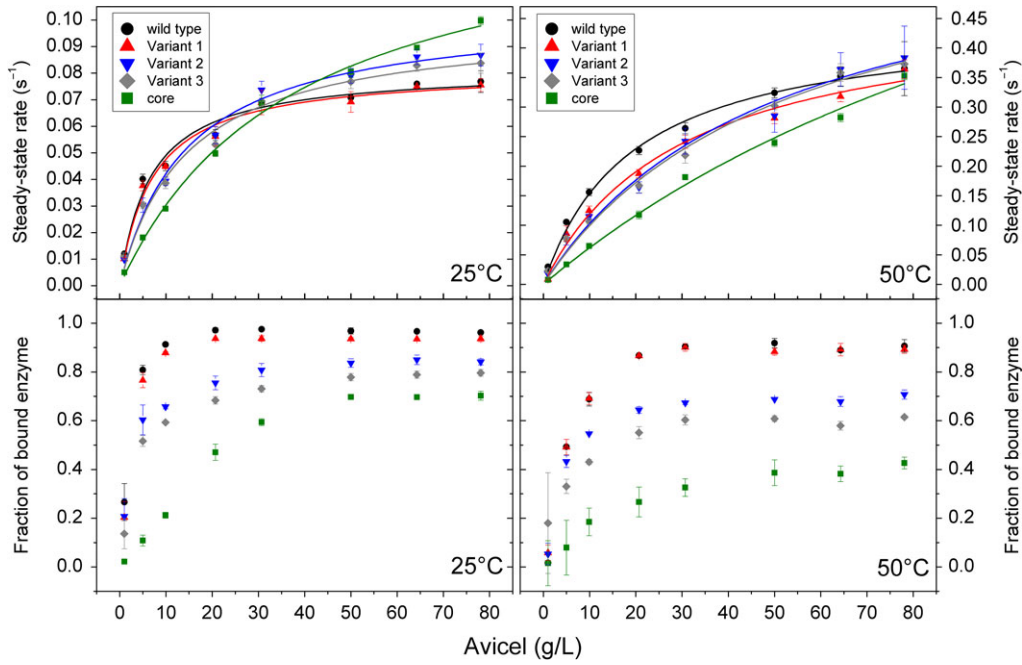


**Fig. 3** Specific enzyme steady-state rates ( $v_{ss}/E_0$ ) and fraction of bound enzyme in the hydrolysis samples. The two upper panels show the kinetic data at 25 and 50°C and the lines here are best fits of the Michaelis–Menten Equation (1). The two lower panels show the fraction of bound enzyme at the end of the hydrolysis experiment. Error bars indicate deviations from triplicates.

**Table I.** Kinetic parameters estimated from non-linear regression analysis on Avicel (Fig. 3) and pNPL including standard errors and the partitioning coefficient  $K_P$  estimated from Fig. 4.

|           | 25°C Avicel                     |                           |                       | 50°C Avicel                     |                           | 25°C pNPL                   |                 |
|-----------|---------------------------------|---------------------------|-----------------------|---------------------------------|---------------------------|-----------------------------|-----------------|
|           | ${}_pV_{\max}/E_0$ ( $s^{-1}$ ) | ${}_pK_M$ ( $g\ l^{-1}$ ) | $K_P$ ( $l\ g^{-1}$ ) | ${}_pV_{\max}/E_0$ ( $s^{-1}$ ) | ${}_pK_M$ ( $g\ l^{-1}$ ) | $V_{\max}/E_0$ ( $s^{-1}$ ) | $K_M$ ( $mM$ )  |
| Cel7A     | $0.082 \pm 0.003$               | $6.6 \pm 1.1$             | 0.77                  | $0.450 \pm 0.014$               | $19.2 \pm 1.7$            | $0.065 \pm 0.0007$          | $0.88 \pm 0.03$ |
| Variant 1 | $0.081 \pm 0.003$               | $7.1 \pm 1.0$             | 0.63                  | $0.477 \pm 0.033$               | $30.1 \pm 5.0$            | $0.068 \pm 0.0009$          | $0.86 \pm 0.03$ |
| Variant 2 | $0.104 \pm 0.004$               | $14.5 \pm 1.9$            | 0.15                  | $0.627 \pm 0.071$               | $51.0 \pm 11.4$           | $0.069 \pm 0.0007$          | $0.86 \pm 0.03$ |
| Variant 3 | $0.099 \pm 0.005$               | $14.2 \pm 2.2$            | 0.15                  | $0.634 \pm 0.060$               | $53.7 \pm 9.9$            | $0.059 \pm 0.0004$          | $0.90 \pm 0.02$ |
| Core      | $0.145 \pm 0.007$               | $37.7 \pm 3.8$            | 0.03                  | $0.993 \pm 0.197$               | $150 \pm 41$              | $0.063 \pm 0.0008$          | $0.91 \pm 0.04$ |

we find that binding-saturation occurs at a substrate load of 20–30 g/l (no further adsorption of enzyme was observed at still higher loads). Conversely, activity remains to increase with substrate loads well above 30 g/l (a constant rate was not even found at the highest substrate loads studied here).

The kinetic data was analyzed with respect to the Michaelis–Menten (MM) Equation

$$\frac{v_{ss}}{E_0} = \frac{{}_pV_{\max}S}{{}_pK_M + S} \quad (1)$$

where  ${}_pV_{\max}$ ,  ${}_pK_M$  and  $S$  are respectively the maximal specific rate (in  $s^{-1}$ ), the Michaelis constant (in g/l) and the load of substrate (g/l). The lines in Fig. 3 show the best fits of Equation (1), and the kinetic parameters derived from this analysis are listed in Table I. We note that while the MM equation is not generally valid for processive cellulases acting on insoluble substrate it may be used under some conditions, particularly when the degree of substrate conversion and enzyme concentration are both low (Cruys-Bagger *et al.*, 2013a). For a processive mechanism, the exact meaning of  ${}_pV_{\max}$  and  ${}_pK_M$  differs

somewhat from conventional MM theory (Cruys-Bagger *et al.*, 2013a), but these parameters nevertheless provide measures of respectively the catalytic activity at saturating loads of substrate and the half-saturation substrate concentration. In the following we will use this interpretation for comparative discussions and we will use the subscript ‘ $p$ ’ in front of the parameters to indicate the relation to a processive reaction mechanism.

The affinity for Avicel is reflected in the  ${}_pK_M$  values in Table I. To support this interpretation of  ${}_pK_M$  and assess substrate affinity directly, we also measured binding isotherms in separate experiments with increasing enzyme concentrations added to 20 g/L Avicel. Results in Fig. 4 show the surface coverage ( $\Gamma$  in  $\mu\text{mol}$  enzyme adsorbed per g Avicel) as a function of the free enzyme concentration,  $E_{\text{free}}$ . These results were fitted to a standard Langmuir isotherm  $\Gamma = \Gamma_{\max} \frac{E_{\text{free}}}{K_d + E_{\text{free}}}$  as indicated by the lines in Fig. 4. On the basis of the Langmuir parameters, we calculated the partitioning coefficient,  $K_P = \Gamma_{\max}/K_d$ , which is traditionally used as a measure of cellulase-substrate affinity (Palonen *et al.*, 1999). Values for  $K_P$  are listed together with the kinetic parameters in Table I. We also estimated kinetic parameters using the soluble substrate pNPL (Table I).



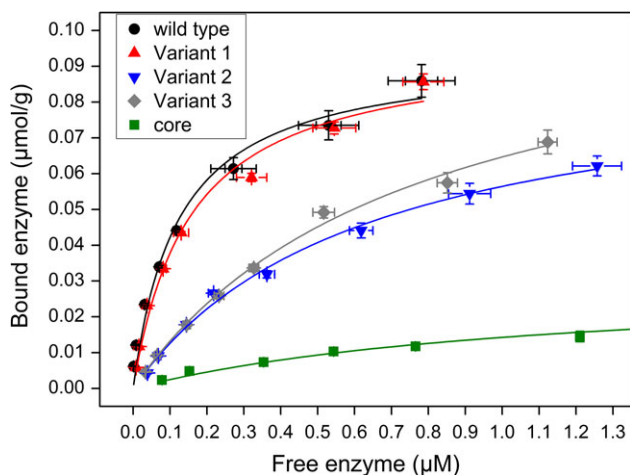


**Fig. 4** Isotherms for the adsorption of Cel7A variants on Avicel (20 g/l). The lines are best fits of simple Langmuir isotherms (see main text for detail). Error bars indicate deviations from triplicates.

## Discussion

The linker region of multi-domain cellulases was originally described as an intrinsically disordered peptide that simply made up a flexible connection between catalytic- and binding domains. Later more specific roles of the linker have been suggested for processive CBHs (Receveur *et al.*, 2002; von Ossowski *et al.*, 2005), including a direct involvement in substrate interactions for Cel7A and Cel6A (Payne *et al.*, 2013). However, only a few experimental studies (see Introduction) have directly addressed the question of a functional role of the linker. Here, we have characterized three linker variants of the CBH Cel7A from *H. jecorina*, and overall, the results showed that moderate changes of the linker can lead to significant modifications of both activity and affinity of this enzyme. To assess substrate affinity of the variants we first note that this property is reflected in the two independently measured parameters  $pK_M$  and  $K_P$  in Table I. As the former is related to the enzyme-substrate dissociation constant (Cruys-Bagger *et al.*, 2013a), while the latter is a binding constant (Palonen *et al.*, 1999), lowered affinity will be reflected in a larger  $pK_M$  but a smaller  $K_P$ . This inverse relationship of changes in  $pK_M$  and  $K_P$  is indeed seen in Table I and this supports the interpretation of these parameters as a measure of substrate affinity.

All variants show comparable activity and affinity (in terms of  $pV_{max}$  and  $pK_M$ ) towards the soluble substrate pNPL and we therefore assume that the modifications of the linker have no effect on the catalytic mechanism in the core domain. On Avicel, however we found that the different linker modifications influenced both activity and affinity. All kinetic- and affinity parameters found here for linker variants were intermediates between the wt and the core variant. Thus, the wt showed higher affinity (*i.e.* highest  $K_P$  and lowest  $pK_M$ , in Table I) and lower or comparable catalytic speed ( $pV_{max}$ ) compared to the variants. Conversely, the core variant without linker and CBM showed the lowest affinity and highest catalytic speed. All linker variants fell between or close to these two limits. Var1, in which a six-residue sequence near the catalytic domain and without glycosylation sites had been truncated (*c.f.* Fig. 1), showed kinetic- and binding properties very close to those of the wt enzyme. Hence, both Michaelis–Menten plots (Fig. 3) and binding isotherms (Fig. 4) at 25°C were essentially superimposed for wt and Var1. At

50°C, we found a small increase in  $pK_M$  for Var1 compared to the wt suggesting a slight reduction of substrate affinity in the variant at higher temperatures. We conclude that the shortening near the catalytic domain in Var1 without changing the number of glycosylation sites was quite neutral with respect to enzyme function and -affinity. This independence speaks against a strictly defined optimal length of the linker, which has been suggested on the basis of a mechanochemical model that considers binding- and catalytic domains as random walkers whose movement is biased by the linker (Ting *et al.*, 2009). Interestingly, Srisodsuk *et al.* (1993) also investigated a Cel7A variant with a deletion in the linker near the catalytic domain. Specifically, they found that the tested 11-residue deletion had little or no effect on the catalytic efficacy, and this result is in perfect accord with the current observations for Var1, which has a related (but smaller) deletion in the same region. A recent work by Strobel *et al.* (2015) also considered modifications of the linker near the catalytic domain. In this case, the linker length was conserved, but the degree of glycosylation increased, and the results again showed negligible changes in the activity against insoluble cellulose. We conclude that moderate changes in length or degree of glycosylation in this region of the linker of Cel7A appear to have little influence on enzyme function.

A different conclusion was reached for Var2 and Var3, which both showed lowered substrate affinity and increased maximal rate compared to the wt (Table I). The design of these variants were quite different with either a substitution near the middle of the linker in which four glycosylation sites were removed (Var2) or a 12-residue insertion near the CBM (Var3) with a total of nine new potential sites for glycosylation (Fig. 1). Judging from the SDS-PAGE data in Fig. 2, the total degree of glycosylation was indeed reduced in Var2 and increased in Var3. Hence, the observation that both of these variants showed lowered affinity for the substrate contradicts a simple relation between the degree of linker glycosylation and affinity. This conclusion is in line with a recent mutational study, where linker variants with either higher or lower degrees of glycosylation showed almost the same  $K_p$ -value on Avicel (Strobel *et al.*, 2015). In addition, different glyco-variants of CBM showed large variation in the binding affinity with no simple relation between glycosylation and substrate affinity (Chen *et al.*, 2014; Guan *et al.*, 2015). Thus attractive forces between glycans and the cellulose surface, which have been identified for both linkers and CBMs (Payne *et al.*, 2013; Chen *et al.*, 2014; Guan *et al.*, 2015), appear to rely strongly on position and conformational restraints. As a result, further knowledge on these interactions may be required before substrate affinity in CBHs can be engineered by inserting or deleting glycosylation sites in the linker. One possible interpretation of these results is that the CBM and the adjoining region of the linker promote affinity together in a cooperative manner, and that this effect is lost upon changes in this part of the linker. We tried to explore this further in a variant with a 9-residue deletion near the CBM, but this construct lost the CBM during expression (data not shown). Clearly, a much larger family of linker variants including members where the number of glycosylation sites has been either increased or reduced at different loci along the linker must be investigated systematically to elucidate this further.

Perhaps the most conspicuous trend in Table I is an inverse relationship of affinity and activity. Thus, we consistently found that variants with lowered substrate affinity showed higher maximal rate. This may seem counterintuitive as adsorption on the substrate surface is a condition for activity. However, increased activity of low-affinity variants has been seen before both for cellulases (Kari *et al.*, 2014;



Sørensen et al., 2015b, 2016) and other processive glycoside hydrolases (Horn et al., 2006), and it probably reflects that dissociation of stalled enzyme complexes is rate limiting (Kurasin and Valjamae, 2011; Cruys-Bagger et al., 2012). Hence, variants with lowered affinity are more readily released from stalled complexes and recruited for a new attack at a different location on the cellulose surface. This mechanism of rate limitation is valid at moderate and high loads of substrate where ‘finding’ an attack sites through random collisions with the surface is fast. In more dilute substrate suspensions finding attack sites inevitably becomes slow, and the rate of association therefore becomes dominant in determining the overall hydrolytic rate (Sørensen et al., 2015a). This shift in rate limiting step is reflected in the cross over of some MM plots in Fig. 3, because low-affinity variants will be worse at low substrate load where finding the attack site is limiting and better at high substrate where dissociation governs the rate. The effect is particularly clear when comparing the wt and core enzymes; the hydrolytic rate at 25°C of the wt is almost twice as high as the core at 10 g/l, while the opposite ratio was found for  $pV_{max}$ . Analogous, although less pronounced cross-over effects were found for the linker variants with lowered affinity (Var2 and Var3). These observations support the conclusions regarding affinity changes in the variants discussed above. On a more practical level, they also call for caution in experimental assessments of Cel7A variants. Thus, testing kinetic properties of variants at only one load of substrate is potentially misleading because the catalytic efficacy may change with the load depending on how the mutation has affected respectively affinity and maximal turnover.

In summary, we have found that moderate modifications in the linker of Cel7A may change enzyme function significantly and that these changes can be quite different depending on the location of the mutation. We found that deletion of a 6-residue peptide near the catalytic domain had almost no effect on enzyme function and this parallels a few earlier studies on mutations in this region. A substitution near the middle of the linker that removed four sites for O-glycosylation as well as an insertion with several new glycosylation sites near the CBM both showed reduced substrate affinity and increased maximal rate compared to the wt. Two main conclusions were drawn from these observations. Firstly, attractive forces between glycans and cellulose that have been identified recently are not simply additive, but appear to depend on the specific location and possibly other factors such as changes in structure and dynamics of the linker peptide. Secondly, we suggest that the inverse relationship of affinity and maximal rate is a manifestation of dissociation controlled reaction at high substrate loads. This has been seen for different variants with weaker substrate binding and hence appears to reflect a generic coupling between affinity and maximal rate rather specific properties of the linker.

## Funding

This work was funded by Innovation Fund Denmark, contract grant numbers [0603-00496B; 5150-00020A] and Carlsbergfondet, contract grant number [2013-01-0208].

## Conflicts of interest

Kim Borch and Kenneth Jensen work at Novozymes A/S, a major manufacturer of industrial enzymes.

## References

- Bansal,P., Hall,M., Realf,M.J., Lee,J.H. and Bommarius,A.S. (2009) *Biotechnol. Adv.*, **27**, 833–848.
- Beckham,G.T., Bomble,Y.J., Matthews,J.F. et al. (2010) *Biophys. J.*, **99**, 3773–3781.
- Borch,K., Jensen,K., Krogh,K., McBrayer,B., Westh,P., Kari,J., Olsen,J., Sørensen,T., Windahl,M. and Xu,H. 2014. WO2014138672 A1 Cellobiohydrolase variants and polynucleotides encoding same.
- Chen,L., Drake,M.R., Resch,M.G., Greene,E.R., Himmel,M.E., Chaffey,P.K., Beckham,G.T. and Tan,Z. (2014) *Proc. Natl. Acad. Sci. USA*, **111**, 7612–7617.
- Cruys-Bagger,N., Elmerdahl,J., Praestgaard,E., Borch,K. and Westh,P. (2013a) *FEBS J.*, **280**, 3952–3961.
- Cruys-Bagger,N., Elmerdahl,J., Praestgaard,E., Tatsumi,H., Spodsborg,N., Borch,K. and Westh,P. (2012) *J. Biol. Chem.*, **287**, 18451–18458.
- Cruys-Bagger,N., Tatsumi,H., Ren,G., Borch,K. and Westh,P. (2013b) *Biochemistry*, **52**, 8938–8948.
- Fox,J.M., Levine,S.E., Clark,D.S. and Blanch,H.W. (2012) *Biochemistry*, **51**, 442–452.
- Gasteiger,E., Hoogland,C., Gattiker,A., Duvaud,S., Wilkins,M.R., Appel,R.D. and Bairoch,A. (2005) Walker,J.M. (ed), *The Proteomics Protocols Handbook Totowa*. Humana Press, New Jersey, pp. 571–607.
- Guan,X.Y., Chaffey,P.K., Zeng,C. et al (2015) *Chem. Sci.*, **6**, 7185–7189.
- Harrison,M.J., Nouwens,A.S., Jardine,D.R., Zachara,N.E., Gooley,A.A., Nevalainen,H. and Packer,N.H. (1998) *Eur. J. Biochem.*, **256**, 119–127.
- Horn,S.J., Sikorski,P., Cederkvist,J.B., Vaaje-Kolstad,G., Sorlie,M., Synstad,B., Vriend,G., Varum,K.M. and Eijsink,V.G.H. (2006) *Proc. Natl. Acad. Sci. USA*, **103**, 18089–18094.
- Kari,J., Olsen,J., Borch,K., Cruys-Bagger,N., Jensen,K. and Westh,P. (2014) *J. Biol. Chem.*, **289**, 32459–32468.
- Knott,B.C., Haddad Momeni,M., Crowley,M.F., Mackenzie,L.F., Götz,A.W., Sandgren,M., Withers,S.G., Ståhlberg,J. and Beckham,G.T. (2014) *J. Am. Chem. Soc.*, **136**, 321–329.
- Kraulis,J., Clore,G.M., Nilges,M., Jones,T.A., Pettersson,G., Knowles,J. and Gronenborn,A.M. (1989) *Biochemistry*, **28**, 7241–7257.
- Kurasin,M. and Valjamae,P. (2011) *J. Biol. Chem.*, **286**, 169–177.
- Langsford,M.L., Gilkes,N.R., Singh,B., Moser,B., Miller,R.C., Warren,R.A. and Kilburn,D.G. (1987) *FEBS Lett.*, **225**, 163–167.
- Le Costaouëc,T., Pakarinen,A., Várnai,A., Puranen,T. and Viikari,L. (2013) *Bioresour. Technol.*, **143**, 196–203.
- Lever,M. (1973) *Biochem. Med.*, **7**, 274–281.
- Maurer,S.A., Bedbrook,C.N. and Radke,C.J. (2012) *Ind. Eng. Chem. Res.*, **51**, 11389–11400.
- Olsen,J.P., Alasepp,K., Kari,J., Cruys-Bagger,N., Borch,K. and Westh,P. (2015) *Biotechnol. Bioeng.*
- Pakarinen,A., Haven,M.O., Djajadi,D.T., Várnai,A., Puranen,T. and Viikari,L. (2014) *Biotechnol. Biofuels.*, **7**, 27.
- Palonen,H., Tenkanen,M. and Linder,M. (1999) *Appl. Environ. Microbiol.*, **65**, 5229–5233.
- Payne,C.M., Resch,M.G., Chen,L. et al (2013) *Proc. Natl. Acad. Sci. U S A*, **110**, 14646–14651.
- Praestgaard,E., Elmerdahl,J., Murphy,L., Nymand,S., McFarland,K.C., Borch,K. and Westh,P. (2011) *FEBS J.*, **278**, 1547–1560.
- Receveur,V., Czjzek,M., Schülein,M., Panine,P. and Henrissat,B. (2002) *J. Biol. Chem.*, **277**, 40887–40892.
- Ruiz,D.M., Turowski,V.R. and Murakami,M.T. (2016) *Sci Rep*, **6**, 28504.
- Sammond,D.W., Payne,C.M., Brunecky,R., Himmel,M.E., Crowley,M.F. and Beckham,G.T. (2012) *PLoS ONE*, **7**, e48615.
- Shen,H., Schmuck,M., Pilz,I., Gilkes,N.R., Kilburn,D.G., Miller,R.C. and Warren,R.A. (1991) *J. Biol. Chem.*, **266**, 11335–11340.
- Srisodsuk,M., Reinikainen,T., Penttilä,M. and Teeri,T.T. (1993) *J. Biol. Chem.*, **268**, 20756–20761.
- Strobel,K.L., Pfeiffer,K.A., Blanch,H.W. and Clark,D.S. (2015) *Biotechnol. Bioeng.*

- Sørensen, T.H., Cruys-Bagger, N., Borch, K. and Westh, P. (2015a) *J. Biol. Chem.*, **290**, 22203–22211.
- Sørensen, T.H., Cruys-Bagger, N., Windahl, M.S., Badino, S.F., Borch, K. and Westh, P. (2015b) *J. Biol. Chem.*, **290**, 22193–22202.
- Sørensen, T.H., Windahl, M.S., Mcbrayer, B., Kari, J., Olsen, J.P., Borch, K. and Westh, P. (2016) *Biochemistry*. Submitted.
- Ting, C.L., Makarov, D.E. and Wang, Z.G. (2009) *J. Phys. Chem. B*, **113**, 4970–4977.
- von Ossowski, I., Eaton, J.T., Czjzek, M., Perkins, S.J., Frandsen, T.P., Schülein, M., Panine, P., Henrissat, B. and Receveur-Bréchet, V. (2005) *Biophys. J.*, **88**, 2823–2832.
- Wilson, D.B. (2009) *Curr. Opin. Biotechnol.*, **20**, 295–299.
- Zhang, S., Irwin, D.C. and Wilson, D.B. (2000) *Eur. J. Biochem.*, **267**, 3101–3115.
- Zhang, S. and Wilson, D.B. (1997) *J. Biotechnol.*, **57**, 101–113.



# In Situ Stability of Substrate-Associated Cellulases Studied by DSC

---

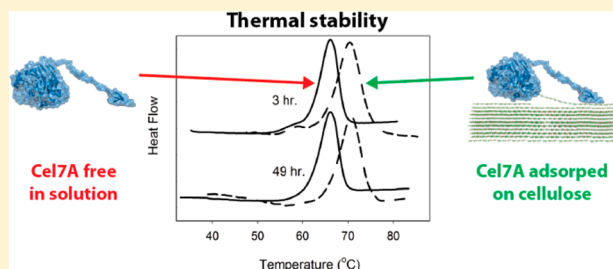
V



## In Situ Stability of Substrate-Associated Cellulases Studied by DSC

Kadri Alasepp,<sup>†</sup> Kim Borch,<sup>‡</sup> Nicolaj Cruys-Bagger,<sup>†</sup> Silke Badino,<sup>†</sup> Kenneth Jensen,<sup>‡</sup> Trine H. Sørensen,<sup>†</sup> Michael S. Windahl,<sup>†,‡</sup> and Peter Westh<sup>\*,†</sup><sup>†</sup>Research Unit for Functional Biomaterials, NSM, Roskilde University. 1 Universitetsvej, Build. 18.1, DK-4000 Roskilde Denmark<sup>‡</sup>Novozymes A/S, Krogshøjvej 36, DK-2880 Bagsværd, Denmark

**ABSTRACT:** This work shows that differential scanning calorimetry (DSC) can be used to monitor the stability of substrate-adsorbed cellulases during long-term hydrolysis of insoluble cellulose. Thermal transitions of adsorbed enzyme were measured regularly in subsets of a progressing hydrolysis, and the size of the transition peak was used as a gauge of the population of native enzyme. Analogous measurements were made for enzymes in pure buffer. Investigations of two cellobiohydrolases, Cel6A and Cel7A, from *Trichoderma reesei*, which is an anamorph of the fungus *Hypocrea jerorina*, showed that these enzymes were essentially stable at 25 °C. Thus, over a 53 h experiment, Cel6A lost less than 15% of the native population and Cel7A showed no detectable loss for either the free or substrate-adsorbed state. At higher temperatures we found significant losses in the native populations, and at the highest tested temperature (49 °C) about 80% Cel6A and 35% of Cel7A was lost after 53 h of hydrolysis. The data consistently showed that Cel7A was more long-term stable than Cel6A and that substrate-associated enzyme was less long-term stable than enzyme in pure buffer stored under otherwise equal conditions. There was no correlation between the intrinsic stability, specified by the transition temperature in the DSC, and the long-term stability derived from the peak area. The results are discussed with respect to the role of enzyme denaturation for the ubiquitous slowdown observed in the enzymatic hydrolysis of cellulose.



## INTRODUCTION

The enzymatic deconstruction of lignocellulosic biomass is a key process for the implementation of sustainable industries based on agricultural residues. This has generated substantial research interest in cellulases, xylanases, lytic monooxygenases, and other enzymes involved in the breakdown of polymers from the plant cell wall.<sup>1–5</sup> Many investigations of these enzymes have found unusual kinetic behavior that could not be readily rationalized by conventional theories. This is at least in part due to the heterogeneous surface of the insoluble substrate and the concomitant diversity of enzyme–substrate complexes, which interconvert on different time scales during the process. One particularly important example of atypical kinetics for cellulolytic enzymes is the ubiquitous slowdown in the hydrolytic activity. Thus, essentially all experimental studies including both monocomponent cellulases and cellulase cocktails and substrates ranging from purified cellulose to complex biomass show a characteristic loss in enzymatic activity as the hydrolysis progresses.<sup>6</sup> This effect can be quite pronounced, and it poses a significant challenge for the industrial application of cellulases as the rate of hydrolysis may fall to exceedingly low levels well before the cellulose is fully converted to soluble sugars. The origins of the slowdown have been discussed extensively, and based on the current understanding it appears reasonable to infer that it relies on several factors. For example, in the later stages of hydrolysis, cellulase activity may be impeded by both accumulated products<sup>7–10</sup> and the depletion of substrate with good reactivity.<sup>11</sup> Another type

of rate retardation has been reported in the very early stages, before the reaction reaches quasi-steady state. Thus, cellulases may show a burst (and subsequent slowdown) in activity within seconds or minutes,<sup>12–16</sup> which is akin<sup>17,18</sup> to that found for other hydrolytic enzymes, which cleaves soluble substrates in conventional homogeneous catalysis.<sup>19–21</sup> These factors, however, cannot fully account for the slowdown, which also appears to depend on intricate enzyme–substrate interactions that affect the hydrolytic activity on intermediate and long time scales.<sup>22–24</sup> Recently, our understanding of these interactions has been promoted by studies using surface methods such as QCM, AFM, and SPR.<sup>25–29</sup> Some of these works have visualized the decay of cellulose particles during enzymatic attack, and others have provided quantitative information on the rate and extent of adsorption and hydrolysis. A recurring result in the latter type of work has been a distinct hysteresis (or irreversibility) of the enzyme–cellulose interaction. Thus, only a limited fraction of the adsorbed enzyme can be washed off the substrate in QCM or SPR when the flow above the cellulose surface reverts from an enzyme solution to a pure buffer.<sup>27,29</sup> This notion of irreversible adsorption also occurs in work on suspended cellulose particles, but conclusions in this area remain divisive. The most commonly studied cellulase, Cel7A, for example, has been reported to show no,<sup>30</sup>

Received: January 13, 2014

Revised: May 8, 2014

Published: May 23, 2014

partial,<sup>31,32</sup> or full<sup>33,34</sup> reversibility when the sample was diluted with buffer. Interestingly, both QCM and SPR showed that the population of enzyme irreversibly bound to cellulose on the measuring chip increased gradually with time,<sup>27,29</sup> and similar behavior, albeit on a much slower time scale, has been found for a bulk suspension of cellulose and Cel7A.<sup>34</sup> This has led to the suggestion that irreversible binding and inactivation may be causally related in the sense that conformational changes of the enzyme underlie both tighter (irreversible) association and inactivation.<sup>29</sup> This latter mechanism is reminiscent of that generally suggested for the irreversible (nonspecific) adsorption of model proteins on different solid sorbents.<sup>35–38</sup> If indeed a population of strongly bound cellulase with non-native conformation tends to build up during hydrolysis, this would clearly have a negative impact on the enzymatic activity and hence would be a contributing factor to the slowdown. This idea is not new, and different types of gradual cellulase inactivation during the hydrolysis have been discussed repeatedly. (See Bansal et al.<sup>6</sup> for a review.) Further insight into this problem appears to rely on better experimental approaches, and in the present work we show that a combination of differential scanning calorimetry (DSC) and standard adsorption and activity measurements may provide quantitative information on the long-term stability of cellulases both free (dissolved in buffer) and in situ during the hydrolysis of insoluble cellulose. We have used this approach in studies of two cellobiohydrolases from *Trichoderma reesei* (an anamorph of the fungus *Hypocrea jecorina*), Cel7A, and Cel6A, which are among the most thoroughly investigated cellulases and candidates for industrial use. Both enzymes consist of a catalytic domain and a carbohydrate binding module (CBM), which are connected by a flexible glycosylated linker. They are thought to hydrolyze cellulose processively, i.e., by sequential catalytic cycles performed on a cellulose strand without dissociation. Cel7A is a retaining enzyme which attacks the reducing end of the cellulose strand, while Cel6A uses the inverting mechanism and starts the processive movement from the nonreducing end.<sup>39</sup> Both enzymes have been reported to hydrolyze microcrystalline cellulose, although recent observations have suggested that Cel6A has a preference for the disordered (noncrystalline) parts<sup>40</sup> of a mixed crystalline/amorphous substrate such as Avicel. (The crystallinity index of Avicel is 0.5–0.7.<sup>41,42</sup>) The maximal enzymatic activity for these enzymes is found at around 55–60 °C,<sup>43,44</sup> and industrial application usually uses temperatures of around 50 °C.

Results of the current work showed that enzyme denaturation may contribute to the slowdown and that the importance of this factor varies strongly with storage temperature and enzyme type.

## ■ EXPERIMENTAL SECTION

**Materials.** Enzymes Cel7A (CBH1) and Cel6A (CBH2) from *Hypocrea jecorina* were cloned, expressed, and purified as described previously.<sup>18,45,46</sup> Enzyme concentrations were derived from measurements of the optical density at 280 nm using theoretical extinction coefficients (86.8 mM<sup>-1</sup> for Cel7A and 96.6 mM<sup>-1</sup> for Cel6A) calculated from the amino acid content.<sup>47</sup> All experiments were conducted in a standard 50 mM acetate buffer at pH 5.0. The substrate was Avicel PH101 (Fluka) at an initial load of 60 g/L. Avicel was chosen because it is the most commonly used model substrate, and initial work showed that it was readily handled at high loads and showed no thermal transitions in the DSC.

**Procedures.** The stability of Cel6A and Cel7A was investigated in thermal stress experiments in which enzyme samples were exposed to

a preset storage temperature ( $T_{\text{store}}$ ) for up to 53 h. Cel6A was tested at  $T_{\text{store}} = 25, 40,$  and  $49$  °C, and for Cel7A we used  $T_{\text{store}} = 25$  and  $49$  °C. Each thermal stress experiment (i.e., one enzyme studied as a function of time at one value of  $T_{\text{store}}$ ) was started by preparing about 20 aliquots of 1000  $\mu\text{L}$  of enzyme solution in 2 mL Eppendorf tubes. Half of the tubes contained substrate (60 g/L Avicel), while the other half were references, with enzyme dissolved in pure buffer. All samples had an enzyme load of 0.63 mg/mL. Henceforth we will refer to samples with and without Avicel as hydrolysis samples and reference samples, respectively. All samples were placed horizontally in a rack on an orbital shaker in a temperature-controlled incubator and agitated so that the liquid moved gently forth and back in the tube. At given time points, samples were removed from the incubator, degassed under vacuum, and loaded into a differential scanning calorimeter (Nano-DSC, TA Instruments, New Castle, DE) to test the thermal stability. The Nano-DSC was equipped with flow-through capillary cells, which were loaded with pipettes mounted on both the inlet and outlet. This enabled rapid liquid movement forth and back in the capillaries and hence the establishment of a homogeneous suspension of the hydrolysis samples in the cell before the start of the calorimetric experiment (this was essential for the data analysis; see below). The reference cell in the DSC was loaded with pure buffer in all runs. Excess sample from the thermal stress experiments that was not used to load the DSC was saved for other types of analyses described below. The stability of the enzyme was tested in heating scans from 20 to about 85 °C at a rate of 2 °C/min. A distinct thermal transition was evident in all enzyme samples while no transitions could be detected in control experiments with (enzyme-free) Avicel suspension in the calorimeter. We used the Nano-Analyze software package (TA Instruments) to analyze enzyme transitions following the subtraction of either a buffer scan or a scan with a pure Avicel suspension. We did not find systematic differences between  $T_{\text{T}}$  and  $\Delta H$  derived by these two procedures, and this corroborates that the results were unaffected by possible thermal transitions in pure Avicel. The transition temperature was simply defined as the apex of the transition peak, and  $\Delta H$  was calculated in the conventional way by normalizing the total heat (the area under the transition peak in  $\mu\text{J}$ ) with respect to the number of moles of enzyme in the calorimetric cell (299  $\mu\text{L}$ ) assuming a homogeneous sample. The total volume required to fill the instrument ( $\sim 700$   $\mu\text{L}$ ) includes both the active volume where the heat signal is detected (299  $\mu\text{L}$ ) and the volume of the access shaft, which must also be filled with sample (but is not heated during a measurement). Effects of inhomogeneity resulting from the precipitation of Avicel with bound enzyme from the vertical access shaft were taken into account as described in the Results and Data Analysis section. In some cases, the sample was cooled in the instrument after the calorimetric scan was completed, equilibrated at 20 °C for 15 min, and taken through a second heating scan to test if any refolding of the denatured enzyme had occurred.

The remainder of the samples (i.e., the liquid not loaded into the DSC) was centrifuged at 10 000g for 3 min. The supernatant was spilt into two and analyzed for the content of soluble sugars (only hydrolysis samples) and the free enzyme (both hydrolysis and reference samples). Free enzyme was quantified by spectrofluorometry using the intrinsic protein fluorescence at an excitation wavelength of 280 nm. The emission at 345 nm was measured in a Shimadzu RF-5301PC instrument and translated into concentration units using standard curves prepared in direct connection to the analysis of the samples. Soluble sugars were quantified in an ICS-5000 ion chromatograph equipped with a CarboPac PA-10 column and an electrochemical detector (Termo Fisher Scientific Waltham, MA). Samples were eluted with a multistep gradient with 50 mM NaOH (0–4 min), 100 mM sodium acetate + 90 mM NaOH (4–28 min), 450 mM sodium acetate + 200 mM NaOH (28–29 min), and 50 mM NaOH (29–35 min). The results were quantified against standards for glucose, cellobiose, and cellotriose run daily.



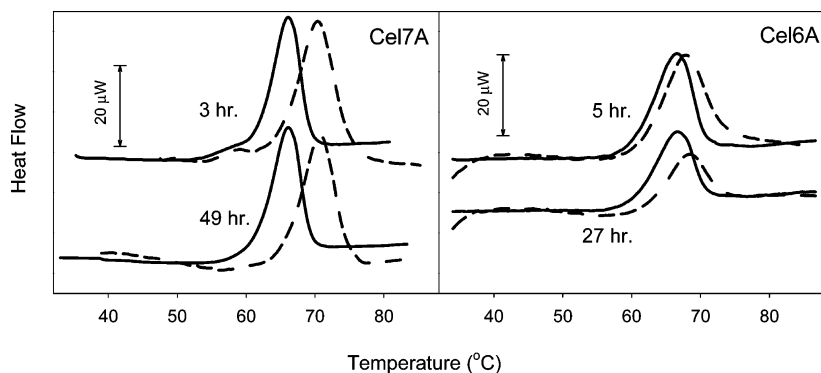


**Figure 1.** Representative DSC data (so-called thermograms) for Cel7A and Cel6A from thermal stress experiments at  $T_{\text{store}} = 49\text{ }^{\circ}\text{C}$ . Samples were retrieved at the stated time points and analyzed in the DSC. Full lines represent reference samples (0.63 mg/mL of enzyme dissolved in buffer), and dashed curves are hydrolysis samples (0.63 mg/mL of enzyme in a 60 g/L Avicel suspension).

## RESULTS AND DATA ANALYSIS

Figure 1 shows representative examples of DSC data (so-called thermograms giving the differential heat flow as a function of temperature). Specifically, thermal transitions of Cel7A and Cel6A are shown for experiments with  $T_{\text{store}} = 49\text{ }^{\circ}\text{C}$ . The samples were retrieved at different time points as stated in the figure. To facilitate comparisons, the thermograms have been shifted vertically so each pair of curves shows a corresponding set of reference (solid line) and hydrolysis (dashed line) samples. For Cel7A, it clearly appears that the presence of substrate displaces the transition temperature,  $T_{\text{T}}$ , in an upward direction; the average shift,  $\Delta T$ , was  $4.4 \pm 0.3\text{ }^{\circ}\text{C}$  (Table 1).

**Table 1. Average Transition Temperatures,  $T_{\text{T}}$ , for Enzymes with and without Substrate<sup>a</sup>**

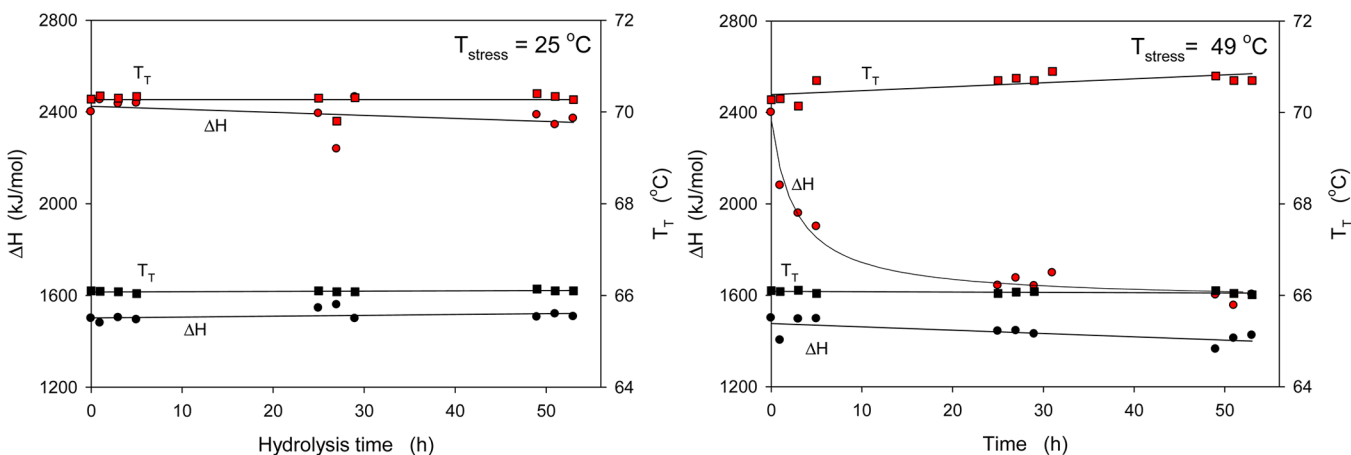
| enzyme | hydrolysis samples (60 g/L Avicel)                  | reference samples (buffer)                           |
|--------|-----------------------------------------------------|------------------------------------------------------|
| Cel7A  | $70.5 \pm 0.3\text{ }^{\circ}\text{C}$ ( $n = 19$ ) | $66.1 \pm 0.03\text{ }^{\circ}\text{C}$ ( $n = 18$ ) |
| Cel6A  | $66.9 \pm 1.3\text{ }^{\circ}\text{C}$ ( $n = 30$ ) | $66.5 \pm 0.2\text{ }^{\circ}\text{C}$ ( $n = 28$ )  |

<sup>a</sup> $T_{\text{T}}$  was independent of the storage temperature and duration of the thermal stress experiment prior to the DSC analysis.

For Cel6A a slight shift also appears in the examples in Figure 1, but for this enzyme  $\Delta T$  was less than the experimental

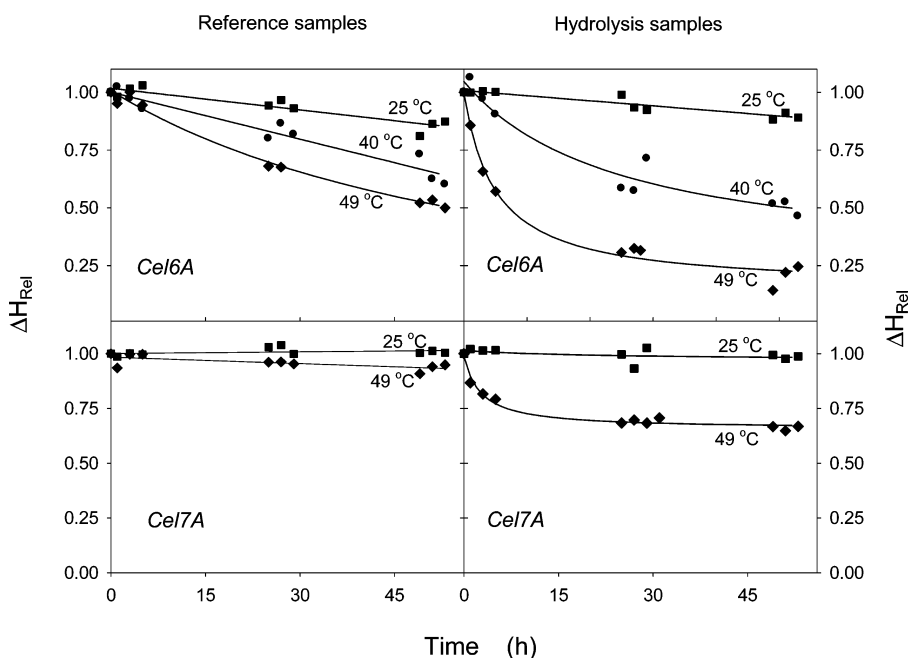
scatter (Table 1). Figure 1 also shows a trend toward smaller peaks (lower  $\Delta H$ ) in samples with long contact times. This is particularly evident for the Cel6A hydrolysis samples, which show a much smaller transition peak after 27 h compared to the 5 h time point. For Cel7A the difference between the two time points is smaller, but the integration of the curves in Figure 1 showed that  $\Delta H$  had decreased by about 20% between the two time points in the figure (further illustrated in Figures 2 and 3). The calorimetric behavior may be illustrated more clearly by plotting both  $T_{\text{T}}$  and  $\Delta H$  as functions of the contact time. Figure 2 shows examples for Cel7A in thermal stress experiments at 25 and 49  $^{\circ}\text{C}$ , and it appears that  $T_{\text{T}}$  was essentially independent of both storage temperature and duration of the thermal stress experiment preceding the DSC measurement. (The  $T_{\text{T}}$  lines in Figure 2 are horizontal.) Average values of  $T_{\text{T}}$  for both enzymes were therefore calculated for hydrolysis and reference samples and are listed in Table 1.

Figure 2 shows that, depending on the conditions,  $\Delta H$  may develop very differently over time in thermal stress experiments. For example,  $\Delta H$  remained constant in reference samples for  $T_{\text{store}} = 25\text{ }^{\circ}\text{C}$  over the entire 53 h experiment but decreased rapidly (particularly during the first 10 h) in hydrolysis samples with  $T_{\text{store}} = 49\text{ }^{\circ}\text{C}$ . Another noticeable



**Figure 2.** Representative calorimetric data from the thermal stress experiments. The results are for Cel7A at storage temperatures of 25 and 49  $^{\circ}\text{C}$ , and the plots show how the transition temperature,  $T_{\text{T}}$  (squares, right ordinate), and the enthalpy change,  $\Delta H$  (circles, left ordinate), vary with contact time. Red symbols identify hydrolysis samples (with 60 g/L Avicel), and black symbols are reference samples where Cel7A is dissolved in buffer. Overall it appears that  $T_{\text{T}}$  is essentially independent of thermal stress and that  $\Delta H$  decreases at high but not at low storage temperature.





**Figure 3.** Relative enthalpy changes,  $\Delta H_{\text{Rel}} = \Delta H/\Delta H_0$ , for respectively reference samples (left panels) and hydrolysis samples (right panels) plotted as a function of the duration of thermal stress. (The storage temperature,  $T_{\text{store}}$  is identified by the labels.) The fitted curves are without theoretical meaning and are included only to facilitate reading.

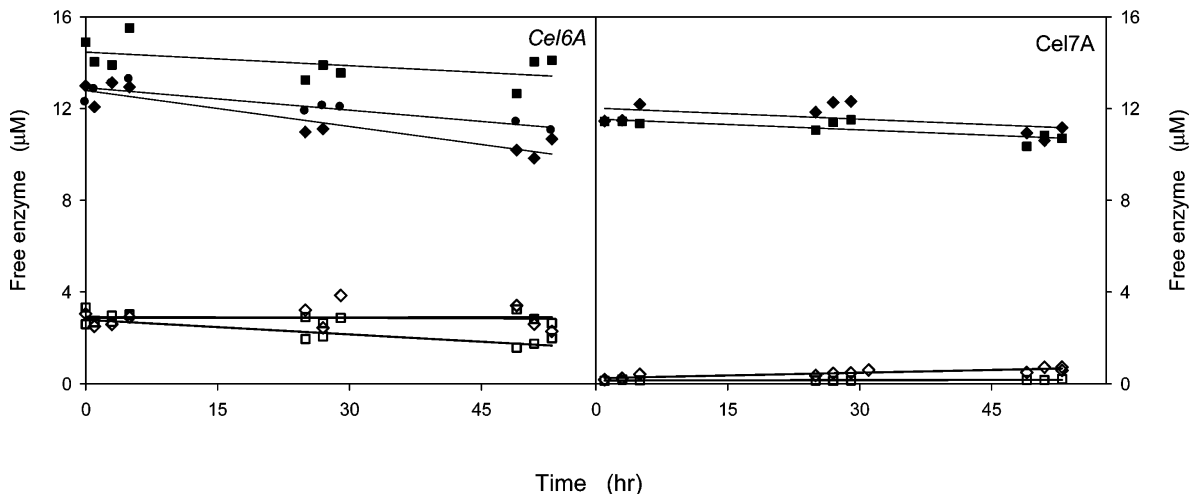


**Figure 4.** Time dependence of the free (aqueous) enzyme concentration in hydrolysis samples (open symbols) and reference samples (filled symbols). The storage temperatures were 25 °C (squares), 40 °C (circles), and 49 °C (diamonds).

result from Figure 2 was that  $\Delta H$  was much higher in hydrolysis samples compared to references. This was expected for two reasons. First, protein–ligand interactions tend to increase  $\Delta H$  due to the extra energy required to break the additional interactions in the complex during the thermal transition.<sup>48</sup> Second, the precipitation of Avicel particles with bound enzyme inevitably increased  $\Delta H$  for the hydrolysis samples. This follows from the design of the instrument (and indeed all commercial high-sensitivity DSCs) with both the active part of the cell and the vertical access shafts filled with sample. For the hydrolysis samples, Avicel particles with bound enzyme sediment from the access shaft into the active part of the cell during the initial equilibration and hence increase the amount of enzyme there. Obviously, this effect will be absent in the (homogeneous) reference samples. We found that the current protocol (with about 30 min initial equilibration) gave

reproducible  $\Delta H$  and that longer equilibration did not change the observed enthalpy change. Also, a visual inspection of a model of the capillary cell of this instrument made of (transparent) tubing showed that all Avicel had settled within a half hour. On the basis of this we conclude that the absolute  $\Delta H$  values for the hydrolysis samples (but not the reference samples) in Figure 2 are dependent on the instrument design and hence without direct physical meaning. However, as the change in  $\Delta H$  is systematic (governed by the volume of the access shaft), the relative changes in  $\Delta H$  can be used to quantify how the denaturation behavior develops during the course of the thermal stress experiments. We therefore calculated the relative enthalpy change  $\Delta H_{\text{Rel}}$  for all trials by normalizing the value at any given time point with the enthalpy change at time = 0,  $\Delta H_0$ . The latter was found by extrapolating plots of  $\Delta H$  vs time to time = 0 (cf. Figure 2). We note that

$\Delta H_0$  values derived in this way were independent of  $T_{\text{store}}$ , but as it appears in the example in Figure 2, extrapolations for  $T_{\text{store}} = 25$  °C, where the  $\Delta H$  function was essentially flat, provided the most precise values for  $\Delta H_0$ . Results in Figure 3 show how  $\Delta H_{\text{Rel}}$  developed with the duration of the thermal stress for all investigated systems.

The Interpretation of the calorimetric data will rely on the populations of free and substrate-associated enzyme in the hydrolysis samples. The results in Figure 4 show that Cel7A is almost fully associated with the substrate under the conditions used here. The free concentrations of this enzyme in the hydrolysis samples were 1–2% ( $T_{\text{store}} = 25$  °C) and 2–5% ( $T_{\text{store}} = 49$  °C) of the concentration in the references (Figure 4). The interaction of Cel6A and Avicel is weaker, but this enzyme is also predominantly substrate-bound with a free population corresponding to 15–18% of the reference samples. Cel6A showed a decreasing trend in the free concentration, particularly in the reference samples. This is possibly associated with a limited aggregation of enzyme, which is removed in the centrifugation step prior to the fluorescence measurements.

The production of sugar in the hydrolysis samples was measured to ensure that the substrate remained mainly unconverted during the experiment. Full conversion of 60 g/L Avicel would approximately make 185 mM cellobiose, and it follows from Figure 5 that the maximal conversion after 53 h

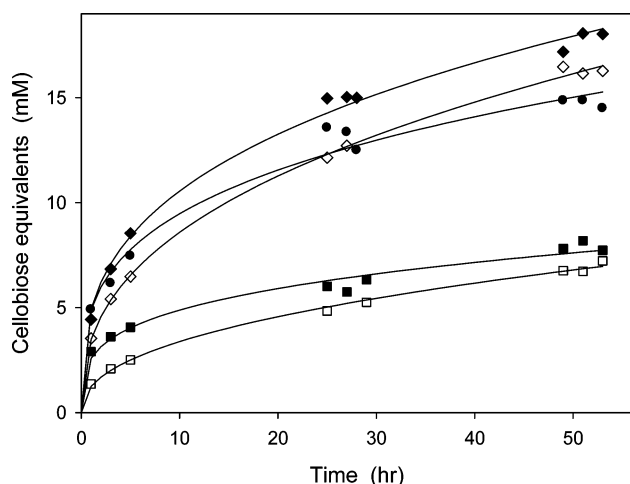


**Figure 5.** Concentration of soluble sugar in the samples analyzed by DSC. The product was predominantly cellobiose, but small amounts of glucose and cellotriose were also found. Results are given as cellobiose equivalents, i.e.,  $\frac{1}{2}[\text{glucose}] + [\text{cellobiose}] + \frac{1}{2}[\text{cellotriose}]$ . Open symbols show data for Cel7A, and filled symbols are for Cel6A. The storage temperatures were 25 °C (squares), 40 °C (circles), and 49 °C (diamonds). The rate of the hydrolytic reaction was estimated from the slope of the fitted lines (sum of two exponentials).

was about 10%. The progress curves in Figure 5 were also used to assess the heat produced by the enzymatic reaction as this could potentially affect the DSC measurement. Thus, for the hydrolysis samples the enzyme was still catalytically active when the DSC measurement commenced; therefore, the thermal output necessarily reflected the sum of the heats from the thermal transition in the protein molecule (as seen in the reference samples) and a contribution from hydrolytic reaction. To assess the latter, we fitted an empirical function (a sum of two exponentials) to the progress curves and used the slope to

estimate the hydrolytic rate. This analysis showed that for the first few time points the maximal slope in Figure 5 (for  $T_{\text{store}} = 49$  °C) was about 1 mM/h. The hydrolytic heat flow ( $\text{HF}_{\text{hyd}}$  in units of J/s) is given as  $\text{HF}_{\text{hyd}} = V_{\text{cell}} \Delta H_{\text{hyd}} v_{\text{hyd}}$ , and the insertion of the enthalpy of Avicel hydrolysis  $\Delta H_{\text{hyd}} \approx -4$  kJ/(mol cellobiose),<sup>49</sup> the volume of the calorimetric cell  $V_{\text{cell}} = 299$   $\mu\text{L}$ , and the rate  $v_{\text{hyd}} \approx 1$  mM/h found above yields an expected  $\text{HF}_{\text{hyd}}$  of about 0.3  $\mu\text{W}$ . This is negligible compared to the peak height in Figure 1, and even if  $\text{HF}_{\text{hyd}}$  increased 2- or 3-fold as the DSC temperature was raised from 49 °C (the temperature where  $\text{HF}_{\text{hyd}}$  was estimated) toward the maximal enzyme activity at around 60 °C,<sup>43</sup> it is still much smaller than the amplitude of the transition peaks in Figure 1 (20–35  $\mu\text{W}$ ). We therefore conclude that the contribution to the DSC signal arising from the hydrolysis reaction can be ignored in samples taken after 1 h. For samples taken at later stages the hydrolytic rate is lower (Figure 5) and  $\text{HF}_{\text{hyd}}$  will still be smaller. The absence of detectable effects from  $\text{HF}_{\text{hyd}}$  was also supported by the lack of a systematic upward curvature of the pretransition range of the DSC traces for hydrolysis samples. The small heat of reaction in the samples also rules out heating the Eppendorf tubes to temperatures above  $T_{\text{store}}$  in the incubator.

## DISCUSSION

It is generally challenging to experimentally appraise the structure and stability of proteins adsorbed to solid surfaces. This relies on both practical limitations and difficulties in the interpretation of experimental observables with contributions from both protein and sorbent. For example, the suite spectroscopic methods that are commonly used in protein structure and stability studies are often limited by scattering, absorption, or competing signals from the solid material.<sup>50</sup> In a few cases, the stability of model proteins such as lysozyme, hemoglobin, or lactalbumin adsorbed on solid surfaces including silica and polystyrene has been assessed by DSC.<sup>50–52</sup> This experimental approach is nonspecific inasmuch as it detects the total heat flow arising from all processes during continuous heating. In the current context, this may provide the advantage of making it insensitive to the presence of the sorbent material as long as this material does not show any thermal transitions in the relevant temperature range. We found this criterion to be fulfilled for Avicel. Moreover, the heat produced by the enzymatic reaction was small enough not to disturb the detection of the transition in the enzyme, and we concluded that DSC can be applied to in situ stability studies of cellulases associated with (and actively hydrolyzing) a model substrate such as Avicel. Preliminary tests with (enzyme-free) lignocellulosic biomass in the DSC showed thermal transitions that could overlap with the denaturation of protein, thus suggesting that the method would be harder to apply for this substrate.

We first address the question of how to extract quantitative stability data from the calorimetric results. To this end we emphasize three general observations from the DSC measurements: (i) The transition temperature,  $T_T$ , was independent of the duration and storage temperature of the thermal stress experiment prior to the calorimetric measurement (Table 1 and Figure 2). (ii) The relative transition enthalpy,  $\Delta H_{\text{Rel}}$ , decreased to different extents depending on the enzyme and the severity of the thermal stress experiment (Figure 3). (iii) Rescanning experiments suggested that all transitions in the DSC were irreversible, both for free and substrate-bound enzyme (no peak observed in the second scan). The simplest

interpretation of these observations is that the native structure (free or substrate-bound) remained unchanged during thermal stress experiments (as  $T_T$  is constant), while the amount of native enzyme decreased to variable extents. This interpretation implies that the reduction in  $\Delta H_{\text{rel}}$  (Figure 3) reflects a gradual, irreversible loss of native enzyme during the experiment. In other words, some enzyme is already non-native before the DSC measurement and hence does not contribute to the transition peak (cf. Figures 1 and 5). This interpretation is along the lines of the so-called Lumry–Eyring (LE) model,<sup>53</sup> which is the most commonly applied description of irreversible protein denaturation. The LE model stipulates that a reversible change in the protein conformation precedes a kinetically controlled inactivation step, and this may be written as  $E \xrightleftharpoons{K} U \xrightarrow{k_i} I$ , where E is the native enzyme, U is an unfolded (or partially unfolded) form, and I represents enzyme that has been irreversibly denatured through aggregation, misfolding, or covalent modifications.<sup>54</sup> Parameters  $K$  and  $k_i$  are, respectively, the equilibrium constant for the first step and the rate constant for the second. In the current context, this scheme pertains to the behavior of the reference samples, but an analogous denaturation process may be written for the substrate (S)-bound enzyme in the hydrolysis samples,  $E'S \xrightleftharpoons{K'} U'S \xrightarrow{k'_i} I'S$ . These LE schemes underscore that two separate descriptors of stability must be distinguished. First, stability may be specified as the resistance toward irreversible inactivation by mild but prolonged thermal stress. This parameter is mainly governed by  $k_i$  (or  $k'_i$ ), and we will henceforth call it long-term stability. (This is often called colloidal stability or kinetic stability in the literature,<sup>55,56</sup> but these terms are ambiguous when working with Avicel suspensions that are highly unstable from a colloidal point of view.) Second, stability may be defined as the resistance against conformational changes at higher temperatures, and we will call this intrinsic stability. For reversible transitions (i.e., when  $k_i = 0$ ), the intrinsic stability is explicitly specified by the equilibrium constant  $K$ , and it can be derived rigorously from the measured transition temperature,  $T_T$ , and the enthalpy change. For irreversible transitions, such as those studied here, the interpretation of  $T_T$  is more complex. In particular  $T_T$  will depend on the scanning rate in a way that can be rationalized on the basis of the LE- picture.<sup>57</sup> We will not apply this detailed analysis here but will simply compare changes in  $T_T$  values obtained at the same scan rate and use these values as an operational measure of the intrinsic conformational stability, as is done in most DSC work on homogeneous systems. Samples from the thermal stress experiments were cooled to 20 °C in the DSC prior to the scan. The use of this low starting temperature was necessary in order to obtain a stable baseline prior to the thermal transition and hence a precise determination of  $\Delta H$ . Clearly, cooling from  $T_{\text{store}}$  to 20 °C could affect both enzyme binding and the  $E \rightleftharpoons U$  equilibrium, and it follows that the subsequent DSC heating scan will detect enzyme that is in dynamic equilibrium (i.e., in the E or U form) while the population captured in the I form will not be detected.

**Intrinsic Stability.** In the terminology specified above, the results in Table 1 show that the intrinsic stability of Cel7A was promoted by its association with substrate ( $T_T$  increased in the presence of substrate), while no significant change was found for Cel6A. The behavior of Cel7A parallels many earlier examples of increased intrinsic stability resulting from protein–ligand interactions in homogeneous solutions<sup>48</sup> but it is in

contrast to DSC studies of the nonspecific adsorption of model proteins on solid surfaces, which showed pronounced reductions in  $T_T$ .<sup>50,52</sup> This probably reflects the specificity of the enzyme–substrate interaction and hence suggests that general properties of proteins on solid sorbents are of minor relevance in discussions of the stability of substrate-adsorbed cellulases. The absence of a measurable increase in the intrinsic stability of Cel6A upon association with substrate may rely on weaker interactions of this enzyme compared to those of Cel7A. This interpretation is in accord with both earlier work<sup>34</sup> and Figure 4, which shows a higher free enzyme concentration in the hydrolysis samples for Cel6A (implying weaker interactions of Cel6A compared to those of Cel7A). However, the behavior of  $T_T$  for Cel6A may also reflect a coupling between the two steps in the LE model. Thus, if the second (irreversible) step is fast (i.e., if  $k'_i$  is large), then the DSC signal will become asymmetric (as the U form is removed rapidly) and its maximum value ( $T_T$ ) will be displaced toward lower temperatures.<sup>57</sup> Therefore, the unchanged value of  $T_T$  for Cel6A in Table 1 could reflect both weaker substrate interactions and a faster irreversible inactivation, which obscures the measurement of  $\Delta T_T$ . The latter suggestion is in accord with both the lower long-term stability of Cel6A (see below) and the higher experimental scatter in  $T_T$  for Cel6A (Table 1), as dominance by the kinetically controlled step generally makes the thermograms more sensitive to technical subtleties.

**Long-Term Stability.** The long-term stability expressed as  $\Delta H_{\text{rel}}$  depended on both the thermal stress and substrate interactions. The best long-term stability was found for Cel7A in buffer at  $T_{\text{store}} = 25$  °C. Under these conditions  $\Delta H_{\text{rel}}$  was unchanged for 53 h (Figure 4), and we conclude that the entire enzyme population remained in the native state (no accumulation of the I form in the sense of the LE scheme). Cel7A also showed good long-term stability at 25 °C in the hydrolysis samples. In this case, a linear fit to all  $\Delta H_{\text{rel}}$  data (Figure 4, left panel) showed a weak negative slope and a  $\Delta H_{\text{rel}}$  value of around 0.97 after 53 h. This value is barely distinguishable from unity ( $\Delta H_{\text{rel}} = 1$  for a stable enzyme) within the experimental scatter (the slope of the fit was  $-5.5 \pm 4$  (SE)  $\times 10^{-4}$  h<sup>-1</sup>). At  $T_{\text{stress}} = 49$  °C,  $\Delta H_{\text{rel}}$  for Cel7A fell to respectively 0.95 in the reference samples and 0.65 in the hydrolysis samples after 53 h. This implies that Cel7A has excellent physical stability in buffer at elevated temperatures but loses about a third of the native population when it is catalytically active. It is noticeable that the lower long-term stability of active enzyme occurred in spite of an increased intrinsic stability; in other words, the increased conformational stability that results from the interaction of Cel7A and its substrate (higher  $T_T$  in Table 1) does not translate into a better long-term stability. Free Cel6A showed approximately the same intrinsic stability as Cel7A, but Cel6A was far inferior with respect to long-term stability, in both reference and hydrolysis samples. At  $T_{\text{store}} = 49$  °C, the  $\Delta H_{\text{rel}}$  data suggested that respectively 50% (reference) and 80% (hydrolysis) of the Cel6A population had been irreversibly denatured over the 53 h experiment. The analogous numbers at  $T_{\text{store}} = 40$  °C were 35 and 50%. These results for Cel6A reiterate the conclusion for Cel7A that the long-term stability is much lower for active enzyme compared to enzyme in buffer. The above conclusions on long-term stability rest on the assumption that all enzyme in the hydrolysis samples was associated with the substrate. For Cel6A, however, a moderate fraction (about 15%, Figure 4) was

in the aqueous phase. The influence of this on the DSC data can be assessed because the DSC behavior of free enzyme is known from the reference samples. Under the assumption that the DSC signal in the hydrolysis samples is a linear combination of contributions from free and bound enzyme, we found that the losses of native Cel6A at  $T_{\text{store}} = 40$  and  $49$  °C were slightly larger than suggested in Figure 3, but the difference was comparable to the experimental scatter and hence was neglected. Molecular origins of the weaker interaction of Cel6A cannot be directly assessed on the basis of the current data. We speculate, however, that it could rely on the shorter and more open catalytic tunnel of Cel6A,<sup>58</sup> which is expected to contribute less to the net affinity than the longer and more closed tunnel of Cel7A.<sup>59</sup> This interpretation is supported by binding data for enzyme variants with no cellulose binding modules, which showed lower cellulose affinity for Cel6A than for Cel7A.<sup>34</sup> Finally, we note that in spite of a lower concentration of bound Cel6A (85%) compared to Cel7A (98%), the enzymatic activity of the former enzyme is comparable to or a bit higher than Cel7A (Figure 5). This is a sign of a slightly higher specific activity of Cel6A under the conditions studied here.

As described in the Introduction, one of the motivating factors of this work was the question of whether the long-term physical instability of the enzyme could be a cause of the slowdown in the hydrolytic rate. Some recent work has indeed supported this inference.<sup>29</sup> The data for Cel7A and  $T_{\text{store}} = 25$  °C speak against any strict relationship because there is essentially no loss in the native population in the hydrolysis samples over the 53 h experiment (Figure 3). However, the hydrolytic rate, specified by the slope in Figure 5, fell by about 1 order of magnitude between 1 and 50 h of hydrolysis. This degree of slowdown is similar to what has previously been observed in a comparable experiment.<sup>7</sup> At higher storage temperatures, and particularly for Cel6A, the situation is quite different, and we found a conspicuous reduction in the native population in hydrolysis samples, particularly over the first 10 h (Figure 4). Taken together, these observations suggest that long-term instability cannot be the only cause of the slowdown but that it may become a significant factor under severe (industrially relevant) temperature conditions. At the higher storage temperatures, the importance of protein denaturation may be assessed by comparing the relative catalytic activity (e.g., the rate at a given time point divided by the initial rate; see Figure 5) and the relative enthalpy change,  $\Delta H_{\text{rel}}$  (Figure 4). Attempts to do so showed that the relative activity always decreased more rapidly than  $\Delta H_{\text{rel}}$ . If we consider the most unstable system studied (Cel6A at  $49$  °C) for  $t = 53$  h, then  $\Delta H$  was about 24% of the value after 1 h while the analogue fraction for the hydrolytic activity was only 8%. For the other (more stable) systems, this discrepancy was even larger, and this again shows that factors other than enzyme denaturation contribute significantly to the slowdown. For the current experiments, with final cellobiose concentrations in the 6–18 mM range, one such factor must be product inhibition.<sup>8–10</sup> It follows that future work combining DSC and more extensive activity measurements also including samples with added  $\beta$ -glucosidase (which converts cellobiose to the much less inhibitory glucose) could be useful in attempts to single out contributions to the slowdown. For the current purpose, we did not use  $\beta$ -glucosidase because the results would then have reflected combined effects of the long-term stability of both the cellobiohydrolase and the  $\beta$ -glucosidase.

We conclude that DSC is a promising tool for in situ measurements of both the intrinsic and long-term stability of cellulases actively associated with insoluble cellulose. Information of this type appears to be important to the understanding of cellulase kinetics, and we are not aware of other experimental approaches which have successfully monitored cellulase stability in situ. It is possible that methods including CD and fluorescence spectroscopy could be developed to provide direct information on structural changes in adsorbed cellulases, and this would be most valuable. However, earlier work has shown that it is difficult to filter out effects originating from the solid material in the spectroscopic data.<sup>50</sup> Another potential of the current method lies in its combined use with surface analysis methods such as QCM and SPR. These latter approaches have proven to be effective in characterizing the adsorption and activity of cellulases,<sup>26–29</sup> and a combination of this and data on the gradual loss of native structure (which cannot be detected by QCM or SPR) appears to be promising in attempts to reveal causes of the slowdown. The current results showed that the intrinsic stability of an adsorbed cellulase is readily measured but is a poor descriptor of long-term stability. Thus, Cel6A and Cel7A have comparable intrinsic stabilities, but Cel6A is much less stable in prolonged hydrolysis trials. We found that substrate association lead to increased (Cel7A) or unchanged (Cel6A) intrinsic stability and that substrate-associated (active) enzyme was less long-term stable than enzyme in pure buffer. This was particularly evident at  $T_{\text{store}} = 49$  °C for Cel7A, which was fully stable in buffer but lost one-third of the native population during 53 h of hydrolysis. This suggests that shelf life tests including so-called “accelerated stability testing”,<sup>60</sup> which are typically used to probe the robustness of industrial proteins, will tend to overestimate the stability of these cellulases. These conclusions were based on experiments with a pure cellulose substrate (Avicel), and no direct inference can be made with respect to the in situ stability of cellulases on lignocellulosic biomass. We suggest, however, that the effects seen here are the result of enzyme–cellulose interactions, which may also be relevant to more complex substrates, although other routes of inactivation may obviously be relevant or even dominant in biomass.

## AUTHOR INFORMATION

### Notes

The authors declare the following competing financial interest: Novozymes is a major enzyme-producing company.

## ACKNOWLEDGMENTS

This work was supported by the Danish Council for Strategic Research, Program Commission on Sustainable Energy and Environment (grant nos. 2104-07-0028 and 11-116772 to P.W.)

## REFERENCES

- (1) Himmel, M. E.; Ding, S. Y.; Johnson, D. K.; Adney, W. S.; Nimlos, M. R.; Brady, J. W.; Foust, T. D. Biomass recalcitrance: Engineering plants and enzymes for biofuels production. *Science* **2007**, *315*, 804–807.
- (2) Horn, S. J.; Vaaje-Kolstad, G.; Westereng, B.; Eijsink, V. G. H. Novel enzymes for the degradation of cellulose. *Biotechnol. Biofuels* **2012**, *5*.
- (3) Kostylev, M.; Wilson, D. B. Synergistic interactions in cellulose hydrolysis. *Biofuels* **2012**, *3*, 61–70.



- (4) Yang, B.; Dai, Z.; Ding, S.-Y.; Wyman, C. E. Enzymatic hydrolysis of cellulose biomass. *Biofuels* **2011**, *2*, 421–450.
- (5) Wilson, D. B. Cellulases and biofuels. *Curr. Opin. Biotechnol.* **2009**, *20*, 295–299.
- (6) Bansal, P.; Hall, M.; Realff, M. J.; Lee, J. H.; Bommarius, A. S. Modeling cellulase kinetics on lignocellulosic substrates. *Biotechnol. Adv.* **2009**, *27*, 833–848.
- (7) Bezerra, R. M. F.; Dias, A. A.; Fraga, I.; Pereira, A. N. Cellulose Hydrolysis by Cellobiohydrolase Cel7A Shows Mixed Hyperbolic Product Inhibition. *Appl. Biochem. Biotechnol.* **2011**, *165*, 178–189.
- (8) Gruno, M.; Valjamae, P.; Pettersson, G.; Johansson, G. Inhibition of the *Trichoderma reesei* cellulases by cellobiose is strongly dependent on the nature of the substrate. *Biotechnol. Bioeng.* **2004**, *86*, 503–511.
- (9) Murphy, L.; Bohlin, C.; Baumann, M. J.; Olsen, S. N.; Sorensen, T. H.; Anderson, L.; Borch, K.; Westh, P. Product inhibition of five *Hypocrea jecorina* cellulases. *Enzyme. Microb. Technol.* **2013**, *52*, 163–169.
- (10) Teugas, H.; Valjamae, P. Product inhibition of cellulases studied with <sup>14</sup>C-labeled cellulose substrates. *Biotechnol. Biofuels* **2013**, *6*, 104.
- (11) Zhang, S.; Wolfgang, D. E.; Wilson, D. B. Substrate heterogeneity causes the nonlinear kinetics of insoluble cellulose hydrolysis. *Biotechnol. Bioeng.* **1999**, *66*, 35–41.
- (12) Murphy, L.; Cruys-Bagger, N.; Damgaard, H. D.; Baumann, M. J.; Olsen, S. N.; Borch, K.; Lassen, S. F.; Sweeney, M.; Tatsumi, H.; Westh, P. Origin of Initial Burst in Activity for *Trichoderma reesei* endo-Glucanases Hydrolyzing Insoluble Cellulose. *J. Biol. Chem.* **2012**, *287*, 1252–1260.
- (13) Cruys-Bagger, N.; Elmerdahl, J.; Praestgaard, E.; Tatsumi, H.; Spodsberg, N.; Borch, K.; Westh, P. Pre-steady state kinetics for the hydrolysis of insoluble cellulose by *Trichoderma reesei* Cel7A. *J. Biol. Chem.* **2012**, *287*, 18451–18458.
- (14) Jalak, J.; Kurashin, H.; Teugas, H.; Valjamae, P. Endo-exo synergism in cellulase hydrolysis revisited. *J. Biol. Chem.* **2012**, *287*, 28802–28815.
- (15) Jalak, J.; Valjamae, P. Mechanism of Initial Rapid Rate Retardation in Cellobiohydrolase Catalyzed Cellulose Hydrolysis. *Biotechnol. Bioeng.* **2010**, *106*, 871–883.
- (16) Kurasin, M.; Valjamae, P. Processivity of Cellobiohydrolases Is Limited by the Substrate. *J. Biol. Chem.* **2011**, *286*, 169–177.
- (17) Kipper, K.; Valjamae, P.; Johansson, G. Processive action of cellobiohydrolase Cel7A from *Trichoderma reesei* is revealed as 'burst' kinetics on fluorescent polymeric model substrates. *Biochem. J.* **2005**, *385*, 527–535.
- (18) Praestgaard, E.; Elmerdahl, J.; Murphy, L.; Nymand, S.; McFarland, K. C.; Borch, K.; Westh, P. A kinetic model for the burst phase of processive cellulases. *FEBS J.* **2011**, *278*, 1547–1560.
- (19) Harkins, T. T.; Lindsley, J. E. Pre-steady-state analysis of ATP hydrolysis by *Saccharomyces cerevisiae* DNA topoisomerase II. I. A DNA-dependent burst in ATP hydrolysis. *Biochemistry* **1998**, *37*, 7292–7298.
- (20) Knight, C. G. Active-site titration of peptidases. In *Proteolytic Enzymes: Aspartic and Metallo Peptidases*; Barrett, A. J., Ed.; Academic Press: San Diego, 1995; Vol. 248, pp 85–101.
- (21) Takahashi, K.; Weiner, H. Nicotinamide adenine-dinucleotide activation of the esterase reaction of horse liver aldehyde dehydrogenase. *Biochemistry* **1981**, *20*, 2720–2726.
- (22) Howell, J. A.; Mangat, M. Enzyme deactivation during cellulose hydrolysis. *Biotechnol. Bioeng.* **1978**, *20*, 847–863.
- (23) Monschein, M.; Reisinger, C.; Nidetzky, B. Enzymatic hydrolysis of microcrystalline cellulose and pretreated wheat straw: A detailed comparison using convenient kinetic analysis. *Bioresour. Technol.* **2013**, *128*, 679–687.
- (24) Olsen, S. N.; Lumby, E.; McFarland, K.; Borch, K.; Westh, P. Kinetics of Enzymatic High-Solid Hydrolysis of Lignocellulosic Biomass Studied by Calorimetry. *Appl. Biochem. Biotechnol.* **2011**, *163*, 626–635.
- (25) Bubner, P.; Plank, H.; Nidetzky, B. Visualizing cellulase activity. *Biotechnol. Bioeng.* **2013**, *110*, 1529–1549.
- (26) Cheng, G.; Liu, Z. L.; Murton, J. K.; Jablin, M.; Dubey, M.; Majewski, J.; Halbert, C.; Browning, J.; Ankner, J.; Akgun, B.; Wang, C.; Esker, A. R.; Sale, K. L.; Simmons, B. A.; Kent, M. S. Neutron Reflectometry and QCM-D Study of the Interaction of Cellulases with Films of Amorphous Cellulose. *Biomacromolecules* **2011**, *12*, 2216–2224.
- (27) Maurer, S. A.; Bedbrook, C. N.; Radke, C. J. Competitive Sorption Kinetics of Inhibited Endo- and Exoglucanases on a Model Cellulose Substrate. *Langmuir* **2012**, *28*, 14598–14608.
- (28) Turon, X.; Rojas, O. J.; Deinhammer, R. S. Enzymatic kinetics of cellulose hydrolysis: A QCM-D study. *Langmuir* **2008**, *24*, 3880–3887.
- (29) Ma, A. Z.; Hu, Q.; Qu, Y. B.; Bai, Z. H.; Liu, W. F.; Zhuang, G. Q. The enzymatic hydrolysis rate of cellulose decreases with irreversible adsorption of cellobiohydrolase I. *Enzyme. Microb. Technol.* **2008**, *42*, 543–547.
- (30) Kyriacou, A.; Neufeld, R. J.; Mackenzie, C. R. Reversibility and competition in the adsorption of *trichoderma-reesei* cellulase components. *Biotechnol. Bioeng.* **1989**, *33*, 631–637.
- (31) Beldman, G.; Voragen, A. G. J.; Rombouts, F. M.; Searle van Leeuwen, M. F.; Pilnik, W. Adsorption and Kinetic-Behavior of Purified Endoglucanases and Exoglucanases from *Trichoderma viride*. *Biotechnol. Bioeng.* **1987**, *30*, 251–257.
- (32) Nidetzky, B.; Steiner, W.; Claeysens, M. Cellulose hydrolysis by cellulases from *Trichoderma reesei*: adsorptions of two cellobiohydrolases, two endocellulases and their core protein on filterpaper, and their relation to hydrolysis. *Biochem. J.* **1994**, *303*, 817–823.
- (33) Bothwell, M. K.; Wilson, D. B.; Irwin, D. C.; Walker, L. P. Binding reversibility and surface exchange of *Thermomonospora fusca* E-3 and E-5 and *Trichoderma reesei* CBHI. *Enzyme. Microb. Technol.* **1997**, *20*, 411–417.
- (34) Palonen, H.; Tenkanen, M.; Linder, M. Dynamic interaction of *Trichoderma reesei* cellobiohydrolases Cel6A and Cel7A and cellulose at equilibrium and during hydrolysis. *Appl. Environ. Microbiol.* **1999**, *65*, 5229–5233.
- (35) Bentaleb, A.; Abele, A.; Haikel, Y.; Schaaf, P.; Voegel, J. C. FTIR-ATR and radiolabeling study of the adsorption of ribonuclease A onto hydrophilic surfaces: Correlation between the exchange rate and the interfacial denaturation. *Langmuir* **1998**, *14*, 6493–6500.
- (36) Norde, W. Adsorption of proteins from solution at the solid-liquid interface. *Adv. Colloid Interface Sci.* **1986**, *25*, 267–340.
- (37) Norde, W.; Anusiem, A. C. I. Adsorption, desorption and readsorption of proteins on solid-surfaces. *Colloids Surf.* **1992**, *66*, 73–80.
- (38) Wertz, C. F.; Santore, M. M. Effect of surface hydrophobicity on adsorption and relaxation kinetics of albumin and fibrinogen: Single-species and competitive behavior. *Langmuir* **2001**, *17*, 3006–3016.
- (39) Teeri, T. T. Crystalline cellulose degradation: New insight into the function of cellobiohydrolases. *Trends Biotechnol.* **1997**, *15*, 160–167.
- (40) Ganner, T.; Bubner, P.; Eibinger, M.; Mayrhofer, C.; Plank, H.; Nidetzky, B. Dissecting and Reconstructing Synergism in situ visualization of cooperativity among cellulases. *J. Biol. Chem.* **2012**, *287*, 43215–43222.
- (41) Hall, M.; Bansal, P.; Lee, J. H.; Realff, M. J.; Bommarius, A. S. Cellulose crystallinity - a key predictor of the enzymatic hydrolysis rate. *FEBS J.* **2010**, *277*, 1571–1582.
- (42) Park, S.; Baker, J. O.; Himmel, M. E.; Parilla, P. A.; Johnson, D. K. Cellulose crystallinity index: measurement techniques and their impact on interpreting cellulase performance. *Biotechnol. Biofuels* **2010**, *3*, 10.
- (43) Boer, H.; Koivula, A. The relationship between thermal stability and pH optimum studied with wild-type and mutant *Trichoderma reesei* cellobiohydrolase Cel7A. *Eur. J. Biochem.* **2003**, *270*, 841–848.
- (44) Wu, I.; Arnold, F. H. Engineered thermostable fungal Cel6A and Cel7A cellobiohydrolases hydrolyze cellulose efficiently at elevated temperatures. *Biotechnol. Bioeng.* **2013**, *110*, 1874–1883.

(45) Baumann, M. J.; Borch, K.; Westh, P. Xylan oligosaccharides and cellobiohydrolase I (TrCel7A) interaction and effect on activity. *Biotechnol. Biofuels* **2011**, *4*, 45.

(46) Murphy, L.; Baumann, M. J.; Borch, K.; Sweeney, M.; Westh, P. An enzymatic signal amplification system for calorimetric studies of cellobiohydrolases. *Anal. Biochem.* **2010**, *404*, 140–148.

(47) Gasteiger, E.; Gattiker, A.; Hoogland, C.; Ivanyi, I.; Appel, R. D.; Bairoch, A. ExPASy: the proteomics server for in-depth protein knowledge and analysis. *Nucleic Acids Res.* **2003**, *31*, 3784–3788.

(48) Jelesarov, I.; Bosshard, H. R. Isothermal titration calorimetry and differential scanning calorimetry as complementary tools to investigate the energetics of biomolecular recognition. *J. Mol. Recognit.* **1999**, *12*, 3–18.

(49) Murphy, L.; Borch, K.; McFarland, K. C.; Bohlin, C.; Westh, P. A calorimetric assay for enzymatic saccharification of biomass. *Enzyme. Microb. Technol.* **2010**, *46*, 141–146.

(50) Haynes, C. A.; Norde, W. Structures and stabilities of adsorbed proteins. *J. Colloid Interface Sci.* **1995**, *169*, 313–328.

(51) Kleijn, M.; Norde, W. The adsorption of proteins from aqueous solution on solid surfaces. *Heterogen. Chem. Rev.* **1995**, *2*, 157–172.

(52) Steadman, B. L.; Thompson, K. C.; Middaugh, C. R.; Matsuno, K.; Vrona, S.; Lawson, E. Q.; Lewis, R. V. The effects of surface-adsorption on the thermal-stability of proteins. *Biotechnol. Bioeng.* **1992**, *40*, 8–15.

(53) Lumry, R.; Eyring, H. Conformation changes of proteins. *J. Phys. Chem.* **1954**, *58*, 110–120.

(54) Chi, E. Y.; Krishnan, S.; Randolph, T. W.; Carpenter, J. F. Physical stability of proteins in aqueous solution: Mechanism and driving forces in nonnative protein aggregation. *Pharm. Res.* **2003**, *20*, 1325–1336.

(55) Chi, E. Y.; Krishnan, S.; Kendrick, B. S.; Chang, B. S.; Carpenter, J. F.; Randolph, T. W. Roles of conformational stability and colloidal stability in the aggregation of recombinant human granulocyte colony-stimulating factor. *Protein Sci.* **2003**, *12*, 903–913.

(56) Sanchez-Ruiz, J. M. Protein kinetic stability. *Biophys. Chem.* **2010**, *148*, 1–15.

(57) Sanchezruiz, J. M. Theoretical-analysis of lumry-eyring models in differential scanning calorimetry. *Biophys. J.* **1992**, *61*, 921–935.

(58) Koivula, A.; Ruohonen, L.; Wohlfahrt, G.; Reinikainen, T.; Teeri, T. T.; Piens, K.; Claeysens, M.; Weber, M.; Vasella, A.; Becker, D.; Sinnott, M. L.; Zou, J. Y.; Kleywegt, G. J.; Szardenings, M.; Stahlberg, J.; Jones, T. A. The active site of cellobiohydrolase Cel6A from *Trichoderma reesei*: The roles of aspartic acids D221 and D175. *J. Am. Chem. Soc.* **2002**, *124*, 10015–10024.

(59) Divne, C.; Stahlberg, J.; Teeri, T. T.; Jones, T. A. High-resolution crystal structures reveal how a cellulose chain is bound in the 50 angstrom long tunnel of cellobiohydrolase I from *Trichoderma reesei*. *J. Mol. Biol.* **1998**, *275*, 309–325.

(60) Franks, F. Accelerated stability testing of bioproducts - attractions and pitfalls. *Trends Biotechnol.* **1994**, *12*, 114–117.



Reversibility of Substrate Adsorption for the  
Cellulases Cel7A, Cel6A and Cel7B from  
*Hypocrea jecorina*

---

VI





## Reversibility of Substrate Adsorption for the Cellulases Cel7A, Cel6A, and Cel7B from *Hypocrea jecorina*

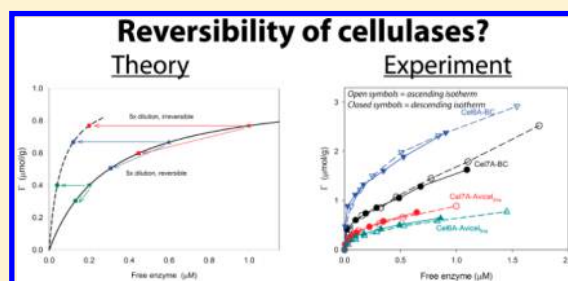
Vanessa O. A. Pellegrini,<sup>†,‡</sup> Nina Lei,<sup>†</sup> Madhuri Kyasaram,<sup>†</sup> Johan P. Olsen,<sup>†</sup> Silke F. Badino,<sup>†</sup> Michael S. Windahl,<sup>†,§</sup> Francieli Colussi,<sup>†</sup> Nicolaj Cruys-Bagger,<sup>†</sup> Kim Borch,<sup>§</sup> and Peter Westh<sup>\*,†</sup>

<sup>†</sup>Research Unit for Functional Biomaterials, NSM, Roskilde University, 1 Universitetsvej, Build. 18.1, DK-4000 Roskilde, Denmark

<sup>‡</sup>Department of Physics and Informatics, University of São Paulo, São Carlos/SP, Brazil

<sup>§</sup>Novozymes A/S, Krogshøjvej 36, DK-2880 Bagsværd, Denmark

**ABSTRACT:** Adsorption of cellulases on the cellulose surface is an integral part of the catalytic mechanism, and a detailed description of the adsorption process is therefore required for a fundamental understanding of this industrially important class of enzymes. However, the mode of adsorption has proven intricate, and several key questions remain open. Perhaps most notably it is not clear whether the adsorbed enzyme is in dynamic equilibrium with the free population or irreversibly associated with no or slow dissociation. To address this, we have systematically investigated adsorption reversibility for two cellobiohydrolases (Cel7A and Cel6A) and one endoglucanase (Cel7B) on four types of pure cellulose substrates. Specifically, we monitored dilution-induced release of adsorbed enzyme in samples that had previously been brought to a steady state (constant concentration of free enzyme). In simple dilution experiments (without centrifugation), the results consistently showed full reversibility. In contrast to this, resuspension of enzyme–substrate pellets separated by centrifugation showed extensive irreversibility. We conclude that these enzymes are in a dynamic equilibrium between free and adsorbed states but suggest that changes in the physical properties of cellulose caused by compaction of the pellet hampers subsequent release of adsorbed enzyme. This latter effect may be pertinent to both previous controversies in the literature on adsorption reversibility and the development of enzyme recycling protocols in the biomass industry.



### INTRODUCTION

Enzymatic hydrolysis of cellulose is an example of heterogeneous catalysis. It is an atypical example in the sense that it involves a diffusive catalyst (the cellulase) and one diffusive reactant (water), while the other reactant (cellulose) makes up the solid sorbent. Evidently, adsorption of the enzyme must precede catalysis, and many studies have addressed the adsorption of cellulases or their carbohydrate binding modules (CBMs) on different types of celluloses and biomass, both from kinetic and equilibrium points of view (see refs 1 and 2 for reviews). This work has uncovered intricate modes of interaction, and several key questions remain unresolved. Perhaps most noticeably, it is not clear whether adsorption is reversible or not. This question has a number of important ramifications ranging from the feasibility of enzyme recycling in industrial applications to strategies for kinetic modeling the enzymatic process. Regarding the latter, any model must in some way account for the adsorption process as an integral part of the catalytic mechanism, and modeling is made difficult if this step is poorly understood. The controversy regarding reversibility may be illustrated by work on the cellobiohydrolase Cel7A, the most thoroughly studied cellulase. Some reports have concluded that this enzyme (or its carbohydrate binding module, CBM) adsorbs irreversibly<sup>3,4</sup> or almost irreversibly<sup>5</sup> to pure cellulose. Other works have reached the opposite

conclusion<sup>6–9</sup> and suggested full reversibility, while still other reports have concluded that the interaction is “partially reversible”.<sup>10,11</sup> The molecular origin of the observed irreversibility remains to be fully elucidated, but some reports have suggested that it relies on either strong binding of the CBM or conformational changes in the enzyme.<sup>5,10–12</sup> Different degrees of reversibility, which have also been found for other cellulases than Cel7A,<sup>3,8,12–16</sup> likely relies in part on experimental challenges as well as differences in the structure and properties of the investigated substrates, but in some cases it is also related to vague definitions of “reversibility”. From a stringent point of view, a reversible process is constituted of a succession of equilibrium states,<sup>17</sup> i.e., steps for which  $\Delta G = 0$ . Changes along any other path are irreversible. One consequence of this is that any spontaneous process ( $\Delta G < 0$ ) is irreversible. This is true even if the process can be readily reverted in a subsequent step where conditions (temperature, pressure, or composition) are changed to favor the initial state. In protein adsorption studies, this stringent definition is not normally used and probably not practical. The pivotal point here is whether a dynamic equilibrium is established within the

Received: June 27, 2014

Revised: September 9, 2014

Published: October 3, 2014

experimental time frame and not how it is reached. Consequently, experimental efforts usually focus on how readily adsorbed enzyme can be resolubilized for example following dilution with buffer. In this sense, full reversibility is achieved when the adsorption isotherm measured upon gradual increase of the enzyme concentration (the so-called ascending isotherm) superimposes the isotherm obtained by sequentially diluting a saturated sorbent (the descending isotherm).<sup>18</sup> Rigorously, superposition of the ascending and descending isotherms signifies the absence of hysteresis and not reversibility in the thermodynamic sense, but we will henceforth use the latter term (reversibility) to be in line with the vast majority of earlier literature in the area. This and its relationship to the current experiments are further illustrated in Figure 1.

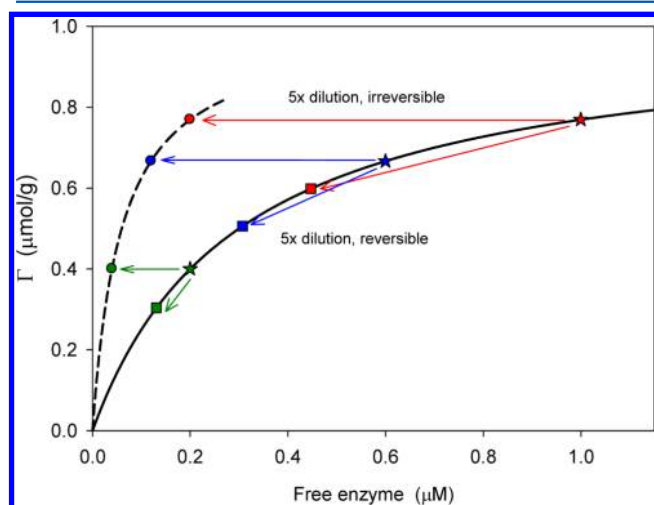


**Figure 1.** Illustration of how one-step dilution experiments with samples of different initial enzyme concentrations can be interpreted with respect to adsorption reversibility. The solid black line represents a Langmuir isotherm, eq 1, with the parameters  $\Gamma_{\max} = 1 \mu\text{mol/g}$  and  $K_d = 0.3 \mu\text{M}$ . We consider three samples (star-shaped symbols) with initial free enzyme concentrations of respectively  $1 \mu\text{M}$  (red),  $0.6 \mu\text{M}$  (blue), and  $0.2 \mu\text{M}$  (green). The substrate load in this example is  $2 \text{ g/L}$ , and all samples are diluted 5-fold. If the adsorption is irreversible, dilution will shift the point horizontally to the left (circles) and define a descending isotherm (dashed line), which is different from the ascending isotherm. For reversible adsorption, the points (squares) will be located on a lower position of the original isotherm, and the ascending and descending isotherms overlap. See text for more details.

In the current work we have investigated the reversibility of cellulose–cellulase interactions through comparisons of ascending and descending binding isotherms. We found that three of the most studied cellulases, Cel7A, Cel 6A, and Cel7B from *Hypocrea jecorina* (*Trichoderma reesei*), showed essentially full reversibility on different types of pure cellulose in simple dilution experiments. This suggests the interaction can be characterized as a dynamic equilibrium between a bound and a free enzyme population—at least within the time scales and concentration ranges studied here. We also found that centrifugation of the enzyme–cellulose complex caused significant loss of reversibility, and we speculate that this can be one of the reasons for the divisive literature on cellulase adsorption reversibility.

## EXPERIMENTAL SECTION

**Materials.** All experiments were conducted in  $50 \text{ mM}$  acetate buffer, pH 5.0. Adsorption and dilution measurements were made in either  $2 \text{ mL}$  “Protein LoBind” Eppendorf tubes (Eppendorf AG, Hamburg, Germany) or  $15 \text{ mL}$  “SuperClear” centrifuge tubes (VWR, Leuven, Belgium). These vials were chosen after control experiments (without substrate) had shown that their adsorption of the investigated cellulases was small compared to the experimental scatter (in contrast to a number of other tested vials). The enzymes Cel7A, Cel6A, and Cel7B from *Hypocrea jecorina* were produced heterologously in *Aspergillus oryzae* as described previously.<sup>19–22</sup> Bacterial cellulose (BC) from *Acetobacter xylinum* was purified from the commercial product “Nata de Coco” (Monika, Fitrite Incorporated, Novaliches Quezon City, Philippines) using the principles of Våljamäe et al.<sup>23</sup> as described elsewhere.<sup>24</sup> Three other types of substrate were made from Avicel PH-101 (Sigma-Aldrich). Avicel consists of microcrystalline cellulose with a crystallinity index  $I_{\text{Cr}}$  of  $0.55–0.70$ <sup>25,26</sup> and a typical particle size (reported by the manufacturer) of  $50 \mu\text{m}$ . One Avicel-based substrate, henceforth called Avicel<sub>coarse</sub>, was made simply by suspending the powder in buffer. As we were interested in possible effects of particle size, we used a coaxial disperser (IKA ultra-Turrax T8, IKA-Werke GmbH, Staufen, Germany) to prepare Avicel suspensions with smaller particles. Specifically,  $10 \text{ g/L}$  Avicel<sub>coarse</sub> in buffer was cooled on ice and dispersed for  $5 \text{ min}$  at medium intensity ( $12\,000 \text{ rpm}$ ). This dispersion has a nominal ultimate fineness around  $10 \mu\text{m}$ , and in the following we will call the dispersed substrate, Avicel<sub>fine</sub>. The third substrate based on Avicel PH-101 was regenerated amorphous cellulose (RAC). This was prepared according to a slightly modified<sup>27</sup> version of the method introduced by Zhang and Lynd.<sup>28</sup> All four substrate preparations have previously been characterized<sup>29</sup> with respect to their  $I_{\text{Cr}}$  and degree of polymerization (DP) using respectively solid-state  $^{13}\text{C}$  cross-polarization/magic angle spinning (CP/MAS NMR)<sup>30</sup> and the phenol–sulfuric acid/bicinchoninate method.<sup>31</sup> The crystallinity index was  $0.87$  for BC,  $0.60$  for Avicel<sub>coarse</sub>,  $0.57$  for Avicel<sub>fine</sub>, and  $<0.05$  for RAC. This suggests that RAC is essentially amorphous and that coaxial dispersion of Avicel has limited effect on its crystallinity. The number-average degree of polymerization fell in the range  $180–240$  glucopyranoside units per cellulose chain for all four substrate preparations studied here.

**Enzyme Concentration.** The concentration of enzyme in stock solutions was determined from  $\text{OD}_{280 \text{ nm}}$  measurements using the extinction coefficients  $86.8 \text{ mM}^{-1} \text{ cm}^{-1}$  for Cel7A,  $96.6 \text{ mM}^{-1} \text{ cm}^{-1}$  for Cel6A, and  $72.8 \text{ mM}^{-1} \text{ cm}^{-1}$  for Cel7B, which were calculated from the primary structure.<sup>32</sup> Measurements of  $\text{OD}_{280 \text{ nm}}$  were not sufficiently sensitive for adsorption reversibility experiments, and instead we measured intrinsic fluorescence at  $280 \text{ nm}/345 \text{ nm}$  (excitation/emission) in a Shimadzu RF-5301PC fluorometer and quantified the output against standard curves made daily in the same buffer.

**Standard Dilution Assay.** Reversibility of enzyme–substrate interactions was tested in a standard dilution assay, where substrate suspensions in eight vials were added enough enzyme stock to yield total enzyme concentrations ( $E_0$ ) of respectively  $0, 0.25, 0.50, 0.75, 1.00, 1.50, 2.00,$  and  $3.00 \mu\text{M}$ . The load of substrate,  $S_0$  (in  $\text{g/L}$ ), was the same in the eight samples but varied between different trials and for the different types of substrate. Thus, based on preliminary measurements,  $S_0$  was adjusted so that the ascending binding isotherm rolled off toward saturation for the highest studied values of  $E_0$ . Typical values for  $S_0$  (after the addition of enzyme stock) were  $5 \text{ g/L}$  for Avicel<sub>coarse</sub>,  $2 \text{ g/L}$  for Avicel<sub>fine</sub>, and  $0.5 \text{ g/L}$  for BC and RAC. The total sample volume was  $2000 \mu\text{L}$ . After the enzyme was added, the samples were mixed on a rotating wheel at  $30 \text{ rpm}$  for  $30 \text{ min}$  at room temperature ( $24 \pm 1 \text{ }^\circ\text{C}$ ). The choice of  $30 \text{ min}$  contact time was based on initial measurements of the adsorption of Cel7A to all four substrates, which showed that the concentration of free enzyme leveled off to a constant value within  $3–15 \text{ min}$  (depending on the substrate load and enzyme concentration). Based on this, it was concluded that  $30 \text{ min}$  contact time is long enough to establish a steady state condition (and short enough to ensure limited conversion

of substrate; see below). Upon removal from the wheel, the suspensions were kept homogeneous through manual agitation, and a 500  $\mu\text{L}$  subset was retrieved. The subset was centrifuged for 3 min at 14000g, and the concentration of enzyme in the supernatant was measured and used as the free enzyme concentration before dilution,  $E_{\text{free}}^{\text{ascen}}$  (see eq 4). The remaining 1500  $\mu\text{L}$  was diluted with pure buffer (either 10 or 1.5 mL) and put back on the rotating wheel for 60 min. Finally, the concentration of enzyme in the supernatant of the diluted sample was measured fluorometrically and used as the free enzyme after dilution,  $E_{\text{free}}^{\text{descend}}$  (see eq 5).

In addition to these buffer-dilution experiments we also tested reversibility of Cel7A/Avicel<sub>fine</sub> interactions in experiments where systems in steady state (i.e., after 30 min contact time) were perturbed by the addition of either more enzyme or substrate. The procedure was the same as above except that instead of diluting with pure buffer after 30 min contact time, we either added 100  $\mu\text{L}$  of 10  $\mu\text{M}$  Cel7A stock or 300  $\mu\text{L}$  of 2 g/L Avicel<sub>fine</sub>.

**Dilution Assay with Centrifugation.** In the standard dilution assay described above, centrifugation is only used to isolate supernatant (before or after dilution) for measurements of free enzyme concentrations. The enzyme–substrate complex is *not* exposed to centrifugation before the dilution. This is in contrast to many earlier works, which have assessed reversibility by resuspending pelleted cellulose with adsorbed enzyme. To assess possible effects of this, we also tested adsorption reversibility in pellet separated by centrifugation. The procedure followed the standard assay to the point where 2000  $\mu\text{L}$  samples had been mixed for 30 min on the rotating wheel. The samples were then centrifuged for 3 min at 4000g, and the supernatant was gently removed and tested for its concentration of enzyme ( $E_{\text{free}}^{\text{ascen}}$ ). The pellet was resuspended in 10 mL of buffer, equilibrated for 60 min on the rotating wheel, and tested for free enzyme ( $E_{\text{free}}^{\text{descend}}$ ) as in the standard assay. We note that ascending isotherms produced either with or without centrifugation follow exactly the same protocol (differences only occur in the subsequent dilution steps). As a result, assessment of effects of centrifugation is based on pairs of identical samples diluted either with or without centrifugation. When such pairs are prepared with different enzyme concentrations the effect can be evaluated over the whole isotherm (cf. Figure 1).

**Ion Chromatography.** To assess the degree of cellulose conversion, we used ion chromatography with pulsed amperometric detection. Concentrations of soluble sugars were measured in supernatants from samples with the highest enzyme concentration (3  $\mu\text{M}$ ) in an ICS-5000 ion chromatograph equipped with a CarboPac PA-10 column and an electrochemical detector (Termo Fisher Scientific Waltham, MA). Samples were eluted with a multistep gradient with 50 mM NaOH (0–4 min), 100 mM sodium acetate + 90 mM NaOH (4–28 min), 450 mM sodium acetate + 200 mM NaOH (28–29 min), and 50 mM NaOH (29–35 min). The results were quantified against standards for glucose, cellobiose, and celotriose run daily.

**Theory.** To quantitatively illustrate reversibility in dilution experiments, we use the Langmuir isotherm for independent and thermodynamically identical sites. This simple isotherm has often been used to characterize cellulose–cellulase interactions, and we therefore use it as an example here. We stress, however, that the general conclusions regarding shifts or superposition of ascending and descending isotherms, which are discussed in this section, are valid for any adsorption mechanism.

The Langmuir isotherm may be written

$$\Gamma = \Gamma_{\text{max}} \frac{E_{\text{free}}}{K_d + E_{\text{free}}} \quad (1)$$

where  $\Gamma_{\text{max}}$  and  $K_d$  are the usual Langmuir parameters, i.e., respectively saturation coverage in  $\mu\text{mol}$  of enzyme bound per g of cellulose at saturation and the dissociation constant (in  $\mu\text{M}$ ). The variables  $\Gamma$  and  $E_{\text{free}}$  are respectively the substrate coverage ( $\mu\text{mol}$  of enzyme/g) and the free enzyme concentration (in  $\mu\text{M}$ ).

In the current context we are interested in dilution experiments, i.e., perturbation of an established adsorption equilibrium by the addition of one dose of buffer. The total concentration of enzyme in the diluted sample,  $E_0$ , can be readily calculated from the original and added volumes, and we may write a mass conservation for enzyme as

$$E_0 = E_{\text{free}} + E_{\text{bound}} \quad (2)$$

In eq 2,  $E_{\text{bound}}$  is the molar concentration of bound enzyme after dilution and it may be expressed  $E_{\text{bound}} = \Gamma S_0$ , where  $S_0$  is the load of substrate (in g/L). If we insert this expression into eq 2 and combine with eq 1, we get a quadratic equation in  $E_{\text{free}}$  that relates the free enzyme concentration and the parameters  $K_d$ ,  $\Gamma_{\text{max}}$ ,  $E_0$ , and  $S_0$ , which are all known in a dilution experiment. The (physically meaningful) solution may be written

$$E_{\text{free}} = \frac{(K_d + \Gamma_{\text{max}} S_0 - E_0) - \sqrt{(K_d + \Gamma_{\text{max}} S_0 - E_0)^2 + 4E_0 K_d}}{2} \quad (3)$$

Figure 1 exemplifies how eq 3 can be used to illustrate adsorption reversibility for one of the experimental protocols used here (simple dilution without centrifugation). Thus, it is shown how  $E_{\text{free}}$  and  $\Gamma$  would change upon a 5-fold dilution in the two extreme cases of either fully reversible or fully irreversible adsorption. In the example in Figure 1, the full line is the (ascending) isotherm calculated from eq 1 using  $\Gamma_{\text{max}} = 1 \mu\text{mol/g}$  and  $K_d = 0.3 \mu\text{M}$ , which are typical values for the adsorption of Cel7A on Avicel.<sup>33</sup> We now consider dilution of three equilibrated samples on this isotherm (indicated by stars) with initial free enzyme concentrations of respectively 1  $\mu\text{M}$  (red), 0.6  $\mu\text{M}$  (blue), and 0.2  $\mu\text{M}$  (green). In this example the load of substrate was 2 g/L. If the interaction is irreversible, dilution of these samples will not change  $\Gamma$  (no release of enzyme). Hence, the only result of the dilution is a 5-fold reduction of  $E_{\text{free}}$  and this is indicated by the horizontal arrows and circles in the figure. If this is done for a number of samples with different initial  $E_{\text{free}}$ , the shifted points will define a new line (dashed line in Figure 1), which is the descending isotherm for a 5-fold dilution experiment in the case of irreversible adsorption. If, on the other hand, the adsorption is fully reversible,  $E_{\text{free}}$  and  $\Gamma$  after dilution can be calculated from eqs 1 and 3. This is illustrated by sloping arrows and squares in Figure 1, and the most important result is that dilution establishes a new equilibrium condition at a lower position of the original (ascending) isotherm. If the descending isotherm falls between the two extremes in Figure 1, the adsorption is often described as “partially reversible”. We will use this one-step dilution principle for several samples with different  $E_{\text{free}}$  to assess reversibility.

We emphasize that the overall interpretation of superposition and left shift, exemplified here for Langmuir adsorption, is valid regardless of the mode of interaction, and in the current work we will focus on an empirical analysis of reversibility based on these principles. Attempts to resolve the relevance of different adsorption models or the associated mathematical expressions for various cellulase–cellulose systems are beyond the current scope.

## RESULTS

The coverage in  $\mu\text{mol}$  of enzyme/g of cellulose before dilution,  $\Gamma_{\text{ascen}}$ , was calculated as

$$\Gamma_{\text{ascen}} = \frac{E_0 - E_{\text{free}}^{\text{ascend}}}{S_0} \quad (4)$$

where  $E_{\text{free}}^{\text{ascend}}$  is the measured free enzyme concentration before dilution (see methods), and  $E_0$  and  $S_0$  are the total loads of respectively enzyme ( $\mu\text{M}$ ) and cellulose (g/L). The coverage after dilution,  $\Gamma_{\text{descend}}$  (descending isotherm), was calculated from the measured free enzyme concentration,  $E_{\text{free}}^{\text{descend}}$ , and three volumes. These are the initial sample volume,  $V_0$ , the volume of the subset,  $V_R$ , retrieved for measurement of  $E_{\text{free}}^{\text{ascend}}$  in the standard dilution assay, and the volume of buffer added in the dilution step,  $V_{\text{add}}$ . In the analysis of data from the assay



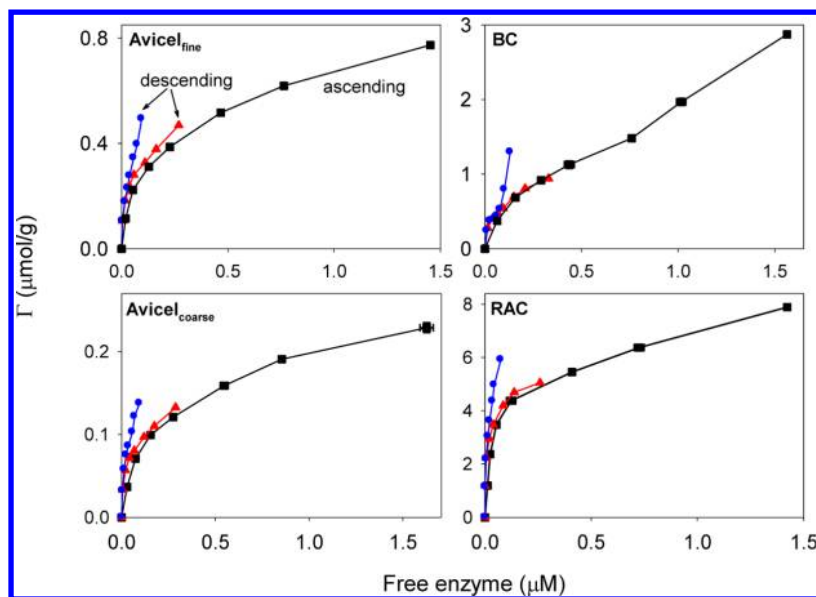


**Figure 2.** Adsorption reversibility for the cellobiohydrolase Cel7A on four kinds of cellulose: Avicel<sub>fine</sub>, BC, Avicel<sub>coarse</sub>, and RAC. Black squares show data for ascending isotherms,  $\Gamma_{\text{ascend}}$ . As the initial conditions were identical in experiments with and without centrifugation, points for the ascending isotherms represent the average of these experiments with (bidirectional) standard deviations. In many cases the standard deviations are comparable to the size of the symbol and difficult to see. Blue circles and red triangles identify descending isotherms,  $\Gamma_{\text{descend}}$ , for assays with and without centrifugation, respectively. The key observation is that  $\Gamma_{\text{descend}}$  superimposes  $\Gamma_{\text{ascend}}$  for the simple assay without centrifugation (red) while  $\Gamma_{\text{descend}}$  is shifted to the left when the enzyme–substrate complex was pelleted by centrifugation (blue).

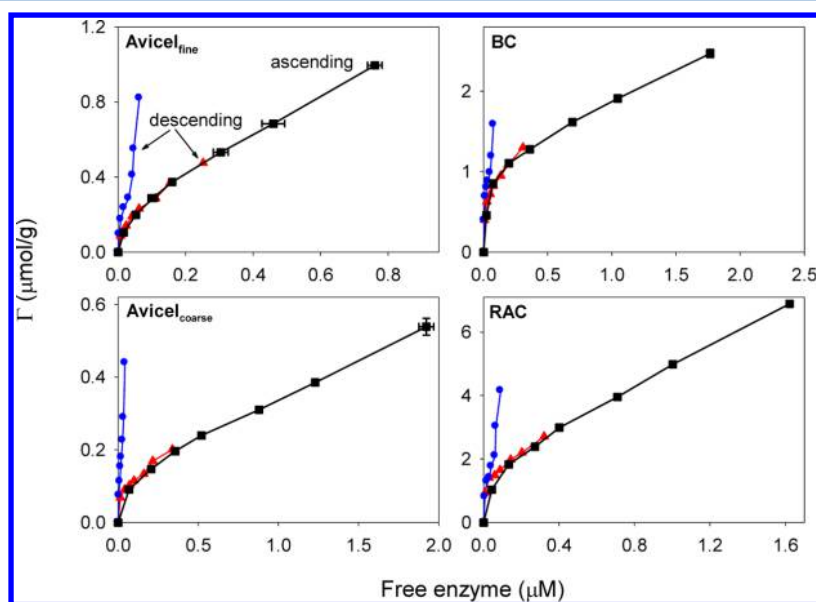


**Figure 3.** Adsorption reversibility for the cellobiohydrolase Cel6A on four kinds of cellulose: Avicel<sub>fine</sub>, BC, Avicel<sub>coarse</sub>, and RAC. The symbols are the same as in Figure 2.

with centrifugation we assumed that all cellulose was precipitated and that the entire bulk phase is removed with the supernatant (i.e., we neglected the small amount of buffer between the precipitated cellulose particles). Under these conditions  $\Gamma_{\text{descend}}$  in the assay with centrifugation may be expressed as

$$\Gamma_{\text{descend}} = \frac{(E_0 - E_{\text{free}}^{\text{ascend}})V_0 - E_{\text{free}}^{\text{descend}}(V_0 + V_{\text{add}})}{S_0V_0} \quad (5)$$

In the standard dilution assay (without centrifugation) some cellulose is removed from the sample together with the subset

used for determination of  $E_{\text{free}}^{\text{ascend}}$ , and the expression for  $\Gamma_{\text{descend}}$  becomes

$$\Gamma_{\text{descend}} = \frac{(V_0 - V_R)E_0 - (V_0 - V_R + V_{\text{add}})E_{\text{free}}^{\text{ascend}}}{S_0(V_0 - V_R)} \quad (6)$$

We calculated  $\Gamma_{\text{ascend}}$  and  $\Gamma_{\text{descend}}$  according to eqs 4–6 for Cel7A and Cel6A on all four substrates, and for Cel7B on RAC, Avicel<sub>fine</sub>, and Avicel<sub>coarse</sub> (the Cel7B-BC system was not investigated as Cel7B is known to have low activity against this substrate), and plotted these functions against the free concentration of Cel7A (Figure 2), Cel6A (Figure 3), and Cel7B (Figure 4). In these figures each panel shows results for

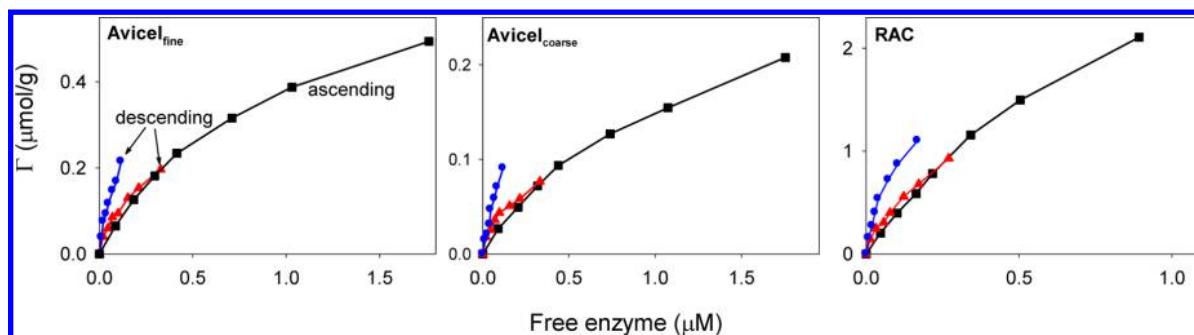


**Figure 4.** Adsorption reversibility for the endoglucanase Cel7B on three types of cellulose: Avicel<sub>fine</sub>, Avicel<sub>coarse</sub>, and RAC. The symbols are the same as in Figure 2.

one type of substrate. In Figures 2–4 the volumes  $V_0$ ,  $V_R$ , and  $V_{add}$  were respectively 2.00 mL, 0.50 mL, and 10 mL, and this corresponds to a 5-fold dilution of the substrate in the experiments with centrifugation and a 6.7-fold dilution of the substrate in the simple dilution experiments. We also tested reversibility at moderate dilution levels for selected enzyme–substrate systems. In this case we only used the simple dilution protocol (no centrifugation), and the volumes  $V_0$ ,  $V_R$ , and  $V_{add}$  were respectively 2.00 mL, 0.50 mL, and 1.50 mL (corresponding to a 2-fold dilution of the substrate).

Some noticeable trends were found by comparing the ascending and descending isotherms in Figures 2–4. Thus, all descending isotherms from the simple dilution assay (red triangles) superimposed the ascending isotherms (black squares). This signifies dynamic equilibrium between the adsorbed and free enzyme populations for the 11 investigated systems (cf. Figure 1). In contrast to this, descending isotherms from the assay using resuspension of centrifuged pellet (blue circles) were consistently steeper (i.e., shifted to the left) compared to the corresponding ascending curves (black). As illustrated in Figure 1, this implies (partial) irreversibility of the adsorption process, when the pellet had been separated by centrifugation.

The degree of reversibility in the assay with centrifugation varied for the three investigated enzymes. To assess this we first note that following centrifugation, essentially all free enzyme is removed with the supernatant before the pellet is resuspended. This means that in contrast to the example in Figure 1, the descending isotherm for a fully irreversible interaction will overlay the ordinate. (If there is no dissociation in the diluted sample, the free enzyme concentration will be zero except from a small contribution due to imperfect removal of the supernatant.) This is practically the situation for Cel6A–Avicel<sub>coarse</sub> in Figure 3, and we conclude that this interaction becomes fully irreversible upon centrifugation. The highest degree of reversibility for centrifuged samples was found for the Cel7B–RAC system (Figure 4). In this case the free enzyme concentration was over 60% of the value predicted from the ascending isotherm. In most other cases this value ranged from 10 to 30%, signifying a predominantly irreversible adsorption.

In addition to the comparisons of ascending and descending curves in Figures 2–4, it is worth noting that the specific binding capacity varies strongly with the physical properties of cellulose. As an example, RAC bound 20–30-fold more Cel7A compared to Avicel<sub>coarse</sub>. This probably reflects differences in the specific accessible surface area of the substrates,<sup>34</sup> but the current data do not allow a detailed analysis.

Results from reversibility tests at moderate (2-fold) dilution are shown in Figure 5. This protocol has the advantage that

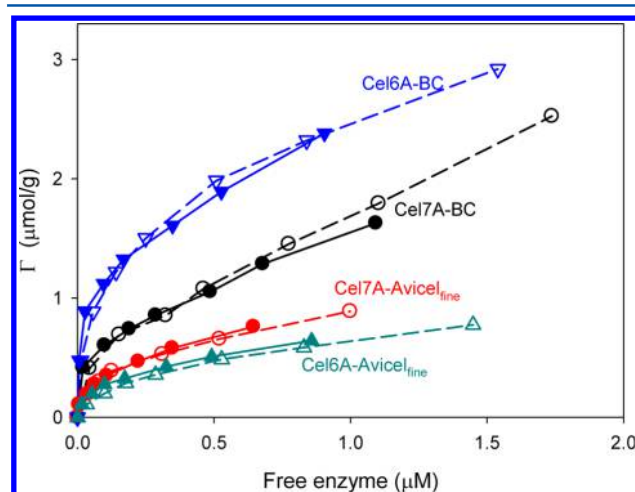


**Figure 5.** Reversibility of the adsorption for selected enzyme–substrate systems following 2-fold dilution in the standard assay with no centrifugation. Open symbols with dashed lines represent ascending isotherms, and closed symbols with full lines are descending isotherms.

ascending and descending data can be compared over a broader range of enzyme concentrations, and results in Figure 5 confirm the picture from Figures 2–4 as all investigated systems show accordance of ascending and descending data.

The pronounced effect of centrifugation seen in Figures 2–4 underscores that reversibility may depend on the experimental procedure, and in the light of this, we tested different means of perturbing steady-state systems. In Figures 2–4 the strategy was to shift the initial state by the addition of pure buffer, but the perturbation could equally well be brought about by the addition of either enzyme or substrate. We tested the latter two strategies for the Cel7A/Avicel<sub>fine</sub> system in the simple assay without centrifugation. Adding enzyme inevitably shifts both  $E_{free}$  and  $\Gamma$  to higher values (i.e., right and upward in the left panel of Figure 6), while adding more substrate shifts the points in the opposite direction. More importantly, it appeared that the points shifted by either perturbation (open symbols in Figure 6) always fell near the original ascending isotherm (closed symbols), and this implies reversibility also for these alternative means of perturbation.

The concentration of cellobiose in the samples with the highest enzyme load (3  $\mu\text{M}$ ) was measured by ion chromatography for all investigated enzyme–substrate systems

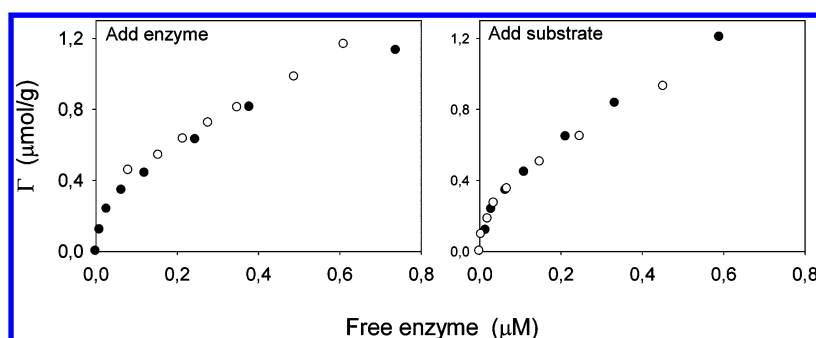


**Figure 6.** Reversibility of the interaction of Cel7A and Avicel<sub>fine</sub> tested by adding either more enzyme (left) or substrate (right) to a previously equilibrated enzyme–substrate mixture. This type of perturbation differs from the procedure underlying data in Figures 2–5, where the equilibrated system was diluted by pure buffer. Filled symbols show the original isotherm, and open symbols represent the new condition after the perturbation. It appears that adding enzyme shifts the points upward while adding substrate has the opposite effect. More importantly, these shifted points all remain near the original (ascending) isotherm, and this implies reversibility also for these types of perturbations.

both before dilution and after re-equilibration of the diluted samples (using the standard dilution assay). The degree of substrate conversion calculated from these measurements ranged from 7% for the Cel7B–RAC system to 0.5% for Cel7A–BMCC, with most cases between 1 and 2%. These values are small or comparable to the experimental scatter in the adsorption measurements, and we did not implement a correction in the substrate load but used the initial value,  $S_0$ , in the calculations of enzyme coverage (eqs 4–6).

## DISCUSSION

Molecular descriptions of enzymatic hydrolysis of cellulose require consideration of a number of distinct reaction steps.<sup>22,35–37</sup> One key process is the association of the enzyme and its insoluble substrate, and in many cases this has been described along the lines of different equilibrium adsorption theories. While the analogy to conventional surface adsorption appears obvious several provisos remain. Most importantly, many studies have found that the interaction is irreversible or partially irreversible (see Introduction) and hence that equilibrium reaction schemes, which underlie simple adsorption models, are not justified. Second, cellulose–cellulase mixtures are reacting systems. This implies that the amount and structure of the sorbent change gradually and hence that equilibrium descriptions will be reasonable only on time scales that are short compared to these changes (and ultimately the full hydrolysis of the solid phase). A third caveat comes from the physical instability of the enzymes. Thus, like any protein conformation, cellulases are prone to irreversible denaturation, and this will complicate the description of the adsorption process. If, as suggested repeatedly,<sup>5,10,12,38</sup> non-native forms bind strongly to the cellulose surface, the concentration of free enzyme (which is the observable in most experiments) will be a complex function of both the affinity of native and denatured forms and the rate of the denaturation process. Indeed, this balance between affinity and stability has often been used to rationalize general aspects of nonspecific adsorption of proteins to solid surfaces.<sup>18,39,40</sup>

In the light of this we have made a systematic study of adsorption reversibility for short contact times where effects of substrate conversion and enzyme denaturation are as small as possible. The results consistently showed accordance of ascending and descending curves in experiments with simple dilution after 30 min. This means that within the experimental conditions used here (i.e., enzyme loads around 1  $\mu\text{M}$ , substrate

loads around 1 g/L, and time scales of about 1 h) the adsorption was fully reversible. In other words, there is a dynamic equilibrium between the populations of free and adsorbed enzyme. Indeed, irreversible adsorption is hard to reconcile with the general picture of a rapid initial adsorption followed by a steady state with constant free enzyme concentration which has been reported in many cases.<sup>6,33,36,41–44</sup> Thus, irreversibility implies very low desorption rate, and if the adsorption is relatively fast, as suggested by the rapid initial decline in free enzyme, one would clearly expect continuous buildup on the surface and a concomitant loss of free enzyme rather than a stable free concentration. This latter scenario with a slow, continuous adsorption has been described for cellulase mixtures hydrolyzing newspaper<sup>45</sup> and most recently for Cel7A and Cel7B attacking supported thin films of cellulose.<sup>5</sup> In the latter case, the interaction showed high reversibility for short contact times (minutes), but extensive irreversibility (70–90%) was found already after an hour at room temperature. A similar behavior with gradual buildup of an irreversibly bound population of Cel7A and Cel7B has also been found in a study using bacterial cellulose in suspension.<sup>7</sup> In this case, however, the loss of reversibility (at 30–40 °C) happened on a much slower time scale (days).

The results in Figures 2–4 consistently showed that descending isotherms made by resuspending centrifuged pellets were much steeper than the corresponding ascending isotherms. As illustrated in Figure 1, this is a hallmark of irreversibility. Hence, the shift to the left of the descending isotherms in these figures implies a limited release of adsorbed enzyme in diluted samples over the time scale studied here. As discussed in the Introduction, the precise term for this is hysteresis between the ascending and descending processes, but we have used the commonly accepted term, irreversibility, here. For the cellobiohydrolases Cel7A and Cel6A the results corresponded to a predominately irreversible interaction whereas the endoglucanase Cel7B showed moderate reversibility. We looked for a “dose–response relationship” with respect to the severity of centrifugation but did not find systematic differences between samples centrifuged for 3 min at respectively 1500g, 4000g (as in Figures 2–4), or 14000g (data not shown). Mechanistic analyses of the centrifugation-induced irreversibility await further investigation, but we speculate that compression of the pellet could change the substrate in a way that tends hamper or delay subsequent release of the enzyme. This interpretation may be seen as an analogy to so-called

hornification that results from lowering the water content in cellulosic suspensions either by drying or wet-pressing. Thus, moderate dehydration of wood pulp (to solid contents above 40–50%) may lead to extensive and irreversible reduction in pore volume and a concomitant reduction in enzymatic digestibility.<sup>46,47</sup> If similar changes occur in pellets made by e.g. centrifugation or filtration,<sup>16</sup> this might impede the subsequent release of enzyme originally adsorbed in wider pores. We note, however, that centrifugation does not *per se* lead to lower surface accessibility because control experiments where the substrate was centrifuged prior to the addition of enzyme showed the same ascending binding isotherm as noncentrifuged substrate. Irrespectively of the molecular origin, the pronounced irreversibility resulting from centrifugation may be pertinent to both cellulase recycling protocols in biomass industries and attempts to reconcile discordant conclusions in earlier literature on cellulase adsorption (see Introduction). Regarding the former, it is clear that the simple cellulose substrates and short time scales studied here only provide information on some of the interactions that govern adsorption of cellulases onto complex biomass. Nevertheless, the results suggest a potential role of mechanical processing and emphasize that centrifugation and possibly other types of compaction could compromise recyclability of cellulases. With respect to deviant conclusions on reversibility in the literature, we note that many earlier works have used resuspension of centrifuged or filtered pellets in their experimental protocols. In the light of the current results it appears that such protocols may have negatively influenced reversibility. However, we emphasize that irreversible adsorption of cellulases has also been reported in simple dilution experiments. In particular, a number of recent studies on the adsorption to supported cellulose films have shown a considerable degree of non-reversibility.<sup>5,10,15</sup> Some of these works have reported a gradually growing population of irreversibly bound enzyme, and we suggest that further studies on the temporal development of reversibility in cellulose suspensions could be fruitful in attempts to understand the process in more detail.

Toward the end of this work, we became aware of a study by Jalak and Våljamäe<sup>48</sup> that suggested irreversibility at very low (nM) enzyme concentrations. Interestingly, enlargements of the dilute range of Figures 2–4 showed a similar behavior for both centrifuged and noncentrifuged samples although these effects were on the verge of the current experimental sensitivity. It appears, however, that future work specifically addressing this low concentration range might be rewarding for a better understanding of adsorption reversibility.

## ■ SUMMARY AND CONCLUSIONS

We found superposition of ascending and descending isotherms for the adsorption of three commonly studied cellulases on different types of pure cellulose substrates. The relationship between superposition of isotherms and reversibility was illustrated in Figure 1 for the simple case of Langmuir adsorption (eq 1), but superimposed isotherms signify reversibility in general regardless of the adsorption mechanism. Hence, the results imply that for short contact times (~1 h) and moderate enzyme and substrate loads (about 1  $\mu$ M and 1 g/L, respectively), the systems are in a state of dynamic equilibrium. This supports the validity of using simple equilibrium reaction schemes in kinetic models at least for the three cellulases studied here. Other investigations, discussed above, have suggested that this simplified interpretation may

not be valid for long contact times and high degrees of conversion. The work also showed that reversibility was mainly lost upon centrifugation. We speculate that this could reflect structural changes such as pore collapse in the cellulose and that it could be one of the reasons for divisive conclusions on reversibility in the literature.

## ■ AUTHOR INFORMATION

### Corresponding Author

\*E-mail: pwesth@ruc.dk (P.W.).

### Notes

The authors declare the following competing financial interest(s): One co-author works at Novozymes, which is a major producer of industrial enzymes.

## ■ ACKNOWLEDGMENTS

We are indebted to Dr. H. W. Bagger for first directing our attention to the role of centrifugation and to Dr. Priit Våljamäe for making results available to us prior to their publication. The technical assistance of Kadri Alasepp, Helen Ruul, and Søren Myhre is gratefully acknowledged. This work was supported by the Danish Council for Strategic Research, Program Commission on Sustainable Energy and Environment (Grant # 2104-07-0028 and 11-116772 to P.W.) and by the Carlsberg Foundation (2013-01-0208 to P.W.).

## ■ REFERENCES

- (1) Bansal, P.; Hall, M.; Realf, M. J.; Lee, J. H.; Bommaris, A. S. Modeling cellulase kinetics on lignocellulosic substrates. *Biotechnol. Adv.* **2009**, *27* (6), 833–848.
- (2) Zhang, Y. H. P.; Lynd, L. R. Toward an aggregated understanding of enzymatic hydrolysis of cellulose: Noncomplexed cellulase systems. *Biotechnol. Bioeng.* **2004**, *88* (7), 797–824.
- (3) Kyriacou, A.; Neufeld, R. J.; Mackenzie, C. R. Reversibility and competition in the adsorption of trichoderma-reesei cellulase components. *Biotechnol. Bioeng.* **1989**, *33* (5), 631–637.
- (4) Pinto, R.; Moreira, S.; Mota, M.; Gama, M. Studies on the cellulose-binding domains adsorption to cellulose. *Langmuir* **2004**, *20* (4), 1409–1413.
- (5) Maurer, S. A.; Bedbrook, C. N.; Radke, C. J. Competitive sorption kinetics of inhibited endo- and exoglucanases on a model cellulose substrate. *Langmuir* **2012**, *28* (41), 14598–14608.
- (6) Linder, M.; Teeri, T. T. The cellulose-binding domain of the major cellobiohydrolase of *Trichoderma reesei* exhibits true reversibility and a high exchange rate on crystalline cellulose. *Proc. Natl. Acad. Sci. U. S. A.* **1996**, *93* (22), 12251–12255.
- (7) Palonen, H.; Tenkanen, M.; Linder, M. Dynamic interaction of *Trichoderma reesei* cellobiohydrolases Cel6A and Cel7A and cellulose at equilibrium and during hydrolysis. *Appl. Environ. Microbiol.* **1999**, *65* (12), 5229–5233.
- (8) Bothwell, M. K.; Wilson, D. B.; Irwin, D. C.; Walker, L. P. Binding reversibility and surface exchange of *Thermomonospora fusca* E-3 and E-5 and *Trichoderma reesei* CBHI. *Enzyme Microb. Technol.* **1997**, *20* (6), 411–417.
- (9) Carrard, G.; Linder, M. Widely different off rates of two closely related cellulose-binding domains from *Trichoderma reesei*. *Eur. J. Biochem.* **1999**, *262* (3), 637–643.
- (10) Ma, A. Z.; Hu, Q.; Qu, Y. B.; Bai, Z. H.; Liu, W. F.; Zhuang, G. Q. The enzymatic hydrolysis rate of cellulose decreases with irreversible adsorption of cellobiohydrolase I. *Enzyme Microb. Technol.* **2008**, *42* (7), 543–547.
- (11) Nidetzky, B.; Steiner, W.; Claeysens, M. Cellulose hydrolysis by cellulases from *Trichoderma reesei*: adsorptions of two cellobiohydrolases, two endocellulases and their core protein on filterpaper, and their relation to hydrolysis. *Biochem. J.* **1994**, *303*, 817–823.



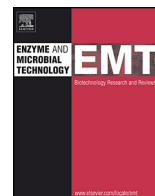
- (12) Beltrame, P. L.; Carniti, P.; Focher, B.; Marzetti, A.; Cattaneo, M. Cotton cellulose - enzyme adsorption and enzymatic-hydrolysis. *J. Appl. Polym. Sci.* **1982**, *27* (9), 3493–3502.
- (13) Beldman, G.; Voragen, A. G. J.; Rombouts, F. M.; Searle van Leeuwen, M. F.; Pilnik, W. Adsorption and kinetic-behavior of purified endoglucanases and exoglucanases from *Trichoderma viride*. *Biotechnol. Bioeng.* **1987**, *30* (2), 251–257.
- (14) Jung, H.; Wilson, D. B.; Walker, L. P. Binding and reversibility of *Thermobifida fusca* Cel5A, Cel6B, and Cel48A and their respective catalytic domains to bacterial microcrystalline cellulose. *Biotechnol. Bioeng.* **2003**, *84* (2), 151–159.
- (15) Moran-Mirabal, J. M.; Bolewski, J. C.; Walker, L. P. Reversibility and binding kinetics of *Thermobifida fusca* cellulases studied through fluorescence recovery after photobleaching microscopy. *Biophys. Chem.* **2011**, *155* (1), 20–28.
- (16) Wang, Q. Q.; Zhu, J. Y.; Hunt, C. G.; Zhan, H. Y. Kinetics of adsorption, desorption, and re-adsorption of a commercial endoglucanase in lignocellulosic suspensions. *Biotechnol. Bioeng.* **2012**, *109* (8), 1965–1975.
- (17) Callen, H. B. *Thermodynamics*; John Wiley and Sons: New York, 1960; p 376.
- (18) Norde, W.; Haynes, C. A. Reversibility and the Mechanism of Protein adsorption. In *Proteins at Interfaces II: Fundamentals and Applications*; Horbett, T. A., Brash, J. L., Eds.; American Chemical Society: Washington, DC, 1995.
- (19) Baumann, M. J.; Borch, K.; Westh, P. Xylan oligosaccharides and cellobiohydrolase I (TrCel7A) interaction and effect on activity. *Biotechnol. Biofuels* **2011**, *4*, 45.
- (20) Murphy, L.; Baumann, M. J.; Borch, K.; Sweeney, M.; Westh, P. An enzymatic signal amplification system for calorimetric studies of cellobiohydrolases [*Anal. Biochem.* **2010**, *404*, 140]. *Anal. Biochem.* **2011**, *408* (2), 361–361.
- (21) Murphy, L.; Cruys-Bagger, N.; Damgaard, H. D.; Baumann, M. J.; Olsen, S. N.; Borch, K.; Lassen, S. F.; Sweeney, M.; Tatsumi, H.; Westh, P. Origin of initial burst in activity for *Trichoderma reesei* endo-glucanases hydrolyzing insoluble cellulose. *J. Biol. Chem.* **2012**, *287*, 1252–1260.
- (22) Praestgaard, E.; Elmerdahl, J.; Murphy, L.; Nymand, S.; McFarland, K. C.; Borch, K.; Westh, P. A kinetic model for the burst phase of processive cellulases. *FEBS J.* **2011**, *278* (9), 1547–1560.
- (23) Valjamae, P.; Sild, V.; Nutt, A.; Pettersson, G.; Johansson, G. Acid hydrolysis of bacterial cellulose reveals different modes of synergistic action between cellobiohydrolase I and endoglucanase I. *Eur. J. Biochem.* **1999**, *266* (2), 327–334.
- (24) Cruys-Bagger, N.; Tatsumi, H.; Ren, G.; Borch, K.; Westh, P. Transient kinetics and rate-limiting steps for the processive cellobiohydrolase Cel7A: Effects of substrate structure and carbohydrate binding domain. *Biochemistry* **2013**, *52* (49), 8938–8948.
- (25) Hall, M.; Bansal, P.; Lee, J. H.; Realf, M. J.; Bommarius, A. S. Cellulose crystallinity - a key predictor of the enzymatic hydrolysis rate. *FEBS J.* **2010**, *277* (6), 1571–1582.
- (26) Park, S.; Baker, J. O.; Himmel, M. E.; Parilla, P. A.; Johnson, D. K. Cellulose crystallinity index: measurement techniques and their impact on interpreting cellulase performance. *Biotechnol. Biofuels* **2010**, *3*, 10.
- (27) Murphy, L.; Baumann, M. J.; Borch, K.; Sweeney, M.; Westh, P. An enzymatic signal amplification system for calorimetric studies of cellobiohydrolases. *Anal. Biochem.* **2010**, *404* (2), 140–148.
- (28) Zhang, Y. H. P.; Cui, J. B.; Lynd, L. R.; Kuang, L. R. A transition from cellulose swelling to cellulose dissolution by o-phosphoric acid: Evidence from enzymatic hydrolysis and supramolecular structure. *Biomacromolecules* **2006**, *7* (2), 644–648.
- (29) Murphy, L. Thermochemical screening of lignocellulosic enzymes for second generation bioethanol production. Ph.D., Roskilde University, 2011.
- (30) Vanderhart, D. L.; Atalla, R. H. Studies of microstructure in native celluloses using solid-state C-13 NMR. *Macromolecules* **1984**, *17* (8), 1465–1472.
- (31) Zhang, Y. H. P.; Lynd, L. R. Determination of the number-average degree of polymerization of dextrins and cellulose with application to enzymatic hydrolysis. *Biomacromolecules* **2005**, *6* (3), 1510–1515.
- (32) Gasteiger, E.; Gattiker, A.; Hoogland, C.; Ivanyi, I.; Appel, R. D.; Bairoch, A. ExPASy: the proteomics server for in-depth protein knowledge and analysis. *Nucleic Acids Res.* **2003**, *31* (13), 3784–3788.
- (33) Stahlberg, J.; Johansson, G.; Pettersson, G. A new model for enzymatic-hydrolysis of cellulose based on the 2-domain structure of cellobiohydrolase-I. *Biotechnology* **1991**, *9* (3), 286–290.
- (34) Hong, J.; Ye, X. H.; Zhang, Y. H. P. Quantitative determination of cellulose accessibility to cellulase based on adsorption of a nonhydrolytic fusion protein containing CBM and GFP with its applications. *Langmuir* **2007**, *23* (25), 12535–12540.
- (35) Chundawat, S. P. S.; Beckham, G. T.; Himmel, M. E.; Dale, B. E.; Prausnitz, J. M. Deconstruction of lignocellulosic biomass to fuels and chemicals. *Annu. Rev. Chem. Biomol. Eng.* **2011**, *2*, 121–145.
- (36) Jalak, J.; Kurasin, M.; Teugjas, H.; Valjamae, P. Endo-exo synergism in cellulose hydrolysis revisited. *J. Biol. Chem.* **2012**, *287* (34), 28802–28815.
- (37) Kostylev, M.; Moran-Mirabal, J. M.; Walker, L. P.; Wilson, D. B. Determination of the molecular states of the processive endoglucanase *Thermobifida fusca* Cel9A during crystalline cellulose depolymerization. *Biotechnol. Bioeng.* **2012**, *109* (1), 295–299.
- (38) Howell, J. A.; Mangat, M. Enzyme deactivation during cellulose hydrolysis. *Biotechnol. Bioeng.* **1978**, *20* (6), 847–863.
- (39) Bentaleb, A.; Abele, A.; Haikel, Y.; Schaaf, P.; Voegel, J. C. FTIR-ATR and radiolabeling study of the adsorption of ribonuclease A onto hydrophilic surfaces: Correlation between the exchange rate and the interfacial denaturation. *Langmuir* **1998**, *14* (22), 6493–6500.
- (40) Wertz, C. F.; Santore, M. M. Effect of surface hydrophobicity on adsorption and relaxation kinetics of albumin and fibrinogen: Single-species and competitive behavior. *Langmuir* **2001**, *17* (10), 3006–3016.
- (41) Liu, H.; Zhu, J. Y.; Chai, X. S. In situ, rapid, and temporally resolved measurements of cellulase adsorption onto lignocellulosic substrates by UV-vis spectrophotometry. *Langmuir* **2011**, *27* (1), 272–278.
- (42) Steiner, W.; Sattler, W.; Esterbauer, H. Adsorption of *Trichoderma reesei* cellulase on cellulose - experimental-data and their analysis by different equations. *Biotechnol. Bioeng.* **1988**, *32* (7), 853–865.
- (43) Moran-Mirabal, J. N.; Santhanam, N.; Corgie, S. C.; Craighead, H. G.; Walker, L. P. Immobilization of cellulose fibrils on solid substrates for cellulase-binding studies through quantitative fluorescence microscopy. *Biotechnol. Bioeng.* **2008**, *101* (6), 1129–1141.
- (44) Cruys-Bagger, N.; Elmerdahl, J.; Praestgaard, E.; Tatsumi, H.; Spodsberg, N.; Borch, K.; Westh, P. Pre-steady state kinetics for the hydrolysis of insoluble cellulose by *Trichoderma reesei* Cel7A. *J. Biol. Chem.* **2012**, *287*, 18451–18458.
- (45) Castanon, M.; Wilke, C. R. Adsorption and recovery of cellulases during hydrolysis of newspaper. *Biotechnol. Bioeng.* **1980**, *22* (5), 1037–1053.
- (46) Haggkvist, M.; Li, T. Q.; Odberg, L. Effects of drying and pressing on the pore structure in the cellulose fibre wall studied by H-1 and H-2 NMR relaxation. *Cellulose* **1998**, *5* (1), 33–49.
- (47) Luo, X. L.; Zhu, J. Y.; Gleisner, R.; Zhan, H. Y. Effects of wet-pressing-induced fiber hornification on enzymatic saccharification of lignocelluloses. *Cellulose* **2011**, *18* (4), 1055–1062.
- (48) Jalak, J.; Våljamäe, P. Multi-Mode Binding of Cellobiohydrolase Cel7A from *Trichoderma reesei* to Cellulose. *PLoS ONE* **2014**, *9* (9), e108181 DOI: 10.1371/journal.pone.0108181.

A Pyranose Dehydrogenase-based Biosensor for  
Kinetic Analysis of Enzymatic Hydrolysis of  
Cellulose by Cellulases

---

**VII**





## A pyranose dehydrogenase-based biosensor for kinetic analysis of enzymatic hydrolysis of cellulose by cellulases



Nicolaj Cruys-Bagger<sup>a,b,\*</sup>, Silke Flindt Badino<sup>a</sup>, Radina Tokin<sup>a</sup>, Mark Gontsarik<sup>a</sup>, Samin Fathalinejad<sup>a</sup>, Kenneth Jensen<sup>b</sup>, Miguel Duarte Toscano<sup>b</sup>, Trine Holst Sørensen<sup>a,b</sup>, Kim Borch<sup>b</sup>, Hirosuke Tatsumi<sup>c</sup>, Priit Väljamäe<sup>d</sup>, Peter Westh<sup>a,\*\*</sup>

<sup>a</sup> Research Unit for Biomaterials, NSM, Roskilde University, Universitetsvej 1, DK-4000 Roskilde, Denmark

<sup>b</sup> Novozymes A/S, Krogshøjvej 36, DK-2880 Bagsværd, Denmark

<sup>c</sup> Department of Chemistry, Faculty of Science, Shinshu University, Matsumoto, Nagano 390-8621, Japan

<sup>d</sup> Institute of Molecular and Cell Biology, University of Tartu, Riia 23b – 202, 51010 Tartu, Estonia

### ARTICLE INFO

#### Article history:

Received 22 August 2013

Received in revised form 3 March 2014

Accepted 4 March 2014

Available online 12 March 2014

#### Keywords:

Pyranose dehydrogenase

Biosensor

Cellulase kinetics

*Hypocrea jecorina*

Cellobiohydrolase

Cel6A

### ABSTRACT

A novel electrochemical enzyme biosensor was developed for real-time detection of cellulase activity when acting on their natural insoluble substrate, cellulose. The enzyme biosensor was constructed with pyranose dehydrogenase (PDH) from *Agaricus meleagris* that was immobilized on the surface of a carbon paste electrode, which contained the mediator 2,6-dichlorophenolindophenol (DCIP). An oxidation current of the reduced form of DCIP, DCIPH<sub>2</sub>, produced by the PDH-catalyzed reaction with either glucose or cellobiose, was recorded under constant-potential amperometry at +0.25 V (vs. Ag/AgCl). The PDH-biosensor was shown to be anomer unspecific and it can therefore be used in kinetic studies over broad time-scales of both retaining- and inverting cellulases (in addition to enzyme cocktails). The biosensor was used for real-time measurements of the activity of the inverting cellobiohydrolase Cel6A from *Hypocrea jecorina* (HjCel6A) on cellulosic substrates with different morphology (bacterial microcrystalline cellulose (BMCC) and Avicel). The steady-state rate of hydrolysis increased towards a saturation plateau with increasing loads of substrate. The experimental results were rationalized using a steady-state rate equation for processive cellulases, and it was found that the turnover for HjCel6A at saturating substrate concentration (i.e. maximal apparent specific activity) was similar (0.39–0.40 s<sup>-1</sup>) for the two substrates. Conversely, the substrate load at half-saturation was much lower for BMCC compared to Avicel. Biosensors covered with a polycarbonate membrane showed high operational stability of several weeks with daily use.

© 2014 Elsevier Inc. All rights reserved.

### 1. Introduction

A common observation in the kinetics of enzymatic cellulose degradation is a declining hydrolysis rate with both time and conversion [1,2]. The origin of the slowdown remains unclear and both enzyme- and substrate related properties have been proposed [1,3] and further progress in this area seems to require better

**Abbreviations:** AmPDH, pyranose dehydrogenase from *Agaricus meleagris*; BQ, 1,4-benzoquinone; Fc, ferrocene; Fc<sup>+</sup>, ferricinium ion; Fc<sup>+</sup>PF<sub>6</sub><sup>-</sup>, ferricinium hexafluorophosphate; DCIP, 2,6-dichloroindophenol.

\* Corresponding author at: Research Unit for Functional Biomaterials, NSM, Roskilde University, Universitetsvej 1, 4000 Roskilde, Denmark. Tel.: +45 4674 3577.

\*\* Corresponding author at: Research Unit for Functional Biomaterials, NSM, Roskilde University, Universitetsvej 1, 4000 Roskilde, Denmark. Tel.: +45 4674 2879; fax: +45 4674 3011.

E-mail addresses: [nicolaj@ruc.dk](mailto:nicolaj@ruc.dk) (N. Cruys-Bagger), [pwesth@ruc.dk](mailto:pwesth@ruc.dk) (P. Westh).

<http://dx.doi.org/10.1016/j.enzmictec.2014.03.002>

0141-0229/© 2014 Elsevier Inc. All rights reserved.

descriptions of structural and kinetic aspects. Fundamental insights into the complex enzymatic hydrolysis process can be obtained from kinetic studies, but such work is challenged by the insoluble and heterogeneous nature of cellulose. Some progress has been obtained using novel real-time experimental approaches such as quartz crystal microbalance (QCM) measurements [4–8], electrochemical sensors [9] and isothermal titration calorimetry (ITC) [10–13]. Enzyme biosensors constitute another real-time approach, which in some cases provides advantageous sensitivity, specificity, and response time. This was utilized in the development of amperometric enzyme biosensors for cellulase activity based on immobilized enzymes including glucose oxidase (GOx), pyrroloquinoline quinine-dependent glucose dehydrogenase (GDH) or cellobiose dehydrogenase (CDH) [14–16]. The CDH biosensor was found to have a particularly high resolution in time and analyte concentration, and this allowed elucidation of the pre-steady state kinetics of the cellobiohydrolase Cel7A [17,18] and endoglucanase

Cel7B [16] from *Hypocrea jecorina* (anamorph: *Trichoderma reesei*) on their insoluble substrates. Sensors based on either GOx, GDH or CDH share the feature of specifically detecting the  $\beta$ -anomer of their analytes. In some special cases this specificity provides analytical advantages, but in general activity measurements, it sets up a number of severe limitations. Hence, these sensors cannot be directly used when the product of the enzymatic reaction is an  $\alpha$ -anomer (e.g. for inverting cellulases such as Cel6A). More importantly, anomeric specificity limits the time-scales over which a biosensor can be used for any hydrolytic enzyme in real-time measurements. This is because mutarotation (i.e. equilibration of the  $\alpha$ - $\beta$  distribution) will occur in parallel with the enzymatic hydrolysis, and hence impede quantification of the product. In practice this means that the anomer-specific biosensors can be used over time-scales that are either much faster or much slower than the mutarotation because under these conditions mutarotation will either be negligible or fully equilibrated and hence easy to account for. Between these extremes there will be a broad interval where biosensor measurements will be either unfeasible or dependent on extensive and error-prone corrections [14]. In the light of this, a biosensor without anomeric specificity appears useful in attempts to elucidate cellulolytic enzymes and their ubiquitous activity loss.

Pyranose dehydrogenase (PDH, pyranose:acceptor oxidoreductase, EC 1.1.99.29) (PDH) is a glycosylated, extracellular, monomeric flavin-dependent sugar oxidoreductase secreted by several wood degrading fungi and a member of the glucose-methanol-choline oxidoreductase family [19,20]. PDH from *Agaricus meleagris* (AmPDH) appears promising for biosensor-based cellulase activity studies because it shows a broad electron-donor substrate specificity which includes both mono-, di- and oligosaccharides, is inert towards oxygen, shows broad optimal pH range (pH 4–10) and is stable for months when stored at 4 °C [19,21]. AmPDH can perform both single oxidizations on the C-1, C-2 or C-3 position or double oxidation (C-1,2 or C-3,4 positions) depending on the substrate and it is not specific to one of the anomeric forms [21]. AmPDH has been successfully “wired” with Osmium redox polymers and immobilized on electrodes both for detection of sugars [22,23] and as anode in enzymatic biofuel cells [24–26].

In the present work a mediated amperometric biosensor based on immobilized AmPDH was developed and the biosensor was applied for real-time activity measurements of a cellulase hydrolyzing insoluble cellulose. The experimental results were analyzed with respect to a recent published steady-state rate equation for processive cellulases [27].

## 2. Methods and materials

### 2.1. Chemicals

Unless otherwise stated, all chemicals were of HPLC grade (>99% purity) and supplied by Sigma–Aldrich (St. Louis, USA).  $\alpha$ -D-(+)-Glucose (>99.0%) was supplied by Acros Organics (NJ, USA),  $\beta$ -D-(+)-Glucose (>99.0%) was from ChromaDex™ (Irvine, USA) and Cellotriose (Fine grade, >95%) was purchased from Seikagaku Biobusiness Corporation (Tokyo, Japan). All solutions were prepared with 50 mM sodium acetate and 2 mM CaCl<sub>2</sub> buffer adjusted to pH 5.0. Stock solutions of sugars were prepared at least 24 h before use to achieve mutarotative equilibrium except in the mutarotation test experiments where the solutions were prepared immediately before use.

### 2.2. Cellulose substrate preparations

Avicel PH-101 was from Fluka (Biochemika, Ireland). Avicel consists of aggregates of microcrystalline cellulose with a crystallinity index of 0.55–0.70 [28,29] and an average particle size (reported by the manufacturer) of 50  $\mu$ m. Bacterial cellulose (BC) was prepared by laboratory fermentation of *Gluconobacter xylinum* as described in detail elsewhere [30]. BC consists of long, thin ribbons that are around 50 nm wide [31] that both have crystalline- and some less ordered amorphous regions. Bacterial microcrystalline cellulose (BMCC) was prepared by treatment of the BC with hydrochloric acid which hydrolyses the amorphous regions. This leads to a large reduction in the degree of polymerization and gives a cellulose substrate with a crystallinity index above 0.90 [32]. The cellulose suspensions were prepared in

50 mM acetate buffer, pH 5.0 and added 0.01% sodium azide to prevent bacterial growth.

### 2.3. Enzyme production and purification

#### 2.3.1. Pyranose dehydrogenase

Pyranose dehydrogenase from *A. meleagris* was expressed, fermented and purified as described in the Supporting Information. The protein concentration was determined from absorbance measurement at 280 nm with the theoretical molar extinction coefficient ( $\epsilon_{280} = 67,840 \text{ M}^{-1} \text{ cm}^{-1}$ ) derived from the amino acid sequence. The thermal stability was tested by differential scanning calorimetry (VP-DSC, MicroCal, USA) and a transition mid-point of 75.9 °C was measured.

#### 2.3.2. Cel6A from *H. jecorina*

The inverting cellobiohydrolase, Cel6A, from *H. jecorina* (HjCel6A) was expressed, fermented and purified as described in the Supporting Information. The absence of cellobiose activity in the purified product was confirmed as lack of detectable activity against the chromogenic substrate analogue *p*-nitrophenyl- $\beta$ -D-glucopyranoside (pNPG). The protein concentration was determined from absorbance measurement at 280 nm with the theoretical molar extinction coefficient ( $\epsilon_{280} = 96,600 \text{ M}^{-1} \text{ cm}^{-1}$ ) derived from the amino acid sequence.

### 2.4. Preparation of enzyme-modified electrodes

Mediator-mixed carbon paste electrodes were prepared as described elsewhere [14,17]. Four different mediators (1,4-benzoquinone (BQ), 2,6-dichloroindophenol (DCIP), ferricenium cation (Fc<sup>+</sup>) as the salt composed with hexafluorophosphate (PF<sub>6</sub><sup>-</sup>) or ferrocene (Fc)) was tested by adding a weighed amount (5–25 mg) of one mediator to graphite powder (100 mg) and liquid paraffin (35  $\mu$ l). The mixture was thoroughly hand-mixed in an agate mortar until a homogenized paste was obtained. A portion of the resulting mediator-carbon paste was packed into carbon paste holders (Bioanalytical Systems, United Kingdom) with a working geometric area of 0.071 cm<sup>2</sup> and the surface was polished using waxed weighing-paper. The enzyme modification of the electrode surface was carried out by adding a 10- $\mu$ l aliquot of a freshly prepared solution of a 1:1 mixture of AmPDH stock and 1% glutaraldehyde (glutaraldehyde solution, 25% in H<sub>2</sub>O) onto the polished electrode surface. The enzyme droplet was carefully smeared-out and allowed to evaporate at room temperature for 30 min. The electrodes were then stored at 4 °C in an inverted position in a closed vessel under humid condition. Enzyme cross-linking and immobilization was allowed to proceed overnight. The electrode surface was thoroughly rinsed with MQ-water and the PDH-biosensor was allowed to stabilize in the buffer between 2 and 4 h and then in 1 mM glucose overnight at an applied potential sufficient to oxidize the mediator. Some PDH-biosensors were covered with a polycarbonate membrane with a pore-size of either 15 or 100 nm (Nuclepore polycarbonate Track Etch membrane Whatmann®, USA) and a nylon mesh with a Teflon-tube fitted over the membrane assembly to fixate them. Some of these were further drop-coated with 10  $\mu$ l Nafion (0.5%, v/v diluted in buffer) that was allowed to air dry for 30 min and stabilized in the buffer overnight before use.

A GOx-benzoquinone-carbon paste electrode was also prepared [33]. The procedure followed that described above with 10 mg benzoquinone mixed in the graphite paste and then glucose oxidase as the sensing enzyme. The glucose oxidase-biosensor was covered with a polycarbonate membrane with a pore-size of 15 nm.

### 2.5. Electrochemical instrumentation and measurements

A conventional electrochemical setup employed the PDH-biosensor as the working electrode, an Ag|AgCl|3M NaCl electrode as the reference electrode (Bioanalytical Systems, United Kingdom) and a platinum coiled wire as auxiliary electrode. Cyclic voltammetry was carried out using a VersaSTAT 3F (Princeton Applied Research, Princeton, NJ). Amperometric measurements were carried out with type-1112 potentiostats from Husou Seisakusyo Co. (Kawasaki, Japan) which were connected to a computer via an Agilent 34401A DMM and a LabVIEW 2012 data acquisition software (National Instruments, Austin, TX, USA). In the amperometric measurements calibrant- and enzyme solutions were delivered through a FEP tube (ID 0.15 mm) from a syringe (SGE Analytical Science) mounted in a syringe pump (Fusion 100, Chemyx, Stafford, USA). The syringe pump was controlled via the LabVIEW program. Calibrations were conducted by consecutive titrations of 5–20  $\mu$ l aliquots of degassed cellobiose solution into buffer. All electrochemical measurements were performed in a water-jacketed glass-cell connected to a water bath (Julabo F12, Seelbach, Germany).

#### 2.5.1. Test of mutarotation effect on PDH-biosensor response

The absence of a preference for one anomeric form was confirmed in trials on respectively  $\alpha$ -glucose,  $\beta$ -glucose and  $\beta$ -cellobiose. Specifically the sugar solutions were freshly prepared in cold buffer, mixed for 60 s and an aliquot titrated to the electrochemical cell with either the PDH- or GOx-biosensor. The response from the enzyme biosensors to an equilibrated glucose solution before and after the measurement was used to check the sensitivity of the sensors.



### 2.5.2. Enzymatic cellulose hydrolysis experiments

An AmPDH biosensor with the DCIP mediator covered with a 15 nm pore-size polycarbonate membrane and used for detection of cellobiose released during enzymatic cellulose hydrolysis experiments. An applied potential of +0.25 V was used as this was found to be the optimal detection potential for the PDH-DCIP-biosensor (see Section 3). Measurements were made on 5-mL degassed samples of the cellulose suspensions.

All experiments were conducted at  $25.0 \pm 0.1^\circ\text{C}$  and a magnetic stirrer at 500 rpm provided convective transport during the amperometric measurements. Data were collected at  $1\text{ s}^{-1}$ .

## 3. Results and discussion

### 3.1. Mediator selection for PDH-biosensor

From the steady-state kinetic parameters of AmPDH with various electron acceptors reported by Sygmond et al. [19]  $\text{Fc}^+$ , BQ and DCIP were tested for the development of a AmPDH biosensor. BQ and ferrocene have been used as electron mediators in second-generation enzyme biosensors [14–17,33–38]. DCIP is frequently used in enzyme assays in solution and as a pH/redox indicator. It is electrochemically active and has been used as a redox coupling agent in detection of NADH [39,40] and in enzyme immunoassays [41–43]. DCIP has also successfully been used as mediator in enzyme biosensors with glucose dehydrogenase [44] and lactate oxidase [45]. Preliminary experiments showed that PDH-biosensors prepared with DCIP showed the best performance and this mediator was therefore selected for further biosensor optimization. Variations of DCIP dosage in the carbon paste showed that the optimal amount was between 10 and 20 mg to 100 mg graphite powder (data not shown).

### 3.2. Cyclic and hydrodynamic voltammetry of the PDH-DCIP-biosensor

Cyclic voltammetry (CV) of DCIP shows two oxidation peaks at respectively +0.05 to 0.01 V and +0.5 V (vs. Ag/AgCl) [39,46]. The two oxidizable groups are the 2,6-dichloro-4-hydroxyphenyl-imino group and the phenolic group (the structure of DCIP can be seen in Fig. 3). The cyclic voltammogram shows well-defined reduction and oxidation waves of the 2,6-dichloro-4-(hydroxyphenyl-imino)-quinone) group if the scan is stopped before +0.4 V (pH 7.8) [47]. Oxidation of the phenolic ring occurs at a potential higher than +0.5 V and is irreversible. It has been suggested that the product of the second oxidation can lead to electropolymerization on the electrode surface, and hence cause electrode fouling [39]. CV was performed to characterize the bioelectrocatalysis properties of the PDH-DCIP-biosensor (non-membrane covered) in the potential range +0.05 to +0.4 V. Results in Fig. 1 show that the PDH-DCIP-biosensor produces an anodic wave for the electrode reaction of reduced DCIP ( $\text{DCIPH}_2$ ) when glucose is added to the buffer solution. This reflects the production of  $\text{DCIPH}_2$  by the PDH-catalyzed reaction.

Hydrodynamic voltammetry was performed to find the optimal detection potential of the PDH-DCIP-biosensor. This was performed with a PDH-biosensor that was covered with a 15 nm pore-size polycarbonate membrane and drop-coated with a layer of Nafion. The hydrodynamic voltammogram of the PDH-DCIP-biosensor can be seen in Fig. 2 and it appears that the anodic current increase from +0.05 V to +0.25 V, where a plateau was observed with only a small increase up to +0.45 V. At still higher potentials (>+0.5 V) the current response dropped. This was expected due to fouling of the electrode surface from electropolymerization of DCIP at high potentials as discussed above. The detection potential was therefore set to +0.25 V in all subsequent measurements. This value is in line with the detection potentials of reduced DCIP used earlier [39,42,45]. The measuring principle of the PDH-biosensor with DCIP serving

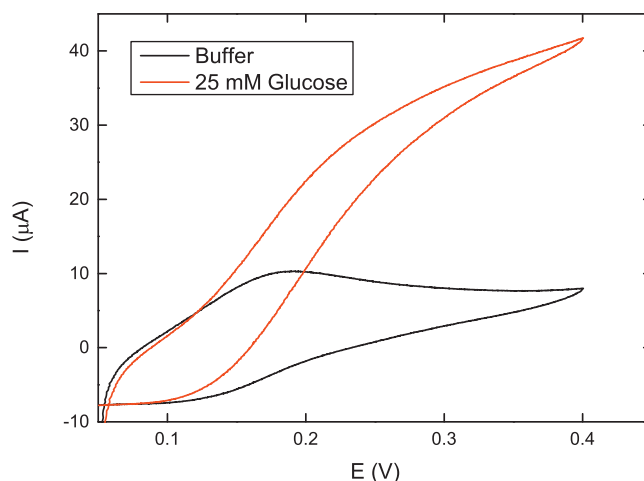


**Fig. 1.** Cyclic voltammogram obtained with the PDH-DCIP-biosensor (no membrane) at  $25^\circ\text{C}$  in buffer (black line) and buffer containing 25 mM glucose (red line). Scan rate:  $1\text{ mV s}^{-1}$ . The potential was scanned from negative to positive. Buffer solution: 50 mM sodium acetate, pH 5.0. (For interpretation of the references to color in this figure legend, the reader is referred to the web version of the article.)

as mediator can be seen in Fig. 3. As a control a DCIP-sensor without PDH immobilized was calibrated at +0.25 V and did not give any anodic current response in the range 0.01–1 mM glucose (data not shown). It should be noted that reduced DCIP ( $\text{DCIPH}_2$ ) can be re-oxidized by oxygen dissolved in the solution [39]. This reaction is slow, but in experiments running over long time, it could potentially influence the current response.

### 3.3. Calibration and analytical performance of the PDH-DCIP-biosensor

The current response of a polycarbonate-covered (100 nm pore size) PDH-biosensor during successive additions of cellobiose at an applied potential of +0.25 V (vs. Ag/AgCl) is shown in Fig. 4. Upon injection the anodic current reached a steady state response within 30 s. The amperometric current response for cellobiose was linear in the range from 10 to  $100\ \mu\text{M}$  (Fig. 4) with a sensitivity around  $6\text{ nA}/\mu\text{M}$  (correlation coefficient of  $>0.999$ ,  $n=9$ ). The detection limit was  $0.3\ \mu\text{M}$  ( $S/N=3$ ). The PDH-biosensors that were not

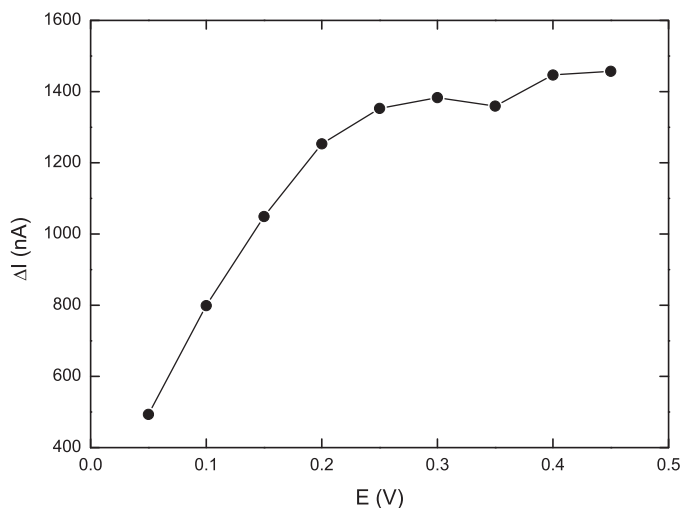


**Fig. 2.** Hydrodynamic voltammogram of a Nafion-polycarbonate (15 nm pore size) covered PDH-DCIP-biosensor. The amperometric response towards 1 mM glucose was recorded after a baseline was obtained. The applied potential was varied from +0.05 to 0.45 V (vs. Ag/AgCl) in steps of 0.05 V.

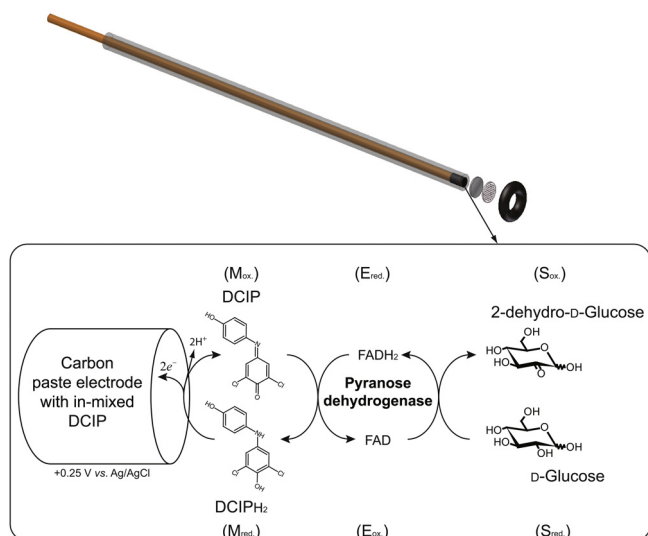


**Fig. 3.** Schematic illustration of the mediated bioelectrocatalytic measuring principle for the amperometric pyranose dehydrogenase-biosensor with DCIP serving as mediator.

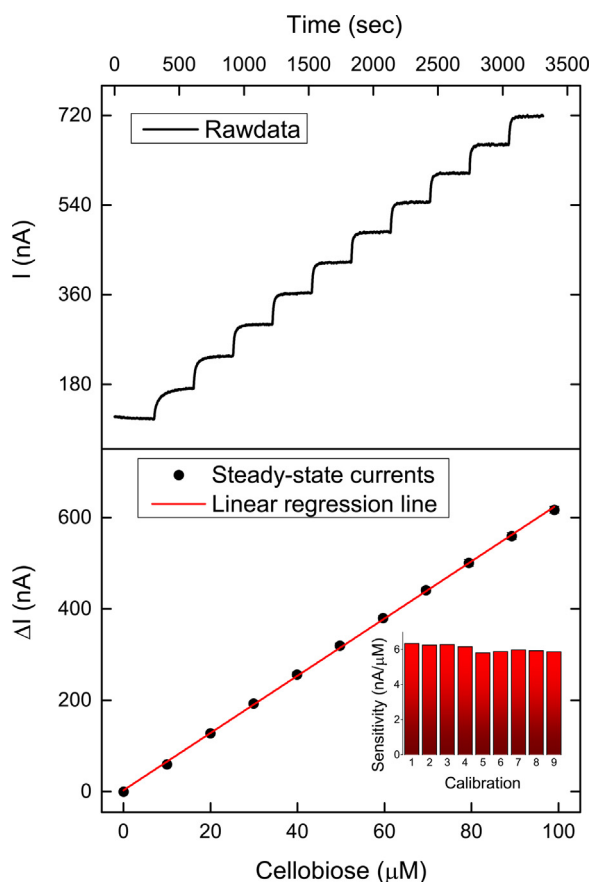


**Fig. 4.** The upper panel shows the amperometric response of the polycarbonate (100 nm) covered PDH-DCIP-biosensor to successive additions of cellobiose at 25 °C in 50 mM sodium acetate buffer, pH 5 (stirring rate 500 rpm). The applied potential was +0.25 V (vs. Ag/AgCl). The lower panel shows the calibration plot of the steady-state currents vs. the cellobiose concentration for a single experiment. The steady-state currents were corrected for the background current so the point of zero current at zero substrate concentration could be included in the linear regression. The insert shows the performance stability in the form of the change in the sensitivity as a function of the calibration number. Single calibration experiments performed between some of the enzymatic cellulose hydrolyses experiments are shown in Fig. 6.

covered with a membrane had a reduced upper limit of the linear range ( $<10 \mu\text{M}$  cellobiose). Sensors with a 15 nm pore-size polycarbonate membrane showed a linear range up to 4 mM cellobiose with a sensitivity of  $0.54 \text{ nA}/\mu\text{M}$  and a response time of 45 s. The PDH-DCIP-biosensors that were both covered with 15 nm pore-size polycarbonate membrane and drop-coated with Nafion also gave highly stable responses with a lower detection limit around  $12 \mu\text{M}$  glucose. However, these biosensors had a much slower response-time ( $>120\text{--}150 \text{ s}$ ) and also required longer time to give a stable background current ( $>1 \text{ h}$ ). The sensitivity, linear range and lifetime of the PDH-biosensor can hence be modulated with membrane coverage. The effect of membrane coverage on the response from enzyme biosensors based on carbon paste electrodes with incorporated mediator is discussed in [48] and references within.

### 3.4. Mutarotation effect on PDH-biosensor response

Enzymatic hydrolysis of  $\beta$ -glycosidic bonds may proceed via two different acid/base-catalyzed mechanisms that results in either retention or inversion of the anomeric configuration of the product [49–51]. Subsequently, so-called mutarotation will shift the population of product towards the equilibrium distribution of the  $\alpha$ - and  $\beta$ -anomer at a rate that depends strongly on temperature and pH [52,53]. One of the main purposes of the current work was to design a biosensor that was unaffected by this and to test if the PDH-DCIP response was indeed insensitive to mutarotation the temporal

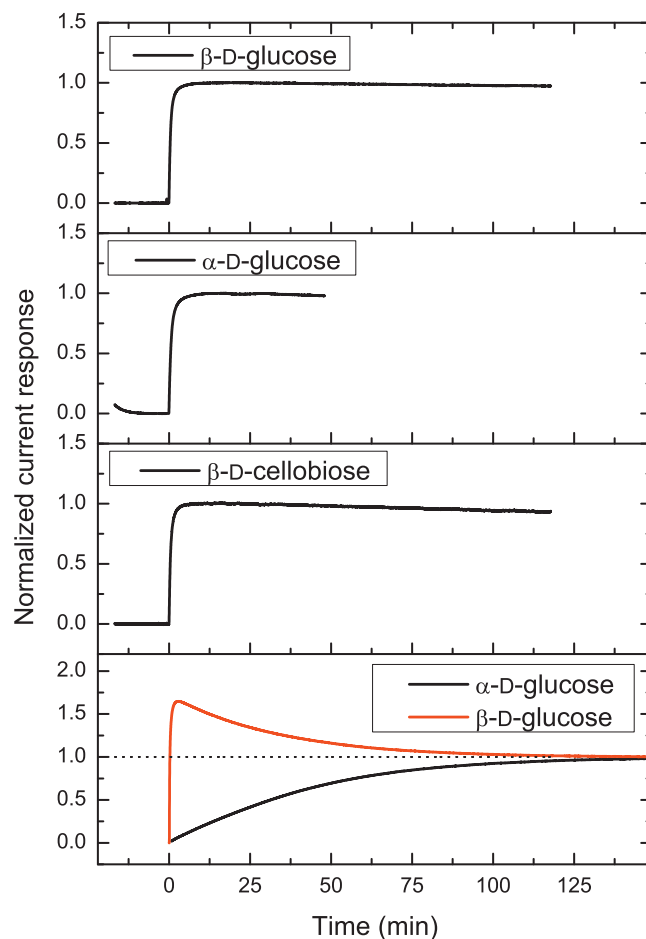


**Fig. 5.** Mutarotation effect on the current response of the PDH-DCIP-biosensor. The normalized current response of 1 mM of  $\beta$ -D-glucose,  $\alpha$ -D-glucose and  $\beta$ -D-cellobiose are shown. For comparison the last panel shows the normalized current response for a glucose oxidase-benzoquinone-carbon paste electrode to either 5 mM  $\alpha$ -D-glucose or  $\beta$ -D-glucose (applied potential +0.6 V).

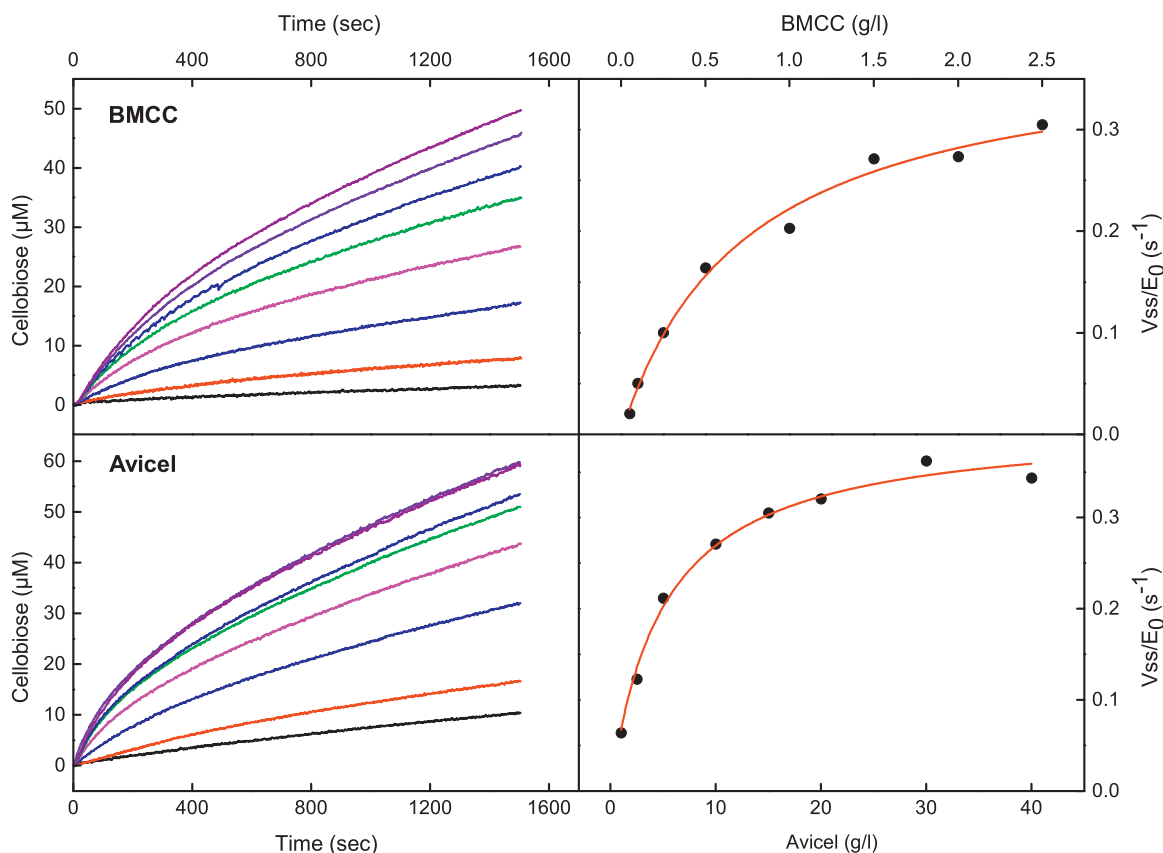


**Fig. 6.** *HjCel6A* (0.1  $\mu\text{M}$ ) activity on cellulosic substrates with different surface morphology and crystallinity. The steady state rate was found by linear regression between 500 and 600 s and plotted as function of the substrate load. The red line is the nonlinear regression to  $V_{ss}/E_0 = k_{cat,app} * S/(pK_M + S)$ . (For interpretation of the references to color in this figure legend, the reader is referred to the web version of the article.)

development in the signals from solutions that were initially 1 mM with respect to either  $\alpha$ -D-glucose,  $\beta$ -D-glucose or  $\beta$ -D-cellobiose was measured. The results are shown in Fig. 5, together with a control experiment where 5 mM solutions of the  $\alpha$  and  $\beta$  forms of glucose are monitored over time with a GOx-based electrode (see Section 2). It is clear that the PDH-DCIP sensor generates a time-independent signal in these tests while the GOx-sensor, which specifically senses the  $\beta$ -anomer, shows a gradual change towards a constant value. This provides strong experimental evidence that the PDH-biosensor exhibits the expected non-specificity (unlike the GOx-sensor) and that the new sensor can be used directly to monitor cellulase activity without any interference from mutarotation. This conclusion was further supported by comparisons with the signal from a CDH-sensor [14].

### 3.5. Application of the PDH-biosensor to real-time measurements of enzymatic hydrolysis of cellulose

A PDH-DCIP-biosensor covered with a 100 nm pore-size polycarbonate membrane was used for real-time measurements of the initial kinetics of the inverting cellobiohydrolase, *HjCel6A*. The sensor was calibrated against cellobiose, which is the major product of *HjCel6A* [54]. The results can be seen in Fig. 6. The left panels show the release of cellobiose from two different cellulosic substrates, BMCC and Avicel, when the dosage of cellulose is increased and the enzyme load is kept constant. The right panels in Fig. 6 show the steady state hydrolysis rate (the slope between 500 and 600 s in the left panels) plotted as function of the substrate dosage. Results of a Michaelis–Menten-type analysis [27] of this data are shown in Table 1. The two substrates differ in physical properties [2,55] and this translates into the kinetic constants. Thus, while the turnover at

saturation substrate load ( $k_{cat,app}$ ) is similar for the two substrates,  $pK_M$  was lower for BMCC. This implies that the affinity of *HjCel6A* is higher for BMCC than for Avicel, and this observation may simply reflect that the accessible area per mass unit (and hence probably the number of binding sites) is much higher for BMCC compared to Avicel [56,57].

### 3.6. Operational stability and reproducibility of preparing the PDH-biosensors

The PDH-biosensors generally showed very good operational stability. The sensor covered with a 100 nm pore-size polycarbonate membrane, for example, had a RSD% of 3.4 for the sensitivity over two days while in continuous use (insert in the lower panel in Fig. 4). Such a slow drop can readily be handled through regular calibrations. PDH-DCIP sensors could be produced quite uniformly, and the sensitivity for three sensors prepared in the same way varied 10% (see Fig. 7). These PDH-biosensors had a RSD% of 17.4, 3.9 and

**Table 1**

Kinetic parameters for *HjCel6A* acting on bacterial microcrystalline cellulose (BMCC) and Avicel. The parameters were found from analysis of the data in the right panels in Fig. 6 with respect to a Michaelis–Menten type equation for processive cellulases.

|        | $k_{cat,app}$ ( $\text{s}^{-1}$ ) <sup>a</sup> | $pK_M$ (g/L) <sup>b</sup> | $k_{cat,app}/pK_M$ ( $(\text{g/L})^{-1} \text{s}^{-1}$ ) <sup>c</sup> | $R^2$  |
|--------|------------------------------------------------|---------------------------|-----------------------------------------------------------------------|--------|
| BMCC   | 0.386                                          | 0.74                      | 0.52                                                                  | 0.9892 |
| Avicel | 0.404                                          | 5.0                       | 0.081                                                                 | 0.9891 |

<sup>a</sup>  $k_{cat,app}$  is the maximal apparent specific activity; i.e. the asymptotic value in the right panels in Fig. 6.

<sup>b</sup>  $pK_M$  is the processive dissociation-constants.

<sup>c</sup> Substrate specificity.



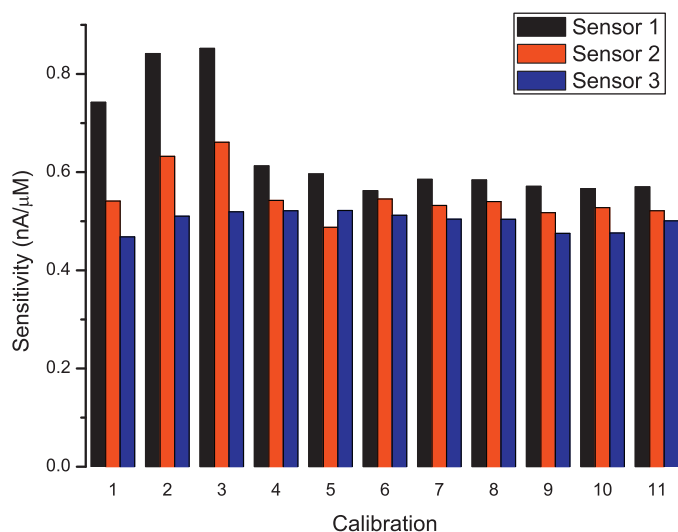


Fig. 7. Change in the sensitivity for three Nafion-polycarbonate (15 nm)-PDH-DCIP-biosensors over a two-week period with continuous use.

9.3 for the sensitivity over two-week period while in continuous use in enzymatic hydrolysis experiments.

#### 4. Conclusion

In conclusion, it has been shown that a mediated amperometric biosensor using immobilized pyranose dehydrogenase from *A. meleagris* on a carbon paste electrode and DCIP as mediator provides an advantageous approach to kinetic studies of cellulases. The PDH-biosensor is anomer unspecific and can therefore be used in continuous studies of both retaining- and inverting cellulases over different time-scales. The PDH-DCIP-biosensor showed high sensitivity and when covered with a polycarbonate membrane the stability was several weeks with daily use. The new sensor had a reasonable time resolution, which allowed steady-state recordings within tens of seconds, but it did not respond fast enough to capture transient enzyme kinetics as in the case of some CDH-sensors [14,17]. The PDH-biosensor was used to measure the initial activity of the inverting cellobiohydrolase *HjCel6A* acting on its natural insoluble substrate, cellulose. For *HjCel6A* acting on substrates with different morphology the dependence of the steady-state rate on the amount of substrate could be rationalized by a steady-state equation for processive cellulases.

#### Conflict of interest statement

Novozymes is a enzyme producing company.

#### Acknowledgments

This work was supported by the Danish Agency for Science, Technology and Innovation, Programme Commission on Sustainable Energy and Environment (Grant # 2104-07-0028 to P.W.) and the Ministry of Education, Culture, Sports, Science, and Technology in Japan (grant-in-aid for young scientists # 23760746 and special coordination funds for promoting science and technology to H.T.).

#### Appendix A. Supplementary data

Supplementary data associated with this article can be found, in the online version, at <http://dx.doi.org/10.1016/j.enzmictec.2014.03.002>.

#### References

- [1] Mansfield SD, Mooney C, Saddler JN. Substrate and enzyme characteristics that limit cellulose hydrolysis. *Biotechnol Prog* 1999;15:804–16.
- [2] Zhang YHP, Lynd LR. Toward an aggregated understanding of enzymatic hydrolysis of cellulose: noncomplexed cellulase systems. *Biotechnol Bioeng* 2004;88:797–824.
- [3] Yang B, Dai Z, Ding S, Wyman CE. Enzymatic hydrolysis of cellulosic biomass. *Biofuels* 2011;2:421–50.
- [4] Turon X, Rojas OJ, Deinhammer RS. Enzymatic kinetics of cellulose hydrolysis: a QCM-D study. *Langmuir* 2008;24:3880–7.
- [5] Maurer SA, Bedbrook CN, Radke CJ. Competitive sorption kinetics of inhibited endo- and exoglucanases on a model cellulose substrate. *Langmuir* 2012;28:14598–608.
- [6] Martin-Sampedro R, Rahikainen JL, Johansson L-S, Marjamaa K, Laine J, Kruus K, et al. Preferential adsorption and activity of monocomponent cellulases on lignocellulose thin films with varying lignin content. *Biomacromolecules* 2013;14:1231–9.
- [7] Suchy M, Linder MB, Tammelin T, Campbell JM, Vuorinen T, Kontturi E. Quantitative assessment of the enzymatic degradation of amorphous cellulose by using a quartz crystal microbalance with dissipation monitoring. *Langmuir* 2011;27:8819–28.
- [8] Hu G, Heitmann JA, Rojas OJ. Quantification of cellulase activity using the quartz crystal microbalance technique. *Anal Chem* 2009;81:1872–80.
- [9] Cruys-Bagger N, Tatsumi H, Borch K, Westh P. A graphene modified screen-printed carbon electrode for measurements of unoccupied active sites in a cellulase. *Anal Biochem* 2014;447:162–8.
- [10] Murphy L, Baumann MJ, Borch K, Sweeney M, Westh P. An enzymatic signal amplification system for calorimetric studies of cellobiohydrolases. *Anal Biochem* 2010;404:140–8.
- [11] Murphy L, Borch K, McFarland KC, Bohlin C, Westh P. A calorimetric assay for enzymatic saccharification of biomass. *Enzyme Microb Technol* 2010;46:141–6.
- [12] Olsen SN, Bohlin C, Murphy L, Borch K, McFarland KC, Sweeney MD, et al. Effects of non-ionic surfactants on the interactions between cellulases and tannic acid: a model system for cellulase-poly-phenol interactions. *Enzyme Microb Technol* 2011;49:353–9.
- [13] Murphy L, Bohlin C, Baumann MJ, Olsen SN, Sorensen TH, Anderson L, et al. Product inhibition of five *Hypocrea jecorina* cellulases. *Enzyme Microb Technol* 2013;52:163–9.
- [14] Cruys-Bagger N, Ren G, Tatsumi H, Baumann MJ, Spodsberg N, Andersen HD, et al. An amperometric enzyme biosensor for real-time measurements of cellobiohydrolase activity on insoluble cellulose. *Biotechnol Bioeng* 2012;109:3199–204.
- [15] Tatsumi H, Katano H, Ikeda T. Kinetic analysis of enzymatic hydrolysis of crystalline cellulose by cellobiohydrolase using an amperometric biosensor. *Anal Biochem* 2006;357:257–61.
- [16] Murphy L, Cruys-Bagger N, Damgaard HD, Baumann MJ, Olsen SN, Borch K, et al. Origin of initial burst in activity for *Trichoderma reesei* endo-glucanases hydrolyzing insoluble cellulose. *J Biol Chem* 2012;287:1252–60.
- [17] Cruys-Bagger N, Elmerdahl J, Praestgaard E, Tatsumi H, Spodsberg N, Borch K, et al. Pre-steady-state kinetics for hydrolysis of insoluble cellulose by cellobiohydrolase Cel7A. *J Biol Chem* 2012;287:18451–8.
- [18] Cruys-Bagger N, Tatsumi H, Ren G, Borch K, Westh P. Transient kinetics and rate limiting steps for the processive cellobiohydrolase Cel7A: effects of substrate structure and carbohydrate binding domain. *Biochemistry* 2013;52:8938–48.
- [19] Sygmund C, Kittl R, Volc J, Halada P, Kubatova E, Haltrich D, et al. Characterization of pyranose dehydrogenase from *Agaricus meleagris* and its application in the C-2 specific conversion of D-galactose. *J Biotechnol* 2008;133:334–42.
- [20] Kittl R, Sygmund C, Halada P, Volc J, Divne C, Haltrich D, et al. Molecular cloning of three pyranose dehydrogenase-encoding genes from *Agaricus meleagris* and analysis of their expression by real-time RT-PCR. *Curr Genet* 2008;53:117–27.
- [21] Sedmera P, Halada P, Kubatova E, Haltrich D, Prikylova V, Volc J. New biotransformations of some reducing sugars to the corresponding (di)hydro(glycosyl) aldehydes or aldonic acids using fungal pyranose dehydrogenase. *J Mol Catal B: Enzym* 2006;41:32–42.
- [22] Tasca F, Timur S, Ludwig R, Haltrich D, Volc J, Antiochia R, et al. Amperometric biosensors for detection of sugars based on the electrical wiring of different pyranose oxidases and pyranose dehydrogenases with osmium redox polymer on graphite electrodes. *Electroanalysis* 2007;19:294–302.
- [23] Yakovleva ME, Killyeni A, Ortiz R, Schulz C, MacAodha D, Conghaile PO, et al. Recombinant pyranose dehydrogenase-A versatile enzyme possessing both mediated and direct electron transfer. *Electrochem Commun* 2012;24:120–2.
- [24] Tasca F, Gorton L, Kujawa M, Patel I, Harreither W, Peterbauer CK, et al. Increasing the coulombic efficiency of glucose biofuel cell anodes by combination of redox enzymes. *Biosens Bioelectron* 2010;25:1710–6.
- [25] Minling S, Zafar MN, Sygmund C, Guschin DA, Ludwig R, Peterbauer CK, et al. Mutual enhancement of the current density and the coulombic efficiency for a bioanode by entrapping bi-enzymes with Os-complex modified electrodeposition paints. *Biosens Bioelectron* 2013;40:308–14.
- [26] Shao M, Zafar MN, Falk M, Ludwig R, Sygmund C, Peterbauer CK, et al. Optimization of a membraneless glucose/oxygen enzymatic fuel cell based on a bioanode with high coulombic efficiency and current density. *Chemphyschem* 2013;14:2260–9.
- [27] Cruys-Bagger N, Elmerdahl J, Praestgaard E, Borch K, Westh P. A steady state theory for processive cellulases. *FEBS J* 2013;280:3952–61.

- [28] Hall M, Bansal P, Lee JH, Realf MJ, Bommarius AS. Cellulose crystallinity – a key predictor of the enzymatic hydrolysis rate. *FEBS J* 2010;277:1571–82.
- [29] Park S, Baker JO, Himmel ME, Parilla PA, Johnson DK. Cellulose crystallinity index: measurement techniques and their impact on interpreting cellulase performance. *Biotechnol Biofuels* 2010;3:10.
- [30] Velleste R, Teugjas H, Väljamäe P. Reducing end-specific fluorescence labeled celluloses for cellulase mode of action. *Cellulose* 2010;17:125–38.
- [31] Boisset C, Fraschini C, Schulein M, Henrissat B, Chanzy H. Imaging the enzymatic digestion of bacterial cellulose ribbons reveals the endo character of the cellobiohydrolase Cel6A from *Humicola insolens* and its mode of synergy with cellobiohydrolase Cel7A. *Appl Environ Microbiol* 2000;66:1444–52.
- [32] Väljamäe P, Sild V, Nutt A, Pettersson G, Johansson G. Acid hydrolysis of bacterial cellulose reveals different modes of synergistic action between cellobiohydrolase I and endoglucanase I. *Eur J Biochem* 1999;266:327–34.
- [33] Tatsumi H, Katano H. Kinetics of the surface hydrolysis of raw starch by glucoamylase. *J Agric Food Chem* 2005;53:8123–7.
- [34] Tatsumi H, Katano H, Ikeda T. Activity measurements of chitosanase by an amperometric biosensor. *Anal Sci* 2009;25:825–7.
- [35] Ikeda T, Hamada H, Miki K, Senda M. Glucose-oxidase immobilized benzoquinone carbon paste electrode as a glucose sensor. *Agric Biol Chem* 1985;49:541–3.
- [36] Ikeda T, Hamada H, Senda M. Electrocatalytic oxidation of glucose at a glucose oxidase-immobilized benzoquinone mixed carbon paste electrode. *Agric Biol Chem* 1986;50:883–90.
- [37] Cass AEG, Davis G, Francis GD, Hill HAO, Aston WJ, Higgins IJ, et al. Ferrocene-mediated enzyme electrode for amperometric determination of glucose. *Anal Chem* 1984;56:667–71.
- [38] Wang J, Wu LH, Lu ZL, Li RL, Sanchez J. Mixed ferrocene glucose-oxidase carbon paste electrode for amperometric determination of glucose. *Anal Chim Acta* 1990;228:251–7.
- [39] Tang HT, Hajizadeh K, Halsall HB, Heineman WR. Flow-injection analysis with electrochemical detection of reduced nicotinamide adenine-dinucleotide using 2,6-dichloroindophenol as a redox coupling agent. *Anal Biochem* 1991;192:243–50.
- [40] Dicu D, Munteanu FD, Popescu IC, Gorton L. Indophenol and O-quinone derivatives immobilized on zirconium phosphate for NADH electro-oxidation. *Anal Lett* 2003;36:1755–79.
- [41] Tang HT, Halsall HB, Heineman WR. Electrochemical enzyme-immunoassay for phenytoin by flow-injection analysis incorporating a redox coupling agent. *Clin Chem* 1991;37:245–8.
- [42] Yao H, Halsall HB, Heineman WR, Jenkins SH. Electrochemical dehydrogenase-based homogeneous assays in whole-blood. *Clin Chem* 1995;41:591–8.
- [43] Barlag RE, Halsall HB, Heineman WR. Amperometric homogeneous competitive immunoassay in a perfluorocarbon emulsion oxygen therapeutic (PEOT). *Anal Bioanal Chem* 2013;405:3541–7.
- [44] Mullen WH, Churchouse SJ, Vadgama PM. Enzyme electrode for glucose based on the quinoprotein glucose-dehydrogenase. *Analyst* 1985;110:925–8.
- [45] Hirano K, Yamato H, Kunimoto K, Ohwa M. Design of novel electron transfer mediators based on indophenol derivatives for lactate sensor. *Biosens Bioelectron* 2002;17:315–22.
- [46] Hassan RYA, Bilitewski U. A viability assay for *Candida albicans* based on the electron transfer mediator 2,6-dichlorophenolindophenol. *Anal Biochem* 2011;419:26–32.
- [47] Barlag RE, Halsall HB, Heineman WR. Cyclic voltammetry in a perfluorocarbon emulsion blood substitute. *Electroanalysis* 2007;19:1139–44.
- [48] Cruys-Bagger N. Development of isothermal microcalorimetry with in-situ electrochemical enzyme sensors. Denmark: Roskilde University; 2010 <http://rudar.ruc.dk/handle/1800/5428>
- [49] Davies G, Henrissat B. Structures and mechanisms of glycosyl hydrolases. *Structure* 1995;3:853–9.
- [50] McCarter JD, Withers SG. Mechanisms of enzymatic glycoside hydrolysis. *Curr Opin Struct Biol* 1994;4:885–92.
- [51] Withers SG. Mechanisms of glycosyl transferases and hydrolases. *Carbohydr Polym* 2001;44:325–37.
- [52] Kabayama MA, Patterson D. The thermodynamics of mutarotation of some sugars. 1. Measurement of the heat of mutarotation by microcalorimetry. *Can J Chem* 1958;33:557–62.
- [53] Kendrew JC, Moelwyn-Hughes EA. The kinetics of mutarotation in solution. *Proc R Soc Lond A: Math Phys Sci* 1940;176:0352–367.
- [54] Koivula A, Kinnari T, Harjunpää V, Ruohonen L, Telemann A, Drakenberg T, et al. Tryptophan 272: an essential determinant of crystalline cellulose degradation by *Trichoderma reesei* cellobiohydrolase Cel6A. *FEBS Lett* 1998;429:341–6.
- [55] Zhang YHP, Himmel ME, Mielenz JR. Outlook for cellulase improvement: screening and selection strategies. *Biotechnol Adv* 2006;24:452.
- [56] Hong J, Ye X, Zhang YHP. Quantitative determination of cellulose accessibility to cellulase based on adsorption of a nonhydrolytic fusion protein containing CBM and GFP with its applications. *Langmuir* 2007;23:12535–40.
- [57] Jalak J, Väljamäe P. Mechanism of initial rapid rate retardation in cellobiohydrolase catalyzed cellulose hydrolysis. *Biotechnol Bioeng* 2010;106:871–83.



Temperature Effects on Kinetic Parameters and  
Substrate Affinity of Cel7A Cellobiohydrolases

---

VIII



# Temperature Effects on Kinetic Parameters and Substrate Affinity of Cel7A Cellobiohydrolases\*

Received for publication, April 16, 2015, and in revised form, July 15, 2015 Published, JBC Papers in Press, July 16, 2015, DOI 10.1074/jbc.M115.658930

Trine Holst Sørensen<sup>‡</sup>, Nicolaj Cruys-Bagger<sup>‡</sup>, Michael Skovbo Windahl<sup>‡§</sup>, Silke Flindt Badino<sup>‡§</sup>, Kim Borch<sup>§</sup>, and Peter Westh<sup>‡1</sup>

From <sup>‡</sup>Roskilde University, Nature, Systems, and Models, Research Unit for Functional Biomaterials, 1 Universitetsvej, Building 28, DK-4000 Roskilde, Denmark and <sup>§</sup>Novozymes A/S, Krogshøjvej 36, DK-2880 Bagsværd, Denmark

**Background:** Temperature concomitantly modulates kinetic and adsorption properties in heterogeneous enzyme catalysis.

**Results:** Affinity-activity relationships for four Cel7A cellobiohydrolases are characterized over a broad temperature interval.

**Conclusion:** Cellobiohydrolases are strongly activated by temperature at high, but not at low, substrate loads.

**Significance:** Fundamental insight into cellulolytic mechanisms at high (industrially relevant) temperatures is gained.

We measured hydrolytic rates of four purified cellulases in small increments of temperature (10–50 °C) and substrate loads (0–100 g/liter) and analyzed the data by a steady state kinetic model that accounts for the processive mechanism. We used wild type cellobiohydrolases (Cel7A) from mesophilic *Hypocrea jecorina* and thermophilic *Rasamsonia emersonii* and two variants of these enzymes designed to elucidate the role of the carbohydrate binding module (CBM). We consistently found that the maximal rate increased strongly with temperature, whereas the affinity for the insoluble substrate decreased, and as a result, the effect of temperature depended strongly on the substrate load. Thus, temperature had little or no effect on the hydrolytic rate in dilute substrate suspensions, whereas strong temperature activation ( $Q_{10}$  values up to 2.6) was observed at saturating substrate loads. The CBM had a dual effect on the activity. On one hand, it diminished the tendency of heat-induced desorption, but on the other hand, it had a pronounced negative effect on the maximal rate, which was 2-fold larger in variants without CBM throughout the investigated temperature range. We conclude that although the CBM is beneficial for affinity it slows down the catalytic process. Cel7A from the thermophilic organism was moderately more activated by temperature than the mesophilic analog. This is in accord with general theories on enzyme temperature adaptation and possibly relevant information for the selection of technical cellulases.

Cel7 cellobiohydrolases (cellulose 1,4- $\beta$ -cellobiosidase (reducing end): EC 3.2.1.176) are among the most effective cellulolytic enzymes and play an essential role in decomposition processes performed for example by ascomycete fungi. They also make up the dominant component in enzyme mixtures used industrially to convert lignocellulosic biomass to fermentable sugars (so-called saccharification). Both of these aspects have generated a substantial research interest in this group of

enzymes (1, 2), and many structural, mechanistic, and phylogenetic questions have been elucidated over the past decades. This work has established that some cellobiohydrolases follow a quite extraordinary reaction path with an initial attack on the end of the cellulose strand followed by sequential release of cellobiose as the enzyme slides along the cellulose crystal with a single polysaccharide strand threaded through a long tunnel with the catalytic site located toward the end. This processive mechanism is considered an effective way (3–5) to overcome the high chemical and physical stability of cellulose (6, 7) and therefore an important element in natural carbon cycling.

One key question in both fundamental and applied Cel7A research is how temperature affects this complex process, and different aspects of this have been addressed in earlier studies. Many of these have been motivated by industrial questions or aimed at clarifying the optimal temperature range for different wild type enzymes or engineered variants with improved thermal stability (8–13). This type of work typically quantifies the amount of soluble sugar produced from an insoluble substrate in end point measurements at variable temperatures with other experimental parameters kept constant. Some studies have applied a broader methodology and investigated temperature effects as a function of contact time and the loads of enzyme and (insoluble) substrate, respectively, and used this to identify optimal hydrolysis conditions (14, 15). In many cases, the overall rate of cellulose hydrolysis for purified enzyme or enzyme mixtures has been measured at different temperatures and interpreted along the lines of the Arrhenius equation. However, reported activation energies,  $E_a$ , vary (16–22), and in some cases, it is difficult to assign a physical meaning to reported  $E_a$  values as they are not defined with respect to a specific reaction scheme. Some studies have analyzed temperature effects on cellulolytic activity with respect to specific kinetic models. The majority of this work has used soluble substrate analogs, which are convenient to assay and allow interpretation within the Michaelis-Menten framework (1, 23, 24). This approach has provided important knowledge of the temperature response of cellulases including insight into differences between enzymes from organisms adapted to different temperatures. In contrast, work on small soluble substrates obviously does not capture any special behavior pertaining to processive hydrolysis of an insol-

\* This work was supported by Danish Council for Strategic Research, Program Commission on Sustainable Energy and Environment Grants 2104-07-0028 and 11-116772 (to P. W.) and by Carlsberg Foundation Grant 2013-01-0208 (to P. W.). Novozymes is a major enzyme-producing company.

<sup>1</sup> To whom correspondence should be addressed. Tel.: 45-4674-2879; Fax: 45-4674-3011; E-mail: pwesth@ruc.dk.



## Temperature Activation of Cel7A Cellobiohydrolases

uble substrate. A few studies have addressed this latter issue and analyzed the results with respect to deterministic models. Examples of this includes work by Zhang *et al.* (16), who studied the hydrolysis of rice straw by a crude cellulase extract between 37 and 50 °C and used a fractal kinetic model to rationalize the results. More recently, Ye and Berson (26) tested a kinetic model that accounted for both hydrolysis and enzyme inactivation against experimental data for a commercial enzyme mixture at different temperatures. Their results suggested that  $E_a$  for hydrolysis and inactivation was of comparable size (~70 kJ/mol). Brown *et al.* (27) tested a number of previously developed steady state models against a set of data based on lignocellulosic biomass and a fungal enzyme mixture. They concluded that a three-parameter model, which accounted for the number of reactive sites covered by the enzymes, represented their data well. This approach gave a linear Arrhenius plot with an activation energy of 48 kJ/mol.

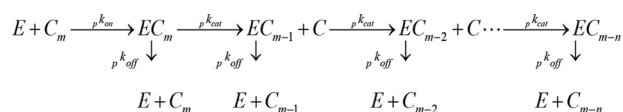
However, systematic investigations of temperature effects on the hydrolysis of insoluble substrate are scarce, and we are not aware of any earlier studies on monocomponent cellulases that report systematic temperature-activity data and rationalize them with respect to a relevant theoretical framework. To address this, we implemented a medium throughput assay and measured activity and adsorption in small increments of temperature (10–50 °C) and substrate load (0–100 g/liter). Results from 1-h trials with a pure cellulose substrate (Avicel) were used to estimate steady state reaction rates at low degrees of conversion and were analyzed with respect to a Michaelis-Menten-type model for processive enzymes described previously (28). We report the temperature dependence of kinetic parameters for four processive enzymes, which were selected to clarify affinity-activity relationships and the effect of natural adaptation to higher temperatures. Specifically, we compared Cel7A enzymes from *Hypocrea jecorina* (often identified by the name of its anamorph, *Trichoderma reesei*) and the thermophile *Rasamsonia emersonii* (previously *Talaromyces emersonii*) (29). The catalytic domains of these two enzymes are structurally homologous and have a sequence identity of 66% (30), but the intact enzymes are distinctively different in the sense that *H. jecorina* Cel7A has a two-module architecture with a catalytic domain and a family I carbohydrate binding module (CBM)<sup>2</sup> connected through a flexible, glycosylated linker (31). Conversely, *R. emersonii* Cel7A only consists of a catalytic domain (30, 32). In addition to these two wild type enzymes, we also studied two enzyme variants designed to highlight the role of the CBM. One was the catalytic domain of *H. jecorina* Cel7A without CBM and linker, and the other was a chimeric protein composed of the linker and CBM from *H. jecorina* Cel7A and the *R. emersonii* enzyme. Henceforth, we will refer to these enzymes by their origin (*Hj* or *Re*) followed by subscript “CORE” or “CBM” for one- and two-domain variants, respectively (e.g.  $Hj_{CBM}$  for the *H. jecorina* wild type).

<sup>2</sup> The abbreviations used are: CBM, carbohydrate binding domain; CORE, catalytic domain;  $Hj_{CBM}$ , cellobiohydrolase Cel7A from *H. jecorina* (wild type with CORE and CBM);  $Hj_{CORE}$ , *H. jecorina* Cel7A variant without CBM;  $Re_{CORE}$ , Cel7A from *R. emersonii* (wild type without CBM);  $Re_{CBM}$ , chimeric enzyme with CORE from *R. emersonii* and CBM from *H. jecorina*; Bis-Tris, 2-[bis(2-hydroxyethyl)amino]-2-(hydroxymethyl)propane-1,3-diol.

## Experimental Procedures

**Enzymes**—*H. jecorina* Cel7A and *R. emersonii* Cel7A wild types were expressed in *Aspergillus oryzae* as described previously (33). Expression of the fusion protein ( $Re_{CBM}$ ) and the *H. jecorina* Cel7A core ( $Hj_{CORE}$ ) (residues 18–453 of UniProt entry G0RVK1) has also been described earlier (33). All enzymes were purified from fermentation broths by hydrophobic interaction chromatography followed by ion exchange chromatography on the ÄKTA system (GE Healthcare). Fermentation broths were filtered through a bottle polyethersulfone top filter with a 0.22- $\mu$ m cutoff, and ammonium sulfate was added to make a 1.8 M solution. Subsequently, the fermentation broths were applied to a 200-ml phenyl-Sepharose® 6 (high sub) FastFlow column XK50 (GE Healthcare), which had been pre-equilibrated with 1.8 M ammonium sulfate, 25 mM HEPES, pH 7.0. The column was washed with equilibration buffer followed by 0.54 M ammonium sulfate. Cel7As were batch-eluted with 25 mM HEPES, pH 7.0 and desalted on a Sephadex™ G-25 (medium) column (GE Healthcare) equilibrated with 25 mM MES, pH 6.0. Next, the Cel7As were applied to a 60-ml SOURCE™ 15Q column (GE Healthcare) equilibrated with 25 mM MES, pH 6.0. Cel7As from *H. jecorina* were eluted with a linear 50–300 mM sodium chloride gradient for 3 column volumes, whereas *R. emersonii* enzymes were eluted with a 100–200 mM sodium chloride gradient for 1.5 column volumes followed by 1.5 column volumes of 300 mM sodium chloride. Fractions were analyzed for the presence of Cel7A by SDS-PAGE using 12-well NuPAGE® 4–12% Bis-Tris gel (GE Healthcare). As estimated by SDS-PAGE and non-denaturing PAGE, the cellulases were purified to apparent homogeneity. The concentration of purified enzyme stocks was measured by amino acid analysis. Protein samples were dried down and hydrolyzed in 18.5% HCl, 0.1% phenol at 110 °C for 16 h. Amino acid analyses were performed by precolumn derivatization using the Waters AccQ-Tag Ultra method. In short, amino acids were derivatized by the AccQ-Tag Ultra reagent, separated with reversed phase ultraperformance LC (Waters), and the derivatives were quantitated based on UV absorbance. Enzyme concentrations were also measured by conventional UV absorption (34) at 280 nm. We used the following molar extinction coefficients:  $Hj_{CBM}$ , 86,760 M<sup>-1</sup> cm<sup>-1</sup>;  $Hj_{CORE}$ , 80,550 M<sup>-1</sup> cm<sup>-1</sup>;  $Re_{CBM}$ , 81,135 M<sup>-1</sup> cm<sup>-1</sup>; and  $Re_{CORE}$ , 74,925 M<sup>-1</sup> cm<sup>-1</sup>. No systematic differences between these two methods were detected.

**Activity Assay**—Hydrolysis of insoluble cellulose was quantified by the *para*-hydroxybenzoic acid hydrazide method (35). Avicel PH101 (Sigma-Aldrich) was washed six times in Milli-Q water and twice in buffer (50 mM acetate, pH 5.0; henceforth called standard buffer). Washed Avicel PH101 was suspended in 50 mM acetate, pH 5.0, and aliquots of 230  $\mu$ l with loads between 0 and 106 g/liter were transferred to 96-well plates (96F 26960, Thermo Scientific). The outermost wells of the microtiter plate were not used for hydrolysis experiments. The plates were initially equilibrated at the experimental temperature (10–50 °C) for 20 min in an Eppendorf Thermomixer, and the reaction was started by the addition of 20  $\mu$ l of enzyme stocks to a final concentration of 400 nM. The plates were mixed



SCHEME 1. Simplified reaction scheme used to characterize processive activity of Cel7A enzymes against insoluble cellulose.

at 1100 rpm at the desired temperature for 1 h, and the reaction was then stopped by centrifugation for 3 min at 3500 rpm at 5 °C (Hereaus Multifuge 3 S-R). The choice of reaction time and enzyme concentration was made after initial trials had shown readily detectable product concentrations ( $> \sim 1 \mu\text{M}$ ) at the lowest temperatures and substrate loads studied here. It was also suitable in the sense that product concentrations in samples with the highest substrate loads were much lower than published inhibition constants for Cel7A (36–38). Hence, we neglected product inhibition in the data analysis. To measure the concentration of soluble, reducing sugars, 50  $\mu\text{l}$  of supernatant was transferred to 96-well PCR sample tubes (0.2-ml non-skirted 96-well PCR plate, AB0600, Thermo Scientific) and 75  $\mu\text{l}$  of 15 mg/ml *para*-hydroxybenzoic acid hydrazide solution (4-hydroxybenzhydrazide; H9882, Sigma) dissolved in buffer (0.18 M potassium sodium tartrate (108087, Merck) was added. Subsequently, the PCR sample tubes were placed in a Peltier thermal cycler and incubated at 95 °C for 10 min and 20 °C for 5 min. One hundred microliters were transferred from the 96-well PCR sample tubes to a 96-well plate (96F 26960, Thermo Scientific). Absorption at 405 nm was determined in a plate reader (Molecular Devices SpectraMax M2), and the soluble reducing sugars were quantified based on standards with 0–0.5 mM cellobiose. Blanks (without enzyme) were included and subtracted for all measurements. All experiments were carried out in triplicates.

**Adsorption**—One hundred microliters of supernatant was retrieved from each sample in the activity assay and transferred to a 96-well microtiter plate (655079, Greiner Bio One). The intrinsic protein fluorescence at 340 nm was determined in a plate reader (Molecular Devices SpectraMax M2) using an excitation wavelength of 280 nm. For these experiments, standard curves ranging from 0 to 800 nM Cel7A ( $Hj_{CBM}$ ,  $Hj_{CORE}$ ,  $Re_{CBM}$ , or  $Re_{CORE}$ ) were included.

**Kinetic Theory**—Measurements of hydrolytic activity were analyzed by a steady state model for processive enzymes (28, 39). The starting point is a simplified scheme (Scheme 1), which uses three rate constants and a processivity number to describe the reaction. It is assumed that the free enzyme,  $E$ , combines with a cellulose strand,  $C_m$ , to form a complex,  $EC_m$ . The complex now goes through consecutive catalytic steps, which release the product cellobiose,  $C$ , and concomitantly shorten the cellulose strand to  $EC_{m-1}$ ,  $EC_{m-2}$ , etc. This course is governed by the rate constants,  $p k_{on}$ ,  $p k_{cat}$ , and  $p k_{off}$  as specified in the scheme (subscript  $p$  in front of the parameter indicates its relationship to the processive Scheme 1). The last parameter,  $n$ , is the average number of steps following one association (the processivity number), which can be measured experimentally albeit with some technical challenges (40). We note that Scheme 1 was chosen as a compromise between the structural and empirical understanding of Cel7A catalysis on one hand and simplicity on the other hand. Other descriptions of the

reaction course could be equally meaningful and able to fit the data, although we surmise that the current level of structural and quantitative data for association and dissociation would be too limited to justify more complex reaction schemes.

The steady state rate of cellobiose production,  $p v_{ss} = d[C]/dt$ , can be expressed (28) as follows.

$$p v_{ss} = \frac{S_0 E_0 p k_{cat} \left( 1 - \left( \frac{p k_{cat}}{p k_{cat} + p k_{off}} \right)^n \right)}{\frac{p k_{off}}{p k_{on}} + S_0} \quad (\text{Eq. 1})$$

where  $E_0$  and  $S_0$  are the total concentration of enzyme (in  $\mu\text{M}$ ) and substrate (in g/liter), respectively. To simplify Equation 1 and illustrate its relationship to the usual Michaelis-Menten equation, we define a maximal processive rate,  $p V_{max}$ , and a processive analog of the Michaelis constant,  $p K_m$ .

$$p V_{max} = E_0 p k_{cat} \left( 1 - \left( \frac{p k_{cat}}{p k_{cat} + p k_{off}} \right)^n \right), \quad p K_m = \frac{p k_{off}}{p k_{on}} \quad (\text{Eq. 2})$$

Inserting Equation 2 into Equation 1 yields the usual hyperbolic form.

$$p v_{ss} = \frac{p V_{max} S_0}{p K_m + S_0} \quad (\text{Eq. 3})$$

We note that  $p v_{ss}$  is an approximation of the steady state rate as Cel7A (as well as other cellulases) show so-called non-linear kinetics where the progress curves never become fully linear. However, we have previously discussed advantages and limitations of Equation 3 and suggested that it is useful for the analysis of short experiments like those considered here (28). The strategy for the current work was to fit Equation 3 to experimental data for  $p v_{ss}(S_0)$  at different temperatures and for different enzymes. The resulting parameters,  $p V_{max}$  and  $p K_m$ , and their temperature dependence were then used to illustrate temperature effects on affinity and kinetics.

## Results

Steady state rates,  $p v_{ss}$ , for the four investigated enzymes were estimated as the ratio of the final cellobiose concentration and the contact time (1 h) and normalized with respect to the total enzyme concentration ( $E_0 = 0.40 \mu\text{M}$ ) to obtain the specific activity,  $p v_{ss}/E_0$ , in units of  $\text{s}^{-1}$ . Fig. 1 illustrates how this parameter changed with substrate load and temperature; *symbols* represent experimental data, and the *lines* are best fits of Equation 3. It appears that the model accounted well for the data under all investigated conditions. The highest conversions of Avicel reached in these experiments were below 1% (in most cases much below).

The kinetic parameters  $p V_{max}/E_0$  and  $p K_m$  derived from the non-linear regression are listed in Table 1 and plotted as a function of temperature in Fig. 2. In most cases, the highest measured rate was close to  $p V_{max}$ , and as a result, the two kinetic parameters in Equation 3 could be well resolved with very low parameter interdependence. However, for one-domain enzymes at the highest investigated temperatures, saturating



# Temperature Activation of Cel7A Cellobiohydrolases

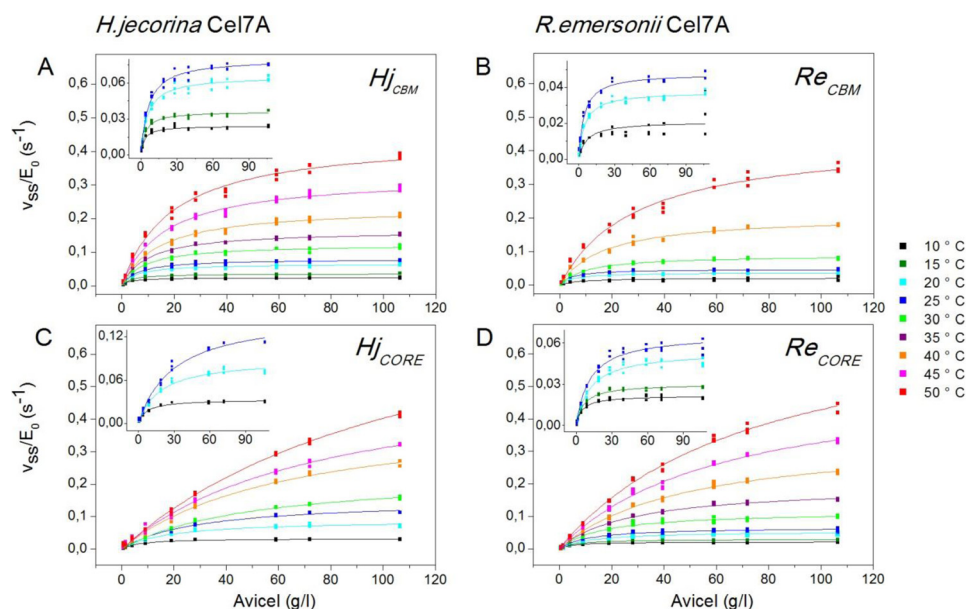


FIGURE 1. Specific enzyme activity ( $v_{ss}/E_0$ ) for  $Hj_{CBM}$  (A),  $Re_{CBM}$  (B),  $Hj_{CORE}$  (C), and  $Re_{CORE}$  (D) plotted as a function of Avicel load (0–106 g/liter) between 10 and 50 °C. Symbols represent all experimental data from triplicate measurements, and lines are the best fit of Equation 3. Insets show enlargements of results at the lower temperatures, which are hard to assess on the main figures.

TABLE 1

Temperature dependence of kinetic and adsorption parameters for two Cel7A wild types,  $Hj_{CBM}$  and  $Re_{CORE}$ , and the corresponding constructs  $Hj_{CORE}$  and  $Re_{CBM}$

Maximal specific rates,  $pV_{max}/E_0$  ( $\pm$ S.E.) and processive Michaelis constants,  $pK_m$  ( $\pm$ S.E.) as defined in Equation 2 were derived from the regression analysis shown in Fig. 1. These two parameters were used to calculate the processive specificity constant,  $p\eta$ , defined in Equation 4. The last column shows the partitioning coefficient calculated from the free enzyme concentration measured at the end of the 1-h hydrolysis experiment (see Fig. 5).

| $T$                           | $pV_{max}/E_0$       | $pK_m$          | $p\eta$                                       | $K_p$           |
|-------------------------------|----------------------|-----------------|-----------------------------------------------|-----------------|
| °C                            | $s^{-1} \times 10^3$ | $g\ liter^{-1}$ | $(\mu\text{mol}\ s^{-1}\ g^{-1}) \times 10^3$ | $liter\ g^{-1}$ |
| <b><math>Hj_{CBM}</math></b>  |                      |                 |                                               |                 |
| 10                            | 24 ± 1               | 2.8 ± 0.3       | 3.4 ± 0.5                                     | 2.0             |
| 15                            | 36 ± 1               | 3.5 ± 0.3       | 4.1 ± 0.6                                     | 2.2             |
| 20                            | 65 ± 1               | 5.5 ± 0.5       | 4.7 ± 0.6                                     | 2.0             |
| 25                            | 80 ± 1               | 6.2 ± 0.5       | 5.1 ± 0.6                                     | 1.5             |
| 30                            | 123 ± 2              | 8.6 ± 0.6       | 5.7 ± 0.6                                     | 0.8             |
| 35                            | 165 ± 2              | 10 ± 0.4        | 6.6 ± 0.6                                     | 1.0             |
| 40                            | 234 ± 4              | 14 ± 0.9        | 6.6 ± 0.6                                     | 0.9             |
| 45                            | 328 ± 7              | 17 ± 1.1        | 7.9 ± 0.6                                     | 0.5             |
| 50                            | 442 ± 10             | 19 ± 1.3        | 9.3 ± 0.8                                     | 0.3             |
| <b><math>Hj_{CORE}</math></b> |                      |                 |                                               |                 |
| 10                            | 33 ± 1               | 7.1 ± 0.5       | 1.9 ± 0.2                                     | -               |
| 20                            | 90 ± 3               | 18 ± 1.7        | 2.0 ± 0.3                                     | 0.09            |
| 25                            | 152 ± 5              | 30 ± 2.6        | 2.0 ± 0.5                                     | 0.05            |
| 30                            | 232 ± 6              | 50 ± 2.6        | 1.9 ± 0.2                                     | 0.05            |
| 40                            | 425 ± 16             | 63 ± 4.7        | 2.7 ± 0.4                                     | 0.04            |
| 50                            | 895 ± 35             | 122 ± 8         | 2.9 ± 0.4                                     | 0.02            |
| <b><math>Re_{CBM}</math></b>  |                      |                 |                                               |                 |
| 10                            | 21 ± 2               | 2.8 ± 2.4       | 2.9 ± 1.0                                     | 2.3             |
| 20                            | 38 ± 1               | 4.5 ± 0.4       | 3.4 ± 0.5                                     | 1.0             |
| 25                            | 48 ± 1               | 4.5 ± 0.3       | 4.3 ± 0.5                                     | 0.5             |
| 30                            | 89 ± 1               | 10 ± 0.7        | 3.4 ± 0.5                                     | 0.7             |
| 40                            | 206 ± 5              | 17 ± 1.4        | 4.9 ± 0.6                                     | 0.3             |
| 50                            | 439 ± 15             | 29 ± 2.7        | 5.0 ± 0.7                                     | 0.6             |
| <b><math>Re_{CORE}</math></b> |                      |                 |                                               |                 |
| 10                            | 22 ± 1               | 4.9 ± 0.6       | 1.8 ± 0.3                                     | 0.5             |
| 15                            | 30 ± 1               | 6.5 ± 0.5       | 1.9 ± 0.3                                     | 0.4             |
| 20                            | 54 ± 1               | 12 ± 1.2        | 1.8 ± 0.3                                     | 0.2             |
| 25                            | 67 ± 2               | 12 ± 1.3        | 2.3 ± 0.4                                     | 0.1             |
| 30                            | 115 ± 4              | 17 ± 1.7        | 2.7 ± 0.6                                     | 0.2             |
| 35                            | 196 ± 3              | 30 ± 1.3        | 2.8 ± 0.5                                     | 0.1             |
| 40                            | 347 ± 9              | 48 ± 2.6        | 2.9 ± 0.4                                     | 0.08            |
| 45                            | 534 ± 15             | 63 ± 3.5        | 3.4 ± 0.4                                     | 0.07            |
| 50                            | 755 ± 28             | 76 ± 5.1        | 4.0 ± 0.5                                     | 0.03            |

conditions were well above the accessible range of substrate loads. This led to parameter interdependence between  $pV_{max}$  and  $pK_m$  and hence larger uncertainty (see Table 1). In these cases, only the initial slope (the specificity constant; see below) was precisely determined. One interesting result here is that at specified temperatures both  $pK_m$  and  $pV_{max}$  are consistently higher for the one-domain enzymes ( $Hj_{CORE}$  and  $Re_{CORE}$ ) compared with enzymes with a CBM ( $Hj_{CBM}$  and  $Re_{CBM}$ ). These differences are quite pronounced. Hence,  $pV_{max}$  is about twice as high for the one-domain enzymes throughout the investigated temperature range, and the effect on the CBM on  $pK_m$  is even larger. Table 1 and Fig. 2 also show the processive analog of the specificity constant,  $p\eta$ .

$$p\eta = \frac{pV_{max}}{pK_m} \quad (\text{Eq. 4})$$

The temperature dependence of this parameter is illustrated in Fig. 2C, and it appears that  $p\eta$  is both larger and more temperature-dependent for two-domain enzymes compared with variants with no CBM.

To further characterize temperature dependence, we made Arrhenius plots (*i.e.* natural logarithm of the parameter plotted against the reciprocal of the absolute temperature) for the data in Fig. 2. The results in Fig. 3 show linear relations, although the experimental scatter for  $p\eta$  was quite high in some cases. Activation energies,  $E_a$ , derived from the slopes in Fig. 3 were 60–70 kJ/mol for  $pV_{max}$  (Fig. 3A), 37–52 kJ/mol for  $pK_m$  (Fig. 3B), and 9–16 kJ/mol for  $p\eta$  (Fig. 3C).

Implications of these energy barriers along with other activation parameters pertaining to Scheme 1 are discussed in the companion article (62). Here, we are only interested in these plots as a practical measure of the temperature dependence of a kinetic parameter. One intuitive way to express the logarithmic relation is the so-called  $Q_{10}$  value, which signifies the relative

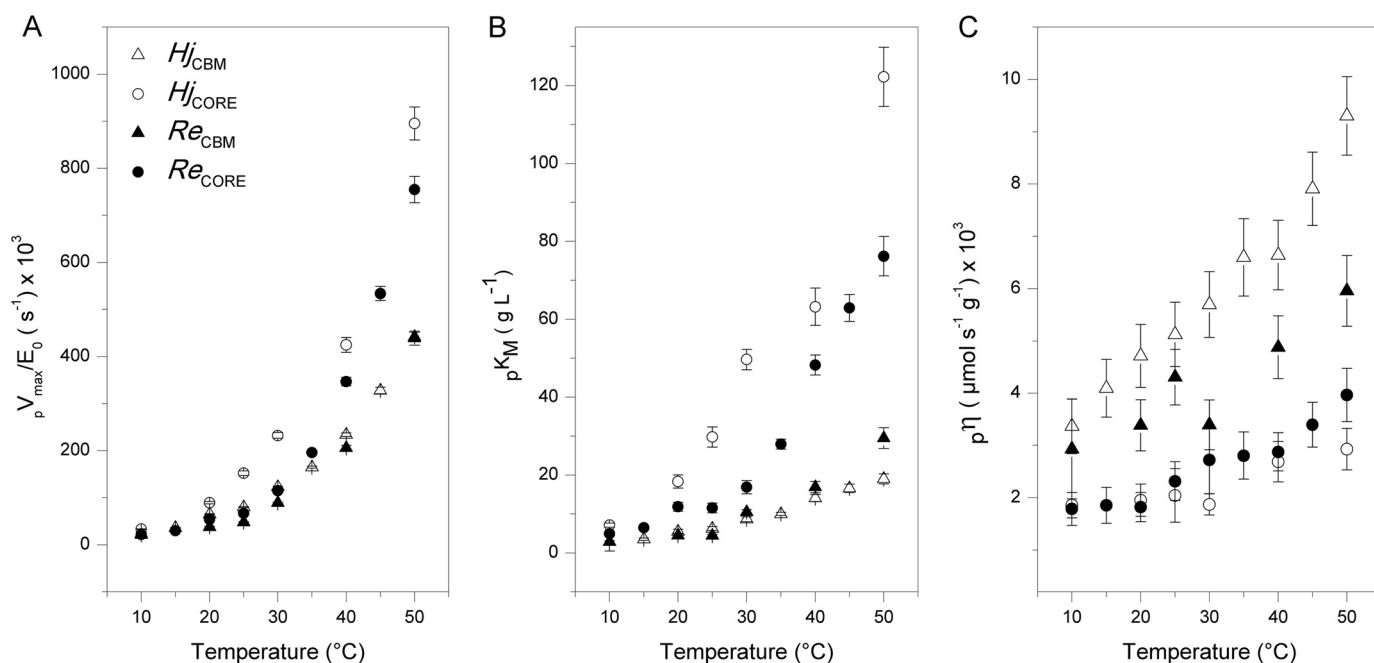


FIGURE 2. Maximum specific rate ( ${}_pV_{max}/E_0$ ; A), Michaelis constant ( ${}_pK_m$ ; B), and specificity constant ( ${}_p\eta$ ; C) plotted as a function of temperature for the four investigated enzymes.

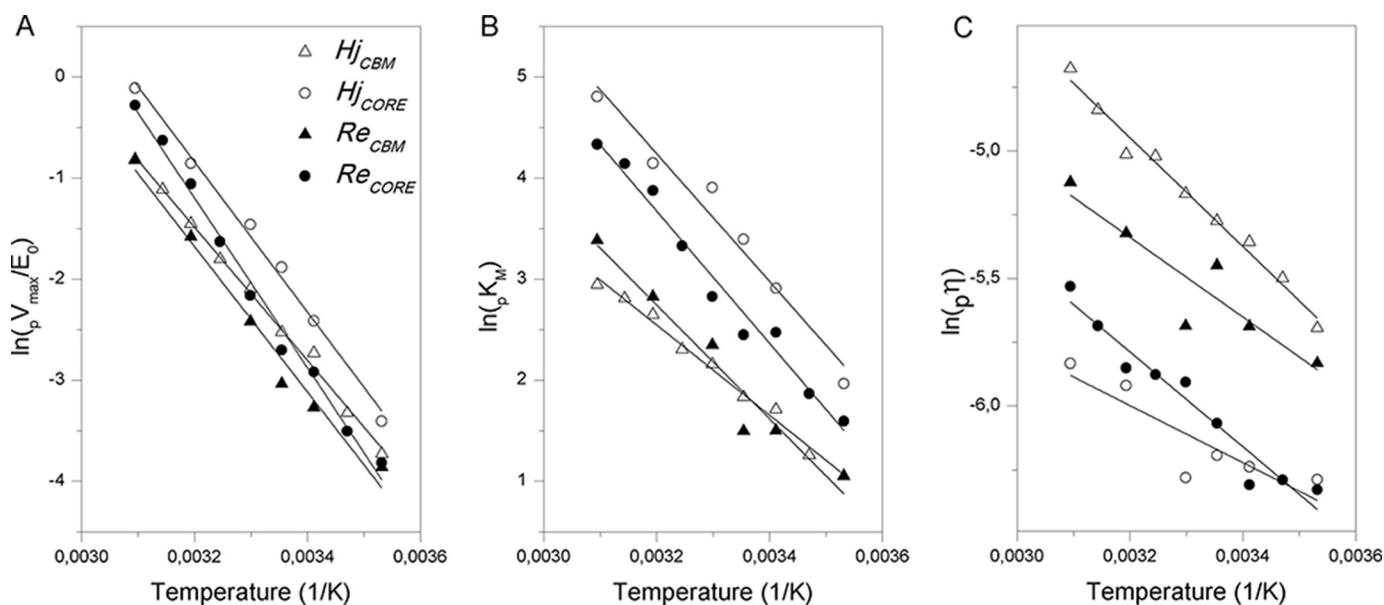


FIGURE 3. Arrhenius plots. The natural logarithm of the maximum specific rate ( ${}_pV_{max}$ ; A), the Michaelis constant ( ${}_pK_m$ ; B), and specificity constant ( ${}_p\eta$ ; C) are plotted against the reciprocal of the absolute temperature.

increment upon a 10 °C temperature increase. For many enzymes reactions around room temperature,  $Q_{10}$  for  $V_{max}$  has been shown to be about 2, thus implying that the reaction rate at saturating substrate loads doubles upon a 10 °C temperature rise ( $Q_{10} = 2$  at room temperature corresponds to an  $E_a$  of about 50 kJ/mol). The results in Fig. 3 corresponded<sup>3</sup> to  $Q_{10}$

<sup>3</sup> The  $Q_{10}$  values can be estimated from the activation energies,  $\ln(Q_{10}) = 10E_a/RT^2$ , at a given temperature. A statistically better approach is to plot the natural logarithm of a parameter against the temperature (rather than the reciprocal temperature). The slope of this plot,  $\alpha$ , is a direct (temperature-independent) measure of  $Q_{10}$ ,  $\ln(Q_{10}) = 10\alpha$ . We tried both ways and found the same results probably because the investigated temperature interval is quite small on the Kelvin scale.

values of 2.1–2.6 for  ${}_pV_{max}$ , whereas it was 1.6–2.1 for  ${}_pK_m$  and only 1.1–1.2 for  ${}_p\eta$ . To illustrate the meaning of this, we first note that the specificity constant,  ${}_p\eta$ , is the slope of the (near-linear) part of the curves in Fig. 1 at low substrate loads (*i.e.* for  $S \ll {}_pK_m$ ). It follows that  ${}_p\eta$  may be interpreted as an apparent second order rate constant, which governs the kinetics at low substrate loads,  $v_{ss} \approx {}_p\eta[E]_0[S]$  (41). This means that the reaction was much more activated by temperature at high substrate loads ( $Q_{10}$  for  ${}_pV_{max}$  was 2.1–2.6) than at low substrate loads ( $Q_{10}$  for  ${}_p\eta$  was 1.1–1.2). It is also interesting to consider average  $Q_{10}$  values for the investigated one- and two-domain enzymes and hence the effect of the CBM on temperature acti-

## Temperature Activation of Cel7A Cellobiohydrolases

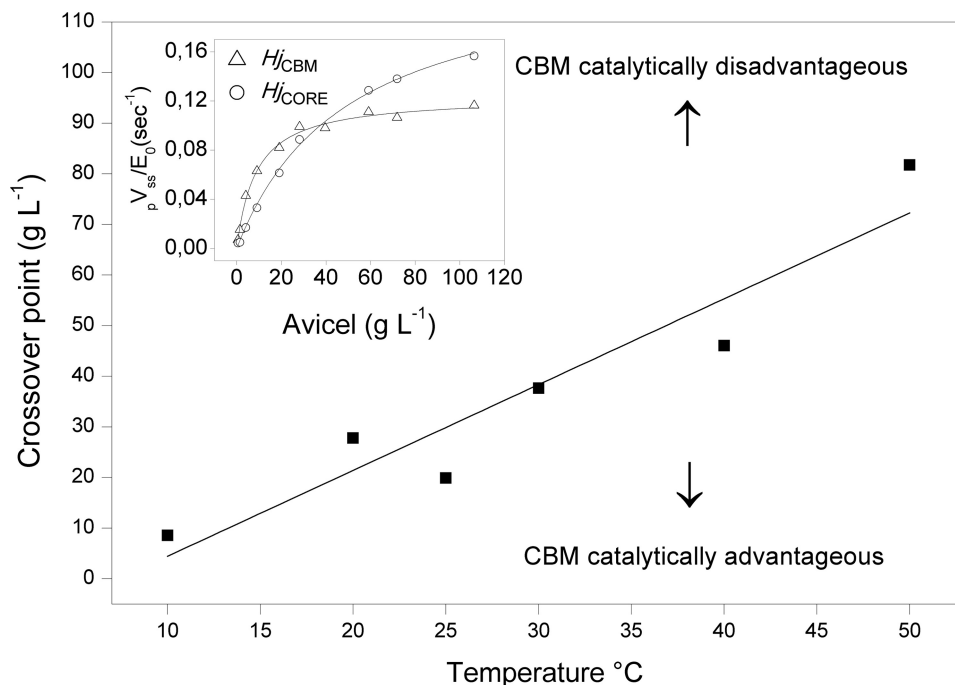


FIGURE 4. **Effects of temperature and binding module on the activity of Cel7A from *H. jecorina*.** The inset shows data from 30 °C of the specific rate versus substrate load. It appears that the one-domain variant was slower at low substrate but became faster than the two-domain enzyme above ~40 g/liter. The main panel shows the location (i.e. substrate load) of this crossover as a function of temperature. The line separates the plane into regions where the CBM promoted (upper left) or reduced (lower right) enzyme activity, respectively.

vation. For enzymes with CBM, we found  $Q_{10}$  values of  $2.17 \pm 0.10$  and  $1.76 \pm 0.16$  for  ${}_pV_{\max}$  and  ${}_pK_m$ , respectively. The analogous (average) values for one-domain enzymes were  $2.44 \pm 0.15$  and  $2.10 \pm 0.09$ , and these numbers revealed that the binding module reduced the sensitivity to temperature of both  ${}_pV_{\max}$  and  ${}_pK_m$ .

To further illustrate relationships among temperature, activity, and the CBM, we replotted data from Fig. 1 to directly compare pairs of enzymes with and without binding module. An example for *H. jecorina* (i.e. a comparison of  $Hj_{CBM}$  and  $Hj_{CORE}$ ) at  $T = 30$  °C is shown in the inset of Fig. 4. It appeared that the two-domain enzyme was more active at low substrate load (below ~35 g/liter), whereas the opposite was true at higher loads. The effect was quite pronounced, and the one-domain enzyme outperformed the wild type by about 40% at the highest loads in Fig. 4. It also appears from the figure that the one-domain enzyme does not reach saturating conditions in the current experiments, and this underlies the observation (Table 1) that the difference in maximal rates for the two variants was even larger (about 2-fold) than the difference in  ${}_pV_{ss}$  shown in Fig. 4. Analogous plots revealed that a crossover occurred at all investigated temperatures (and for both  $Hj$  and  $Re$  enzymes), and the main panel in Fig. 4 shows how the substrate load at the crossover point changed with temperature. This plot shows that at 10 °C the one-domain variant was most active except in very dilute substrate suspensions (below 5–10 g/liter). Conversely, at 50 °C, the two-domain enzyme was more effective over most of the investigated range and only became inferior to the CBM-free variant when the substrate load exceeded 70–80 g/liter.

The distribution between free and adsorbed enzyme was measured in all samples at the end of the hydrolysis experiments.

Results of these measurements are presented in Fig. 5, which shows the fraction of bound enzyme as a function of the substrate load. It appears that adsorption is strongly promoted by the CBM, particularly at high temperatures where a much higher fraction of the two-domain enzymes is bound compared with enzymes without a CBM. Fig. 5 also illustrates that at low substrate loads (below 30–40 g/liter) increasing temperature (at a fixed substrate load) consistently lowers the bound fraction, and this negative effect of temperature on adsorption is more pronounced for the single-domain enzymes. At higher loads of substrate where binding sites were in large excess, enzymes with a CBM were essentially fully adsorbed, and no effect of temperature could be detected. At the lower substrate loads where the effect of temperature on adsorption was largest, the CBM appeared to protect against temperature-induced affinity loss somewhat more in  $Hj_{CBM}$  compared with  $Re_{CBM}$ . As the sequence of the linker and CBM (as well as the expression organism) were the same in both cases, this is unlikely to depend on differences in the CBM itself. It could reflect that the  $Hj_{CBM}$  enzyme with its native linker and binding module showed some kind of cooperative interaction, which was absent in the artificial fusion of the CBM-less  $Re$  wild type and the CBM from *H. jecorina*. To quantify the adsorption data, we converted it to substrate coverage,  $\Gamma$ , in units of  $\mu\text{mol}$  of enzyme/g of cellulose using the relationship  $\Gamma = (E_0 - [E])/S_0$  where  $[E]$  is the measured free enzyme concentration. We plotted  $\Gamma$  against the free enzyme concentration,  $[E]$  (not shown), and determined the slope for  $[E] \rightarrow 0$ . This is the so-called partitioning coefficient,  $K_p$ , which is often used as a measure of the overall affinity of a cellulase for the cellulose surface (42, 43). Values of  $K_p$  are listed in Table 1.

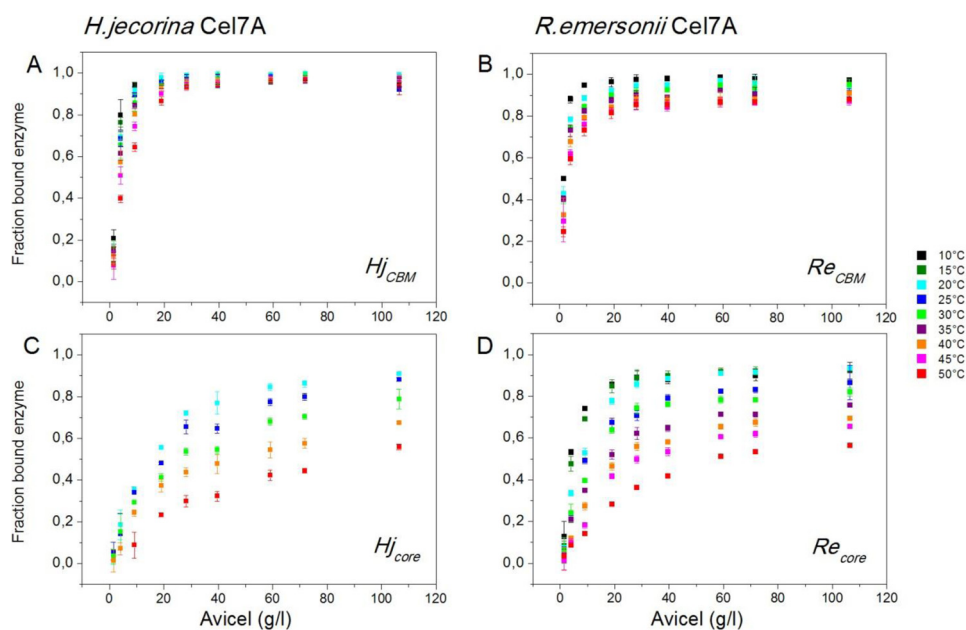


FIGURE 5. Fraction of bound Cel7A in the hydrolysis samples as function of substrate load at temperatures from 10 to 50 °C. The total enzyme concentration was 400 nM in all samples, and the measurements were made after 1-h contact time. All points are average  $\pm$  S.D. (error bars) for triplicate measurements.

## Discussion

The effect of temperature on cellulolytic enzyme activity is of direct interest within different research fields. For example, it has been hypothesized that temperature activation of cellulases and related glycoside hydrolases that decompose soil organic matter could shift natural carbon stocks toward more atmospheric CO<sub>2</sub> as the climate gets warmer (44). If indeed so, this would generate a positive feedback loop for global warming, and any attempt to predict such effects relies heavily on an understanding of the activation of relevant enzymes (1). Within biotechnology, the interest in cellulases is primarily driven by their use in emerging industries that produce bioethanol from lignocellulosic feedstock. In the industrial saccharification process, it is desirable to use as high a temperature and solid loadings as possible (45, 46), and many studies have therefore investigated optimal temperatures both for wild types and thermostable variants (8–13). Although ill-defined from a rigorous point of view (47), the optimal temperature specifies the location of the maximum that usually appears when the activity against a certain substrate is plotted as a function of temperature. It occurs as a result of two independent processes. Catalytic reactions are accelerated as temperature increases, but at the optimal temperature, this is balanced out by thermal inactivation of the enzyme, and at still higher temperatures, activity is reduced due to rapid inactivation. The balance of these two processes must be considered in any enzyme temperature study. For the current enzymes, earlier work has suggested a very small degree of inactivation of *Hj<sub>CBM</sub>* under the conditions studied here (1-h contact with Avicel and  $T < 50$  °C) (48), and as *R. emersonii* Cel7A is significantly more thermostable than the *H. jecorina* enzyme (49), it appears safe to assume that thermal inactivation can be generally neglected in this work. Therefore, we will henceforth interpret the results with respect to the effect of temperature on catalysis and adsorption without interference from enzyme inactivation.

Cellulases perform heterogeneous catalysis, and this implies that only surface-adsorbed enzymes are potentially active. Many earlier works have shown that the adsorbed population of both two-domain Cel7A and isolated CBM decreases with increasing temperature (42, 43, 50, 52, 53), and it follows that temperature-activity relationships on insoluble substrate may be seen as a balance between accelerated reaction steps on one hand and a shift toward less surface-adsorbed (potentially active) enzyme on the other hand. The results in Table 1 allow evaluation of these two contributions. Thus, the parameter  $pV_{\max}/E_0$  is the specific rate at saturating substrate loads where all enzyme is per definition adsorbed. We found strong thermoactivation for this parameter with  $Q_{10}$  values of 2.1–2.6, and we interpret this as a measure of the temperature-induced acceleration of the catalytic reaction devoid of contributions from shifts in the adsorption equilibrium. Earlier studies on soluble substrate analogs have suggested a comparable or moderately lower temperature sensitivity of  $V_{\max}$  for cellobiohydrolases (1, 24, 54), and hence there were no signs of pronounced effects of an insoluble substrate on temperature activation at saturating substrate loads. Comparing the two enzymes, *Re<sub>CBM</sub>* and *Re<sub>CORE</sub>*, from a thermophile organism with the analogous enzymes from the mesophile *H. jecorina* suggested a higher thermoactivation for the former ( $pV_{\max}$  had  $Q_{10}$  values that were higher by 0.2–0.3 unit for *R. emersonii*). This behavior is in line with theories suggesting stronger thermoactivation (*i.e.* higher activation energies) of enzymes adapted to higher temperatures (23, 55), and a similar behavior has been seen in some (54) but not all (1) earlier cellulase studies using soluble substrate analogs.

At low substrate loads, we found a very different picture with a much lower degree of temperature activation. Hence,  $Q_{10}$  values for  $p\eta$ , which is the apparent second order rate constant that governs the hydrolytic rate when  $S \ll pK_m$ , was only 1.1–1.2, and this unusually low temperature sensitivity was the



## Temperature Activation of Cel7A Cellobiohydrolases

result of a strong growth of  ${}_pK_m$ . This parameter typically increased by an order of magnitude upon heating from 10 to 50 °C (Table 1 and Fig. 2B), and the direct meaning of this is that the substrate load required to achieve half of the maximal rate increased about 10-fold in this temperature interval. However, as  ${}_pK_m$  defined in Equation 2 is the ratio of the off- and on-rate constants,  ${}_pK_m$  may also be interpreted as a dissociation constant for the enzyme-substrate complex, and this underscores that its stability decreased noticeably upon heating. The same conclusion was reached from the independently measured  $K_p$  values (Table 1). It should be noted that  $K_p$  corresponds to a binding constant, and hence it is the reciprocal,  $1/K_p$ , that is relevant to compare with  ${}_pK_m$ . It appears from the results in Table 1 that  $1/K_p$  also increased strongly with temperature, and it follows that both kinetic and adsorption data confirm the same trend of a much weaker interaction as temperature increased. This agreement also offers model-independent support for the general validity of the kinetic analysis. Further inspection of Figs. 2B and 3B shows that the temperature-induced loss of affinity was particularly strong for one-domain enzymes. In fact, for enzymes without a CBM,  $Q_{10}$  for  ${}_p\eta$  was essentially 1 (Fig. 3C), thus suggesting that their activity was almost independent of temperature at very low substrate loads. We interpret this behavior as the result of an almost complete balancing between the normal acceleration of the catalytic steps on one hand and a shift toward less enzyme-substrate complex on the other hand. If we combine the observed effects of the CBM at high and low substrate loads, it appears that the binding module exerted a dual role on temperature activation. On one hand, the CBM hampered activation because it reduced growth in the maximal rate ( $Q_{10}$  for  ${}_pV_{\max}$  was smaller for the two-domain enzymes). On the other hand, it favored activation by diminishing the tendency of desorption from the substrate as temperature increased ( $Q_{10}$  for  ${}_pK_m$  was also smaller for two-domain enzymes). As a consequence, the CBM favored activity at low, but not at high, substrate loads as illustrated in Fig. 4. The same conclusion has been reached previously by Viikari and co-workers (56–58), who studied a number of systems and conditions including lignocellulosic substrates and long term experiments with significant conversion. These workers concluded that the increased probability of enzymes to find the substrate at high loads would compensate for the lower affinity of one-domain enzymes (56). This argument is along the lines of Le Chatelier's principle, which stipulates a shift toward the adsorbed form at high loads, and the results in Table 1 are compatible with this. However, the current results suggest that other factors must be considered to rationalize relationships between the CBM and catalytic efficacy. Thus, at saturating substrate loads, the one-domain enzymes were consistently about 2-fold faster than enzymes with CBM, and this cannot depend on adsorption because the whole enzyme population (whether one- or two-domain) is adsorbed at saturation. We conclude that the CBM effects both adsorption and catalysis: it promotes adsorption and hence enzymatic activity at low substrate loads where "finding" the substrate is critical but exerts a negative effect on the rate of catalysis, which becomes evident at high loads. For a processive enzyme, this effect of the CBM could rely on a slow dissociation (*i.e.* low  ${}_pk_{\text{off}}$  in Scheme 1).

Several studies have suggested that at least under some conditions the overall hydrolytic rate is governed by the release of unproductively bound enzymes, which although associated with a cellulose strand are prevented from further processive movement by irregularities on the cellulose surface (39, 59–61). If CBM-cellulose interactions indeed contribute to a slower dissociation, higher maximal rates for the one-domain variants could reflect faster dissociation of unproductively bound enzyme (and hence earlier recruitment for new attacks). This interpretation parallels a recent study where the substrate affinity of  $Hj_{\text{CBM}}$  was lowered by the mutation W38A in the catalytic domain (25). Kinetic analysis of this variant at 25 °C showed a 4-fold increase in  ${}_pK_m$  and a 2-fold increase in  ${}_pV_{\max}$  compared with the wild type. Interestingly, these relative changes are essentially identical to those seen when comparing  $Hj_{\text{CBM}}$  and  $Hj_{\text{CORE}}$  at 25 °C (Table 1). In other words, we find the same inverse correlation between affinity and maximal rate in variants that are modified in very different ways, and although two examples are obviously not sufficient to make any general conclusions, the coincidence supports both the interpretation that  ${}_pk_{\text{off}}$  is rate-limiting and the conclusion that the CBM makes a negative contribution to this rate constant (and hence slows down dissociation).

In conclusion, we have measured activity and adsorption on insoluble substrate of four related cellobiohydrolases in small increments of temperature and substrate load and used a steady state model for processive hydrolysis to analyze their temperature activation. The most temperature-sensitive parameter was the maximal rate, which showed  $Q_{10}$  values up to 2.6. This degree of activation is comparable with or slightly higher than results from earlier studies on cellobiohydrolases acting on soluble substrate analogs. We suggest that this provides a measure of the thermal acceleration of the reactions steps in the investigated enzymes. Other factors including temperature-induced changes in the structure of cellulose cannot be ruled out but appear unlikely. Thus, although earlier works have identified such changes, they were only seen at far higher temperatures (51). Heating was associated with a pronounced reduction in substrate affinity, and this was reflected in  ${}_pK_m$  and  $1/K_p$ , which both grew by about an order of magnitude between 10 and 50 °C. One consequence of this was that the overall hydrolytic rate showed little and in some cases no (see Fig. 2C) increase with temperature in dilute substrate suspensions. The investigated cellobiohydrolases were chosen to elucidate whether the CBM and natural adaptation to higher temperature influenced temperature activation. We consistently found that the CBM lowered both  ${}_pV_{\max}$  and its increment with temperature. This negative contribution of the CBM to activity was counteracted by its promotion of substrate affinity, and as a result, the presence of a CBM was an advantage for activity at low substrate loads but a disadvantage for activity at high loads. The substrate load where the effect of the CBM on activity changed sign increased strongly with temperature (Fig. 4). The effect of the CBM was similar for the *Hj* and *Re* enzymes, although the former is naturally evolved with a CBM, whereas the latter is not. Hence, we did not find signs of additional interactions in the *Re* enzyme, which might have evolved to compensate for the lack of a CBM. The results revealed a moderately higher tempera-

ture activation ( $0.2\text{--}0.3 Q_{10}$  unit) of  $pV_{\max}$  for thermophilic (*Re*) enzymes compared with the mesophilic (*Hf*) analogs, and this behavior was in line with general theories on temperature adaptation of enzymes and may suggest that enzymes from thermophilic organisms are beneficial for technical applications with respect to both physical stability and temperature activation.

**Author Contributions**—T. H. S. and P. W. conceived the study and wrote the paper. N. C. B. contributed to the analysis and interpretation of data based on the steady state model. M. S. W. designed, constructed, and expressed the WT and mutant proteins and revised the work associated with the writing of the article. S. F. B. purified the mutant proteins and designed, performed, and analyzed the experiments in Fig. 5. K. B. and T. H. S. coordinated and made the strategy for the experimental setup. All authors analyzed the results and approved the final version of the manuscript.

## References

- German, D. P., Marcelo, K. R. B., Stone, M. M., and Allison, S. D. (2012) The Michaelis-Menten kinetics of soil extracellular enzymes in response to temperature: a cross-latitudinal study. *Glob. Chang. Biol.* **18**, 1468–1479
- Wilson, D. B. (2009) Cellulases and biofuels. *Curr. Opin. Biotechnol.* **20**, 295–299
- Horn, S. J., Sikorski, P., Cederkvist, J. B., Vaaje-Kolstad, G., Sørli, M., Synstad, B., Vriend, G., Vårum, K. M., and Eijsink, V. G. (2006) Costs and benefits of processivity in enzymatic degradation of recalcitrant polysaccharides. *Proc. Natl. Acad. Sci. U.S.A.* **103**, 18089–18094
- Zhou, W., Irwin, D. C., Escovar-Kousen, J., and Wilson, D. B. (2004) Kinetic studies of *Thermobifida fusca* Cel9A active site mutant enzymes. *Biochemistry* **43**, 9655–9663
- Payne, C. M., Knott, B. C., Mayes, H. B., Hansson, H., Himmel, M. E., Sandgren, M., Ståhlberg, J., and Beckham, G. T. (2015) Fungal cellulases. *Chem. Rev.* **115**, 1308–1448
- Wolfenden, R., and Snider, M. J. (2001) The depth of chemical time and the power of enzymes as catalysts. *Acc. Chem. Res.* **34**, 938–945
- Wolfenden, R., Lu, X. D., and Young, G. (1998) Spontaneous hydrolysis of glycosides. *J. Am. Chem. Soc.* **120**, 6814–6815
- Heinzelman, P., Snow, C. D., Wu, I., Nguyen, C., Villalobos, A., Govindarajan, S., Minshull, J., and Arnold, F. H. (2009) A family of thermostable fungal cellulases created by structure-guided recombination. *Proc. Natl. Acad. Sci. U.S.A.* **106**, 5610–5615
- Voutilainen, S. P., Puranen, T., Siika-Aho, M., Lappalainen, A., Alapuranen, M., Kallio, J., Hooman, S., Viikari, L., Vehmaanperä, J., and Koivula, A. (2008) Cloning, expression, and characterization of novel thermostable family 7 cellobiohydrolases. *Biotechnol. Bioeng.* **101**, 515–528
- Voutilainen, S. P., Murray, P. G., Tuohy, M. G., and Koivula, A. (2010) Expression of *Talaromyces emersonii* cellobiohydrolase Cel7A in *Saccharomyces cerevisiae* and rational mutagenesis to improve its thermostability and activity. *Protein Eng. Des. Sel.* **23**, 69–79
- Wu, I., and Arnold, F. H. (2013) Engineered thermostable fungal Cel6A and Cel7A cellobiohydrolases hydrolyze cellulose efficiently at elevated temperatures. *Biotechnol. Bioeng.* **110**, 1874–1883
- Day, A. G., Goedegebuur, F., Gualfetti, P., Mitchinson, C., Neefe, P., Sandgren, M., Shaw, A., and Stahlberg, J. (February 26, 2004) World Intellectual Property Organization Patent WO2004016760
- Teter, S., Cherry, J., Ward, C., Jones, A., Harris, P., and Yi, J. (April 2, 2009) World Intellectual Property Organization Patent WO2005030926
- Viikari, L., Alapuranen, M., Puranen, T., Vehmaanperä, J., and Siika-Aho, M. (2007) Thermostable enzymes in lignocellulose hydrolysis. *Adv. Biochem. Eng. Biotechnol.* **108**, 121–145
- Vásquez, M. P., da Silva, J. N., de Souza, M. B., Jr., and Pereira, N., Jr. (2007) Enzymatic hydrolysis optimization to ethanol production by simultaneous saccharification and fermentation. *Appl. Biochem. Biotechnol.* **137**, 141–153
- Zhang, Y., Xu, J. L., Qi, W., Yuan, Z. H., Zhuang, X. S., Liu, Y., and He, M. C. (2012) A fractal-like kinetic equation to investigate temperature effect on cellulose hydrolysis by free and immobilized cellulase. *Appl. Biochem. Biotechnol.* **168**, 144–153
- Hu, G., Heitmann, J. A., Jr., and Rojas, O. J. (2009) *In situ* monitoring of cellulase activity by microgravimetry with a quartz crystal microbalance. *J. Phys. Chem. B* **113**, 14761–14768
- Drissen, R. E. T., Maas, R. H. W., Van Der Maarel, M., Kabel, M. A., Schols, H. A., Tramper, J., and Beentink, H. H. (2007) A generic model for glucose production from various cellulose sources by a commercial cellulase complex. *Biocatal. Biotransform.* **25**, 419–429
- Zhang, S., Wolfgang, D. E., and Wilson, D. B. (1999) Substrate heterogeneity causes the nonlinear kinetics of insoluble cellulose hydrolysis. *Biotechnol. Bioeng.* **66**, 35–41
- Subhedar, P. B., and Gogate, P. R. (2014) Enhancing the activity of cellulase enzyme using ultrasonic irradiations. *J. Mol. Catal. B Enzym.* **101**, 108–114
- Deng, S. P., and Tabatabai, M. A. (1994) Cellulase activity of soils. *Soil Biol. Biochem.* **26**, 1347–1354
- Ng, T. K., and Zeikus, J. G. (1981) Comparison of extracellular cellulase activities of *Clostridium thermocellum* LQRI and *Trichoderma reesei* QM9414. *Appl. Environ. Microbiol.* **42**, 231–240
- Lonhienne, T., Gerday, C., and Feller, G. (2000) Psychrophilic enzymes: revisiting the thermodynamic parameters of activation may explain local flexibility. *Biochim. Biophys. Acta* **1543**, 1–10
- Stone, M. M., Weiss, M. S., Goodale, C. L., Adams, M. B., Fernandez, I. J., German, D. P., and Allison, S. D. (2012) Temperature sensitivity of soil enzyme kinetics under N-fertilization in two temperate forests. *Glob. Chang. Biol.* **18**, 1173–1184
- Kari, J., Olsen, J., Borch, K., Cruys-Bagger, N., Jensen, K., and Westh, P. (2014) Kinetics of cellobiohydrolase (Cel7A) variants with lowered substrate affinity. *J. Biol. Chem.* **289**, 32459–32468
- Ye, Z., and Berson, R. E. (2014) Factors affecting cellulose hydrolysis based on inactivation of adsorbed enzymes. *Bioresour. Technol.* **167**, 582–586
- Brown, R. F., Agbogbo, F. K., and Holtzapfel, M. T. (2010) Comparison of mechanistic models in the initial rate enzymatic hydrolysis of AFEX-treated wheat straw. *Biotechnol. Biofuels* **3**, 6
- Cruys-Bagger, N., Elmerdahl, J., Praetgaard, E., Borch, K., and Westh, P. (2013) A steady-state theory for processive cellulases. *FEBS J.* **280**, 3952–3961
- Houbraken, J., Spierenburg, H., and Frisvad, J. C. (2012) *Rasamsonia*, a new genus comprising thermotolerant and thermophilic *Talaromyces* and *Geosmithia* species. *Antonie Van Leeuwenhoek* **101**, 403–421
- Grassick, A., Murray, P. G., Thompson, R., Collins, C. M., Byrnes, L., Birrane, G., Higgins, T. M., and Tuohy, M. G. (2004) Three-dimensional structure of a thermostable native cellobiohydrolase, CBH1B, and molecular characterization of the cel7 gene from the filamentous fungus, *Talaromyces emersonii*. *Eur. J. Biochem.* **271**, 4495–4506
- Tomme, P., Van Tilbeurgh, H., Pettersson, G., Van Damme, J., Vandekerckhove, J., Knowles, J., Teeri, T., and Claeysens, M. (1988) Studies of the cellulolytic system of *Trichoderma reesei* QM 9414. Analysis of domain function in two cellobiohydrolases by limited proteolysis. *Eur. J. Biochem.* **170**, 575–581
- Divne, C., Ståhlberg, J., Reinikainen, T., Ruohonen, L., Pettersson, G., Knowles, J. K., Teeri, T. T., and Jones, T. A. (1994) The three-dimensional crystal structure of the catalytic core of cellobiohydrolase I from *Trichoderma reesei*. *Science* **265**, 524–528
- Borch, K., Jensen, K., Krogh, K., McBrayer, B., Westh, P., Kari, J., Olsen, J. P., Sorensen, T. H., Windahl, M. S., and Xu, H. (September 12, 2014) World Intellectual Property Organization Patent WO2014138672
- Gasteiger, E., Hoogland, C., Gattiker, A., Duvaud, S., Wilkins, M. R., Appel, R. D., and Bairoch, A. (2005) in *The Proteomics Protocols Handbook* (Walker, J. M., ed) pp. 571–607, Humana Press, Totowa, NJ
- Lever, M. (1972) A new reaction for colorimetric determination of carbohydrates. *Anal. Biochem.* **47**, 273–279
- Murphy, L., Bohlin, C., Baumann, M. J., Olsen, S. N., Sørensen, T. H., Anderson, L., Borch, K., and Westh, P. (2013) Product inhibition of five *Hypocrea jecorina* cellulases. *Enzyme Microb. Technol.* **52**, 163–169

## Temperature Activation of Cel7A Cellobiohydrolases

37. Teugjas, H., and Väljamäe, P. (2013) Product inhibition of cellulases studied with C-14-labeled cellulose substrates. *Biotechnol. Biofuels* **6**, 104
38. Gruno, M., Väljamäe, P., Pettersson, G., and Johansson, G. (2004) Inhibition of the *Trichoderma reesei* cellulases by cellobiose is strongly dependent on the nature of the substrate. *Biotechnol. Bioeng.* **86**, 503–511
39. Praestgaard, E., Elmerdahl, J., Murphy, L., Nyman, S., McFarland, K. C., Borch, K., and Westh, P. (2011) A kinetic model for the burst phase of processive cellulases. *FEBS J.* **278**, 1547–1560
40. Horn, S. J., Sørli, M., Vårum, K. M., Väljamäe, P., and Eijsink, V. G. (2012) Measuring processivity. *Methods Enzymol.* **510**, 69–95
41. Fersht, A. (1998) *Structure and Mechanism in Protein Science: a Guide to Enzyme Catalysis and Protein Folding*, W. H. Freeman, New York
42. Linder, M., and Teeri, T. T. (1996) The cellulose-binding domain of the major cellobiohydrolase of *Trichoderma reesei* exhibits true reversibility and a high exchange rate on crystalline cellulose. *Proc. Natl. Acad. Sci. U.S.A.* **93**, 12251–12255
43. Palonen, H., Tenkanen, M., and Linder, M. (1999) Dynamic interaction of *Trichoderma reesei* cellobiohydrolases Cel6A and Cel7A and cellulose at equilibrium and during hydrolysis. *Appl. Environ. Microbiol.* **65**, 5229–5233
44. Davidson, E. A., and Janssens, I. A. (2006) Temperature sensitivity of soil carbon decomposition and feedbacks to climate change. *Nature* **440**, 165–173
45. Larsen, J., Petersen, M. O., Thirup, L., Li, H. W., and Iversen, F. K. (2008) The IBUS process—lignocellulosic bioethanol close to a commercial reality. *Chem. Eng. Technol.* **31**, 765–772
46. Jorgensen, H., Kristensen, J. B., and Felby, C. (2007) Enzymatic conversion of lignocellulose into fermentable sugars: challenges and opportunities. *Biofuel. Bioprod. Bioref.* **1**, 119–134
47. Laidler, K. J., and Peterman, B. F. (1979) Temperature effects in enzyme kinetics. *Methods Enzymol.* **63**, 234–257
48. Alasepp, K., Borch, K., Cruys-Bagger, N., Badino, S., Jensen, K., Sørensen, T. H., Windahl, M. S., and Westh, P. (2014) *In situ* stability of substrate-associated cellulases studied by DSC. *Langmuir* **30**, 7134–7142
49. Voutilainen, S. P., Nurmi-Rantala, S., Penttilä, M., and Koivula, A. (2014) Engineering chimeric thermostable GH7 cellobiohydrolases in *Saccharomyces cerevisiae*. *Appl. Microbiol. Biotechnol.* **98**, 2991–3001
50. Moran-Mirabal, J. M., Bolewski, J. C., and Walker, L. P. (2011) Reversibility and binding kinetics of *Thermobifida fusca* cellulases studied through fluorescence recovery after photobleaching microscopy. *Biophys. Chem.* **155**, 20–28
51. Watanabe, A., Morita, S., and Ozaki, Y. (2006) Temperature-dependent structural changes in hydrogen bonds in microcrystalline cellulose studied by infrared and near-infrared spectroscopy with perturbation-correlation moving-window two-dimensional correlation analysis. *Appl. Spectrosc.* **60**, 611–618
52. Ooshima, H., Sakata, M., and Harano, Y. (1983) Adsorption of cellulase from *Trichoderma viride* on cellulose. *Biotechnol. Bioeng.* **25**, 3103–3114
53. Colussi, F., Sørensen, T. H., Alasepp, K., Kari, J., Cruys-Bagger, N., Windahl, M. S., Olsen, J. P., Borch, K., and Westh, P. (2015) Probing substrate interactions in the active tunnel of a catalytically deficient cellobiohydrolase (Cel7). *J. Biol. Chem.* **290**, 2444–2454
54. Garsoux, G., Lamotte, J., Gerday, C., and Feller, G. (2004) Kinetic and structural optimization to catalysis at low temperatures in a psychrophilic cellulase from the Antarctic bacterium *Pseudoalteromonas haloplanktis*. *Biochem. J.* **384**, 247–253
55. Somero, G. N. (2004) Adaptation of enzymes to temperature: searching for basic “strategies.” *Comp. Biochem. Physiol. B Biochem. Mol. Biol.* **139**, 321–333
56. Le Costaouëc, T., Pakarinen, A., Várnai, A., Puranen, T., and Viikari, L. (2013) The role of carbohydrate binding module (CBM) at high substrate consistency: comparison of *Trichoderma reesei* and *Thermoascus aurantiacus* Cel7A (CBHI) and Cel5A (EGII). *Bioresour. Technol.* **143**, 196–203
57. Pakarinen, A., Haven, M. O., Djajadi, D. T., Várnai, A., Puranen, T., and Viikari, L. (2014) Cellulases without carbohydrate-binding modules in high consistency ethanol production process. *Biotechnol. Biofuels* **7**, 27
58. Várnai, A., Siika-Aho, M., and Viikari, L. (2013) Carbohydrate-binding modules (CBMs) revisited: reduced amount of water counterbalances the need for CBMs. *Biotechnol. Biofuels* **6**, 30
59. Cruys-Bagger, N., Elmerdahl, J., Praestgaard, E., Tatsumi, H., Spodsberg, N., Borch, K., and Westh, P. (2012) Pre-steady-state kinetics for hydrolysis of insoluble cellulose by cellobiohydrolase Cel7A. *J. Biol. Chem.* **287**, 18451–18458
60. Jalak, J., and Väljamäe, P. (2010) Mechanism of initial rapid rate retardation in cellobiohydrolase catalyzed cellulose hydrolysis. *Biotechnol. Bioeng.* **106**, 871–883
61. Eriksson, T., Karlsson, J., and Tjerneld, F. (2002) A model explaining declining rate in hydrolysis of lignocellulose substrates with cellobiohydrolase I (cel7A) and endoglucanase I (cel7B) of *Trichoderma reesei*. *Appl. Biochem. Biotechnol.* **101**, 41–60
62. Sørensen, T. H., Cruys-Bagger, N., Borch, K., and Westh, P. (2015) Free energy diagram for the heterogeneous enzymatic hydrolysis of glycosidic bonds in cellulose. *J. Biol. Chem.* **290**, 22203–22211

PATENT WO/2016/138167  
CELLOBIOHYDROLASE VARIANTS AND  
POLYNUCLEOTIDES ENCODING SAME

---

IX







- (51) **International Patent Classification:**  
*C12N 9/42* (2006.01)
- (21) **International Application Number:**  
PCT/US2016/019404
- (22) **International Filing Date:**  
24 February 2016 (24.02.2016)
- (25) **Filing Language:** English
- (26) **Publication Language:** English
- (30) **Priority Data:**  
62/120,178 24 February 2015 (24.02.2015) US
- (71) **Applicant:** NOVOZYMES A/S [DK/DK]; Krogshoejvej 36, 2880 Bagsvaerd (DK).
- (72) **Inventor; and**  
(71) **Applicant (for BW only):** MCBRAYER, Brett [US/US]; 3712 Kos Island Ave, Sacramento, California 95834 (US).
- (72) **Inventors:** WINDAHL, Michael Skovbo; Møebjergvej 14, 3660 Stenløse (DK). WESTH, Peter; Amagerbrogade 28 4.TH, 2300 Copenhagen (DK). BADINO, Silke Flindt; Krogshoejvej 36, 2880 Bagsvaerd (DK). BORCH, Kim; Vandtårnsvej 18, 3460 Birkerød (DK).
- (74) **Agents:** FECHTER, Eric et al.; Novozymes, Inc., 1445 Drew Avenue, Davis, California 95618 (US).
- (81) **Designated States (unless otherwise indicated, for every kind of national protection available):** AE, AG, AL, AM,

AO, AT, AU, AZ, BA, BB, BG, BH, BN, BR, BW, BY, BZ, CA, CH, CL, CN, CO, CR, CU, CZ, DE, DK, DM, DO, DZ, EC, EE, EG, ES, FI, GB, GD, GE, GH, GM, GT, HN, HR, HU, ID, IL, IN, IR, IS, JP, KE, KG, KN, KP, KR, KZ, LA, LC, LK, LR, LS, LU, LY, MA, MD, ME, MG, MK, MN, MW, MX, MY, MZ, NA, NG, NI, NO, NZ, OM, PA, PE, PG, PH, PL, PT, QA, RO, RS, RU, RW, SA, SC, SD, SE, SG, SK, SL, SM, ST, SV, SY, TH, TJ, TM, TN, TR, TT, TZ, UA, UG, US, UZ, VC, VN, ZA, ZM, ZW.

- (84) **Designated States (unless otherwise indicated, for every kind of regional protection available):** ARIPO (BW, GH, GM, KE, LR, LS, MW, MZ, NA, RW, SD, SL, ST, SZ, TZ, UG, ZM, ZW), Eurasian (AM, AZ, BY, KG, KZ, RU, TJ, TM), European (AL, AT, BE, BG, CH, CY, CZ, DE, DK, EE, ES, FI, FR, GB, GR, HR, HU, IE, IS, IT, LT, LU, LV, MC, MK, MT, NL, NO, PL, PT, RO, RS, SE, SI, SK, SM, TR), OAPI (BF, BJ, CF, CG, CI, CM, GA, GN, GQ, GW, KM, ML, MR, NE, SN, TD, TG).

**Declarations under Rule 4.17:**

- as to the applicant's entitlement to claim the priority of the earlier application (Rule 4.17(iii))

**Published:**

- without international search report and to be republished upon receipt of that report (Rule 48.2(g))
- with sequence listing part of description (Rule 5.2(a))



(54) **Title:** CELLOBIOHYDROLASE VARIANTS AND POLYNUCLEOTIDES ENCODING SAME

(57) **Abstract:** The present invention relates to cellobiohydrolase variants. The present invention also relates to polynucleotides encoding the variants; nucleic acid constructs, vectors, and host cells comprising the polynucleotides; and methods of using the variants.

